USGS
science for a changing world

Latest Pleistocene to Present Geology of Mount Baker Volcano, Northern Cascade Range, Washington

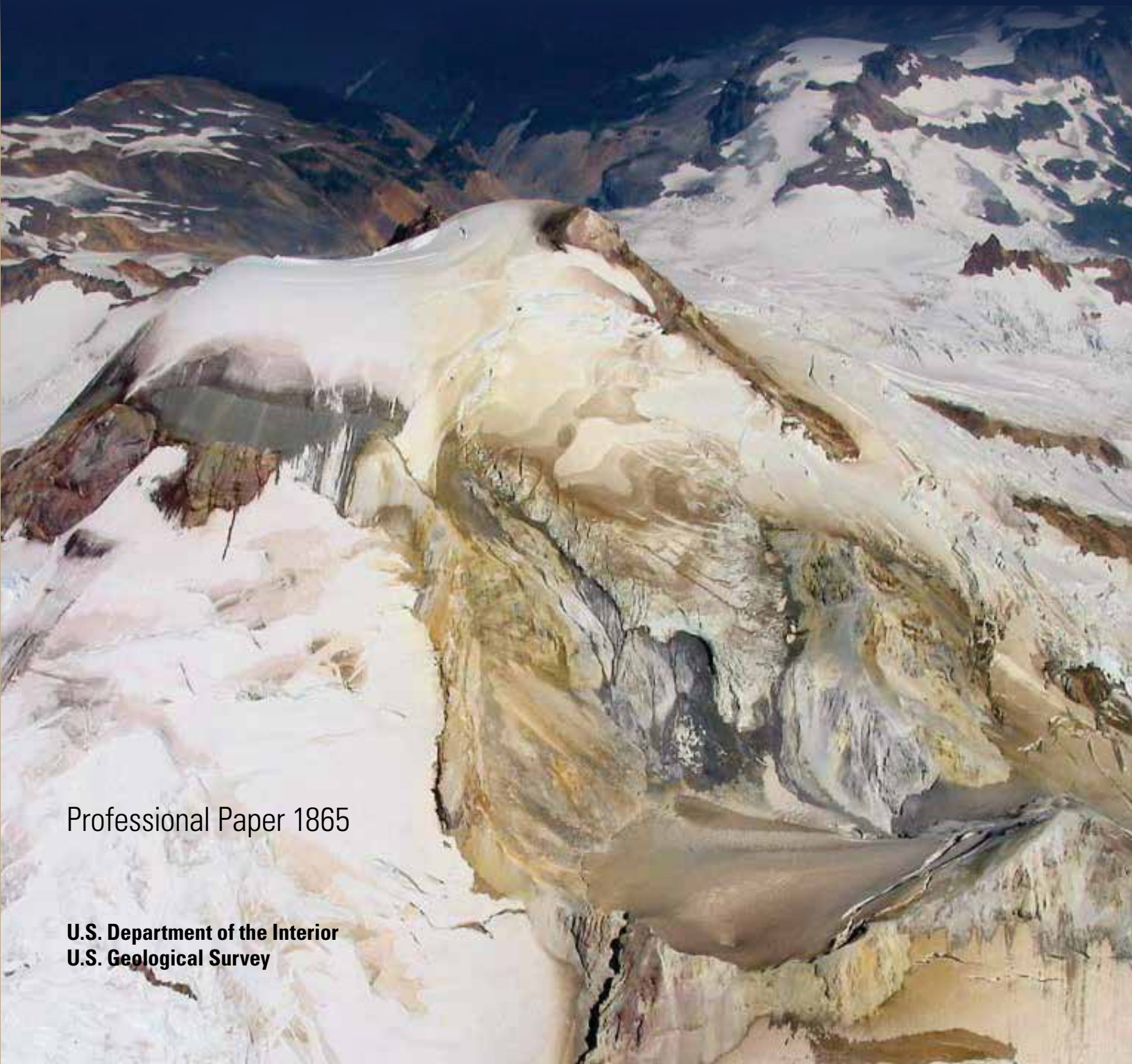

Professional Paper 1865

U.S. Department of the Interior
U.S. Geological Survey

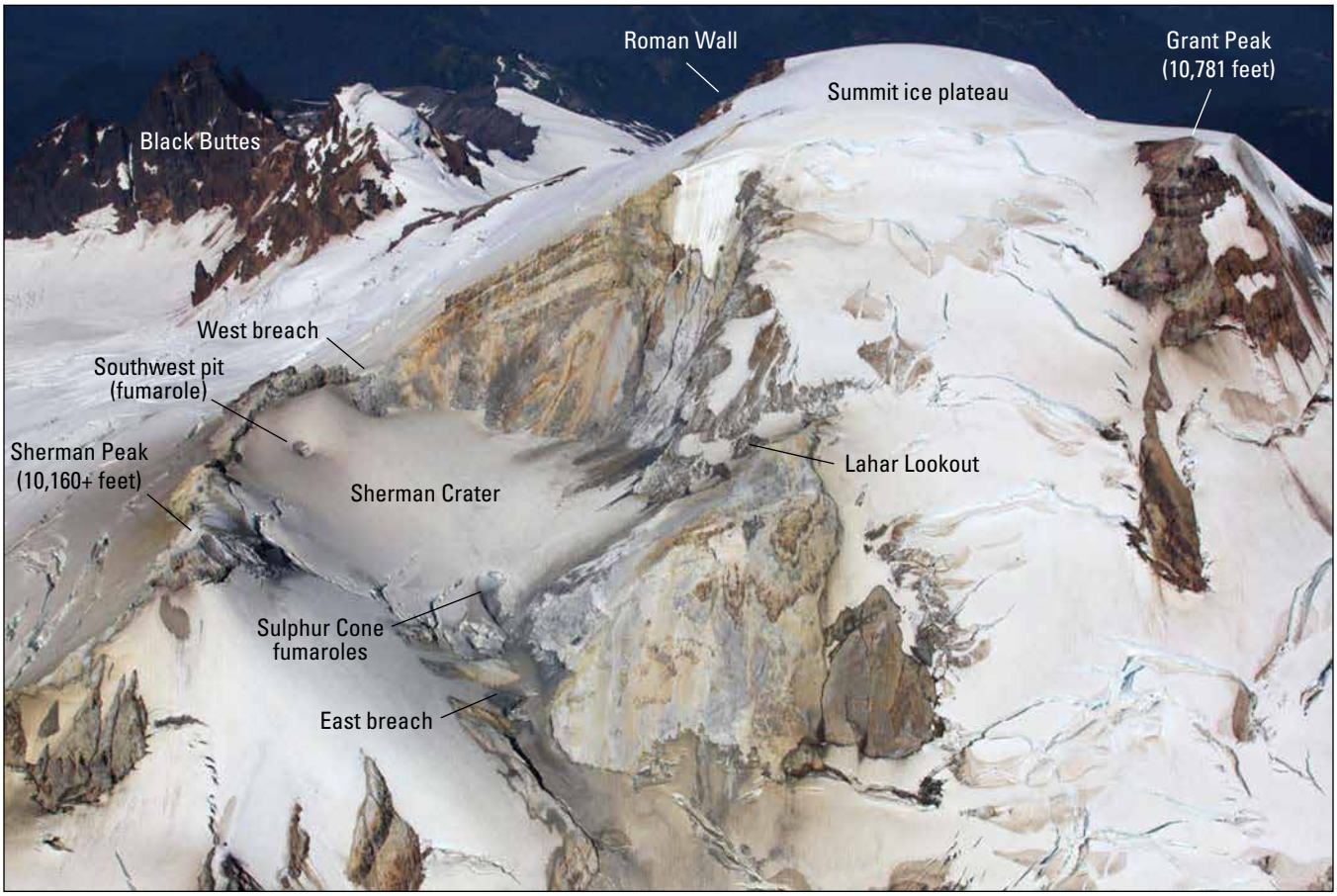

Cover. Aerial view of Mount Baker from the south, illustrating dark-colored, mainly unaltered bedrock of the west flank (on left, including the Roman Wall), and the lighter colored southeast flank (on right), with hydrothermal alteration concentrated at Holocene Sherman Crater. Carmelo Crater is the Pleistocene ice-filled summit crater. Note wind-distributed material on Sherman Crater floor. Photograph by J.H. Scurlock, September 2, 2003, used with permission.

Frontispiece. Aerial view of Mount Baker from the southeast. Photograph by J.H. Scurlock, July 27, 2009, used with permission.

Latest Pleistocene to Present Geology of Mount Baker Volcano, Northern Cascade Range, Washington

By Kevin M. Scott, David S. Tucker, Jon L. Riedel, Cynthia A. Gardner, and John P. McGeehin

Professional Paper 1865

U.S. Department of the Interior
U.S. Geological Survey

U.S. Department of the Interior
DAVID BERNHARDT, Secretary

U.S. Geological Survey
James F. Reilly II, Director

U.S. Geological Survey, Reston, Virginia: 2020

For more information on the USGS—the Federal source for science about the Earth, its natural and living resources, natural hazards, and the environment—visit https://www.usgs.gov or call 1–888–ASK–USGS.

For an overview of USGS information products, including maps, imagery, and publications, visit https://store.usgs.gov.

Any use of trade, firm, or product names is for descriptive purposes only and does not imply endorsement by the U.S. Government.

Although this information product, for the most part, is in the public domain, it also may contain copyrighted materials as noted in the text. Permission to reproduce copyrighted items must be secured from the copyright owner.

Suggested citation:
Scott, K.M., Tucker, D.S., Riedel, J.L., Gardner, C.A., and McGeehin, J.P., 2020, Latest Pleistocene to present geology of Mount Baker Volcano, northern Cascade Range, Washington: U.S. Geological Survey Professional Paper 1865, 170 p., https://doi.org/10.3133/pp1865.

ISSN 2330-7102 (online)

Acknowledgments

The detail of this latest-Pleistocene-to-present history of Mount Baker would not have been possible without many observations of "overburden" shared by Wes Hildreth during his mapping of the volcano's bedrock (Hildreth and others, 2003). We appreciate his counsel during all stages of this study.

We pay tribute to our collaborator, photographer-pilot John H. Scurlock; a few of his thousands of photographs of the volcano illustrate this report. Examples of his aerial images of Mount Baker, the north Cascade Range, and other volcanic and alpine terrains in the western United States and Canada can be viewed at https://jaggedridgeimaging.com.

Unlocking the remarkable history of the mobile debris avalanches in Rainbow Creek and Avalanche Gorge would not have been possible without the alpine and geological skills of David R. Lewis during our traverses of the gorge, two from above, one from below (Lewis and others, 2006). This mentor and earth science teacher at Mount Baker High School inspires his students, fellow teachers, and us.

We are in debt to the first accurate, deposit-based observations of the recent volcanic history of Mount Baker by Joseph Morovits, a miner and pioneer climbing guide who prospected throughout the Baker River watershed east of the volcano from 1891 to about 1917. That spelling of Joseph's name appears in historical accounts but is Morovitz on topographic maps of the U.S. Geological Survey (USGS). USGS policy requires that geologic names reflect spellings on those maps, and consequently we apologize to Morovits' descendants (and to those of Herman Schreiber, of Schriebers Meadow renown). The family name is actually Morvits or Morvitz, according to his grandnephew, volcanologist Richard P. Hoblitt. We cite several observations of 19th-century flows and eruptions by this brilliant but unschooled geologist (accounts and letters in appendix 9). We name the most significant young lahar from Mount Baker after Joseph—the multibranched Morovitz Creek lahar—based on its widespread deposits in the drainage in which he built his "ranch."

Pioneer aerial photographer Lage Wernstedt took the first images showing the debris avalanches in the reaches of Rainbow Creek named Avalanche Gorge after their description by Morovits. The minimum limiting date of the youngest avalanche is confirmed by one of his images (no. 3968).

William E. Scott and Thomas C. Pierson of the USGS reviewed the entire report; Wes Hildreth (USGS) and Pierson reviewed a previous draft; John C. Clague (Simon Fraser University) and Thom Davis (Bentley College) reviewed an early glacier chapter and aspects of an early glacial lake chapter; Karoly Nemeth (Massey University) reviewed the peperite discussions; and Mark Mastin (USGS Washington Water Science Center) reviewed appendix 8 and helped with the solution to that fascinating "detective story."

David Lewis and Kevin Scott received a Partners-in-Science Award from the M.J. Murdock Charitable Trust during 2005 and 2006. David Tucker and Kevin Scott received a 2006–07 research grant from Mazamas, the mountaineering organization of Portland, Oregon, that has a rich history of exploration at Mount Baker. Scott received 2007–09 grants from the Bradley Scholars program of the USGS.

Contents

Figures

Tables

Conversion Factors

U.S. customary units to International System of Units

Multiply	By	To obtain
	Length	
inch (in.)	2.54	centimeter (cm)
inch (in.)	25.4	millimeter (mm)
foot (ft)	0.3048	meter (m)
mile (mi)	1.609	kilometer (km)
yard (yd)	0.9144	meter (m)
	Area	
acre	4,047	square meter (m^2)
acre	0.004047	square kilometer (km^2)
square foot (ft^2)	929.0	square centimeter (cm^2)
square foot (ft^2)	0.09290	square meter (m^2)
square inch (in^2)	6.452	square centimeter (cm^2)
square mile (mi^2)	2.590	square kilometer (km^2)
	Volume	
gallon (gal)	0.003785	cubic meter (m^3)
million gallons (Mgal)	3,785	cubic meter (m^3)
cubic foot (ft^3)	0.02832	cubic meter (m^3)
cubic yard (yd^3)	0.7646	cubic meter (m^3)
cubic mile (mi^3)	4.168	cubic kilometer (km^3)
acre-foot (acre-ft)	1,233	cubic meter (m^3)
	Flow rate	
foot per second (ft/s)	0.3048	meter per second (m/s)
foot per year (ft/yr)	0.3048	meter per year (m/yr)
cubic foot per second (ft^3/s)	0.02832	cubic meter per second (m^3/s)
	Mass	
ounce, avoirdupois (oz)	28.35	gram (g)
ton, short (2,000 lb)	0.9072	metric ton (t)
ton, long (2,240 lb)	1.016	metric ton (t)

International System of Units to U.S. customary units

Multiply	By	To obtain
	Length	
centimeter (cm)	0.3937	inch (in.)
millimeter (mm)	0.03937	inch (in.)
meter (m)	3.281	foot (ft)
kilometer (km)	0.6214	mile (mi)
meter (m)	1.094	yard (yd)
	Area	
square meter (m^2)	0.0002471	acre
square kilometer (km^2)	247.1	acre
square centimeter (cm^2)	0.001076	square foot (ft^2)
square meter (m^2)	10.76	square foot (ft^2)
square centimeter (cm^2)	0.1550	square inch (ft^2)
square kilometer (km^2)	0.3861	square mile (mi^2)
	Volume	
cubic meter (m^3)	264.2	gallon (gal)
cubic meter (m^3)	0.0002642	million gallons (Mgal)
cubic meter (m^3)	35.31	cubic foot (ft^3)
cubic meter (m^3)	1.308	cubic yard (yd^3)
cubic kilometer (km^3)	0.2399	cubic mile (mi^3)
cubic meter (m^3)	0.0008107	acre-foot (acre-ft)
	Flow rate	
meter per second (m/s)	3.281	foot per second (ft/s)
meter per year (m/yr)	3.281	foot per year (ft/yr)
cubic meter per second (m^3/s)	35.31	cubic foot per second (ft^3/s)
	Mass	
gram (g)	0.03527	ounce, avoirdupois (oz)
metric ton (t)	1.102	ton, short [2,000 lb]
metric ton (t)	0.9842	ton, long [2,240 lb]

Abbreviations

BF	buried forest
GPS	Global Positioning System
PJB	prismatically jointed blocks
RS	reference section
USGS	U.S. Geological Survey
UTM	Universal Transverse Mercator
XRF	X-ray fluorescence

Latest Pleistocene to Present Geology of Mount Baker Volcano, Northern Cascade Range, Washington

By Kevin M. Scott,[1] David S. Tucker,[2] Jon L. Riedel,[3] Cynthia A. Gardner,[1] and John P. McGeehin[1]

Mount Baker looms over the city of Bellingham, Washington, 46 kilometers (30.5 miles) west of the volcano. Telephotograph by D.S. Tucker, December 28, 2006.

[1]U.S. Geological Survey.

[2]Western Washington University.

[3]National Park Service.

Chapter A

Mount Baker Volcano, Northern Casade Range, Washington

Vapor plume rising from Sherman Crater, the active vent during the Holocene. Such plumes are commonly seen in winter on clear, cold, windless days. View looks east. Photograph by John H. Scurlock, January 9, 2011, used with permission.

Chapter A

Summary

Mount Baker is the northernmost active stratovolcano of the United States' part of the Cascade Range. It is the most recent center of a multivent Quaternary lava field that has been active during the past 1.3 million years (Ma) (Hildreth and others, 2003). The current edifice is built upon the remnants of the older Black Buttes stratovolcano (0.5–0.2 Ma) and was constructed largely between 50 and 10 thousand years ago (ka) (Hildreth and others, 2003). Unlike the central part of the Cascade Arc, mafic centers are sparse; nonetheless, the 9.8 ka eruption of a cinder cone in Schriebers Meadow on the south flank of Mount Baker boasts the most voluminous Holocene lava flow in the Washington Cascade Range north of Mount Adams.

This report summarizes the multifaceted and complex surficial geologic history of Mount Baker just before, during, and after withdrawal of the late Pleistocene Cordilleran ice sheet from the Mount Baker area. Within a backdrop of glacial advances and retreats, we define four eruptive periods: the Carmelo Crater eruptive period (circa [ca.] 14–11.6 ka), Schriebers Meadow eruptive period (ca. 9.8–9.1 ka), Mazama Park eruptive period (ca. 6.7 ka), and Sherman Crater eruptive period (1843–1880 C.E.). Fundamental to our understanding of the timing of volcanic events is the glacial history and the presence of two long-lived glacial lakes—Glacial Lake Concrete and Glacial Lake Baker, the latter of which existed well into the Holocene.

After Mount Rainier, Mount Baker is the most heavily glaciated volcano in the United States' part of the Cascade Range (Kennard and Driedger, 1987). Thus, much of the volcano's history involves interaction with snow and ice. The Fraser glaciation (34–11.6 ka), consisting of the Evans Creek, Vashon, and Sumas stades in the Fraser River valley and Puget Lowland, was the last major glaciation in the Pacific Northwest (Armstrong and others, 1965; fig. 1, table 1). Much of the summit edifice (50–10 ka) was constructed just before or during this time (Hildreth and others, 2003; fig. 1). Exotic clasts (that is, non-Mount Baker andesite) in glacial till on the volcano's flanks are diagnostic in distinguishing Vashon stade deposits, when the Cordilleran ice sheet surrounded the volcano, from those of older (Evans Creek) and younger (Sumas) glacial stades, when only alpine glaciers graced the volcano.

During the Evans Creek stade (ca. 30–21 ka; Armstrong and others, 1965), alpine glaciers at Mount Baker were much more extensive than at any time since. An alpine glacier flowing out of the Baker River valley blocked the Skagit River and created Glacial Lake Concrete, which persisted for about 10,000 years. Radiocarbon ages from lake beds of Glacial Lake Concrete provide maximum ages for the arrival of the Cordilleran ice sheet at Mount Baker. Although alpine glaciers remained extensive during Evans Creek time, they appear to have receded up-valley before the arrival of the Cordilleran ice sheet during Vashon time.

As the Cordilleran ice sheet moved into the Skagit River valley during the Vashon stade, it incorporated fine-grained lacustrine deposits from Glacial Lake Concrete (Riedel, 2007). The Cordilleran ice sheet reached the Mount Baker area after 18 ka and surrounded the volcano to an altitude of about 2,000 meters (m) by 16.3 ka; it was largely gone by 14 ka. As the Cordilleran ice sheet retreated, ice and morainal deposits blocked the outlet of the Baker River and created Glacial Lake Baker, which persisted, at decreasing levels, well into the Holocene.

Mount Baker alpine glaciers advanced again at the same time as the Sumas stade (14–11.6 ka) advance of the Cordilleran ice sheet (Armstrong and others, 1965). In contrast to Evans Creek time, glacial advance was limited. Glaciers extended at most a few kilometers beyond present-day glacial limits. Thick (locally >100 m), volcaniclastic assemblages—the Boulder, Pratt, and Sulphur Creek assemblages, and, perhaps, the Rocky Creek sequence—in drainages on the east and south flanks of the volcano overlie Vashon Drift and tills of early Sumas age, and record the final summit eruptions of Mount Baker during the Carmelo Crater eruptive period (fig. 1, table 1). These assemblages include numerous block-and-ash-flow deposits, clay-poor (noncohesive) lahars, hyperconcentrated flows, and rare pumice derived from summit explosions. Sediment from these assemblages washed into Glacial Lake Baker, forming a mixed lacustrine and volcaniclastic facies. During the Carmelo Crater eruptive period, summit eruptions emplaced tephra set SP (ca. 12.7 ka), the oldest known postglacial tephra. Where found, it provides a useful stratigraphic marker for distinguishing latest Pleistocene deposits from Holocene deposits.

The end of the Carmelo Crater eruptive period marks the end of Mount Baker edifice construction and the beginning of mainly destructional processes (flank failures and resultant lahars) during most of the Holocene. It also marks a shift of vent location from the summit to off-summit locations that persists to the present.

The oldest known Holocene eruptions (~9.8 ka) in the Mount Baker area are from a cinder cone located in Schriebers Meadow on the volcano's south flank. Eruptions there produced scoriaceous tephra set SC and the Sulphur Creek lava flow. The lava flow moved downvalley into Glacial Lake Baker, where it invaded lake sediments and stratigraphically underlies older, latest Pleistocene and early Holocene deposits. On the basis of cinder cone eruptions elsewhere (for example, Paricutín; Luhr and Simkin, 1993), the duration of the cinder cone eruption was likely at most a decade or

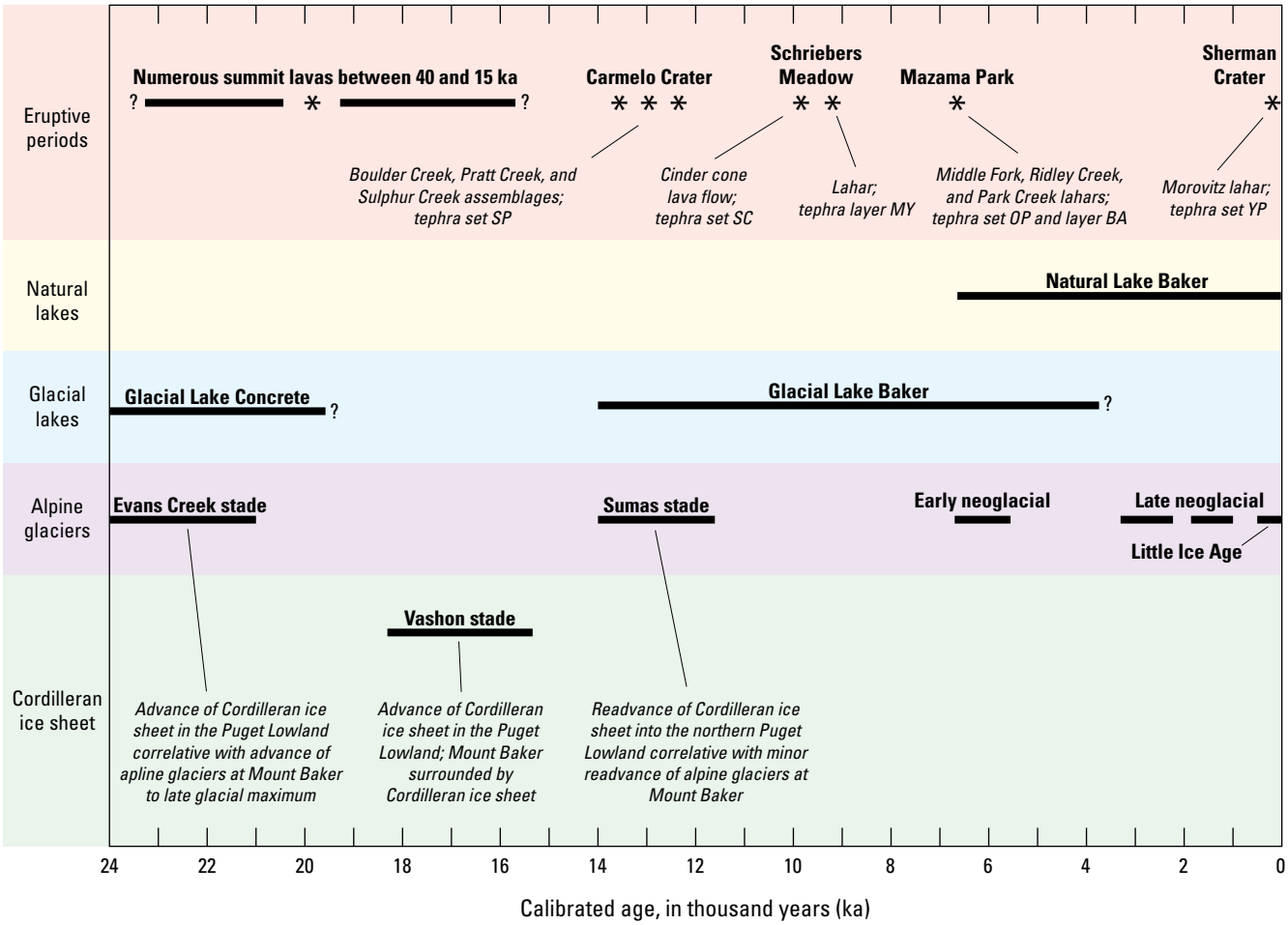

Figure 1. Timeline of major glacial periods, duration of glacial lakes and natural Baker Lake, and eruptive periods at Mount Baker over the past 24 thousand years. Note that we use the geologic-climatic terminology for the glacial periods established by Armstrong and others (1965) because no complementary framework has been established for the northern Cascade Range.

two. We define the Schriebers Meadow eruptive period as beginning with the cinder cone eruption and ending, somewhat arbitrarily, centuries later with two orphan events—the ca. 9.5 ka Schriebers Meadow lahar and decades to centuries later, the younger tephra layer MY—both are from the Mount Baker edifice, although not from the summit (fig. 1, table 1). Both the lahar and tephra fall contain modest amounts of hydrothermally altered material, suggesting that off-summit hydrothermal alteration in the Sherman Crater area had begun by the early Holocene. By the middle Holocene Mazama Park eruptive period (6.7 ka), the shallow hydrothermal system was clearly in place and hydrothermal alteration extensive.

After several millennia of quiescence, the last magmatic and largest Holocene eruptive event at Mount Baker occurred. The ca. 6.7 ka middle Holocene Mazama Park eruptive period began with numerous off-summit (in the vicinity of Sherman Crater) flank failures of hydrothermally altered material that transformed into large clay-rich lahars (Middle Fork, Ridley Creek, and Park Creek lahars), and ended with the most voluminous (0.08 cubic kilometers [km^3] dense rock equivalent) magmatic tephra-fall deposit, layer BA, known in Mount Baker's history. The duration of the eruptive period is unknown, but the major events (flank failures and tephra layer BA) probably occurred over a relatively short time (hours to months to a few years). The farthest traveled lahars were the Middle Fork and Ridley Creek lahars that flowed through the Middle Fork Nooksack River and into the main stem of the Nooksack River. Middle Fork (and probably also Ridley Creek) lahar deposits are found in well logs at Deming, Washington (50 km from source), where the deposit is as much as 15 m thick. During the middle Holocene, the likely flow path of the Nooksack River was northward through the Sumas River valley and across the international border into the Fraser River. At the town of Sumas, Washington, about 75 km from source, a log-rich gravelly layer is seen in well logs above the 7.6 ka Mount Mazama tephra (Cameron, 1989). The log-rich layer is a likely candidate for the Middle Fork lahar, which would extend the flow path another 25 km, or represents extensive post-lahar sedimentation associated with the lahar event. We infer that the flank failures during the Mazama Park eruptive episode were likely triggered by magma intrusion into the edifice that resulted in the emplacement of the phreatic tephra set OP and magmatic tephra layer BA. At the time of the Mazama Park eruptive period, Glacial Lake Baker

Table 1. Summary of postglacial geologic history of Mount Baker illustrated by the events described in this report.

[Named events from this report are in bold. Note that the terminology of the late Pleistocene glacial stades are taken from the Puget Lowland (Armstrong and others, 1965), as a separate framework for the northern Cascade Range has not been developed. ca., circa; ka, thousand years; km, kilometers; m, meters; ft, feet; yr B.P., years before present]

Activity (and age)	Process
Recent activity	
Continuing CO_2 emissions from Sherman Crater (as of 2015)	Phreatic activity from probable stalled magmatic intrusion in the middle 1970s
Increased thermal activity at Sherman Crater (March 1975–76)	Phreatic activity from probable stalled magmatic intrusion in the middle 1970s
Deming Glacier debris flow—Collapse of distal 1.6 km of Deming Glacier (June 1927)	Collapse of stagnant ice; runout as debris flow
Landslide from Lava Divide (1917–32)	Flank collapse; runout as debris avalanche
Rainbow Creek debris avalanche—Landslide from Lava Divide (1889–91)	Flank collapse; runout as debris avalanche and lahar
Sherman Crater eruptive period (1843 to 1880 C.E.)	
Last account of possible incandescent ejecta (1880)	Possible phreatic activity
Younger lahar in Boulder Creek—Reports of forests "swept away" in Boulder Creek (1858[?])	Collapse from Sherman Crater; runout as lahar
Reported ash eruptions from Sherman Crater (1850–54)	Possible phreatic activity
Tree-staining flood of 1856 redated to 1843–50	Entrainment of tephra set YP in runoff to form "bright" stains on trees
Morovitz Creek lahar—Landslide from east side of Sherman Crater (1845–47)	Flank collapse and lahar runout in four drainages
Tephra set YP—Eruption from Sherman Crater	Phreatic eruption
Native American legend flood of 1815	Here eliminated from Skagit River flood history (appendix 7)
Eruption of Mount Baker (ca. 1792–1820)	1792 event ascribed provisionally to Glacier Peak; doubted by some (appendix 5)
Volcanically dormant period (Little Ice Age); debris flows (ca. 6.7 ka to ~1850 C.E.)	
Glacial retreat (ca. 1850)	Retreat of glaciers from late Little Ice Age advance
Advance of Deming Glacier in Middle Fork Nooksack River (430 yr B.P.)	Late Little Ice Age advance
Debris avalanche in Rainbow Creek (ca. 1300 C.E.)	Probable analog of 1889–91 flow
Advance of Deming Glacier (ca. 1 ka)	Advance preceding Little Ice Age
Advance of Deming Glacier (ca. 1.7 and 1.5 ka)	First millennium A.D. advance
Elbow Lake Trailhead debris flow—Probable outburst flood and debris flow (ca. 1.7 ka)	Glacial-outburst flood transformed to debris flow by bulking of alluvium
Lacustrine strata at 131 m (430 ft) altitude in lower Baker River valley; a diminished **Glacial Lake Baker** remained in the lower valley until at least 3.4 ka	Marks the level of Glacial Lake Baker in the middle Holocene
Mazama Park eruptive period (ca. 6.7 ka)	
Older lahar in Boulder Creek—Poorly dated lahar in Boulder Creek	May be correlative and have same origin as Park Creek lahars
Tephra layer BA—Widespread juvenile andesite tephra, largest tephra known from Mount Baker	Magmatic eruption from Sherman Crater; climactic event of eruptive period
Tephra set OP—Lithic tephra dominated by highly altered clasts	Phreatic eruption from Sherman Crater
Ridley Creek lahar—Landslide from west side of Sherman Crater; second largest postglacial lahar at Mount Baker	Flank collapse mobilized to lahar; likely triggered by eruption of tephra set OP
Middle Fork lahar—Landslide from area west of Sherman Crater; largest postglacial lahar at Mount Baker	Flank collapse mobilized to lahar; likely triggered by magmatic intrusion
Park Creek lahars—Landslides from east side of Sherman Crater; third largest postglacial lahar at Mount Baker	Flank collapses mobilized to lahars, the largest of which blocked the upper Baker River valley, creating natural Baker Lake; collapses likely triggered by magmatic intrusion

Table 1. Summary of postglacial geologic history of Mount Baker illustrated by the events described in this report.—Continued

Activity (and age)	Process
Schriebers Meadow eruptive period (ca. 9.8–9.1 ka)	
Tephra layer MY—Lithic hydrothermally altered tephra on south flank of Sherman Crater (ca. 9.1 ka)	Contains highly altered rock from Sherman Crater area; unrelated to Schriebers Meadow cinder cone eruptions
Schriebers Meadow lahar—Landslide from flank of Mount Baker upslope from Schriebers Meadow (ca. 9.5 ka)	Flank collapse of some part of the edifice; mobilized to lahar; triggering mechanism unknown; unrelated to cinder cone eruption
Volcaniclastic lake sedimentation (**facies Vhc, Vu**) following eruption of tephra set SC (ca. 9.6 ka)	Locally deltaic sedimentation into Glacial Lake Baker
Tephra set SC and **Sulphur Creek lava**—Tephra and lava flow(s) from Schriebers Meadow cinder cone (ca. 9.8 ka)	Widespread basaltic tephra; lava flow(s) 8 km down Sulphur Creek and into Glacial Lake Baker; created peperite facies as lava invaded lake sediments
Carmelo Crater eruptive period, Sumas stade (ca. 14–11.6 ka)	
Sustained sedimentation in Glacial Lake Baker (**facies Mhc_1, Mhc_2, Mu**) between 14 and 11.6 ka	Mixed volcaniclastic and lacustrine (volcaniclastic-free) sedimentation
Block-and-ash and lava flows, lahars, their hyperconcentrated runouts and associated fluvial deposits (all post-Vashon [<17 ka] and likely post-Sandy Creek beds [14.1 ka]). At least two of the assemblages overlie till of Sumas age (14–11.6 ka); includes **Boulder, Pratt, Sulphur Creek assemblages**, and possibly the **Rocky Creek sequence**	Thick syneruptive fragmental assemblages on east and southeast flanks likely from collapse of lava flows high on edifice; final additions to Mount Baker edifice; assemblages not correlated; Hildreth and others (2003) have dated summit lava flows of this time period; likely source material for lacustrine facies Mhc_1 and Mu
Moraines of Sumas age in Middle Fork Nooksack River (ca. 12.5 ka), extending <3 km beyond Little Ice Age maximum	Maximum extent of post-Vashon alpine glaciation
Tephra set SP—Juvenile andesite tephra ca. 12.7 ka	Multiple magmatic eruptions of tephra from Carmelo Crater
Sandy Creek beds and **Glacial Lake Baker facies Lsc and Lu**—Volcaniclastic-free sedimentation in Glacial Lake Baker (ca. 14 ka)	Flora-rich sedimentation in Glacial Lake Baker devoid of volcaniclastic material; overlies Vashon till
Vashon stade, Glacial Lake Baker, eruptive activity (ca. 19.5–14.1 ka)	
Cordilleran ice sheet (Vashon) fully retreated from Baker Valley (by 14.1 ka)	Earliest record of Glacial Lake Baker
Cordilleran ice sheet (Vashon) reaches Mount Baker no earlier than 18.2 ka and is at its maximum extent at about 16.3 ka (Troost, 2016)	Cordilleran ice sheet surrounds the volcano to an altitude of 2,000 m
Pre-Cordilleran ice sheet (Vashon) lacustrine deposits dated at 19.5 ka, giving a maximum-limiting age for Cordilleran ice sheet at Mount Baker	Lacustrine deposits from Glacial Lake Concrete; some summit lava flows have age dates within this time period (Hildreth and others, 2003)
Glacial Lake Concrete, Evans Creek stade, and eruptive activity (ca. 29.5–19.5 ka)	
Duration of **Glacial Lake Concrete**	During the Evans Creek stade, alpine glaciers from Mount Baker dammed Skagit River, creating Glacial Lake Concrete, which persisted until at least 19.5 ka; some summit lava flows have age dates within this time period (Hildreth and others, 2003)

occupied only the lower Baker River valley. The Baker River flowed through the upper valley and into Glacial Lake Baker. The largest of the Park Creek lahars blocked the upvalley part of Baker River to create natural Baker Lake, which persisted until the upper valley was dammed in 1959.

A long period of quiescence ensued (6.7 ka to the 19th century) with no known eruptive activity. Glacial Lake Baker persisted until at least 3.5 ka but disappeared sometime between then and when explorers first visited the area in the late 18th to early 19th century (fig. 1). The middle Holocene brought renewed growth of glaciers on Mount Baker, which advanced several times between about 6.8 ka and the middle to end of the 19th century. Little Ice Age moraines (~1350 C.E. to middle 19th century) indicate that it was the most extensive glacier advance during the Holocene.

The historical Sherman Crater eruptive period occurred near the end of the Little Ice Age with the emplacement of the phreatic tephra set YP in 1843 C.E. Historical accounts describe it as resembling a layer of snow (Gibbs, 1873). No juvenile material has been found in tephra set YP deposits.

Within a couple of years, the eastern third of Sherman Crater collapsed, producing a lahar in Boulder Creek, the main drainage from the crater. The lahar was large enough to cross drainage divides and reached the outlet of natural Baker Lake. The impoundment raised lake levels by about 4 m. The lahar deposits are separated from the underlying tephra set YP by a widespread layer of woody debris, indicating that the collapse occurred at least several months after the tephra fall. After these events, eye-witness accounts recorded periods of incandescence and eruption clouds at Mount Baker until about 1880 C.E., after which time such reports ceased. Between 1843 and 1880 C.E., the area was increasingly settled by people who knew Mount Baker to be an active volcano, which lends some credence to the eye-witness accounts. Sherman Crater was reported as ice-filled in 1891 C.E. (C.F. Easton, written commun., 1911–31).

Activity in the late 19th century to present has largely consisted of nonvolcanically triggered flank collapses, debris flows, and floods. In Rainbow Creek, a mobile debris avalanche formed from a collapse of Lava Divide around 1891 C.E. A second Rainbow Creek debris avalanche occurred between 1917 and 1935. Some debris flows have been the result of glacial recession. For example, the stagnant distal 1 km of the Deming Glacier collapsed in July 1927, decades after the end of the Little Ice Age; the resulting flood destroyed a section of a logging railroad.

Significant unrest occurred at Mount Baker in the middle to late 1970s. In 1975, an increase in vapor plumes from Sherman Crater was accompanied by a 10-fold increase in heat flow, increased gas flux (primarily CO_2), and light dustings of lithic ash (Frank and others, 1977); however, these events were not accompanied by significant seismicity or deformation and no magmatic eruption occurred. Increased fumarolic activity continued for several years thereafter, and CO_2 emissions from Sherman Crater remain detectable (Werner and others, 2009). Subsequent research suggests that, in the middle 1970s, magma moved into the edifice but stalled before reaching the surface (Hodge, 2008; Crider and others, 2008, 2011; Werner and others, 2009).

The recent history of Mount Baker has important implications for considering future eruptions. Vent location is of special importance to both style of eruption and areas at risk. The summit of Mount Baker is relatively unaltered, but intensely altered rock exists around Sherman Crater and the Dorr Fumarole Field to thicknesses of greater than 150 m (Finn and others, 2018). Past summit eruptions produced lava flows, some of which collapsed to form pyroclastic flows, clay-poor lahars, and tephra falls. It is difficult to determine the extent of latest Pleistocene lahars and tephra falls because of extensive postglacial reworking; however, an eruption at the summit could potentially affect any flank of the volcano.

There has been no known activity from the summit area in the Holocene. All magmatic and phreatic events have been off summit, either from the cinder cone in Schriebers Meadow or from Sherman Crater, which has funneled material either south or east. Cinder cones are short-lived volcanic features and relatively rare north of Mount Rainier; thus, the likelihood of a future cinder cone eruption is quite low. More likely is renewed activity from Sherman Crater, which is the current location of the most active fumarolic activity and the vent for both the 6.7 ka Mazama Park and historical Sherman Crater eruptive periods. During the 6.7 ka eruption, large collapses of hydrothermally altered material from the Sherman Crater area transformed quickly into far-traveled lahars down south and east drainages. East side lahars reached the Baker River valley—today, similarly sized lahars would flow into the Baker Lake reservoir. On the south side, lahars traveled down the length of the middle fork and main stem of the Nooksack River, which, at 6.7 ka, most likely flowed northward through the Sumas River valley to the Fraser River. Today the Nooksack River flows into Bellingham Bay. However, floods commonly top a low divide near the town of Everson, Wash., causing part of the river flow to inundate the Sumas River valley. Therefore, both the Sumas River valley and lower Nooksack River valley would be at risk from future lahars, hyperconcentrated flows, or post-eruption sediment transport and flooding. The 6.7 ka event culminated in an explosive magmatic eruption that probably lasted several hours and emplaced a couple of centimeters of tephra in a broad swath downwind. The historical Sherman Crater eruptive period was much smaller, but locally devastating. The event consisted of a small-volume hydrothermally altered tephra-fall deposit followed months to years later by a flank collapse that transformed into a lahar that reached the Baker River valley.

Eruptions at Mount Baker have ranged in size, style, and areas affected. Today, as in 1975, any unrest will cause some economic and societal disruption regardless of outcome. On the basis of past events, eruptive activity may cause anything from local damage to a regional disaster for communities on the ground, and minor to moderate disruption for the aviation industry. Mount Baker is not the only variable, however, as to whether the damage will be great or recovery quick—much also depends on society's ability to plan and prepare for the next eruption.

Chapter B

Mount Baker Volcano, Northern Casade Range, Washington

View looking east-southeast of the eroded middle Pleistocene lava flows of Black Buttes (foreground), modern summit cone of Mount Baker (left), and rim of Sherman Crater (right of summit). Peaks of the Mount Baker Wilderness in the background. Photograph by John H. Scurlock, January 24, 2008, used with permission.

Chapter B

Introduction

Mount Baker is the prominent andesitic stratocone that forms the youngest volcanic center in the Mount Baker volcanic field (Hildreth and others, 2003; Hildreth, 2007). Its heavily glaciated cone, rising to 3,286 meters (m) (10,781 feet, ft), is an international landmark, dominating the skyline of Vancouver, British Columbia, even though the volcano is located 25 kilometers (km) south of the international border (fig. 2). Mount Baker caught the attention of scientists and the public alike in 1975–76 during a period of increased steaming, thermal output, and near-vent lithic tephra falls (Frank and others, 1977). Although a magmatic eruption did not ensue, it awoke the populace to the possibility of renewed volcanic activity in the Cascade Range (the first since the 1914–17 eruptions of Lassen Peak, Calif.)—a possibility fulfilled just five short years later with the 1980 eruption of Mount St. Helens in southwest Washington. The 1980 Mount St. Helens eruption, with its dramatic edifice collapse, extraordinary pyroclastic density current, and catastrophic lahars, invigorated the scientific community into studying these then little-known processes. It also highlighted the need to better understand eruptive histories at other Cascade Range volcanoes in order to prepare for future eruptions.

The 1975 unrest also spawned one of the earliest volcano hazard assessments in the Cascade Range, which recognized the rich history of postglacial events at Mount Baker and identified the risk posed by volcanic mudflows, or lahars (Hyde and Crandell, 1978). The focus of this study is to more fully describe the late-glacial to present surficial geology, to better constrain the timing of events (including 19th-century floods), and to dovetail this history with Hildreth and others' (2003) bedrock study.

Geologic Background

Mount Baker is the youngest volcano of a volcanic field that has been active for the past 1.3 million years (Hildreth and others, 2003; Hildreth 2007). The volcanic field is constructed above basement rocks belonging primarily to the Mesozoic and Paleozoic Nooksack Formation and Chilliwack Group

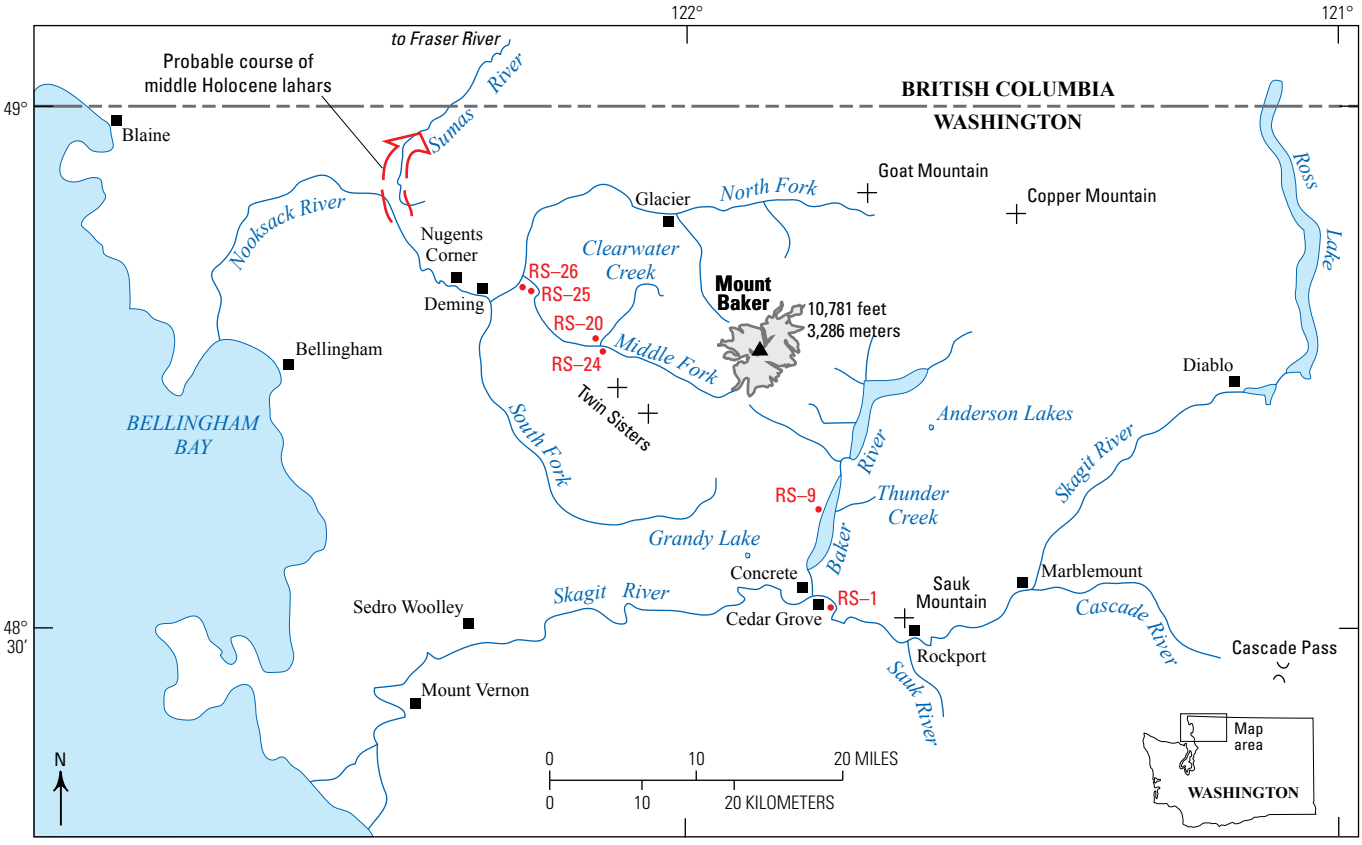

Figure 2. Simplified map of the Mount Baker region in northwestern Washington showing the major river systems and surrounding peaks. Reference sections are marked in red (see also fig. 3). Red arrow in the upper left shows the probable pathway of the large middle Holocene Middle Fork lahar discussed in chapter G.

(Tabor and others, 1989, 2003; Hildreth and others, 2003), which are mostly marine volcanic and associated sedimentary rocks that were accreted to the North American margin. These accreted rocks also crop out in high terrain surrounding the volcano such that clasts of the Nooksack Formation and Chilliwack Group are found on Mount Baker in glacial tills from the Cordilleran ice sheet.

Mount Baker is not only the youngest volcano of the volcanic field, but also one of the youngest stratovolcanoes of the Cascade Range. Hildreth and others (2003) established that most of edifice was built after 50 thousand years ago (ka) and that much of the upper cone is younger than 20 ka, based on high precision K-Ar and $^{40}Ar/^{39}Ar$ dating on some of as many as 200 lava flows dipping outward from the central vent, today marked by ice-filled Carmelo Crater (fig. 3). The edifice is constructed on older rocks of the Mount Baker volcanic field referred to as "pre-Mount Baker." Lavas of the Black Buttes stratocone, the craggy, ice-riven edifice west of Mount Baker (ca. 500–290 ka; Hildreth and others, 2003; fig. 4) is the remnant of a large stratovolcano that occupied approximately the same location as present-day Mount Baker. Other satellite vents that appear contemporaneous with Black Buttes include lava flows of Lava Divide, which separates the Rainbow and Park Creeks, and of Forest Divide, which separates the Sandy and Boulder Creeks (figs. 3, 5; Hildreth and others, 2003). The time period between 290 and 50 ka includes remnants of five lava flows, whose source areas are unknown, as well as several lavas from satellite vents (Hildreth and others, 2003). Activity shifted to a central vent within the gutted Black Buttes stratovolcano after 50 ka and two satellite vents, Schriebers Meadow cinder cone and Sherman Crater (fig. 3), have been the locus of activity during the Holocene.

Although the volcanic field is composed of near-equal amounts of andesite and rhyodacite, the more silicic products are primarily associated with the older part of the field (≥1 Ma; Hildreth and others, 2003). The younger part (<500 ka), which includes Black Buttes and several contemporaneous satellite centers, as well as the present cone of Mount Baker, consists primarily of andesite lava flows and breccias with lesser amounts of dacite and basalt products. Most lava flows are phenocryst rich with plagioclase and either clinopyroxene or orthopyroxene, or both. Olivine and hornblende are less common (Hildreth and others, 2003).

The last edifice construction occurred during the waning stages of the last ice age, about 15–13 ka. Only one known magmatic event has occurred on the edifice during the Holocene. Rather, the Holocene has consisted of numerous flank collapses (some clearly related to volcanic activity, others not) in a 200-degree sector between azimuths N. 30° E. and S. 50° W. (fig. 2). All significant flank collapses have resulted in lahars that have traveled far from their sources.

After Mount Rainier, Mount Baker is the most heavily glaciated volcano in the United States' part of the Cascade Range (Kennard and Driedger, 1987; Brown, 2011), as well as the only one to have experienced both alpine and ice sheet glaciation. Glacial erosion has been so extensive that middle Pleistocene eruptive centers are strongly gutted, and only dikes and occasional remnants remain of early Pleistocene centers (Hildreth and others, 2003). Alpine glaciers and the ice sheet have strongly influenced the distribution of eruptive products and are largely responsible for the paucity of pyroclastic-flow and lahar deposits preserved on and around the edifice.

The west and north flanks of the volcano drain into the Nooksack River system, whereas the south and east flanks drain into the Baker and Skagit River systems. Two hydroelectric reservoirs are on the east to southeast side: Baker Lake (figs. 2, 3, 5) and Lake Shannon. These lakes are impounded by the upper and lower Baker Dams, respectively.

Terminology

We use the Indonesian term lahar to describe a debris flow (>60 percent sediment by volume; Beverage and Culbertson, 1964) that originates at a volcano and apply the term for both flows and their deposits, as used by Crandell (1971) at Mount Rainier and by Hyde and Crandell (1978) at Mount Baker. To emphasize lahar origin and behavior, we differentiate cohesive (clay-rich) flows that contain more than 3–5 percent clay-sized matrix sediment from noncohesive (clay-poor) flows that contain less than 3–5 percent matrix sediment (Scott and others, 1995). As did Crandell (1971), we exclude hyperconcentrated flow (between 20 and 60 percent sediment by volume) under the umbrella of a lahar, although others include it (see Vallance, 2000). Instead, we describe hyperconcentrated flows and their deposits separately. Where a flowage deposit formed by noneruptive processes

Figure 3 (page 9). Simplified map of the Mount Baker area showing the major geographic features, glaciers, rivers, reservoirs, roads, and the outline of Sherman Crater and Carmelo Crater (red hachure). Reference sections (RS) and buried forests (BF) are shown in red. Inset aerial photograph is of the summit region (from 1940) and shows the ice-filled Carmelo Crater, the active vent during the latest Pleistocene (red dashed line shows its bedrock rim and green dashed line shows its tephra rim), and Sherman Crater, the active vent during the Holocene (outlined in black). The crevasse pattern in the inset photograph suggests that the sub-glacial configuration of Carmelo Crater is breached to the north.

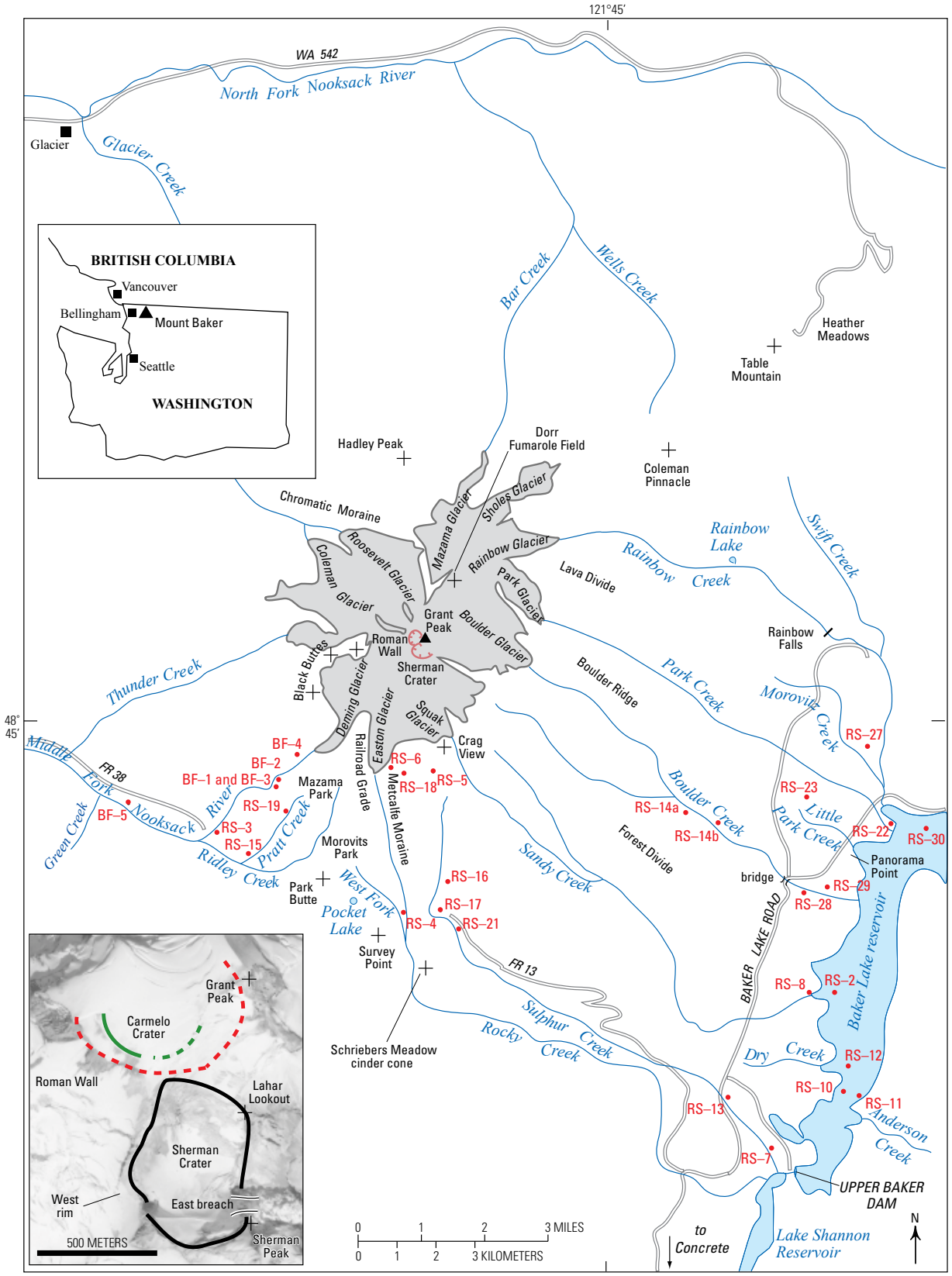
121°45'
WA 542
North Fork Nooksack River
Glacier
Glacier Creek
BRITISH COLUMBIA
Vancouver
Bellingham
Mount Baker
Seattle
WASHINGTON
Bar Creek
Wells Creek
Heather Meadows
Table Mountain
Hadley Peak
Dorr Fumarole Field
Coleman Pinnacle
Chromatic Moraine
Roosevelt Glacier
Coleman Glacier
Mazama Glacier
Sholes Glacier
Rainbow Glacier
Park Glacier
Lava Divide
Rainbow Lake
Rainbow Creek
Swift Creek
Grant Peak
Boulder Glacier
Roman Wall
Sherman Crater
Black Buttes
Deming Glacier
Easton Glacier
Squak Glacier
Crag View
Rainbow Falls
Boulder Ridge
Park Creek
Moraine Creek
Thunder Creek
48° 45'
Middle Fork Nooksack River
FR 38
Green Creek
Ridley Creek
Pratt Creek
Railroad Grade
Metcalfe Moraine
Mazama Park
Morovits Park
Park Butte
West Fork Pocket Lake
Survey Point
Schriebers Meadow cinder cone
Sandy Creek
Forest Divide
Boulder Creek
Little Park Creek
Panorama Point
bridge
BAKER LAKE ROAD
Baker Lake reservoir
FR 13
Sulphur Creek
Rocky Creek
Dry Creek
Anderson Creek
UPPER BAKER DAM
Lake Shannon Reservoir
to Concrete
BF–4
BF–2
BF–1 and BF–3
BF–5
RS–19
RS–3
RS–15
RS–6
RS–18
RS–5
RS–14a
RS–14b
RS–23
RS–27
RS–22
RS–30
RS–29
RS–28
RS–16
RS–17
RS–4
RS–21
RS–8
RS–2
RS–12
RS–10
RS–11
RS–13
RS–7
Grant Peak
Carmelo Crater
Roman Wall
Lahar Lookout
Sherman Crater
West rim
East breach
Sherman Peak
500 METERS
0 1 2 3 MILES
0 1 2 3 KILOMETERS
N

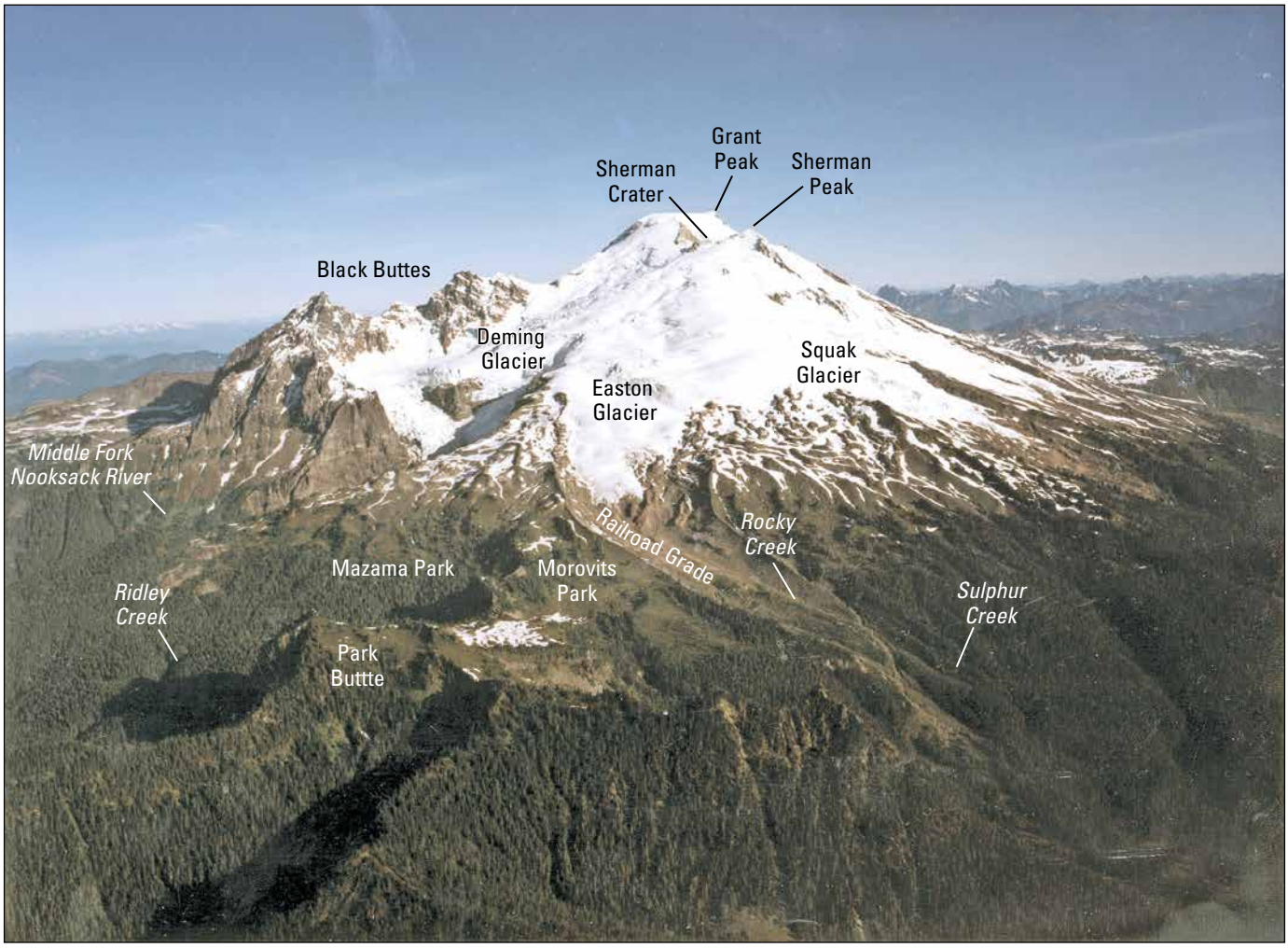

Figure 4. Photograph of Mount Baker from the southeast. To the left are the craggy remnants of Black Buttes, an older stratovolcano (~500–290 thousand years; Hildreth and others, 2003). Grant Peak, the highest point on Mount Baker, is on the southeast rim of Carmelo Crater, the vent from which late Pleistocene cone-building eruptions occurred. Below Grant Peak is Sherman Peak, the highest point on the rim of Sherman Crater and the vent from which middle Holocene and historical eruptive activity occurred. Photograph by A. Post, U.S. Geological Survey.

(for example, rainfall, glacial-outburst flood, stagnant ice failure, and so on), we describe it as a debris flow with the understanding that it could also be categorized as a lahar. We use the modifiers cohesive and noncohesive interchangeably with their more descriptive counterparts, clay-rich and clay-poor.

We describe explosive Holocene eruptions at Mount Baker with equivocal driving forces as phreatic (involving water and heat). We identify no unequivocally phreatomagmatic tephras—that is, those evidenced by the presence of juvenile glass (Heiken and Wohletz, 1985; Morrisey and others, 2000).

In our usage, sector collapses commonly incorporate a volcano's summit and leave a horseshoe-shaped crater, whereas flank collapses do not involve the summit (Scott and others, 2001). Flank collapses are smaller failures than sector collapses.

Where significant, color is described with the Munsell system of terminology based on published rock- and soil-color charts (for example, Geological Society of America, 1995). Where color is not a discriminating characteristic, it is described qualitatively.

We use both volcanologic size terms, in which ash is <2 millimeters (mm), lapilli is 2 to 64 mm, and blocks are >64 mm, as well as sediment (particle) size terms, in which clay is <0.002 mm, silt is 0.002 to 0.0625 mm, sand is 0.0625 to 2.0 mm, granules are 2 to 4 mm, pebbles are 4 to 64 mm, cobbles are 64 to 256 mm, and boulders are >256 mm, to describe tephra and flow deposits. Mud is the total of silt plus clay; gravel consists of all fractions of granule size and coarser. Subdivisions of volcanologic size intervals, in which ash (<2 mm) includes sand-, silt-, and clay-size particles, can be important for interpretations of origin.

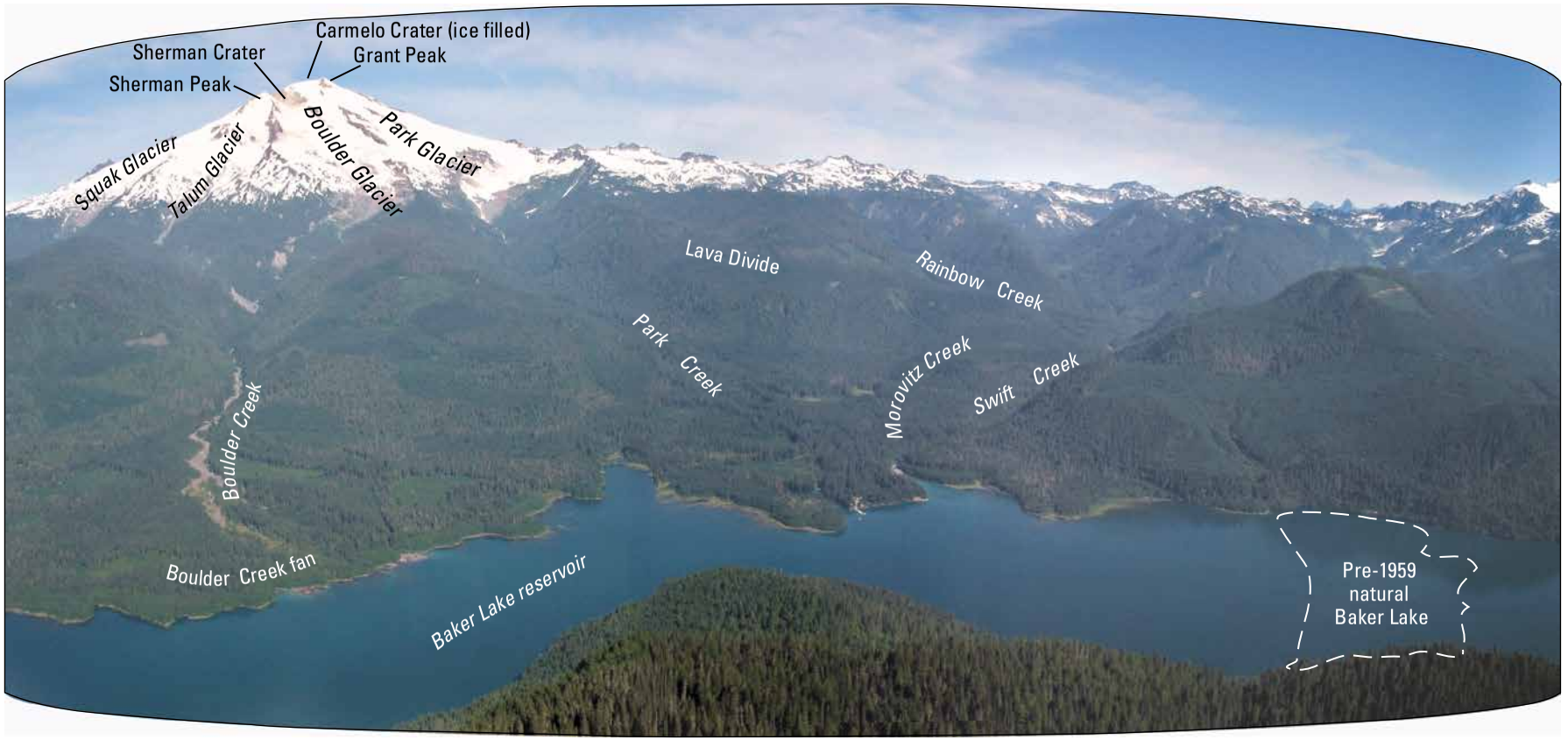

Figure 5. Photograph of the east flank of Mount Baker. In the foreground are the mouths of Boulder, Park, Morovitz, and Swift Creeks, which drain into Baker Lake reservoir. The dashed line shows the extent of "natural" Baker Lake prior to the impoundment of the Baker River in 1959. Lava Divide is the remnant of a pre-Mount Baker edifice (Hildreth and others, 2003), which separates Rainbow Creek to the north from Park Creek to the south. Photograph by K.M. Scott.

Reference Sections and Buried Forests

Key stratigraphic sections, called reference sections, are described in a format that proved effective in D.R. Crandell's classic paper on Mount Rainier (Crandell, 1971), as well as J.E. Beget's postglacial history of Glacier Peak (Beget, 1982). The 30 reference sections are numbered in order of citation (appendix 1). The reference sections record the stratigraphic positions of important radiocarbon samples (see appendixes 2 and 3) and many consist of multiple units that pertain to several chapters. Reference sections located beyond the flanks of Mount Baker are shown in figure 2, those on the flanks are shown in figure 3.

Buried forests are similarly described and included in appendix 1 with the reference sections. Buried forests consist of large concentrations of trees knocked down and buried by lahars or glaciers; they occur at noteworthy geological contacts and date the overlying flow or glacial deposit.

Radiocarbon Dating and Age Conventions

We obtained nearly 80 conventional and accelerator mass spectrometry ages on wood, needles, and charcoal samples. For wood samples, we prefer ages from the outermost rings of logs with bark still in place because they were likely living trees killed by a volcanic or glacial process. Using the outermost rings gives us the greatest confidence that we are sampling the youngest part of the killed tree and that these logs directly date the deposits into which they were incorporated and are not older or younger fragments.

We treat radiocarbon ages as raw data and use calibrated ages in the text to facilitate comparison with argon ages and with results in recently published papers. We report calibrated ages in kilo-annums (ka) (before 1950 C.E.), except those of the past millennium, where we use calendar years (C.E.). We converted radiocarbon ages to 2σ calendar ages using the calibration program OxCal versions 4.2 and 4.3 (Bronk Ramsey, 2001, 2009). Most calibrated ages plot as non-Gaussian, multimodal distributions of probability; thus, even the 2σ range may not contain the correct age. However, reporting all modal distributions becomes unwieldy in a text or table with numerous ages. We show the full range of multimodal distributions in appendix 2. For ease of discussion, we commonly use an approximate age rather than the full 2σ range (for example, 12,949–12,587 calendar years before present [cal. yr B.P.] becomes ca. 12.7 ka). In doing so, we use the modal distribution that we think best represents the range. For dates for which we collected the raw material, we show ranges with two decimal places and an approximation with only one decimal place. Where we cite dates from the literature, we may use only one decimal place or round the date to the nearest thousand and give the citation for the date. Only in the reference (and buried forest) sections do we show the radiocarbon ages (with their uncertainties), as these are the raw data collected at these localities.

A log with bark in the Ridley Creek lahar in upper Rocky Creek produced a calibrated "wiggle-match" age that most accurately defines the age of the middle Holocene Mazama Park eruptive period. Five samples, each comprising several rings from the log's precisely counted ring sequence, were submitted for ^{14}C accelerator mass spectrometry measurements. The technique matches the radiocarbon dates to the "wiggles" of the calibration curve (Bronk Ramsey and others, 2001). The more accurate and precise wiggle-match age statistically narrows the time range in which the event most likely occurred. Because this is a calibrated age, it is not directly correlated to conventional radiocarbon ages.

In appendix 2, most dates are reported with the assumed isotopic fraction ($^{13}C/^{12}C$) value of −25 percent for plant material in the temperate zone. Only some of the most recent ages have the actual ^{13}C correction. The wiggle-match age shows both, but we use the measured ^{13}C correction value as it is the more accurate age.

Dendrochronology

We apply dendrochronology, the dating of deposits from the ages of trees growing on them or from surviving trees buried or scarred by them, to several flow deposits of the 19th-century Sherman Crater eruptive period. Most of our tree-ring ages are based on ring counts of multiple stumps in either clear cuts (logging dates obtained from the U.S. Forest Service) or in areas logged before inundation by Baker Lake reservoir in 1958 and 1959. Pierson (2006) estimates colonization time gap (the time between deposit emplacement and seedling growth to the height sampled by ring counting in stumps or by increment boring) to be 10±7 years for the early-colonizing Douglas fir, *Pseudotsuga menziesii*. We use the colonization time gap to replace the term "ecesis period" because of the latter's many different and conflicting definitions.

Locations and Reference of Geographic Features

Reference sections are located to an estimated accuracy of ±10 m using the Universal Transverse Mercator (UTM) metric grid (North American Datum of 1927, zone 10) shown on U.S. Geological Survey (USGS) topographic maps. These coordinates are given with distance east followed by distance north. Trails shown on topographic maps are commonly incorrectly mapped, have been relocated since the maps were made, or no longer exist. In most cases, UTM grid coordinates were determined from our mapped locations on 7.5′ USGS topographic maps using a transparent overlay grid and, in other

instances, directly from hand-held Global Positioning System (GPS) receivers. To locate reference sections or buried forests, we recommend using the descriptions in the tables, supported by the UTM positions plotted on USGS topographic maps. Although we use the metric system throughout the report, when it comes to specific altitudes of features, we provide the U.S. customary units first, followed by the metric altitude in parentheses, because topographic maps are in feet.

We use names of geographic features (for example, the Chromatic Moraine), as identified on the latest USGS topographic maps, although previous usage may differ. We use spellings by the U.S. Board on Geographic Names as shown on USGS topographic maps (for example, Schriebers Meadow cinder cone, Morovitz Creek lahar) even when those differ from the known surnames of the people commemorated (for example, Schreiber; Morovits, Morvits, or Morvitz). "Morovits Park" is an exception because that name does not appear on any previous map with any spelling, and we use it as shown on figure 4 as submitted by C.F. Easton[4] (written commun., 1911–31) to, but rejected by, the U.S. Geographic Board (modern U.S. Board on Geographic Names). It is a name in common but informal use.

Past and Ongoing Investigations

Serious concern for the potential volcanic hazards of Mount Baker did not begin until the tenfold increase in heat flux and accompanying gas emissions from Sherman Crater in March 1975 (Frank and others, 1977). The reservoirs of Lake Shannon and Baker Lake were completed in 1925 and 1959, respectively, with no concern for volcanic hazards. In response to the 1975 activity, Easterbrook (1975) and Malone and Frank (1975) compiled historical accounts of Mount Baker activity. Also motivated by that activity, Frank and others (1977) analyzed the 20th-century history of heat emission at Sherman Crater and Dorr Fumarole Field, and Frank (1983) reported on hydrothermal activity of the volcano. Frank and others (1975) documented pre-1975 small debris avalanches from the Sherman Crater rim. The first hazard-oriented study based on detailed fieldwork was made by Hyde and Crandell (1978). The most definitive work on the edifice was published by Hildreth and others (2003). Graduate students working under D.J. Easterbrook of Western Washington University have reported on volcanic deposits they encountered while studying glacial deposits on the volcano. Noteworthy contributions cited here include master's theses by Burke (1972), Fuller (1980), Kovanen (1996), and Thomas (1997). More recently, students working under J.G. Crider while she was at Western Washington University (now at University of Washington) have reported on deformation and gravimetry at the volcano, with findings published by Hill and others (2007), Hodge and Crider (2007), and Crider and others (2008). Warren and Watters (2007) studied the strength and stability of altered lavas near Sherman Crater.

The hazard assessment of Hyde and Crandell (1978) was updated by Gardner and others (1995) and is discussed in a USGS Fact Sheet for the public by Scott and others (2000).

Gas emissions and temperatures from the active hydrothermal vents in Sherman Crater have been periodically monitored by the USGS by Symonds and others (2001) and Ingebritsen and others (2014) or with airborne instrumentation by McGee and others (2001). Symonds and others (2003a,b) compared the levels of gas emissions at Sherman Crater with volcanoes elsewhere, and Werner and others (2009) evaluated the long-term record of gas emissions at Mount Baker since the 1975 activity.

Navigating this Report

The report consists of a summary chapter and seven content chapters. Of the seven chapters, five are arranged primarily by geologic process (glacial history, glacial lakes, summit eruptions, tephra, and lahars). Each of these chapters aims to produce evidence regarding the spatial and temporal history of a process at Mount Baker and to provide the foundation for the next process discussed. For example, chapter C on glacial history establishes the foundation for chapter D, glacial lake history. Together these chapters provide the key evidence for the history of the earliest postglacial eruptions, discussed in chapter E. Chapter F focuses on Holocene magmatic events (tephras and lava) and chapter G on the history of lahars and flank failures. Chapter H interprets the data detailed in chapters E–G to define four postglacial eruptive periods and discusses potential hazards from future eruptions of Mount Baker. Nine appendixes follow this report. The first five show data pertinent to this report whereas the others focus on historical accounts of various kinds related to events at the volcano. For example, appendix 8 is a detailed assessment of the 19th-century flood history of the Skagit River and its relation to volcanic events at Mount Baker. In that analysis, we show that the renowned "1815 flood of legend" did not occur.

Many readers may be most interested in a single chapter—for example, glacial history. Consequently, each chapter is designed to be comprehensive with respect to the timing and magnitude of events. The emplacement of the Sulphur Creek lava flow, however, is discussed in both chapter D (glacial lake history) and chapter F (tephras and the Sulphur Creek lava flow).

[4]C.F. Easton (1911–31) compiled a scrapbook of historical accounts and memorabilia collected by the Mount Baker Club titled "Mt. Baker, its trails and legends," which is available in the archives of the Whatcom County Museum of Natural History in Bellingham, Wash. The collection contains items from after 1931, but essentially ends with Easton's death in that year. Much, but not all, of the scrapbook was digitally published as a CD titled "Mount Baker, Stories, Legends, and Exploration" in 1999 by the Whatcom Museum of History and Art in Bellingham. Citations herein are to the manuscript, not the CD.

Chapter C

Mount Baker Volcano, Northern Casade Range, Washington

Terminus of the Coleman Glacier, north flank of Mount Baker. Glaciers on Mount Baker have been important distributors of volcanic deposits, sources of water for far-reaching lahars, and critical to constraining the timing of volcanic events. Photograph by John H. Scurlock, July 20, 2005, used with permission.

Chapter C

Glaciers and Mount Baker

Glaciers grace most of the edifice of Mount Baker (fig. 6). They have been, and will continue to be, important factors in the distribution of volcanic deposits and as sources of water for far-reaching lahars. Additionally, the history of glacial advance and retreat is important to help constrain the timing of volcanic events. In this chapter, we focus on the timing of glacial advance and retreat from the latest Pleistocene through the Holocene to provide a temporal and spatial framework for understanding the timing and distribution of volcanic deposits.

We use the geologic-climatic terminology and ages established by Armstrong and others (1965) for the Fraser River valley and Puget Lowland as our general framework because no complementary framework has been established in the northern part of the Cascade Range. We acknowledge that some of the ages determined by Armstrong and others (1965) are being revised or remain uncertain and that the timing of events in the lowlands may differ from those in the mountains. Regardless, there is some evidence that alpine glacier activity during the late Pleistocene (Sumas stade) was broadly synchronous with that of the Cordilleran ice sheet (Clague and others, 1997; Porter and Swanson, 1998; Osborn and others, 2012; Riedel, 2017).

The last Pleistocene glaciation in the Pacific Northwest is known as the Fraser glaciation, which lasted from approximately 34 to 11.6 ka (Armstrong and others, 1965), and which coincides with the last part of marine isotope stage 3 and all of marine isotope stage 2 (for example, Lisiecki and Raymo, 2005). The Fraser glaciation began with an advance of alpine glaciers to elevations below 100 m above sea level during the Evans Creek stade (ca. 30–21 ka; table 2; Armstrong and others, 1965). Alpine glaciers remained extensive for most of this period before they receded significantly to the flanks of Mount Baker during the Port Moody interstade after about 22.5 ka (Hicock and Lian, 1995; Riedel, 2007, 2017; Riedel and others, 2010). In the Puget Lowland, the glacial maximum occurred around 16.3 ka (Troost, 2016) during the Vashon stade, an event that lagged more than 5,000 years behind the global Last Glacial Maximum at about 21.8 ka (Denton and Hughes, 1981; Porter and Swanson, 1998). During this time, the Cordilleran ice sheet surrounded the volcano to an altitude of 2,000 m but retreated rapidly thereafter from the ridges and valleys around the volcano. After retreating north of 49° N. latitude, the Cordilleran ice sheet made at least two minor re-advances across the Fraser Lowland, regionally known as the

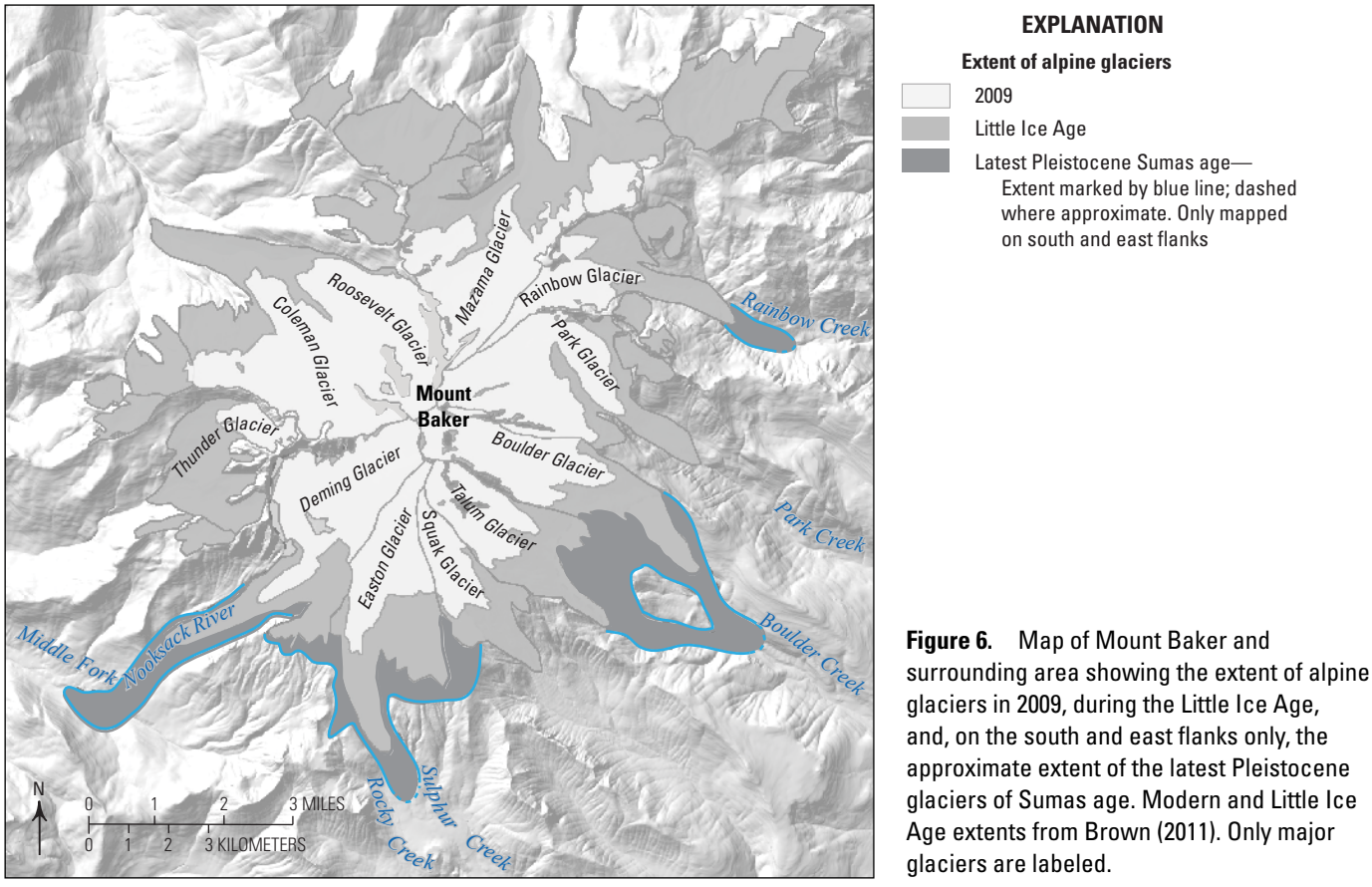

Figure 6. Map of Mount Baker and surrounding area showing the extent of alpine glaciers in 2009, during the Little Ice Age, and, on the south and east flanks only, the approximate extent of the latest Pleistocene glaciers of Sumas age. Modern and Little Ice Age extents from Brown (2011). Only major glaciers are labeled.

Sumas stade (Armstrong and others, 1965) and globally as the Older and Younger Dryas of Europe. Clague and others (1997) limited the age of these advances to before 14–13.5 ka and after 13.3–13 ka. At about the same time, alpine glaciers on Mount Baker underwent a series of minor advances that extended to elevations as low as 1,800 ft (550 m) on Boulder Creek.

Holocene glacial fluctuations are generally ascribed to one of three neoglacial time periods (Porter and Denton, 1967). Recently collected data (Osborn and others, 2012; this report) reveal a complex Holocene glacial record at Mount Baker with possibly four or more cycles of advance and retreat culminating in the Little Ice Age (table 2).

Table 2. Summary of late Pleistocene and Holocene glacial history at Mount Baker.

[Glacial periods as defined by Puget Lowland stratigraphy with pertinent references provided. Age data for the glacial periods are given in years before present (yr B.P.) for radiocarbon ages and thousand years (ka) for calendar ages (OxCal version 4.3; Bronk Ramsey, 2009; Reimer and others, 2013). Mount Baker deposit ages are from this report and given as generalized calendar ages. All ages <1,000 years ago have been calibrated and expressed in years C.E.; see appendixes 2 and 3 for full range data. Descriptions of reference sections (RS) and buried forests (BF) are given in appendix 1. ca., circa; m, meter; km, kilometer]

Glacial period	Mount Baker deposit
Late Holocene	
Little Ice Age, 1350–1900 C.E. (Grove, 1988; Fagan, 2000)	Moraines present in all major drainages. Buried forests include wood beds dated at ca. 1490 C.E. (Osborn and others, 2012) and ca. 1440 C.E. in a moraine of Deming Glacier in the Middle Fork Nooksack River (BF–3). Dates of ca. 1470 C.E. from a log buried beneath till at a site below Easton Glacier (Osborn and others, 2012). Two wood samples near the top of the Coleman Glacier left-lateral moraine gave ages of ca. 1350 and 1380 C.E.
First millennium A.D. advance, 0–1000 C.E. (Reyes and others, 2007)	Log in northwest (right-lateral) moraine of Deming Glacier dated ca. 950 C.E. (BF–4); wood mat at basal unconformity 12 m below the crest of the west (left-lateral) moraine of Coleman Glacier yielded an age of ca. 1100 C.E. (Osborn and others, 2012). Ages of ca. 1.5 ka (BF–1, BF–2) from logs in buried forest in southeast (left-lateral) moraine of Deming Glacier.
Middle Holocene	
Middle neoglacial, 2,960–2,000 yr B.P. (3.2–2 ka) (Porter and Denton, 1967)	Logs buried in till of a right-lateral moraine about 0.5 km below the modern terminus of Deming Glacier yield ages of ca. 2.3 and 2.1 ka (Osborn and others, 2012). About 1.3 km further downvalley, buried logs gave ages of about 3.1 ka (Easterbrook and Donnell, 2007).
Early neoglacial, 6,000–4,600 yr B.P. (6.8–5.3 ka) (Porter and Denton, 1967)	Ages of ca. 6 ka from vegetation mat at base of moraine located about 20 m below the crest of the east (left-lateral) moraine of Easton Glacier (Osborn and others, 2012; RS–6).
Late Pleistocene	
Sumas stade, 11,900–10,000 yr B.P. (14–11.6 ka) (Armstrong and others, 1965)	Moraine complex in the Middle Fork Nooksack River near confluence with Ridley Creek, with ages ranging from 12.7–12.2 ka (RS–3). Moraine near Rocky Creek has charcoal on surface dated at 13.3 ka.
Everson interstade, 13,600–11,900 yr B.P. (16.4–14 ka) (Armstrong and others, 1965)	Sandy Creek beds and other lacustrine deposits of Glacial Lake Baker, including a volcaniclastic facies containing primary and (or) redistributed tephras from Mount Baker; oldest dated lacustrine deposits are ca. 14.1 ka (RS–2)
Vashon stade, 16,333–13,600 yr B.P. (19.6–16.4 ka) (Armstrong and others, 1965; Porter and Swanson, 1998)	Advance of Cordilleran ice sheet in Skagit River (<19.5; RS–1), and withdrawal from flanks of Mount Baker (>14.1 ka; RS–2). At about 16.3 ka (Troost, 2016) the ice sheet surrounds Mount Baker to an altitude of 2,000 m, isolating it in a sea of ice. Ice sheet till contains exotic lithologies and Mount Baker andesite in a blue-gray, clay-rich matrix.
Evans Creek stade, 25,160–17,570 yr B.P. (29.6–21 ka) (Armstrong and others, 1965)	Deposits of alpine glaciers from Mount Baker edifice exposed some valleys. Mount Baker valley alpine glacier blocked Skagit River to form Glacial Lake Concrete (Riedel and others, 2010).

Late Pleistocene Glaciation

Evans Creek Stade

As climate cooled during the Fraser glaciation, glaciers emanating from Mount Baker merged with ice flowing from nonvolcanic terrain to the north and east to form long valley glaciers in the Nooksack and Baker River valleys. The alpine glacier that flowed out of the Baker River valley dammed the Skagit River, forming Glacial Lake Concrete (RS–1, appendix 1; fig 7). Stratigraphic, radiocarbon, and macrofossil evidence from this lake is exposed at several locations on the left bank of the Skagit River near Concrete, Washington. The data show that at least two alpine ice advances occurred between about 30–26.5 and 24–22.5 ka that were separated by a period of glacial recession centered on about 24.2 ka (Riedel, 2007, 2017; Riedel and others, 2010). These ages place the lake deposits within the Evans Creek stade as defined by Crandell and Miller (1974) from the type section at Mount Rainier, and correlate with other similar aged alpine glacier deposits in the region (Riedel and others, 2010). The deposits also show that

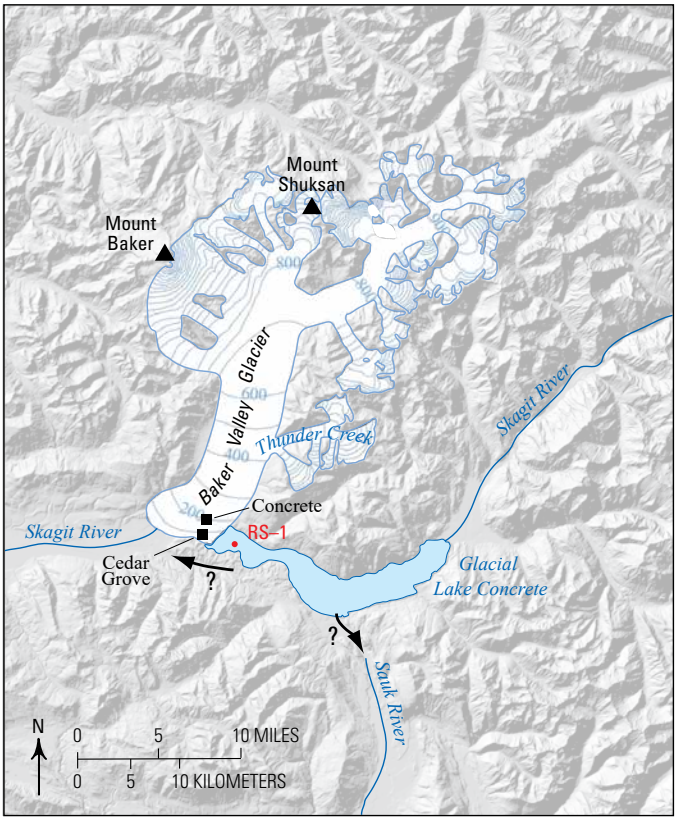

Figure 7. Map showing the extent of Evans Creek glaciation in the Baker River valley. Ice flowing south out of Baker River valley blocked the Skagit River about 29 thousand years ago, creating Glacial Lake Concrete. Arrows mark the two possible outlets for Glacial Lake Concrete. Triangles denote the summits of Mount Baker and nearby Mount Shuksan (formed of Cretaceous greenschist).

the younger advance appears to have been more extensive (figs. 2, 7; Riedel and others, 2010). As the alpine glacier system receded up the Baker River valley sometime after about 22.5 ka (the Port Moody interstade), it left extensive outwash deposits on both sides of the Skagit River valley near Concrete. Lithologies in Evans Creek till and outwash consist primarily of Mount Baker andesite, Shuksan Greenschist, and Chilliwack Group granodiorite in a sandy matrix. The presence of ice-sheet transported erratics at elevations as high as 2,000 m on the flanks of the volcano confirms that alpine glaciers were restricted to the Mount Baker edifice by the time the Cordilleran ice sheet arrived.

Evans Creek deposits are rarely exposed on Mount Baker because they were eroded by the Cordilleran ice sheet or buried by subsequent glacial or volcanic deposits. They and younger alpine till deposits are differentiated from Cordilleran ice sheet till by their matrices and clast lithologies. Mount Baker alpine tills, like many alpine tills in the region, have a sandy matrix owing to glaciers advancing down valleys over their own outwash. Additionally, clasts are from local sources. In contrast, Cordilleran ice sheet tills have a finer grained matrix because, as the ice advanced, it encountered lake deposits formed in valleys during the Evans Creek stade and Port Moody interstade (for example, Glacial Lake Concrete; chapter D). Cordilleran ice sheet tills contain exotic clasts (such as quartzite and metamorphic rocks) in addition to Mount Baker andesite. We infer that a till exposed in lower Pratt Creek (see RS–15, appendix 1) is Evans Creek in age based on (1) the presence of Mount Baker edifice andesite, thereby documenting a late Pleistocene age (the edifice is <50 ka; Hildreth and others, 2003); (2) the absence of erratics transported by the Cordilleran ice sheet; (3) a sandy matrix, and (4) stratigraphic position under inferred Vashon Drift. Based on these criteria, the Evans Creek correlation at Pratt Creek is probable but not proven. Elsewhere in the northern Cascade Range, deposits of what appear to have been alpine glaciation are identified as ice-sheet drift if only small quantities of exotic clasts are present (R.B. Waitt, oral commun., 2004). More detailed study of this section could reveal a few exotic clasts, resulting in its reclassification as a Cordilleran ice sheet deposit.

Vashon Stade

The Cordilleran ice sheet flowed from several directions to surround Mount Baker during the Vashon stade, leaving a complex history of ice flow during advance and retreat (Riedel, 2017). The Puget lobe flowed east up the lower Nooksack and Skagit River valleys (Heller, 1980) and, near the confluence of the Skagit and Sauk Rivers, met a branch of the Okanogan lobe flowing west down Skagit Valley (Riedel, 2011, 2017). The ice sheet ultimately overtopped passes, many summits, and ridges north and east of the volcano and flowed into the headwaters of the Nooksack and Baker River valleys. Glacial striae and erratics record north-to-south flow of ice across divides northeast of Mount Baker in the vicinity

of Coleman Pinnacle and Table Mountain (Ragan, 1961; Heller, 1980; Burrows, 2001; fig. 3). At Cordilleran ice sheet maximum in the Puget Lowland (~16.3 ka; Troost, 2016) the ice sheet encircled Mount Baker, leaving it an island in a sea of ice (fig. 8). Erratics observed as high as 2,000 m on ridges, on low summits, and in mountain passes attest to the ice sheet's surface elevation. Maximum isostatic depression of the area by the 1.5-kilometer-thick Cordilleran ice sheet was about 300 m; most of the recovery occurred in the first few thousand years after deglaciation (Clague and James, 2002).

Reference section 1 (RS–1; appendix 1; figs. 2, 7) provides a near-complete record of the Evans Creek alpine stade and the Vashon ice sheet phase, including the deposition of Cordilleran ice sheet advance outwash and till. Several other key Cordilleran ice sheet units are in the upper half of this section (named the "Big Boy" section after a bull in the terrace above the section)—described in its entirety by Riedel and others (2010)—and at another site located about 2 km downstream at Cedar Grove (fig. 3) on the left bank of the Skagit River. At still another site upstream from RS–1, we obtained an age of 19.94–19.53 ka (appendix 2) on wood in pre-ice-sheet fluvial/lacustrine sediment near the middle of the section. That age is similar to, but slightly younger than, ages we obtained at RS–1. The age represents the youngest maximum limiting date for ice sheet glaciation of the lower Skagit River and Mount Baker. In other words, the Mount Baker edifice could only have been surrounded by the Cordilleran ice sheet after that time. Our age correlates with Porter and Swanson's (1998) age of about 19.7 ka for when the Cordilleran ice sheet crossed the 49th parallel. Using their well-constrained rate of ice advance in the Puget Lowland of 125 meters per year (m/yr), we suggest that Cordilleran ice sheet arrival at the south side of Mount Baker could be no earlier than 18.2 ka.

On the flanks of Mount Baker, Cordilleran ice sheet drift is typically identified by (1) the presence of Mount Baker edifice andesite (confining it to <50 ka); (2) exotic clasts from British Columbia (for example, quartzite) and from downstream sources, such as the Twin Sisters Dunite 15 km southwest of the volcano (figs. 2, 8); (3) glaciolacustrine strata interbedded with till; and (4) a silty, clay-rich matrix. Vashon till lower on the mountain is typically thick and massive with a fine-grained, gray to blue matrix (2.5YR 6/0 to 5PB 5/2; fig. 9). In Sulphur Creek, on the southeast flank of the volcano, however, Cordilleran ice sheet till exposed at two sites near 1,160 m has a sandier than usual matrix, but there it overlies a sandy outwash. It is clearly not an alpine till because it contains granodiorite and nonlocal metamorphic clasts.

Locally, Cordilleran ice sheet drift is overlain by volcaniclastic deposits, by alluvium derived from those deposits, or by lacustrine deposits. As Mount Baker emerged from its isolation by the ice sheet, some of its valleys were blocked by the backwasting ice, creating both small, temporary glacial lakes as well as larger, long-lived lakes, such as the lake in Baker River valley, which we name Glacial Lake Baker even though it persisted long after glacial ice left the valley (Scott and Tucker, 2006). For example, at the mouth

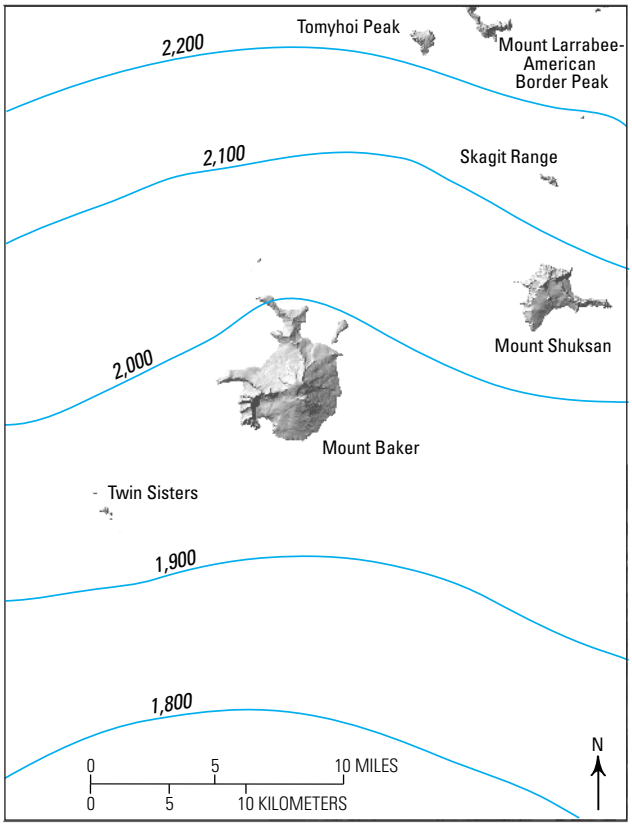

Figure 8. Map showing what Mount Baker (center) would have looked like surrounded by the Cordilleran ice sheet at its maximum extent around 16.3 thousand years ago. Blue lines are ice surface contours in meters. Other major peaks that stood above the ice surface included the Twin Sisters (source of dunite in tills), Mount Shukshan, the Skagit Range, Tomyhoi Peak, and Mount Larrabee-American Border Peak.

Figure 9. Photograph of Cordilleran ice sheet till (Vashon Drift) with typical fine-grained, blue-gray matrix and exotic clasts (right center of photograph) exposed in Baker River valley near the mouth of Sulphur Creek. Penknife for scale. Photograph by D.S. Tucker.

of Sandy Creek (RS–2, appendix 1; fig. 3), glaciolacustrine strata are interbedded with till near the top of the till sequence.

At the mouth of the Baker River valley, the Cordilleran ice sheet constructed a moraine embankment to an altitude of more than 300 m, known locally as Burpee Hills (Booth, 1987; see fig. 13, chapter D). The 135-m-thick moraine embankment extends up the Baker River valley to Thunder Creek (figs. 7, 13) and is composed primarily of stratified advance outwash that coarsens upward and is unconformably overlain by a relatively thin veneer of Vashon till (Riedel, 2011). The U-shaped trough of the Baker River valley, carved out by both alpine glaciers and the Cordilleran ice sheet, would become the basin for Glacial Lake Baker.

Everson Interstade

In the Puget Lowland, 30 km west of Mount Baker, the Everson interstade represents a period of rapid ice sheet retreat and return of marine waters to Puget Sound (Armstrong and others, 1965; Dethier and others, 1995). At the type locality, the interstade occurred after 16.4 ka, based largely on shell dates (Dethier and others, 1995), but the Cordilleran ice sheet maximum is now thought to have been at least 16.3 ka or later (Troost, 2016). In the northern Cascade Range, the timing of this period is not well constrained. Ice sheet deglaciation was rapid between ca. 14.5 and 13.5 ka (Riedel, 2017) and lower Skagit Valley became ice free about 13.8 ka (Dragovich and others, 1997).

At Mount Baker, the first radiocarbon date of ice-free conditions is 14.24–13.95 ka (RS–2; appendixes 1, 2), obtained from lacustrine deposits at the mouth of Sandy Creek (fig. 3). There, Vashon Drift is overlain conformably by the macroflora-fossil-rich Sandy Creek beds of Glacial Lake Baker (unit 2, RS–2). The date indicates that lower Baker River valley was deglaciated before some lowland areas to the west and some mountain valleys, including the Skagit Valley (Riedel, 2017). The ca. 14 ka date is one of only four minimum ages for ice sheet deglaciation in Skagit Valley. Importantly, this and other dates in the lower Skagit Valley suggest that the entire ice sheet phase of glaciation at Mount Baker was less than 3,000 years. The formation of Glacial Lake Baker (chapter D) is the prominent local feature of this period.

A down-wasting ice surface meant that the Cordilleran ice sheet retreated from uplands first, exposing regional hydrologic divides such as the one that separates the Nooksack and Baker River valleys. Exposure of the divides led to the isolation of large ice masses in mountain valleys (Riedel, 2017). The remnant glaciers also retreated by back-wasting up the Baker and Nooksack River valleys, leaving down-valley sloping kame terraces and moraines. In the Baker River valley, a large recessional moraine exists near the mouth of Swift Creek (figs. 3, 5) and gently sloping kame terraces define a south-sloping ice surface draped across the mouth of Thunder Creek on the east side of Baker River valley (figs. 3, 7). Landforms in the Nooksack River valley originally thought to have been left by unusually large alpine glaciers heading on Mount Baker during the later Sumas stage (Kovanen and Easterbrook, 2001), were more likely formed by remnants of the Cordilleran ice sheet, as suggested by the presence of exotic clasts in till and outwash. Frontal retreat of the ice sheet east up Skagit Valley is recorded by a series of lateral moraines and ice-marginal melt-water channels at Hamilton, Concrete, and near the mouth of Illabot Creek, east of Rockport (Riedel, 2017; fig. 2). Retreat of the ice sheet left extensive melt-out till and outwash deposits on the volcano's flanks that were eroded and transported down valleys heading on the volcano. On the southeast side, the flux of sediment from glacial and late Pleistocene eruptive deposits (chapter E) entered Glacial Lake Baker (chapter D) and pinned the later Holocene course of the Baker River against the eastern side of the valley.

Sumas Stade (Older and Younger Dryas)

The Sumas stade was named for the re-advancement of the Cordilleran ice sheet in the Fraser Lowland late in the Fraser glaciation (Armstrong and other, 1965; table 1), and encompasses the Older and Younger Dryas climatic oscillations in the North Atlantic between about 13.8 and 11.6 ka (Stuiver and others, 1995). On the south flank of Mount Baker, the glacial record for this period is represented by alpine moraines and glacial drift observed at multiple sites. A series of four sharp-crested moraines in the valley of the Middle Fork Nooksack River document the advance and retreat of the Deming Glacier in the Sumas stade and represents the most detailed late-glacial record in the region (RS–3, appendix 1; fig. 10). The switchback logging road (U.S. Forest Service Road [FR] 38; fig. 10) crosses the moraines on the north valley-side slope below the confluence of the Middle Fork Nooksack River with Ridley Creek. The first switchback to the right follows the outer edge of the most extensive of these moraines; no post-Vashon-stade alpine glacier extended beyond this terminus. A detailed reconstruction of the Deming Glacier at this time, including its equilibrium line altitude, can be found in Riedel (2007).

Logs in alpine glacier till (unit 3a, RS–3, appendix 1; figs. 3, 10, 11) exposed along the east bank of the Middle Fork Nooksack River yielded four ages between 12.69–12.43 ka and 12.64–12.17 ka. The exposed till correlates with the youngest of the moraines. The ca. 12.5 ka age thus represents a maximum limiting age for the last of the late glacial advances, and a minimum age for the other moraines.

Deposits at RS–3 (appendix 1; figs. 10, 11) have been described by other researchers, who interpreted these deposits differently than we do. Fuller (1980) considered the moraines to be early Little Ice Age, but without direct age control, he acknowledged they could be much older. Kovanen and Easterbrook (2001) dated other logs in RS–3 (unit 3a, appendix 1) and interpreted the overlying diamict (unit 3b, appendix 1) as evidence of extensive alpine glaciers—their Nooksack Alpine Glacial System—during the Younger Dryas (Kovanen and Easterbrook (1996, 2001). Kovanen and

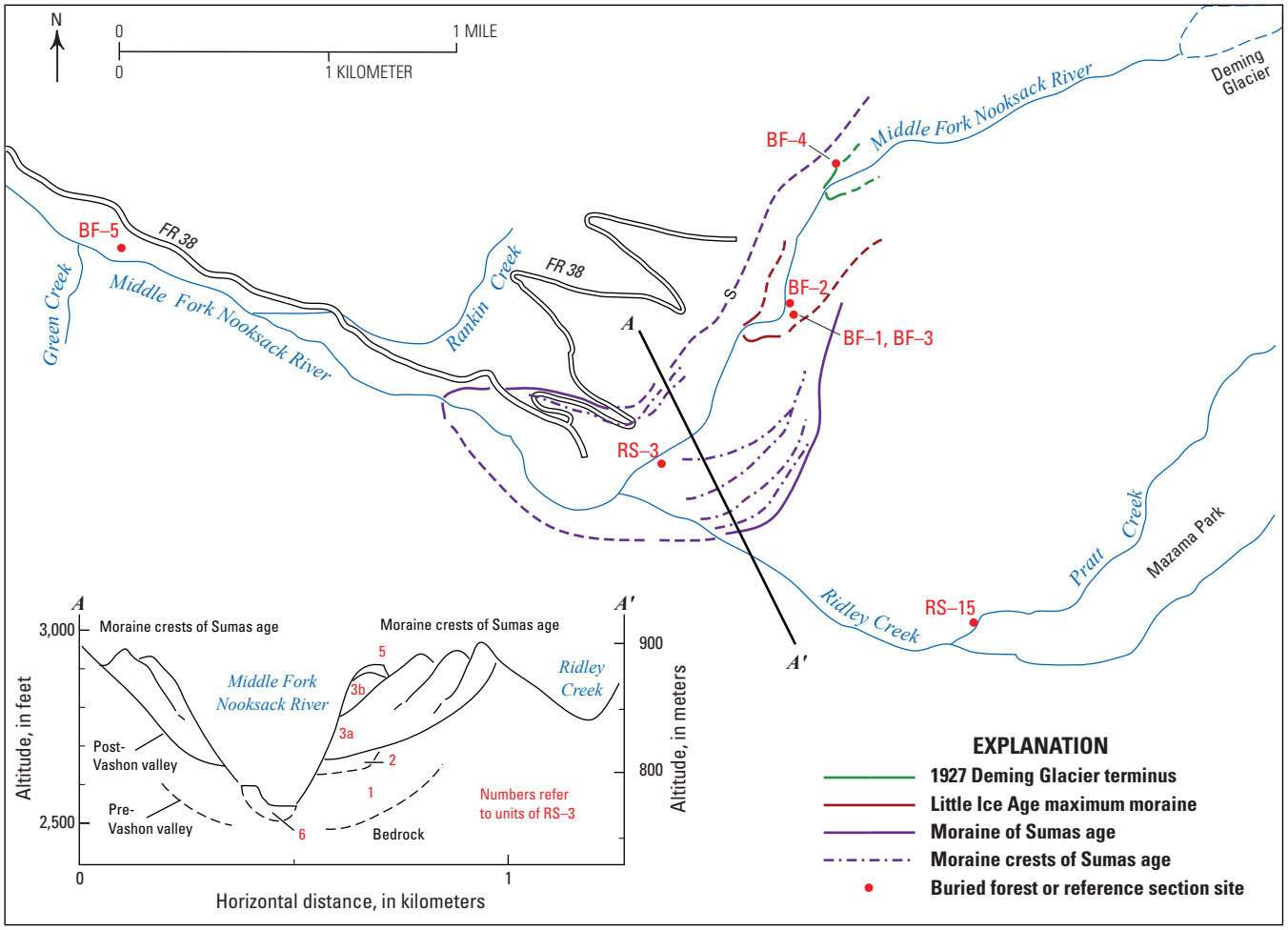

Figure 10. Map showing the extent of moraines of Sumas age (see also Osborn and others, 2012), the maximum extent of Holocene glaciation during the Little Ice Age, and the 1927 terminus of the Deming Glacier. Numbered reference sections and buried forests are marked by red dots (appendix 1). Cross section *A*–*A*′ is shown in the inset. Numbers in the inset refer to units in RS–3 (appendix 1). U.S. Forest Service Road (FR) 38 shown for reference.

Figure 11. Photograph of moraine of Sumas age at RS–3 (unit 3a, appendix 1). The log (at man's waist) yielded an age of 12.64–12.42 thousand years. Photograph by K.M. Scott.

Slaymaker (2005) revisited the area and described part of the section (as noted in RS–3). They suggest that the topography outlined by our purple-dashed line in figure 10 reflects the maximum extent of advance deposits, with presumed glacial limits farther downvalley. In striking contrast with the perfectly preserved moraine crests of Sumas age (fig. 10), we found no deposits or morphology anywhere downstream in the Middle Fork Nooksack River valley that would correlate with more extensive glaciation during the Sumas stade (Kovanen and Easterbrook 2001; Kovanen and Slaymaker; 2005). As stated above, our interpretation of deposits at RS–3 is that they define the maximum extent of alpine glaciers of Sumas age and therefore the maximum extent of post-Vashon alpine glaciation—less than 1.0 km below the confluence of the Middle Fork Nooksack River and Ridley Creek, and less than 3.0 km from the maximum Holocene (Little Ice Age) extent of Deming Glacier (Scott and others, 2003; Osborn and others, 2012). Osborn and others (2012) note that wedge-shaped accumulation zones with small areas above 2,500 m and narrow canyons below 1,700 m did not favor development of exceptionally large alpine glaciers emanating from Mount Baker during the latest Pleistocene. Furthermore, they argue that if there were anomalous late glacial advances on Mount Baker during the Sumas stade, one would expect to see anomalous Little Ice Age advances as well; however, none are seen. Riedel (2017) notes that glacier equilibrium line altitudes during Sumas-stade time were about 200–400 m lower than today, but considerably higher than during the Evans Creek stade when equilibrium line altitudes were 750–1,000 m lower than today. Thus, our, Osborn and others' (2012), and Riedel's (2017) interpretation is that glaciers of Sumas age at Mount Baker were not exceptionally large, consistent with most sites in western North America where such latest moraines are within a few kilometers downvalley of Little Ice Age terminal limits and within about 5 km of current glacial limits (Porter, 1976; Swanson and Porter, 1997; Burrows, 2001; Friele and Clague, 2002; Riedel, 2007, 2017).

Probable alpine moraines and glacial drift of Sumas age were also identified at other sites on the flanks of Mount Baker (fig. 6), but end and lateral moraines are known only in the Middle Fork Nooksack River, Rocky Creek, Boulder Creek, and Rainbow Creek. At Rocky Creek, a sharp-crested ridge on the west (right) bank is composed of diamict with sub-rounded, faceted andesite boulders that is overlain by latest Pleistocene tephra set SP ranging in age between 13.41 and 12.42 ka (RS–4, RS–5, appendixes 1, 2). The older date represents a minimum age for the till and indicates it formed at about the same time that the Cordilleran ice sheet re-advanced into lower Chilliwack River valley (southwestern British Columbia, just north of the map shown in fig. 2) in the early stages of the Sumas stade (Clague and others, 1997). At the same elevation on the opposite side of the valley, there are two sharp-crested moraines that are capped by the early Holocene tephra set SC. The inner end moraine extends about 100 m to the west of the larger lateral moraine and ends abruptly on a younger alluvial surface. The larger, older moraine extends at least 500 m farther upvalley and has a crest that slopes steeply to the south before being truncated by an outwash terrace. Although the precise ages of the moraines are unknown, the presence of the tephra set SC and the close elevation match to the moraine on the other side of Rocky Creek indicates that they represent late-glacial advances of Easton Glacier.

Osborn and others (2012) demonstrated that moraines from Squak Glacier (figs. 3, 6) on the south flank of Mount Baker were covered by early Holocene (ca. 9.8 ka) tephra set SC, and are therefore also likely to be of latest Pleistocene (Sumas stade) age. Others (Thomas and others, 2000; Kovanen and Slaymaker, 2005) have suggested that they may be of early Holocene age, but that interpretation is inconsistent with climatological evidence of relatively warm and dry conditions in western North America during the early Holocene (Whitlock, 1992). Some ridge features previously thought to be early Holocene moraines in this area (Thomas and others, 2000; Kovanen and Slaymaker, 2005) have been reinterpreted as volcanic in origin (Osborn and others, 2012). Latest Pleistocene tephra set SP (ca. 12.8 ka) found in meadows between some of these ridge features (4,850 ft elevation; 1,479 m) indicates that these meadows were not glaciated at the time of tephra set SP fallout nor have they been since, which argues against extensive early Holocene ice. Other moraines of probable Sumas age covered with early Holocene tephra set SC (ca. 9.8 ka) are found west of Railroad Grade (figs. 3, 4) at 5,200 ft elevation (1,585 m) on the south flank of the volcano.

The late Pleistocene advances of alpine glaciers on Mount Baker are broadly correlated with the final advances of the Cordilleran ice sheet across the international border to the northwest (Armstrong and others, 1965; Clague and others, 1997; Easterbrook, 2000; Kovanen, 2001; Kovanen and Easterbrook, 2002; Easterbrook and others, 2007) and with alpine glaciers elsewhere in western North America (Osborn and others, 2012). These include the Crowfoot advance in the Canadian Rockies (Reasoner and others, 1994) and an advance in the Squamish River valley in the southern Coast Mountains of British Columbia (Friele and Clague, 2002). The ages of alpine moraines in the northern Cascade Range east of Mount Baker are poorly constrained, but radiocarbon-limiting dates and ^{10}Be exposure ages at several sites suggest they were deposited during Sumas time (Burrows, 2001; Riedel, 2017).

Holocene Glaciation

Early Holocene

Paleobotanical and geological evidence from throughout western North America indicates that the early Holocene was relatively warm and dry in comparison to today (Whitlock, 1992; Sea and Whitlock, 1995; Bartlein and others, 2011). As Whitlock (1992) states, "the height of postglacial warming in the Pacific Northwest occurred in the early Holocene." We have shown that moraines from Sauk Glacier that were

previously thought to be early Holocene in age have tephra set SC (ca. 9.8 ka) overlying them. The tephra itself does not preclude an early Holocene age, but, coupled with the climatological data, suggests the moraines are more likely latest Pleistocene in age. Additionally, meadows and features interpreted to be early Holocene moraines in the Sulphur Creek drainage (Thomas and others, 2000; Kovanen and Slaymaker, 2005) are overlain by tephra set SP (ca. 12.8 ka) and thus are latest Pleistocene in age. Osborn and others (2012) concluded that during the early Holocene, glaciers on Mount Baker were no more extensive than today.

Middle Holocene

Porter and Denton (1967) originally defined the neoglacial period as an interval of "rebirth or renewed growth, and all subsequent fluctuations of glaciers after the time of maximum Hypsithermal (early Holocene) shrinkage." They identified three phases of glacial resurgence: about 5.3 ka, at 2.8 ka, and within the past 700–800 calendar years. Subsequent work in western North America has moved the beginning of neoglaciation back to about 6.8 ka or possibly earlier (Ryder and Thompson, 1986; Davis and others, 2006, 2009). Recent work near Garibaldi Peak (British Columbia) and on Mount Baker indicates that neoglaciation may have involved more than three episodes of glacier advance (Koch and others, 2007a,b; Osborn and others, 2012).

Radiocarbon ages and the tephras described later in this report constrain the age of an early neoglacial advance on Mount Baker that is correlated with the Garibaldi phase (oldest of the Holocene neoglacial periods) in the Coast Mountains of British Columbia (Ryder and Thompson, 1986). Glacial drift from this advance has been identified in the stratigraphy of the left-lateral moraine of Easton Glacier (RS–6, appendix 1; figs. 3, 6) by Osborn and others (2012). A deformed mat of wood fragments, logs, and peat dated at 6.26–5.91 ka and 6.26–5.89 ka (appendix 3; Osborn and others, 2012) separates two tills. The older till is overlain by early to middle Holocene tephras from Mount Baker, and therefore is likely late Pleistocene in age. The tephras and radiocarbon data provide a maximum age for the younger till. Elsewhere on the volcano, Easterbrook and Burke (1972) dated an advance of the Boulder Glacier sometime after about 6.6 ka. At both the Easton and Boulder Glacier sites, the buried wood was high on the volcanic edifice, indicating that glacial cover in the early Holocene was similar to, if not less than, today.

Forests buried in glacial diamict in lateral moraines in the Middle Fork Nooksack River valley record two advances of the Deming Glacier after 3.2–3.0 ka (Easterbrook and Donnell, 2007) and after 2.2–2.0 ka (Osborn and others, 2012). The later advance is broadly correlative with the Burroughs Mountain Drift on Mount Rainier (Crandell and Miller, 1974) and the Tiedemann advance in the southern Coast Mountains (Ryder and Thompson, 1986). Presumably similar evidence in other valleys on Mount Baker is buried by more extensive later advances or lahar deposits.

Late Holocene—First Millennium A.D.

The late Holocene at Mount Baker is marked by two glacial advances (Osborn and others, 2012). The first of these is known as the "First millennium A.D." advance (Reyes and others, 2007) and the second as the Little Ice Age (table 1). Several ages from logs in buried forests beneath tills in the Middle Fork Nooksack River valley establish an advance of Deming Glacier around 1.5 ka. The ages of these logs are summarized in BF–1 and BF–2 (appendix 1; figs. 3, 10). Together, ages from several sites record a single advance of Deming Glacier over a period of several centuries that was smaller than the subsequent Little Ice Age advance (Osborn and others, 2012).

Late Holocene—Little Ice Age

The most recent significant advance of Mount Baker's glaciers is known globally as the Little Ice Age, which lasted from approximately 1350 to 1900 C.E. (Grove, 1988; Fagan, 2000; table 1). Advance of the Coleman and Deming Glaciers likely began by 1020 C.E. (Osborn and others, 2012), well in advance of the published age for when the Little Ice Age began. Data from the Easton Glacier also support an earlier beginning, because ice had already reached an advanced position at an elevation of about 4,400 ft (ca. 1,340 m), 1.5 km below the modern terminus, by 1370 C.E. Little Ice Age moraines are widespread on Mount Baker and in western North America, and data from most sites confirm that the Little Ice Age was the most extensive glacial advance in the Holocene (Riedel, 1987; Menounos and others, 2009; Osborn and others, 2012). Little Ice Age moraines have been mapped in the valley of Glacier Creek by Heikkinen (1984), in the Middle Fork Nooksack River and Rainbow Creek by Fuller (1980), and in Boulder Creek by Burke (1972). Brown (2011) recently completed mapping the Little Ice Age extent of all glaciers on Mount Baker (fig. 6).

Some of the moraines mapped in the Middle Fork Nooksack River by Fuller (1980) are upstream of, and possibly continuous with, the late Pleistocene moraines shown in figure 10. Fuller (1980) did not recognize the older downstream moraines but did note that a probable upstream extension of at least one of the moraines could be pre-Little Ice Age. Fuller (1980) described the moraines he mapped as pre-13th century (?) and 16th century as having significant soil development. The "soil" in many instances is a deposit of the middle Holocene Middle Fork lahar (see chapter G). The presence of this distinctive lahar deposit on a moraine indicates the moraine is older than the middle Holocene and provides a means of separating moraines of Sumas age (14–11.6 ka; table 2) from those of younger neoglacial period (<6.7 ka) in the Middle Fork Nooksack River drainage.

Ages presented here and by Osborn and others (2012) represent Little Ice Age advances at Mount Baker that are broadly synchronous with those in Garibaldi Provincial Park in Canada (Koch and others, 2007b), the Garda advance at

Mount Rainier (Crandell and Miller, 1974), and at many other sites elsewhere in western North America (Riedel, 2007; Menounos and others, 2009; Osborn and others, 2012).

Chromatic Moraine

The Chromatic Moraine is the large right-lateral Little Ice Age moraine of Roosevelt Glacier (figs. 3, 12). The name (ca. 1900 C.E.) originally described the bi-colored, double crested medial moraine (red and gray) between Roosevelt and Coleman Glaciers and not the moraine that now bears the name (see details in appendix 4). The red debris on modern Coleman Glacier (seen in fig. 12) suggests that it was the source of the original red medial moraine, making Roosevelt Glacier the likely source of the gray medial moraine.

The highest light-colored deposits seen in figure 12 approximate the ice surface of the Roosevelt Glacier sometime after the 1843 C.E. eruption of Sherman Crater that ejected the yellowish-white to pale-yellow tephra set YP (see chapter F). It is not clear if the tephra set YP immediately flowed down the glacier surface to the moraine, or if it was deposited later after glacial transport from a higher elevation.

Modern Glaciers

Glacial cover on Mount Baker is about 35 square kilometers (km^2) (fig. 6), making it the second most heavily glaciated volcano in the United States' part of the Cascade Range, after Mount Rainier (Kennard and Driedger, 1987; Brown, 2011). This area represents a decrease of approximately 30 percent since Little Ice Age maxima. All of the glaciers on Mount Baker are currently receding owing to a strongly negative trend in cumulative balance that began around 1977 (Pelto and Riedel, 2002; Riedel and Larrabee, 2016).

Figure 12. Photograph of present-day Chromatic Moraine, terminus of Roosevelt Glacier, and a tongue of the Coleman Glacier. In the foreground is a rust-colored landslide deposit on Coleman Glacier (rock of similar color is present in parts of the Coleman Glacier headwall). In the early 20th century, the Coleman and Roosevelt Glaciers merged with moraines of two different colors (red and gray). The contrasting colors inspired the original name (see appendix 4), which now only refers to the north lateral moraine of Roosevelt Glacier. Note the difference in height between the level of the upstream-most inset yellow-white tephra set YP deposit and the level of the downstream tephra set YP on Chromatic Moraine. The lower height of the downstream tephra is explained by the presence of an icefall in the middle 19th century that follows the bedrock profile. Photograph by J.H. Scurlock, August 7, 2003, used with permission.

Summary of Latest Pleistocene to Late Holocene Glacial History at Mount Baker

The latest Pleistocene to present glacial history of Mount Baker is summarized in table 2. Below are highlights from the glacial history that pertain to subsequent chapters on glacial lakes and eruptive products.

- The latest Pleistocene Fraser glaciation brought two types of glaciation to Mount Baker: extensive alpine glaciers that flowed from the mountain and inundation by the Cordilleran ice sheet.
- Glacial deposits from the Fraser glaciation and younger are distinguished from older glacial deposits by the presence of andesite from the Mount Baker edifice, which is mainly younger than ca. 50 ka (Hildreth and others, 2003).
- Evans Creek-stade alpine glaciers from Mount Baker merged with ice from upper Baker River valley and flowed into and blocked the Skagit River to form Glacial Lake Concrete. Stratigraphic, geochronologic, and macrofossil data from two exposures of Glacial Lake Concrete beds indicate alpine glaciers remained extensive for most of this period, but receded upvalley to the Mount Baker edifice before arrival of the Cordilleran ice sheet.
- Pre-Vashon stade lacustrine deposits provide a maximum age for the Cordilleran ice sheet of 19.94–19.53 ka. Using a well-constrained rate of ice advance in the Puget Lowland, we estimate that the ice sheet did not arrive at Mount Baker until after 18.2 ka. At its maximum extent at 16.3 ka, the Cordilleran ice sheet surrounded the volcano to an altitude of 2,000 m.
- Ice sheet deglaciation occurred mainly between 14.5 and 13.5 ka (Riedel, 2017). Post-Vashon lacustrine deposits near the mouth of Sandy Creek (RS–2) show that the ice sheet had withdrawn from the Baker River valley by at least 14 ka. The Sandy Creek and lower Skagit River data indicate that the entire Cordilleran ice sheet phase of glaciation of Mount Baker was completed in less than 3,000 years.
- Erosion of its thick ice-advance deposits in the Baker River valley and a back-wasting retreat by the Cordilleran ice sheet in Skagit Valley resulted in the development of Glacial Lake Baker, the prominent local feature of the Everson interstade and a receptacle for late Pleistocene and early Holocene eruptive products. As is discussed in chapter D, Glacial Lake Baker persisted well into the Holocene.
- Near the end of the Fraser glaciation, Mount Baker alpine glaciers advanced a short distance again. In contrast to the earlier Evans Creek stade, glaciers of Sumas age advanced less than 5 km beyond present-day glacier margins. These deposits on Mount Baker conform to the regional age, distribution, and extent of deposits of Sumas age described elsewhere by most previous workers. Like Osborn and others (2012), we find no evidence to support the Kovanen and Easterbrook (1996, 2001) and Kovanen and Slaymaker (2005) hypothesis that alpine glaciers in late glacial and early Holocene times were more extensive at Mount Baker (their Nooksack Alpine Glacial System) than elsewhere in the North American Cordillera.
- The Middle Fork Nooksack River holds one of the most detailed records of latest Pleistocene through Holocene glaciation in western North America.
- The middle Holocene brought renewed growth of the glaciers on Mount Baker, which advanced several times between about 6.8 ka and 100 years ago. Along with data from other valleys, the glacial record on Mount Baker shows that these advances, though separated by several centuries to millennia of recession, were getting bigger. The Little Ice Age was the most extensive advance in the Holocene.
- Glaciers today are about the same size as they were in the early Holocene, as indicated by the presence of buried forests in lateral moraines of Easton and Boulder Glaciers.

Chapter D

Mount Baker Volcano, Northern Casade Range, Washington

View looking east toward the head of Baker Lake reservoir at moderate drawdown level. The fan from Boulder Creek is in the foreground. The reservoir occupies a similar part of the Baker River valley that was once occupied by Glacial Lake Baker. At its maximum extent, Glacial Lake Baker extended eastward 2.8 miles (4.5 kilometers) beyond the current head of Baker Lake reservoir. Photograph by John H. Scurlock, March 2, 2004, used with permission.

Chapter D

Glacial Lakes Concrete and Baker

Lakes formed in the glaciated mountain valleys around Mount Baker by glacial impoundment during and at the end of the last ice age. The two most important of these were Glacial Lake Concrete (Riedel, 2007) and Glacial Lake Baker (Scott and Tucker, 2006). Glacial Lake Concrete was formed during the Evans Creek stade when an alpine glacier advancing south out of the Baker River valley dammed the Skagit River valley. Glacial Lake Baker was formed later during retreat of the Cordilleran ice sheet at the end of the Vashon stade; a lake remnant remained in the Baker River valley well into the Holocene (we call both Glacial Lake Baker). The presence or absence of volcanic detritus in fine-grained sediment deposited in Glacial Lake Baker records periods of volcanic activity and quiescence at Mount Baker and its satellite vent, the Schriebers Meadow cinder cone. An important feature in the Glacial Lake Baker record is the subaqueous invasion of lacustrine sediment by the early Holocene Sulphur Creek lava flow erupted from the Schriebers Meadow cinder cone. A peperite carapace (defined as a clastic rock formed by disintegration of magma intruding and mingling with unconsolidated or poorly consolidated wet sediment [White and others, 2000; Skilling and others, 2002]) formed on the invading lava flow, which can be confused with a volcaniclastic breccia, an interpretation that would lead to an erroneous conclusion about eruption history. Tucker and Scott (2009) described the structures and facies associated with the peperite sill; here we focus on the interaction of the lava with Glacial Lake Baker sediments.

Glacial Lake Concrete

Glacial Lake Concrete formed when an alpine valley glacier flowed out of the Baker River valley and blocked the Skagit River near the present town of Concrete (figs. 2, 7) at about 29 ka (Riedel and others, 2010). The lake drained via two possible stable outlets (the Sauk or Skagit River valleys; fig. 7), and therefore did not undergo dump-and-fill cycles common with some ice-dammed lakes. This configuration allowed the lake to persist for at least 9,000 years (~29–20 ka) and to record the environmental history of the early Fraser glaciation. Lake deposits are exposed at a few sites along the Skagit River in the reach upstream and downstream from Concrete. Massive accumulations of outwash from Baker River valley filled the western end of Glacial Lake Concrete and are exposed along both sides of the Skagit River south and east of Concrete. At Cedar Grove (figs. 2, 7), alpine glacial deposits contain abundant clasts of Mount Baker andesite of unknown age.

It is unclear when Glacial Lake Concrete ceased to exist. It likely remained for some time after the alpine valley glacier retreated, but the upper part of lacustrine section at RS–1 (Big Boy) was removed by Cordilleran ice sheet erosion as evidenced by an unconformity between units 6 and 7 (see Riedel and others, 2010). In the middle part of the Big Boy section (RS–1, unit 6), we obtained an age of 20.03–19.57 ka (appendix 1); thus, this age represents a maximum date for the disappearance of Glacial Lake Concrete.

Glacial Lake Baker

Sometime after the local glacial maximum around 16.3 ka (Troost, 2016), the Cordilleran ice sheet began withdrawing from the area. Evidence summarized in chapter C indicates that the ice sheet withdrew as a back-wasting ice margin up Skagit and Baker River valleys. As ice retreated, Glacial Lake Baker formed in lower Baker River valley and drained through the Tyee spillway (fig. 13). The spillway followed a meandering, low-gradient course across Cordilleran ice sheet deposits (locally known as Burpee Hills) before dropping steeply into Skagit Valley along lower Grandy Creek, where it entered a marine embayment in lower Skagit Valley and left behind a coarse-grained delta (Riedel, 2011). As ice continued to retreat in the upper Baker River valley, lake levels dropped and the Tyee spillway was abandoned.

Deposits at RS–2 near the mouth of Sandy Creek (appendix 1; fig. 13) record the transition from Cordilleran ice sheet drift, with isolated granitoid boulders, to silt- and clay-rich, laminated, lacustrine beds (fig. 14; table 3). Plant macrofossils from the beds, which are probably correlative with the strata described in drill logs as varved clays by Stearns and Coombs (1959), include abundant alder leaves (*Alnus* sp.), conifer cones, and charcoal. A lodgepole pinecone and a piece of charcoal yield dates of 14.24–13.95 and 13.76–13.55 ka, respectively. The early Holocene eruption of the Schriebers Meadow cinder cone (ca. 9.8 ka) deposited a thick tephra blanket that washed into Glacial Lake Baker. Deltaic top-set beds containing reworked Schriebers Meadow tephra in downstream reaches of Sulphur Creek at RS–7 and near the mouth of Sandy Creek (RS–8, appendix 1; figs. 2, 15, 16) occur at an elevation of approximately 797 ft (243 m), indicating that the level of Glacial Lake Baker remained high nearly 4,000 years after these early lacustrine beds were deposited (table 3; fig. 16).

As the ice sheet retreated east up Skagit Valley, a new outlet opened for the lake to drain into the Skagit River at the present location of Lower Baker Dam near the town of

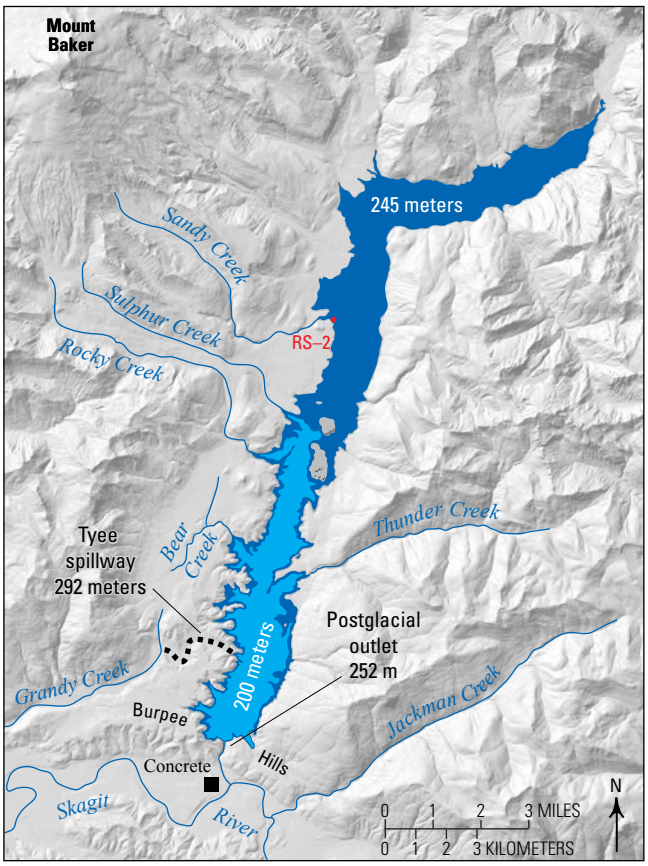

Figure 13. Map showing the latest Pleistocene and middle Holocene extent of Glacial Lake Baker. As the Cordilleran ice sheet retreated into Baker River headwaters, the lower valley was partly ice free and meltwater drained through the Tyee spillway (292 meters [m], 890 feet [ft]: Riedel, 2011) into Grandy Creek. As the ice retreated upvalley, lake levels lowered and the Tyee spillway was abandoned with a new outlet draining southward through the Burpee Hills into the Skagit River valley. Two lake levels are shown. The maximum pool level of 245 m (800 ft) is in dark blue and marks when the entire valley was ice free circa (ca.) 14.0 thousand years ago (ka). During the Holocene, lake levels began to drop as the outlet was incised such that by the middle Holocene (ca. 6.7 ka) the lake existed only in the lower valley at an estimated height of ca. 200 m (<722 ft), shown in light blue. By 3.4 ka, the lake level had further declined to about 128 m (420 ft; table 3). When early European explorers reached the lower Baker River valley in the middle 19th century, no lake existed.

Figure 14. Photograph of Sandy Creek beds at RS–2 (unit 2), showing rhythmites with abundant macroflora fossils that overlie Vashon Drift. Section RS–2 was buried by flood deposits in 2003. Penny for scale. Photograph by K.M. Scott.

Figure 15. Photograph of a deltaic sequence overlying lava in Sulphur Creek at RS–7 (appendix 1; fig. 3). View is of the left valley-side slope (looking upstream), where cross-strata is inclined 30–36° below subhorizontal gravel topset beds. The deltaic sediment represents infilling of Glacial Lake Baker by streams after emplacement of the early Holocene Sulphur Creek lava flow. Photograph by D.S. Tucker.

Table 3. Glacial Lake Baker and its Holocene levels through time as constrained by reference sections (RS) and calibrated radiocarbon dates in lake sediment.

Calibrated age, in thousand years (ka)	Lake level altitude, in meters (feet)	Evidence
~3.4	>128 (>420)	Highest layer in lacustrine section on west bank of Lake Shannon reservoir near Bear Creek (RS–9)
~6.7	<220 (<722)	Subaerially deposited Park Creek lahar; exposed on right bank Swift Creek below modern Baker Lake reservoir full pool level (RS–22)
~7.6	>213 (>700)	Level of crossbedded and ripple cross-laminated lake sediment interstratified with redeposited strata of tephra layer O (RS–10, RS–12)
Post-9.8	>232–235 (>760–770)	Highest deltaic deposits overlying Sulphur Creek lava flow in Sulphur Creek (RS–7) and containing lava flow clasts. Mega-crossbedding records deposition in Glacial Lake Baker
Post-9.8	>235 (>770)	Top of lacustrine terrace containing tephra set SC in Sandy Creek (RS–8)
~14.0	>244–247 (>800–810)	Highest deltaic deposits in Sandy, Park, and lower Swift Creeks. Date is that of earliest lake deposits overlying Vashon till (RS–2)
Post-Vashon	252 (825)	Approximate height of ice sheet moraine (Burpee Hills) at lower Lake Shannon dam outlet
Post-Vashon	292 (890)	Elevation of the Tyee spillway; age of use unknown, but likely before 14 ka

Concrete (fig. 13). By 6.7 ka, the lake's elevation had dropped below 220 m (<722 ft) and the Baker River valley above Sulphur Creek was lake free as indicated by the subaerial deposition of the Park Creek lahar (table 3, fig. 16; see chapter G).

As Glacial Lake Baker drained into Skagit River via its southern outlet, its channel incised through about 100 m (330 ft) of glacial drift comprising the Burpee Hills (fig. 13) before drainage incision was slowed by bedrock (the present site of Lower Baker Dam) at 137 m (450 ft). Outlet erosion limited by bedrock allowed the lake to persist into the late Holocene, as confirmed by the 3.55–3.36 ka age of lacustrine deposits at RS–9 (appendixes 1, 2, 3; figs. 2, 16; table 3). The exact timing of the demise of Glacial Lake Baker is unknown; however, no lake existed in lower Baker River valley when European explorers visited the area in the early 19th century (appendix 7).

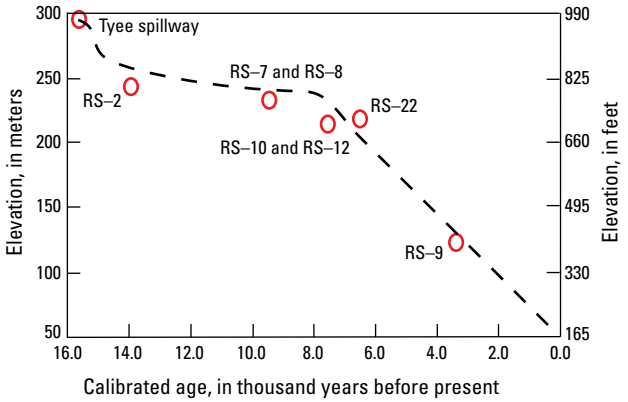

Figure 16. Plot of Glacial Lake Baker surface-level history from the latest Pleistocene through today. Glacial Lake Baker disappeared sometime after 3 thousand years ago. Reference section units constrain lake levels at certain periods in time. The dramatic decrease in lake level from Tyee spillway to RS–2 reflects rapid melting of the Cordilleran ice sheet in the upper Baker River valley, which allowed broadening of the lake area. Note current elevation (time 0) of 55 meters (m) (180 feet [ft]), which is the elevation of the outlet channel below the Lower Baker Dam that impounds Lake Shannon. Full pool heights of the Baker Lake and Lake Shannon reservoirs are about 221 m (725 ft) and 134 m (440 ft), respectively. See appendix 1 (reference sections) and table 3 (lake-level heights) for more details.

Stratigraphy of Glacial Lake Baker Deposits

Lacustrine deposits in Glacial Lake Baker are interbedded with volcaniclastic sediment and lava from Mount Baker and its satellite vent, the Schriebers Meadow cinder cone, produced during late Pleistocene to early Holocene eruptions. The sedimentary lake record therefore provides age control for these events. Three facies are distinguished in the deposits of Glacial Lake Baker.

Lacustrine, Lsc (Sandy Creek) or Lu (undifferentiated).—Facies overlies Vashon Drift (figs. 14, 17, 18) and consists of blue-gray (5PB 5/2, wet) clay with a minor silt-size component and without detectable volcaniclastic material. We interpret it as a period without significant volcanism when runoff into the lake was dominated by glacial meltwater. The facies are rhythmically bedded at the type section at the mouth of Sandy Creek (RS–2, appendix 1; figs. 3, 14, 17, 18). The facies also may be massive. At Horseshoe Cove (RS–10, appendix 1; figs. 3, 17, 18), the clayey matrix of the peperitic carapace is assumed to be facies Lu that partly fluidized and adhered to the rubbly top of the invading lava flow. In addition, we infer on the basis of texture (that is, fine-grained lake sediments devoid of volcaniclastic material but containing plant material) that rip-up clasts at the base of facies Mhc_1 (mixed facies, Horseshoe Cove; figs. 17, 18) are also derived from facies Lu.

At its type locality at the mouth of Sandy Creek (RS–2, appendix 1), the Lsc facies is 1.7 m thick and consists of clay-rich sediment eroded from Vashon Drift exposed during deglaciation and conformably overlies clay-rich, blue-gray Cordilleran ice sheet lodgment till (figs. 14, 17, 18). At approximately 14 ka, the facies represents the oldest known deposits of Glacial Lake Baker. At RS–2, the facies is overlain by volcaniclastic facies Vu from the early Holocene eruption of the Schriebers Meadow cinder cone.

Volcaniclastic, Vhc (Horseshoe Cove) or Vu (undifferentiated).—Facies consists of gray (10YR 5/1) to black (10YR 2/1) fluvial deposits from the early Holocene eruption of the Schriebers Meadow cinder cone (see chapter F). Deposits consist of sand-size grains of reworked scoriaceous tephra (set SC) or basaltic lava fragments from the Sulphur Creek lava flow (fig. 18). They are typically well stratified and locally contain graded, turbidite-like strata inferred to record pulses of flood sedimentation. Locally, where tephra particles

Figure 17 (page 31). Map of modern reservoirs in Baker River valley and simplified stratigraphic columns at select reference sections. Also shown are the inferred peak level of Glacial Lake Baker ~800 feet (~244 meters) when the Sulphur Creek lava flow entered the lake and locally invaded lacustrine deposits about 9.8 thousand years (ka) ago and the lake level at 3.4 ka when the lake was restricted to the lower valley. Reference sections are compiled in appendix 1 where there is a more complete explanation of units and corresponding ages. Note that at RS–12 (Dry Creek) we show two examples of the stratigraphy along a 240-meter exposure (from mouth of Dry Creek and south) with lateral variation. Radiocarbon ages (in ka) are calibrated and designated without corresponding range. Tephra layer O (RS–10, RS–12) is ash from the 7.6 ka eruption of Mount Mazama (Crater Lake) in Oregon. ca., circa.

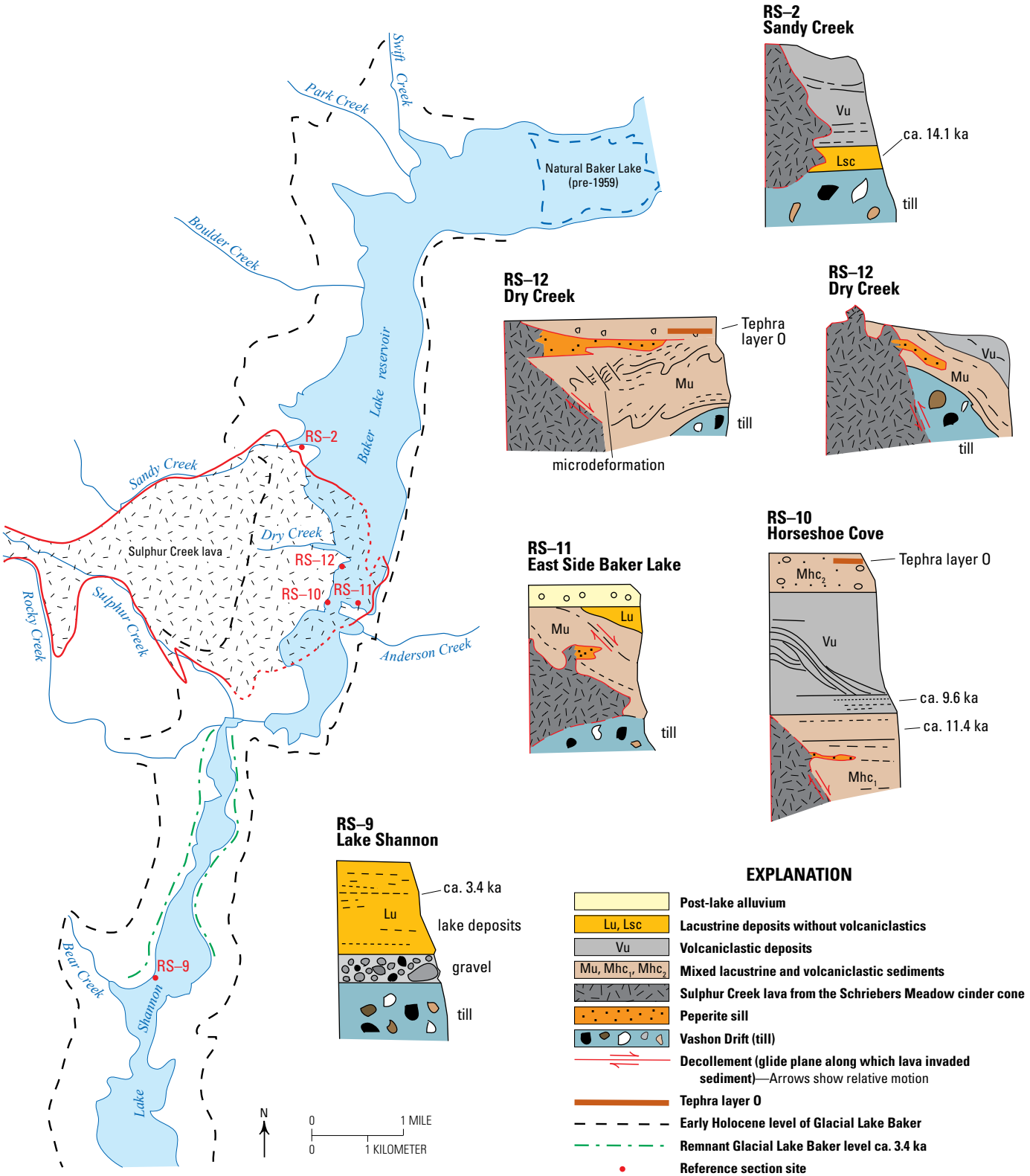
Swift Creek
Park Creek
Natural Baker Lake (pre-1959)
Boulder Creek
Baker Lake reservoir
RS–2
Sandy Creek
Dry Creek
Sulphur Creek lava
RS–12
RS–10
RS–11
Rocky Creek
Sulphur Creek
Anderson Creek
Bear Creek
RS–9
Shannon Lake
N
0 1 MILE
0 1 KILOMETER
RS–2
Sandy Creek
Vu
ca. 14.1 ka
Lsc
till
RS–12
Dry Creek
Tephra layer O
Mu
till
microdeformation
RS–12
Dry Creek
Vu
Mu
till
RS–11
East Side Baker Lake
Lu
Mu
till
RS–10
Horseshoe Cove
Tephra layer O
Mhc2
Vu
ca. 9.6 ka
ca. 11.4 ka
Mhc1
RS–9
Lake Shannon
ca. 3.4 ka
Lu
lake deposits
gravel
till
EXPLANATION
Post-lake alluvium
Lu, Lsc
Lacustrine deposits without volcaniclastics
Vu
Volcaniclastic deposits
Mu, Mhc1, Mhc2
Mixed lacustrine and volcaniclastic sediments
Sulphur Creek lava from the Schriebers Meadow cinder cone
Peperite sill
Vashon Drift (till)
Decollement (glide plane along which lava invaded sediment)—Arrows show relative motion
Tephra layer O
Early Holocene level of Glacial Lake Baker
Remnant Glacial Lake Baker level ca. 3.4 ka
Reference section site

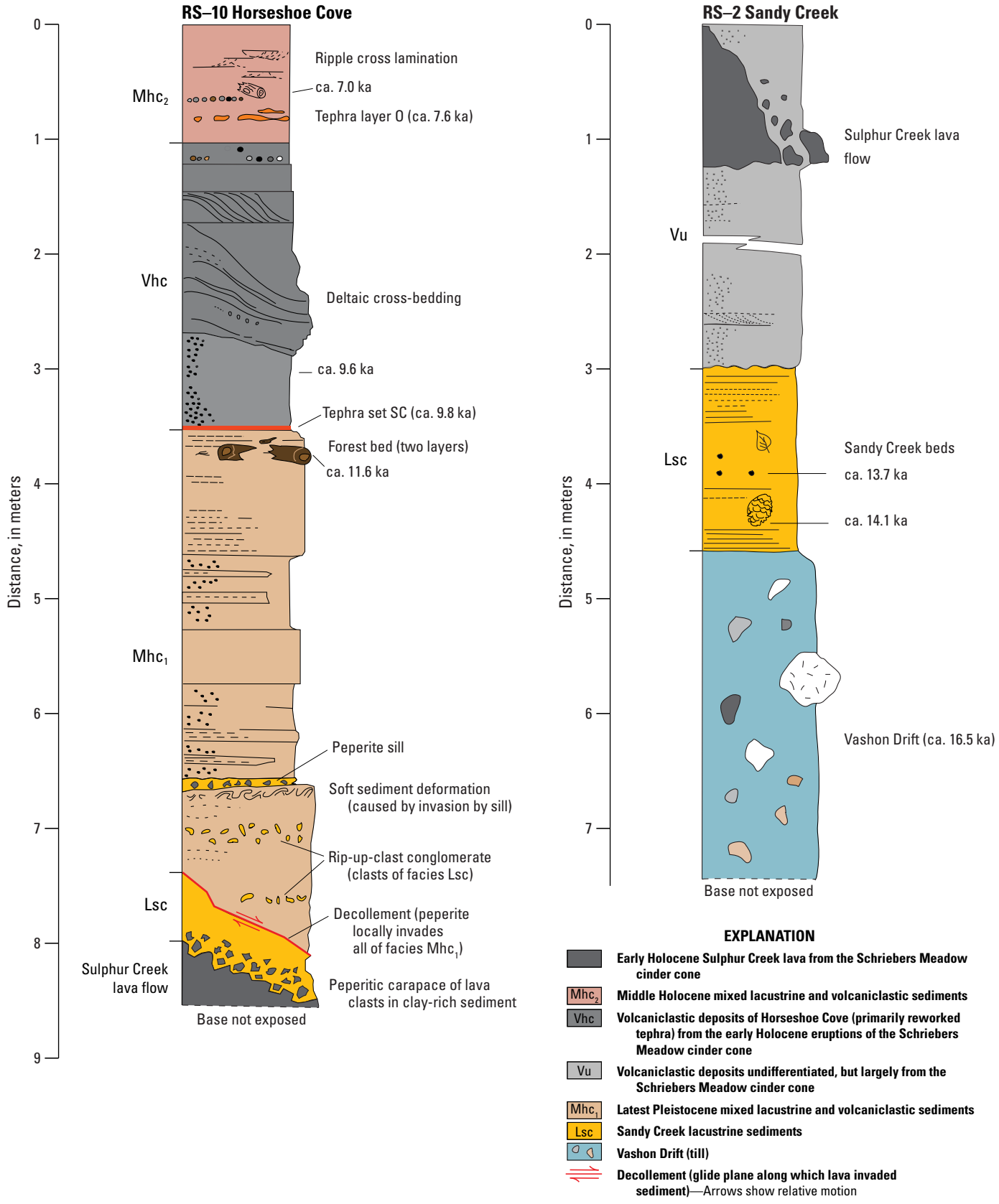
RS–10 Horseshoe Cove
RS–2 Sandy Creek
Distance, in meters
0
1
2
3
4
5
6
7
8
9
Mhc2
Vhc
Mhc1
Lsc
Sulphur Creek lava flow
Ripple cross lamination
ca. 7.0 ka
Tephra layer O (ca. 7.6 ka)
Deltaic cross-bedding
ca. 9.6 ka
Tephra set SC (ca. 9.8 ka)
Forest bed (two layers)
ca. 11.6 ka
Peperite sill
Soft sediment deformation (caused by invasion by sill)
Rip-up-clast conglomerate (clasts of facies Lsc)
Decollement (peperite locally invades all of facies Mhc1)
Peperitic carapace of lava clasts in clay-rich sediment
Base not exposed
Vu
Sulphur Creek lava flow
Sandy Creek beds
ca. 13.7 ka
ca. 14.1 ka
Vashon Drift (ca. 16.5 ka)
Base not exposed
EXPLANATION
Early Holocene Sulphur Creek lava from the Schriebers Meadow cinder cone
Mhc2 Middle Holocene mixed lacustrine and volcaniclastic sediments
Vhc Volcaniclastic deposits of Horseshoe Cove (primarily reworked tephra) from the early Holocene eruptions of the Schriebers Meadow cinder cone
Vu Volcaniclastic deposits undifferentiated, but largely from the Schriebers Meadow cinder cone
Mhc1 Latest Pleistocene mixed lacustrine and volcaniclastic sediments
Lsc Sandy Creek lacustrine sediments
Vashon Drift (till)
Decollement (glide plane along which lava invaded sediment)—Arrows show relative motion

Figure 18 (page 32). Stratigraphic columns of reference sections in Horseshoe Cove (RS–10) and Sandy Creek (RS–2). The detailed composite Horseshoe Cove section shows the invasion of the early Holocene Sulphur Creek lava flow into latest Pleistocene lacustrine (Lsc) and mixed volcaniclastic and lacustrine (Mhc_1) facies. Clasts from the lava flow are surrounded by lake sediment to form a peperite carapace above the lava flow whereas a peperite sill invaded facies Mhc_1. At RS–2 in Sandy Creek, lacustrine deposits (Lsc) overlie Vashon Drift and contain organic material that can be correlated to other lacustrine sections (Lu) around the lake. ca., circa.

are oxidized, deposits are tan to yellow in color. Large-scale crossbeds represent deltaic sedimentation into Glacial Lake Baker (RS–7, RS–10; appendix 1). Facies Vhc at Horseshoe Cove (fig. 18) is as much as 5-m thick and records the influx of sediment from both Sulphur and Sandy Creeks. Charcoal, about a meter above the base of the facies, yielded a date of 9.69–9.54 ka (RS–10; appendixes 1, 2, 3), slightly younger than dates on the primary tephra fall deposits (see chapter F).

Mixed, Mhc_1 and Mhc_2 (Horseshoe Cove) or Mu (undifferentiated).—Facies is composed of interbedded units of lacustrine (light gray 10YR 7/2) and volcaniclastic (dark gray 10YR 4/1) sediment. At Horseshoe Cove, two mixed facies exist, Mhc_1 and Mhc_2, separated by facies Vhc (RS–10; fig. 18). The lower sequence, Mhc_1, is of latest Pleistocene age based on a date of 11.61–11.27 ka (appendixes 1, 2, 3) from the outer rings of a log in a forest bed—which consists of one or more layers of conifer needles, wood fragments, and logs—near the upper contact of Mhc_1.

The volcaniclastic parts of facies Mhc_1 and Mu are distinctly finer grained (fine sand and silt) than those of facies Vhc and Vu (coarse sand) and are composed of unaltered andesite grains. At RS–11 (fig. 17, appendix 1) on the east side of Baker Lake, facies Mu is similar lithologically to facies Mhc_1 and, like Mhc_1, underlies a forest bed with dates of 12.41–12.01 ka (on wood) and 11.61–11.27 ka (on needles). A twig in facies Mu, 12 centimeters (cm) below the forest bed, yielded a date of 12.11–11.72 ka (appendixes 2, 3).

At the Sandy Creek section (RS–2), facies Mu is absent (figs. 17, 18) even though RS–2 is only 2 to 2.5 km north of Dry Creek (RS–12) and Horseshoe Cove (RS–10), where facies Mhc_1 and Mu are 0 to >4 m thick. We suggest several reasons for this absence: (1) there are no post-Vashon fragmental volcanic deposits in the Sandy Creek drainage; (2) no volcaniclastic debris exists upslope of RS–2, only lava flows; and (3) in late Pleistocene time, Sandy Creek likely flowed south, after leaving the mountain front, into a valley that was later filled by the Sulphur Creek lava flow (figs. 17, 20). The creek has since incised through the lakebeds, revealing the section at RS–2.

At Horseshoe Cove (RS–10; figs. 17, 18), a second mixed lacustrine and volcaniclastic facies, Mhc_2, lies above facies Vhc. Facies Mhc_2 contains reworked, water-deposited tephra layer O (ca. 7.6 ka; Zdanowicz and others, 1999) from the climactic eruption of Mount Mazama, gravel clasts of Sulphur Creek lava (low in the section), sparsely distributed reworked andesitic tephra grains (likely reworked Vhc or Vu), and woody debris. The outer rings of the higher of two logs yield an age of 7.16–6.95 ka (appendixes 2, 3). Facies Mhc_2 accumulated during a ca. 2,000-year period after lake sedimentation was dominated by the influx of tephra set SC (ca. 9.8 ka). It documents a volcanically quiet time at Mount Baker and the continued existence of Glacial Lake Baker in the upper part of the Baker River valley into the middle Holocene.

The origin of the forest bed (figs. 18, 19) is unknown and its thickness suggests it accumulated through time, but whether that time period was as long as 1,000 years, as suggested by the range of age dates (12.41–11.22 ka; appendix 2), seems unlikely. We prefer the younger age for the forest bed as dated by conifer needles. The older age is from wood that didn't have bark on it, so it is impossible to know whether the wood reflects the most youthful part of a killed tree or the oldest. Additionally, the age on a twig below the forest bed at RS–11 supports a younger age of likely no more than 12 ka. Further work is needed to understand the origin and accumulation period of this important stratigraphic unit.

Figure 19. Photograph of forest bed (dark-gray material behind knife handle) within facies Mu at RS–11 (appendix 1; figs. 3, 17), east side of Baker River valley. The forest bed is a widespread layer of conifer needles and wood deposited in Glacial Lake Baker near the Pleistocene-Holocene boundary around 11.6 thousand years ago. Penknife for scale. Photograph by D.S. Tucker.

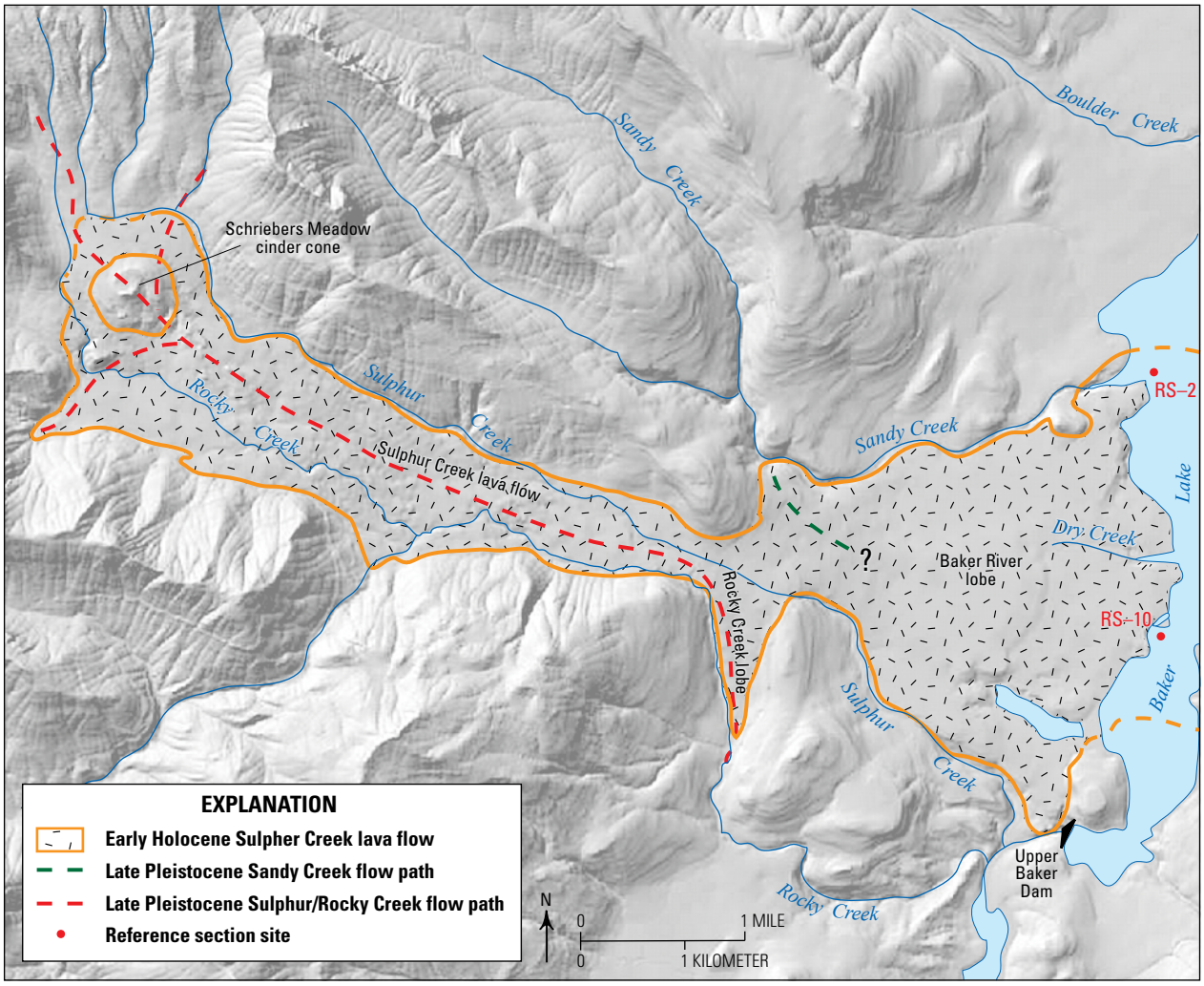

Figure 20. Map showing the inferred late Pleistocene flow path of Sandy Creek (dashed green line) and Sulphur/Rocky Creek drainages (red dashed line) compared to current drainages. Volcaniclastic-free lacustrine beds at RS–2 (facies Lsc) formed during the late Pleistocene prior to the emplacement of the early Holocene Schriebers Meadow cinder cone and Sulphur Creek lava flow (stipple pattern). In the late Pleistocene, Sandy Creek likely flowed southward into the valley later filled by the Sulphur Creek lava flow and may have been a tributary to either Sulphur or Rocky Creek. After emplacement of the lava flow, Sandy Creek reestablished itself on the north side of the lava flow and incised through lake sediment revealing the section at RS–2. Horseshoe Cove, RS–10, contains evident volcaniclastic deposits (likely tephra set SC) from before emplacement of the Sulphur Creek lava flow.

Invasion of Glacial Lake Baker by the Early Holocene Lava Flow, Basalt of Sulphur Creek

Early Holocene eruptions at the Schriebers Meadow cinder cone culminated in a lava flow (basalt of Sulphur Creek [unit bsc]; Hildreth and others, 2003) that traveled down Sulphur Creek and into Glacial Lake Baker (fig. 20). Flow of the lava into the lake resulted in deposits with unique sedimentary textures, facies, and structures, which are described and discussed in detail by Tucker and Scott (2009). Here we focus on lava inundation processes. Exposures illustrating the interaction between the lacustrine deposits and the invading lava are only available for study when the reservoirs of Baker Lake and Lake Shannon are seasonally lowered.

Where it invaded the lake deposits, the lava flow formed a carapace of peperite. At Glacial Lake Baker, the most common form of peperite consists of lava fragments in a matrix of clay-rich Pleistocene sediment, derived from the basal part of the lacustrine sequence, facies Lu (figs. 17, 18, 21). The formation of peperite is generally ascribed to fuel-coolant interaction causing the explosive vaporization of water in saturated sediment invaded by fragmenting lava (Kokelaar, 1986). The style of peperite formation in Glacial Lake Baker,

Figure 21. Photograph of the depositional sequence at Horseshoe Cove (RS–10; fig. 18), where late Pleistocene mixed lacustrine and volcanoclastic facies, Mhc_1, is intruded from below by the Holocene lava flow from Schriebers Meadow cinder cone (basalt of Sulphur Creek, Hildreth and others, 2003) along a decollement. Note the sequence beneath the decollement that consists of: A, clay-rich facies Lsc gradationally above B, a zone of peperite formed of lava fragments in facies Lu matrix, above C, fractured lava. The lava flow is well dated at about 9.8 thousand years (ka); thus, facies Vhc, which consists primarily of tephra set SC and has deltaic crossbedding, is contemporaneous with or slightly older than the lava flow. Unit Mhc_1 is also older than the underlying lava flow. Scale provided by vertical 85-centimeter ice ax (upper left of photograph) with point marking the stratigraphic level of the forest beds (marked by dashed line), which are dated here at circa (ca.) 11.4 ka. Much of the interval labeled Mhc_1 is surface wash derived from unit Vhc. Facies Mhc_2 (unit 5, RS–10) lies out of the photograph frame. Arrows show the direction of relative movement along the decollement. Photograph by K.M. Scott.

however, was of a more passive nature—one of fluidization and mixing of the lacustrine deposits with the rubbly lava carapace with little evidence of violently explosive activity. The invaded strata are, in fact, remarkably little disturbed (whether the contact is invasive or along a decollement), resulting in the possible misinterpretation that the stratigraphic relations are primary (that is, the lava flow is older than the sediment). The key to interpreting these sections is recognizing the difference in age of the host lacustrine sediment (latest Pleistocene) and the invading lava (early Holocene).

The fluidized fragmental lava and invaded lacustrine sediment were injected as thin dikes and sills extending as much as 10 m away from the lava-flow margin. The dikes and sills range from a centimeter or less to several tens-of-centimeters thick (fig. 22). Soft-sediment deformation associated with sill injection locally resembles convoluted bedding and curved transverse laminae like so-called dishes of dish-and-pillar structures (fig. 23). Dish-and-pillar structures develop by migration of fine sediment within a coarser deposit, commonly toward the top of a mass-emplaced volcaniclastic deposit during dewatering (see Scott and others, 1995). The laminae (fig. 23) may reflect the same process, with fluid (and probably steam) radiating outward from the invading, overlying sill. Invasion of the peperite into coarser grained sediment was locally associated with microfaulting (fig. 24; RS–12, appendix 1).

Figure 22. Photograph of three peperite intrusions into facies Mu near Dry Creek (RS–12). Lowermost dike (or sill) (marked A on photograph) tapers from 4 to 0 centimeters (cm) in thickness from right to left, branching from the base of the overlying 30-cm-thick sill (B). Uppermost sill (C), <7 cm thick, is mainly fluidized sediment with few lava fragments. Note the orange zones of hydrothermal alteration bounding the upper sill and the angularity of homogeneous lava clasts in peperite sill (B). Pencil (14 cm) for scale. Photograph by K.M. Scott.

Figure 23. Photograph of sediment deformation in late Pleistocene lacustrine facies, Lsc, just beneath the Holocene peperite sill (far upper left, rubbly texture, mostly eroded). At Horseshoe Cove, lava invaded from left to right. Note the faint dish-like texture in the lower half of the photograph in sediment below the nickel. Photograph by K.M. Scott.

Figure 24. Photograph of microfaulting of graded (coarse to fine) turbidite-like strata in Holocene facies Vu near Dry Creek (RS–12, appendix 1). The deformation is inferred to have been caused by invasion of the peperite carapace into granular, sand-size sediment containing tephra set SC. In this case, the peperite sill invades overlying strata of nearly the same age. Pencil (14 centimeters) for scale. Photograph by K.M. Scott.

The lava flow crossed the Baker River valley by invading the lacustrine sequence of Glacial Lake Baker. In some places, the lava flow is separated from the overlying sequence by one or more decollements (fig. 25). At other localities, however, the lava-sediment contact is a zone of fluidized peperite, and yet at other locations the lava flow was so thick that it simply bulldozed through and displaced the lake deposits. In all cases, the hackly, quenched, fractured character of the lava, as described in Tucker and Scott (2009), is similar.

We have found as much as 8 m of lake strata (facies Lu and Mhc_1) overlying the lava, but drill logs show that the lake sediment was thicker at other sites. Stearns and Coombs (1959) recorded at least 35 m of "varved clay and silt deposited in shallow glacial lakes" (drill holes J, K, and BR-20) in their drill logs. We suggest that the differences in the lake strata thickness above the lava flow indicate that the lava flow did not always invade the lake sediment at its base (that is, in places there may be sediment beneath the lava flow as well). The depth of Glacial Lake Baker was approximately 80 m (260 ft) when the Sulphur Creek lava flow entered the lake, assuming the base of the lava recorded in drill logs was on top of the lake strata (fig. 26; Tucker and Scott, 2009).

The nature of the decollement changes among outcrops. In figure 21, the decollement formed along a bedding plane of the invaded strata (facies Lsc) with almost no deformation; in contrast, in figure 25 the decollement is a bedding plane of the invaded sequence (facies Lu), which is gently deformed. At other locations, invasion of the peperite carapace occurred along a fluidized zone without any apparent discrete glide plane. In each of these three cases, the lack of deformation in the invaded sequence is noteworthy, other than at the small scale illustrated in figures 23 and 24.

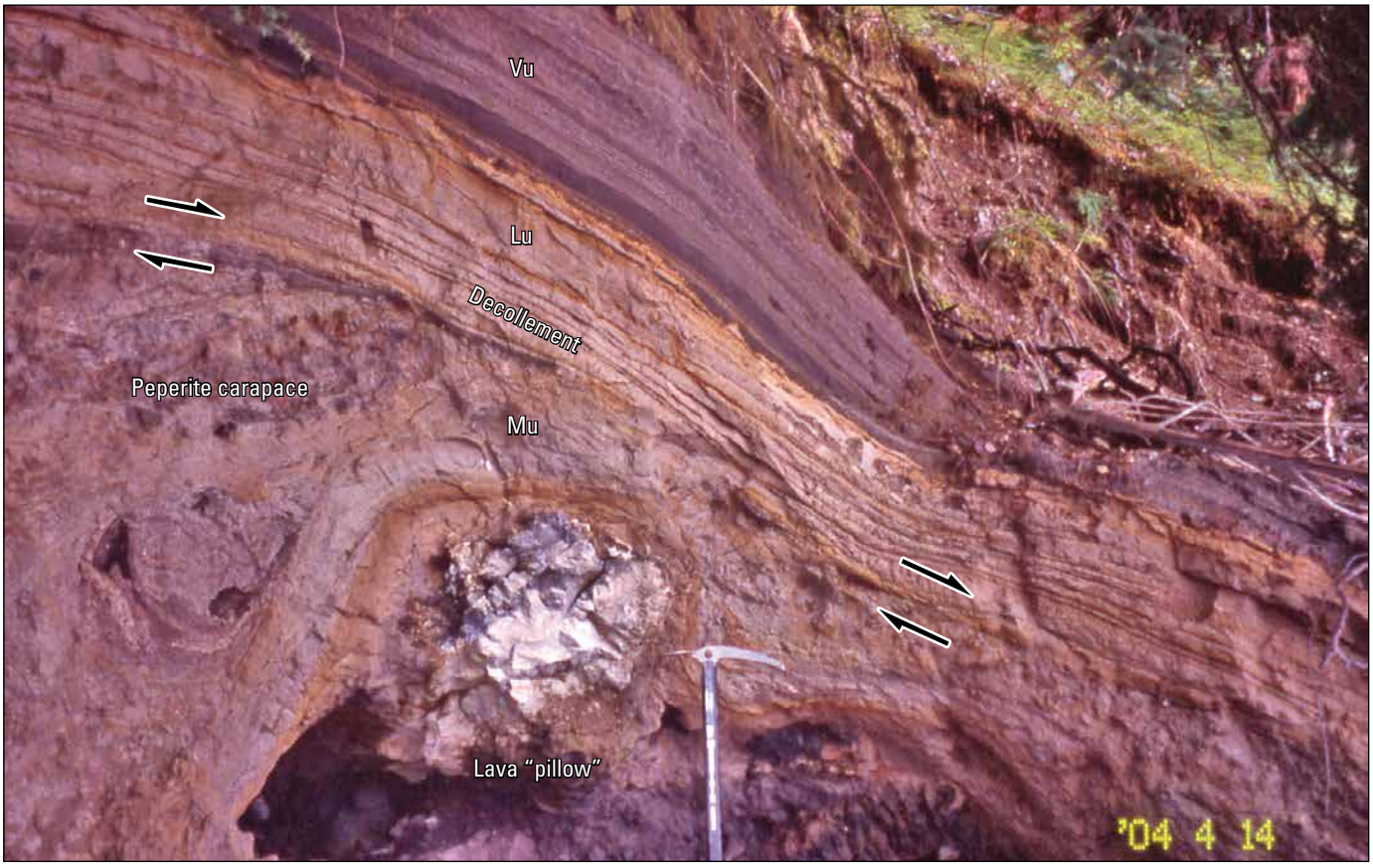

Figure 25. Photograph of deposits on the east side of modern Baker Lake reservoir at RS–11 (appendix 1), where lacustrine sediment is intruded and deformed by the lava flow from Schriebers Meadows cinder cone, forming pillow-like masses of rapidly quenched, radially jointed lava within the sequence. The overlying volcaniclastic facies Vu probably correlates with facies Vhc (RS–10 at Horseshoe Cove; figs. 17, 18). The decollement is a plane along which lava and its peperite carapace were emplaced from the right (west). This outcrop is exposed only at low reservoir levels. Ice ax (85 centimeters) for scale. Photograph by K.M. Scott.

Erosion in the Upper Baker River Valley after Emplacement of Sulphur Creek Lava Flow

Drill holes west of Upper Baker Dam (Swiger, 1958; Stearns and Coombs, 1959) show that a previous course (likely pre-glacial) of the Baker River was west of the 125-m high bedrock knob that presently supports the west abutment of the dam (fig. 26). The paleochannel ran approximately beneath the West Pass Dike Dam, the rockfill dam extending north and west from the bedrock knob (site of the present boat launch). This paleochannel was sufficiently filled with glacial drift and lava from the Sulphur Creek lava flow that, when the surface level of Glacial Lake Baker declined in the middle Holocene, the area east of the bedrock knob was lower and became the course of Baker River.

Glacial Lake Baker was still present at Horseshoe Cove (RS–10) at 7 ka; thus, the lava flow (~9.8 ka) remained submerged beneath the surface of Glacial Lake Baker for about 3,000 years—enough time for it to have been mantled by additional lacustrine sediment, at least in the center of the valley. Post-lava sedimentation included significant thicknesses of sandy material, Mount Mazama tephra layer O (~7.6 ka), and gravel of mixed lithologies (see RS–10 and RS–12). After about 7 ka, the level of Glacial Lake Baker gradually fell and by 6.7 ka Baker River had reestablished itself. In the middle of the valley (fig. 26), the river initially meandered across a flat, newly exposed lakebed, but through time it incised through the lacustrine sediments and lava flow. The incision produced a steep-sided gorge consisting of two wide meander loops, now submerged beneath Baker Lake reservoir (the name Horseshoe Cove refers to one of these meander loops or horseshoe bends). The meander pattern differed from the braided pattern in the valley upstream and suggests that when this part of upper Baker River valley was first exposed, the Baker River flowed across a low-gradient floodplain into the remnant lake. The meanders would have initially formed in the highly erodible sandy lacustrine sediment covering the lava (post-lava lacustrine sediment), facies Lsc and Mu that had been invaded by, and rafted onto, the flow, and the peperite carapace. As lake level continued to fall, the gradient on Baker River increased and it incised through the pervasively shattered lava flow preserving the meanders. Walls of the now-submerged canyon are nearly vertical (fig. 26). The canyon was cut for roughly 7,000 years, between the time waters of Glacial Lake Baker receded below the lava surface and renewed inundation by Baker Lake reservoir. The lava flow surface is at about 220 m in the center of the valley and the bottom of the now-drowned canyon cut into the lava flow is at about 168 m, giving an incision rate of 52 m/7,000 years or 0.7 m/100 years. This is slightly less than the rate of 0.9 m/100 years given by Tucker and Scott (2009). The difference is we use calibrated ages, whereas they used radiocarbon ages.

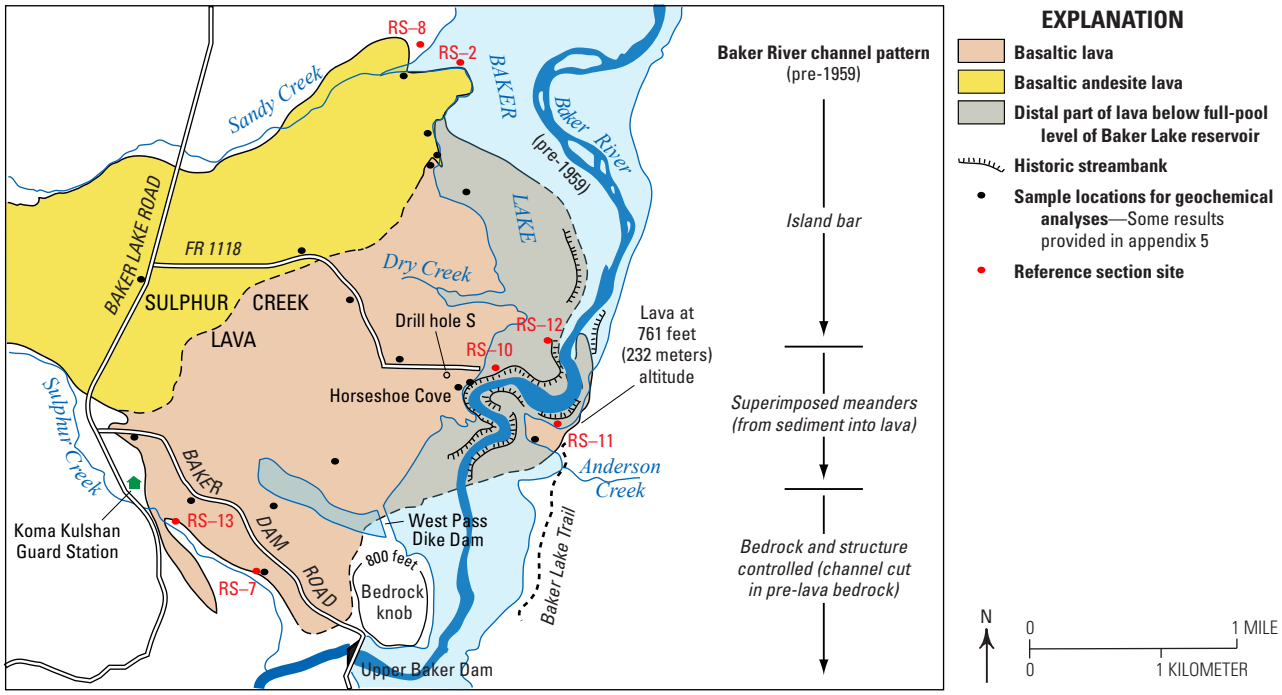

Figure 26. Map of the distal part of the basalt of Sulphur Creek (Hildreth and others, 2003) and the pre-1959 channel pattern of Baker River prior to impoundment by Upper Baker Dam. Shoreline location at time of lava emplacement is unknown, but reference sections shown were subaqueous at that time. Channel pattern is from pre-1959 topographic maps, 1959 aerial photographs, and topographic maps in Swiger (1958). Drill hole S penetrates the base of the lava flow at its deepest known level (Swiger, 1958). Reference sections RS–2, RS–10, RS–11, and RS–12 are visible only when Baker Lake reservoir is below full-pool level; RS–2 was buried by flood alluvium in 2003. Topographic elevation line around the bedrock knob is in feet. Figure modified from Tucker and Scott (2009).

Natural Baker Lake and Current Reservoirs

Shortly after 7 ka, upper Baker River valley was lake free. Natural Baker Lake (as shown on pre-1959 maps before reservoir inundation) was formed by the damming of the Baker River by the largest Park Creek lahar ca. 6.7 ka (see chapter G). Its level was further raised by the historical Morovitz Creek lahar in 1845–47 C.E. Darwin (1921) conducted a bathymetric survey of the lake and reported a lake level of 661.5 ft (202 m) and a maximum lake depth of 116.5 ft (35.5 m), which placed the altitude of the valley bottom at ≤545 ft (166 m). Darwin's (1921) reported lake level is similar to the lake altitude of 663 ft (203 m) reported on the pre-dam 1952 Lake Shannon 15-minute quadrangle.

Lower Baker River valley became ice free sometime after 3 ka. At that time, Baker River flowed some 50 km southward from its headwaters into the Skagit River. In the middle 1920s, as part of a hydroelectric project, Lower Baker Dam was constructed across a narrow gorge about 1.6 km upstream of the mouth of Baker River. The lower dam created the Lake Shannon reservoir. In the late 1950s, the Upper Baker Dam was constructed, which effectively drowned the upper valley (including natural Baker Lake) and created the Baker Lake reservoir.

Summary of Glacial Lake History

In summary, there were three natural lakes near the base of Mount Baker that captured sediment recording the volcano's eruptive history (table 4) from the latest Pleistocene to late Holocene. Now the only lakes in the valley are reservoirs.

- Glacial lakes that formed near Mount Baker during and after alpine and Cordilleran ice sheet glaciation provided depositional environments that record glacial and volcanic activity.
- Glacial Lake Concrete was formed by blockage(s) of the Skagit River valley during the Evans Creek stade by an alpine valley glacier that extended down Baker River valley (Riedel and others, 2010). Glacial Lake Concrete persisted for about 9,000 years. At the "Big Boy" section (RS–1), lakebeds are overlain by Vashon (ice sheet) till and outwash.
- As the Cordilleran ice sheet retreated, the Baker River valley gradually became ice free, while ice was still present in the Skagit River valley. Ice in the Skagit River valley (and later ice-marginal deposits; Riedel, 2011) blocked the Baker River, creating Glacial Lake Baker (Scott and others, 2003; Scott and Tucker, 2006).

Table 4. History of latest Pleistocene to Holocene lakes and reservoirs in the Baker and Skagit valleys near Mount Baker.

[m, meters; ka, thousand years; ca., circa]

Lake	Description	Age	Deposits
Modern reservoirs	Baker Lake reservoir	July 1959	Reservoir sedimentation
	Lake Shannon	November 1925	Reservoir sedimentation
Natural Baker Lake	Natural Baker Lake (as shown on 1952 Lake Shannon 15-minute quadrangle)	Blockage mainly emplaced in the middle Holocene by Park Creek lahar and raised by Morovitz Creek lahar in 1845–47	Blockage drowned by Baker Lake reservoir but outcrops of lahar can be seen at times of reservoir drawdown
Glacial Lake Baker	Persists because outlet incision is slowed by bedrock	Lake level above 128 m at ca. 3.4 ka; lake history is summarized in figure 16 and table 3	See RS–9 (appendix 1)
	Lake initially dammed by deposits of retreating and (or) downwasting of Vashon glacier	Earliest dates on lake are basal rhythmite deposits at 14.2–13.5 ka, suggesting formation during the latest Pleistocene; see Sandy Creek beds at RS–2	Lacustrine, volcaniclastic, and mixed facies; see RS–10 (appendix 1)
Glacial Lake Concrete	Lake formed in Skagit River valley in response to damming of Skagit River by Evans Creek valley glaciers that extended down Baker River valley (Riedel and others, 2010)	ca. 30.3–19.3 ka	Lacustrine strata locally preserved; see "Big Boy" section of RS–1 (appendix 1)

The lake persisted into the Holocene (fig. 16; table 3), declining slowly to near the present full-pool level of Lake Shannon reservoir by ca. 3.4 ka. The lake ceased to exist sometime after 3.4 ka.

- Clay-rich lacustrine deposits (facies Lsu and Lu) at the mouth of Sandy Creek (RS–2, appendix 1; figs. 14, 17, 18; facies Lsc) and elsewhere are the oldest dated deposits of Glacial Lake Baker at about 14 ka. This sediment is devoid of fresh volcaniclastic material, indicating it was deposited during a quiet period at Mount Baker.
- Facies Lsu and Lu are overlain by a mixed assemblage of lacustrine and volcaniclastic deposits. This mixed assemblage (facies Mhc_1 and Mu) is loosely bracketed in age between 14 ka (the age of facies Lsc) and an overlying organic-rich layer, herein called the forest bed, dated at about 11.6 ka. The fine-grained, unaltered andesite grains in facies Mhc_1 and Mu indicate renewed eruptive activity at Mount Baker with the source vent at Carmelo Crater.
- Primary and reworked tephra from the early Holocene (ca. 9.8 ka) eruption of Schriebers Meadow cinder cone, a vent on the southeast flank of Mount Baker, is preserved as a thick deposit of nearly pure volcaniclastic material (facies Vhc, Vu; figs. 17, 18) above the forest bed. These deposits are overlain by another mixed lacustrine and volcaniclastic deposit, facies Mhc_2. The volcaniclastic material in Mhc_2 appears to be mostly reworked tephra from the Schriebers Meadow cinder cone eruption. We have not looked closely enough at the volcanic material to see if some of it is altered and perhaps from some unknown eruptions at Sherman Crater. The paucity of volcaniclastic material in Mhc_2 compared with facies Vhc and Vu, as well as indications that most of the grains are reworked tephra, indicate that Mhc_2 was deposited during a quiet period at Mount Baker.
- Concurrent with the deposition of facies Vhc and Vu, a lava flow from the Schriebers Meadow cinder cone moved down the Sulphur Creek valley and entered Glacial Lake Baker. The Sulphur Creek lava flow invaded the latest Pleistocene clay-rich sediment and in outcrop sits stratigraphically below facies Lsc and Lu even though the lava flow is 4,000 to 5,000 years younger.
- The invasion of the Sulphur Creek lava flow into Glacial Lake Baker deposits created a peperite carapace on the lava flow. Misinterpretation of the stratigraphic position and of the carapace as a volcanic breccia could lead one to erroneously postulate a pre-Lsc volcanic event.
- There is no evidence that the Sulphur Creek lava flow ever blocked the Baker River. The lava intruded sediment at the bottom of the lake and at no time was a barrier to river flow.
- Shortly after 7 ka, the upper Baker River valley was lake free. However, a remnant of Glacial Lake Baker remained in lower Baker River valley into the late Holocene (after 3.4 ka).
- Natural Baker Lake formed when the largest of the middle Holocene (ca. 6.7 ka) Park Creek lahars flowed into upper Baker River valley and dammed Baker River. It was raised again by the Morovitz Creek lahar sometime between 1845 and 1847 C.E. Natural Baker Lake persisted from 6.7 ka onwards until it was drowned by Baker Lake reservoir in 1959.

Chapter E

Mount Baker Volcano, Northern Casade Range, Washington

A stack of lavas underlies the north ridge of Mount Baker. During the late Pleistocene, steeply dipping lava flows like these failed, spawning block-and-ash flows and lahars that are preserved in volcaniclastic assemblages on the south and southeast flanks of the volcano. Photograph by John H. Scurlock, January 14, 2003, used with permission.

Chapter E

Latest Pleistocene Assemblages of Lava Flows and Fragmental Deposits

Assemblages of latest Pleistocene deposits from summit eruptions are found in several drainages on the southern flanks of Mount Baker. The assemblages consist of lava flows, block-and-ash flows, lahars, hyperconcentrated-flow deposits, tephra fall, and associated reworked deposits. They are preserved as the incised remnants of deposits that originally filled several valleys, notably Boulder, Pratt, and Sulphur Creek valleys (fig. 27). The assemblages were emplaced after Cordilleran ice sheet (Vashon) glacial activity (<~16 ka) and before early Holocene volcanic activity associated with the Schriebers Meadow cinder cone (>9.8 ka); below we suggest a more confined range in age. Block-and-ash flows, originating from lava-flow-front collapse (Hildreth and others, 2003), also contain some bombs and rare pumice documenting that some explosive activity accompanied the effusive activity. We propose that, as the hot block-and-ash flows moved downslope, they mixed with and melted snow and ice to generate syneruptive lahars. Deposition of the coarser material transformed some lahars to hyperconcentrated flows, which make up a major portion of the distal assemblages.

Burke (1972) was the first to describe a fragmental sequence in Boulder Creek that was later described as the Boulder Creek assemblage by Hyde and Crandell (1978) and recognized by Hildreth and others (2003) as the youngest fragmental deposits on the edifice. The Boulder Creek assemblage and potentially three other latest Pleistocene fragmental assemblages in Pratt, Sulphur, and perhaps upper Rocky Creeks mark the beginning of the late- to postglacial eruptive activity of Mount Baker. No similar fragmental sequences are known from the other sectors of the volcano; however, an intracanyon lava flow, the andesite of Glacier Creek (unit age of Hildreth and others, 2003), is of post-Vashon age and thus may be correlative in age to these assemblages.

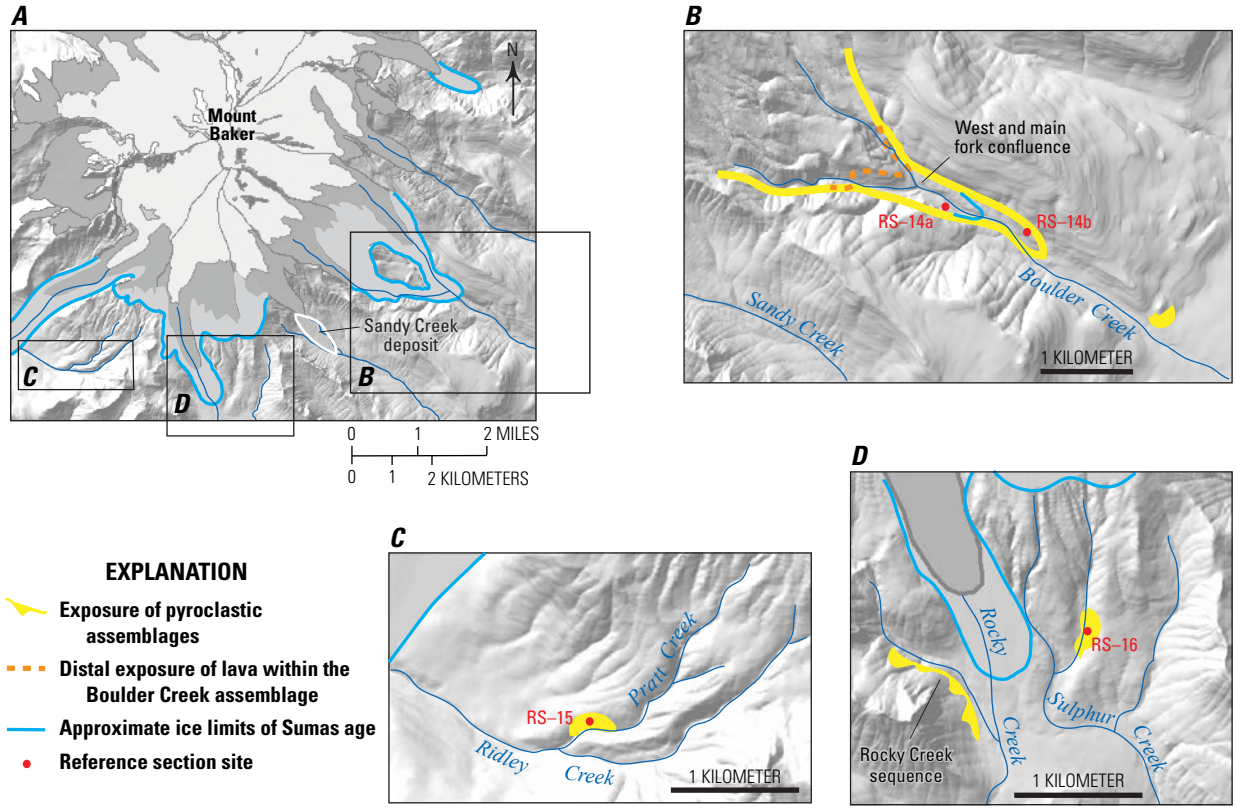

Figure 27. Maps showing locations of pyroclastic assemblages and corresponding reference sections. *A*, Mount Baker summit area and south flank of the volcano showing the location of maps *B*, *C*, and *D*, as well as the location of the Sandy Creek deposit that Hildreth and others (2003) postulated may also be a fragmental assemblage. Light-gray area near summit shows the current glacier extent, dark gray shows Little Ice Age glacier limits, and medium-gray areas within blue lines show approximate ice limits of Sumas age (see fig. 6). *B*, Exposures of Boulder Creek assemblage are located between yellow lines and in the yellow area on the left bank of Boulder Creek at the mountain front. *C*, Exposure of Pratt Creek assemblage located near the confluence with Ridley Creek. *D*, Exposures of Sulphur Creek assemblage on left bank of Sulphur Creek and Rocky Creek sequence on the right bank of the west fork tributary to Rocky Creek.

Boulder Creek Assemblage

The Boulder Creek assemblage formed a broad fan of primary and reworked fragmental material that filled the Boulder Creek valley (Hyde and Crandell, 1978; Hildreth and others, 2003; Tucker and Scott, 2004). It is now incised and exposed continuously on both sides of Boulder Creek, 2.0 to 5.5 km upstream from Baker Lake Road (figs. 3, 27) at stream altitudes of ca. 420 to 954 m as described in RS–14a and RS–14b (appendix 1; fig. 3). It also forms an isolated exposure in a roadcut 100 m northeast (upstream) of the bridge at the mouth of the Boulder Creek valley.

The Boulder Creek assemblage is the thickest of the exposed assemblages and consists of lava flows and deposits of rubbly block-and-ash flows, lahars, sand-rich hyperconcentrated flows, and their alluvial runouts (fig. 28). A stack of two-pyroxene andesite lava flows dominates the assemblage in the upper valley. In the west fork of Boulder Creek, 1 km upvalley from the confluence with the main fork, at least four lava flows, 5 to 50 m in thickness, are intercalated with fragmental deposits (Tucker and Scott, 2004); no lava flows, however, extend below the confluence (fig. 27).

Fragmental deposits of the Boulder Creek assemblage are exposed along the main fork of Boulder Creek for nearly 2 km below the west fork confluence. The assemblage thins downvalley (although measurements here are in kilometers upstream from the Baker Lake Road bridge across Boulder Creek) from ~250 m (5.5 km) to ~230 m (RS–14a; 3 km) to ~80 m (RS–14b; 2 km; fig. 27*B*).

The Boulder Creek assemblage type section of Hyde and Crandell (1978; RS–14b; figs. 27, 28), on the northeast side of Boulder Creek, consists of ~80 m of deposits with 24 individual units ranging in thickness from 0.5 to more than 6 m (table 5). It consists primarily of fragmental, monolithologic flow deposits characterized by a coarse mode of unaltered clasts of Mount Baker andesite set in a uniformly clay poor (noncohesive), granular matrix. Mean grain sizes of the lowest lahar deposit (unit 2; table 6) are typically in the coarse pebble fraction (−5.0 to −6.0 ϕ; 32–64 mm). The subrounded coarse mode is commonly in the boulder fraction (>−8.0 ϕ; 256 mm) and represents bed material of Boulder Creek entrained during flow. The matrix generally is nearly devoid of silt-size (4.0 to 8.0 ϕ; 0.0625–0.004 mm) and clay-size (<8.0 ϕ; 0.004 mm) sediment (table 6). Most deposits

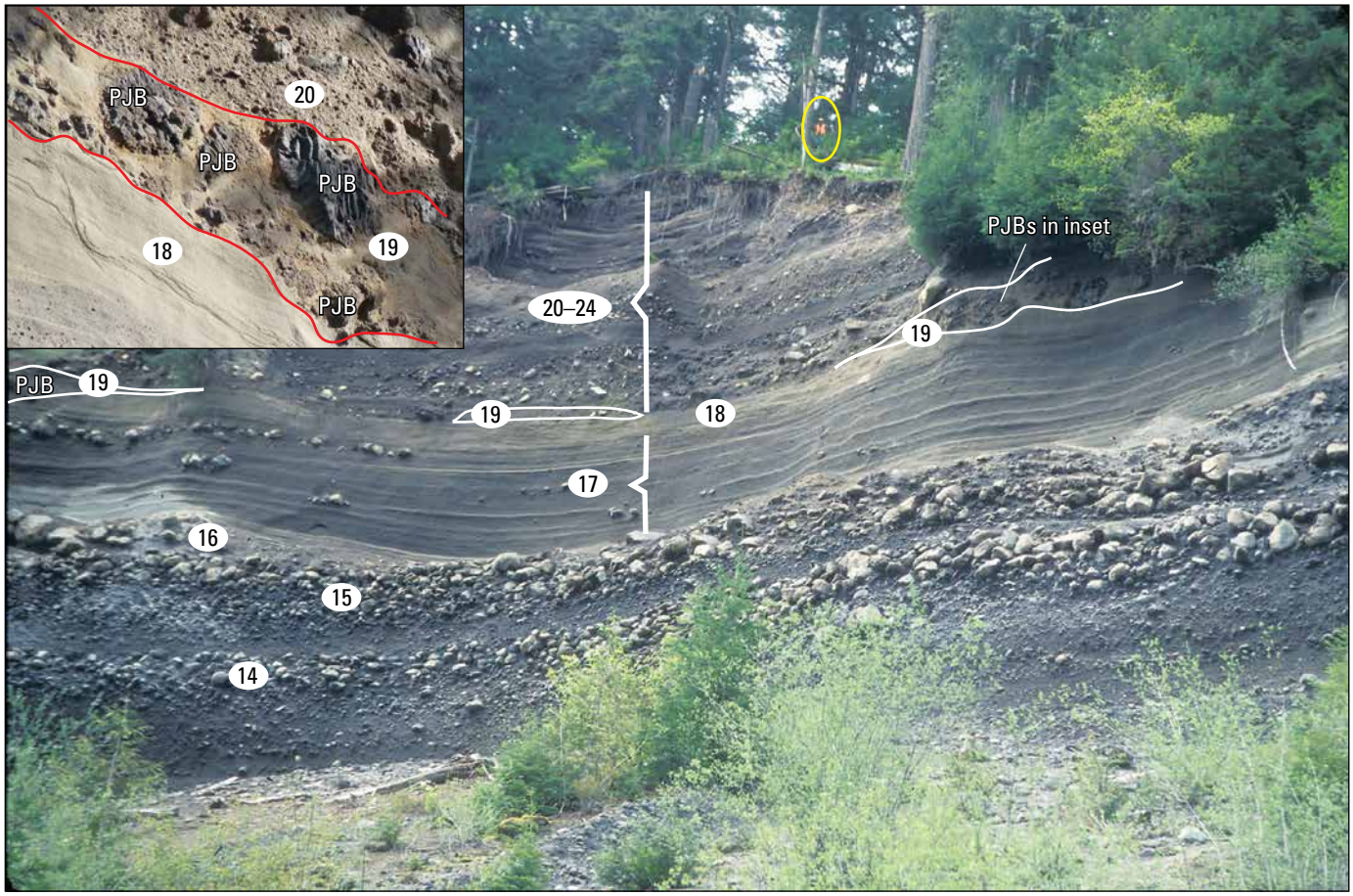

Figure 28. Foreshortened telephotographic view of the upper half of the Boulder Creek assemblage type section of Hyde and Crandell (1978) at RS–14b (appendix 1; figs. 3, 27). Unit numbers correspond to those in table 5. Note the fine-grained hyperconcentrated-flow deposits in unit 17 (see table 5). Six-foot-tall individual in orange (circled in yellow) at top of section for scale. Inset photograph is a close-up view of the prismatically jointed blocks (PJBs) in unit 19. Photographs by D.S. Tucker.

Table 5. Detailed stratigraphy of left-bank type section (RS–14b) of the Boulder Creek assemblage; measured on rappel by D.S. Tucker.

[Clast diameters in parentheses are estimates. Sediment size terminology is applied to all units; volcanologic size terms (ash, lapilli, and blocks) also apply to block-and-ash flows. m, meters; cm, centimeters]

Unit	Thickness (m)	Description	Diameter of largest lithic clast (cm)	Interpretation of origin
24	10	Subrounded andesitic pebbles, sand matrix; crude stratification	15	Alluvium
23	10	Subrounded andesitic cobbles, sand matrix; crude stratification; overall normal grading	(30)	Alluvium
22	3	Poorly sorted diamict; dispersed phase with small boulders; crude reverse grading	(50)	Lahar
21	1	Massive sand with rare dispersed pebbles	(10)	Hyperconcentrated flow
20	3	Poorly sorted diamict; dispersed phase with small boulders; crude reverse grading	(50)	Lahar
19	2	Massive sand; angular andesite grains and crystals; numerous prismatically jointed blocks; local dune structures	(200[a])	Block-and-ash flow
18	0–1	Stratified gray sand, locally cross-cutting	(<1)	Alluvium
17	6.5	Rhythmically bedded sequence of 8 massive, 0.5- to 1-m-thick units of sand with dispersed angular pebbles and rounded pumice, separated by 10- to 30-cm-thick interbeds of stratified sand. Reverse grading at base of units; normal grading above	(5–10)	Hyperconcentrated flow; lahar transitional to hyperconcentrated flow; alluvium (interbeds)
16	1.5	Multiple, massive-to-stratified units of sand and pebbles; base covered	(4–6)	Alluvium
15	3.5	Poorly sorted diamict with andesite boulders and scoria in sand matrix; rare rounded pumice pebbles	(200)	Block-and-ash flow transitional to lahar
14	3.5	Poorly sorted diamict with andesite boulders and scoria in sand matrix; rare rounded pumice pebbles	(200)	Block-and-ash flow transitional to lahar
13	2	Moderately well-sorted subangular-to-rounded andesite cobbles in sand	(50)	Alluvium
12	3.5	Poorly sorted diamict with andesite boulders and scoria in sand matrix; rare rounded pumice pebbles	(200)	Block-and-ash flow transitional to lahar
11	3	Poorly sorted diamict	(200)	Lahar
10	0.5	Stratified sand with subrounded pebbles; normal grading	(2)	Alluvium
9	4	Poorly sorted diamict with andesite boulders and scoria in sand matrix; rare rounded pumice pebbles	(150)	Block-and-ash flow transitional to lahar
8	4	Poorly sorted diamict with andesite boulders and scoria in sand matrix; rare rounded pumice pebbles	(100)	Block-and-ash flow transitional to lahar
7	3.5	Well-sorted pebbly sand with subangular-to-subrounded lithic and crystal grains	(2)	Alluvium
6b	4	Poorly sorted diamict	(200)	Lahar
6a	0.5	Massive sand	1	Hyperconcentrated flow
5	2	Stratified pebbly sand	6–8	Alluvium
4	2	Poorly sorted diamict with andesite boulders and scoria in sand matrix; rare rounded pumice pebbles	300	Lahar
3	1.5	Coarse angular sandy gravel	100	Alluvium
2	6	Diamict of andesite (and 1 percent metamorphic) clasts set in oxidized matrix of sand, silt, and clay; some hydrothermally altered andesite clasts	200	Lahar[b]
1	>3	Diamict of angular, poorly sorted andesite clasts in 5–15 percent clay and silt matrix	300	Till; base covered

[a]Prismatically jointed block.

[b]Particle-size analysis of matrix shown in table 6.

Table 6. Deposit texture of lahar in the Boulder Creek assemblage (unit 2 of RS–14b).

[Graphical measures after Folk (1980); $\phi = -\log_2$(size in mm). Laboratory analyses by dry or wet sieving. Sedigraph analyses of fine sediment. Percentages of individual coarse fractions (>−1.0 ϕ; 2 mm) and of total matrix (<−1.0 ϕ; 2 mm) are field measurements. NA, not applicable; %, percent; mm, millimeter; cm, centimeter]

Deposit	Mean diameter (ϕ)	Sorting	Skewness	Kurtosis	Clay[1]	Silt + clay[1]	Matrix clay[2]	Matrix silt + clay[2]	Matrix[3]
	Mz	σ_G	Sk_G	K_G	%	%	%	%	%
Middle of unit 2	−5.03	4.64	+0.30	0.84	<0.01	0.7	<0.01	4.7	15
20–30 cm above base	−1.57	2.55	+0.02	0.83	<0.01	1.0	NA	NA	unimodal
Base of unit 2	−2.23	2.09	+0.22	0.91	<0.01	1.0	NA	NA	unimodal

[1]Refers to texture of entire deposit.

[2]Refers to texture of matrix only.

[3]Proportion of sand, silt, and clay in total deposit.

in the section contain variable proportions of prismatically jointed and breadcrusted blocks and reveal the spectrum of emplacement processes from hot block-and-ash flows spawned by collapse of the fronts of upslope lava flows, to water-mobilized slurries. Unit 19, 27 m below the top of RS–14b, contains a concentration of 1–2 m blocks of prismatically jointed andesite blocks in a sandy matrix (fig. 28). Interpretations of hyperconcentrated-flow deposits (RS–14b; table 5) are based on the textural and structural similarity to the type examples described by Pierson and Scott (1985) and Scott (1988a) at Mount St. Helens. Remobilized, rounded clasts of pumice, 3–15 cm in diameter, are concentrated in units 15 and 17 (table 5).

At the highway bridge across Boulder Creek, a prominent fan slopes eastward into the Baker River valley, displacing the river against the valley's east side. This 6-km^2 fan is composed of distal deposits of pyroclastic flows and lahars as well as reworked Boulder Creek assemblage sediment. Two 19th-century lahar deposits mantle the fan surface. Fan construction probably began during the initial formation of the assemblage after the Vashon glacier withdrew from the valley and continued thereafter, eventually extending into Glacial Lake Baker and likely contributing to lake facies Mu.

Burke (1972) obtained an age for the Boulder Creek assemblage of 12.75 to 7.79 ka (8,700±1,000 ^{14}C yr B.P.; appendix 3) from wood in a mudflow beneath a lava flow interbedded in the Boulder Creek assemblage. The date originally was interpreted to suggest that the assemblage was Holocene in age. The validity of the date, however, is questionable because of the small sample size and technical problems encountered during sample analysis (Hyde and Crandell, 1978); furthermore, the large uncertainty makes the date of limited use. Nonetheless, it remains the only direct date on any of the assemblages. We constrain the age by stratigraphic relations. At RS–14a (appendix 1), the Boulder Creek assemblage overlies alpine till of probable Sumas age and is overlain by the 9.8 ka set-SC tephra-fall deposit from the Schriebers Meadow cinder cone (fig. 29). At RS–14b, the Boulder Creek assemblage overlies Vashon Drift as this section is below the alpine limit of Sumas age, with no minimum limiting age information. A radiocarbon date from the base of Pocket Lake (fig. 3), an alpine moraine-damned lake of presumed Sumas age, yielded an age of 13.57–13.11 ka (Osborne and others, 2012). Additionally, outer rings of logs in till of Sumas age in the Middle Fork Nooksack River (RS–3; appendix 1) yield ages between 13.69–13.43 ka and 12.64–12.17 ka. Thus, the Boulder Creek assemblage is likely no older than about 13.5 ka. At Horseshoe Cove (RS–10) and on the east side of Baker Lake (RS–11; figs. 17, 18), the mixed facies of volcaniclastic and lacustrine sediment (Mhc_1 and Mu) is largely below the ca. 11.6 ka forest bed. Assuming the assemblages contributed to the volcaniclastic part of the mixed facies, it places the age of the Boulder Creek assemblage between 13.5 and 11.6 ka. Hildreth and others (2003) estimated an age of 12–11 ka for the Boulder Creek assemblage, presumably based on their interpretation that the assemblage was post-Vashon and pre-tephra set SC.

Pratt Creek Assemblage

In Pratt Creek, a 30-m-thick sequence of fragmental flow deposits, remarkably similar to the Boulder Creek assemblage, rests on more than 10 m of Vashon and possibly Evans Creek glacial deposits (RS–15, appendix 1; figs. 3, 27*C*, 30). Geochemical analyses, however, indicate that blocks in the Pratt Creek assemblage have lower silica contents (57–60 weight percent SiO_2) than the Boulder Creek assemblage lavas (61–63 weight percent SiO_2; Hildreth and others, 2003), indicating that these two assemblages were probably not derived from the same eruptive event. The Pratt Creek assemblage contains several coarse cobble- and boulder-bearing beds that are 0.5 to 3.0 m thick. At RS–15 (unit 5, appendix 1), the lowermost of these coarse beds is a 1- to 2-m-thick block-and-ash flow deposit dominated by prismatically jointed blocks and breadcrusted bombs.

Figure 29. Photograph of person sampling the upper part of RS–14a, where the bright-orange early Holocene tephra set SC (circa [ca.] 9.8 thousand years ago [ka]; see chapter F) overlies an organic-rich silt and diamict (units 4 and 5 of RS–14a), which overlie a soil formed in the ~230-meter-thick Boulder Creek assemblage. Location is on the right valley wall of Boulder Creek. Photograph by K.M. Scott.

The age of the Pratt Creek assemblage, like that of the Boulder Creek assemblage, is constrained between underlying glacial till and overlying tephra set SC. In this valley there are no glacial deposits of Sumas age (fig. 27*A*), thus the Pratt Creek assemblage overlies glacial deposits of likely Vashon age owing to the presence of a significant proportion of Twin Sisters Dunite (2 percent of gravel-sized clasts), whose source area is southwest of Mount Baker (fig. 8). To get the dunite into the Pratt Creek drainage requires transport from the Twin Sisters up the Middle Fork Nooksack River and Ridley Creek, which only could have been accomplished by continental ice. At RS–15 (appendix 1; fig. 27*C*), unit 7 is a 0 to 1.5-m-thick soil horizon that overlies the assemblage and contains early Holocene tephra set SC fall (ca. 9.8 ka) in the upper 0.2 to 0.3 m. No organic matter has been found in this horizon suggesting that the postglacial landscape had not yet been extensively revegetated.

Sulphur Creek Assemblage

In the middle fork of Sulphur Creek, the Sulphur Creek assemblage is a >25-m-thick section of fragmental deposits that overlies a sequence of late Pleistocene lava flows with thin interbeds of lava breccias and sparse scoria. The Sulphur Creek assemblage (RS–16; appendix 1; figs. 27*D*, 31) is well stratified and consists mainly of hyperconcentrated and alluvial runouts of noncohesive lahar deposits. Although, in general, texturally finer than either the Pratt Creek or Boulder Creek assemblages, this fragmental sequence is lithologically similar and is inferred to be the distal, water-mobilized portion of proximally hot, syneruptive block-and-ash flow deposits. Many of the deposits contain a significant proportion of prismatically jointed blocks and some units contain upwards of 5–15 percent pumice.

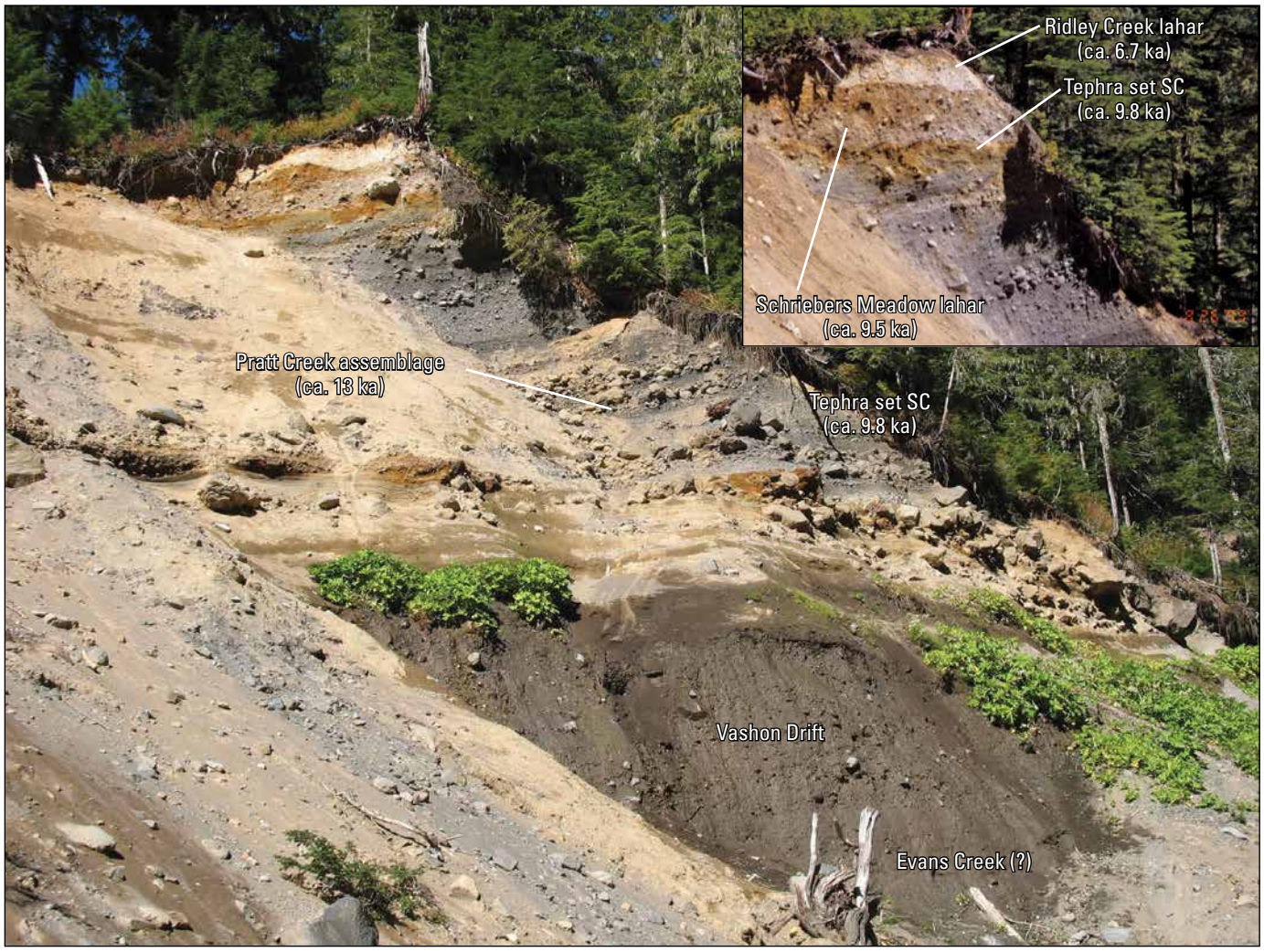

Figure 30. Photograph of RS–15 (appendix 1) showing glacial deposits overlain by the Pratt Creek assemblage near the confluence of Pratt Creek and Ridley Creek. Inset photograph (upper right) shows the Pratt Creek assemblage overlain by deposits of the early Holocene tephra set SC and Schriebers Meadow lahar and middle Holocene Ridley Creek lahar discussed in chapters F and G. ka, thousand years. Photographs by K.M. Scott. ca., circa.

Lava flows underlying the Sulphur Creek assemblage and upstream (unit acv of Hildreth and others, 2003) are geochemically more mafic (58.2–59.0 weight percent SiO_2) than blocks in either the Pratt Creek or Boulder Creek assemblages. Near RS–16, the K-Ar age date of the underlying lavas (unit 1) is 36±14 ka (unit acv of Hildreth and others, 2003). Unit acv, however, consists of as many as 40 separate lava flows, and 2 km upslope from RS–16, an upper unit acv flow has a date of 11±9 ka (fig. 12 of Hildreth and others, 2003), just barely outside the lower (1σ) limit of the 36 ka age. We surmise that the Sulphur Creek assemblage was derived from upvalley unit acv lava flows, but do not have chemical data to confirm the relation.

A latest Pleistocene age for the Sulphur Creek assemblage is supported by organic material in units just overlying the assemblage. Thomas (1997) obtained a date of 13.05–12.73 ka (appendix 3) from charcoal fragments at the top of a diamict in upper Sulphur Creek, which was also reported by Kovanen and others (2001). We obtained ages of 12.96–12.69 and 13.26–12.66 ka (appendix 2) from charcoal fragments in a thin layer of colluvial silt directly overlying the Sulphur Creek assemblage at RS–16 (appendix 1; fig. 3), which was confirmed later to also be Thomas' sampling site (P.A. Thomas, oral commun., 2005). All three ages indicate a minimum limiting age for the Sulphur Creek assemblage between 13.3 and 12.7 ka.

Volcaniclastic Sequence in Rocky Creek

A stratified fragmental sequence is exposed in several isolated locations on the right valley wall of the unnamed west fork of Rocky Creek between 3,600 and 3,950 feet (1,090–1,190 m; figs. 27*D*, 32). Its base is not exposed, and vegetation

Figure 31. Photograph of RS–16 (appendix 1) shows the Sulphur Creek assemblage (unit 3) on the left bank of the middle fork of Sulphur Creek (fig. 27*D*). Vashon Drift (unit 2 of RS–16), just out of view in this photograph, sits stratigraphically between a lava flow dated at about 36±14 thousand years (ka) (Hildreth and others, 2003) and the Sulphur Creek assemblage. Units 4–11 contain numerous Holocene tephra layers from Mount Baker and tephra layer O from the 7.6 ka eruption of Mount Mazama (Bacon, 1983; Zdanowicz and others, 1999). Photograph by D.S. Tucker.

or colluvium covers the upper parts of the sequence; the thickest exposure is at least 110 m. The stratified, normally graded clastic units consist entirely of andesite clasts as large as 1 meter across in a sandy matrix. Angular clasts dominate, although subrounded blocks are also present, including vesicular blocks and scoriaceous-to-breadcrusted vitric clasts. Rounded tan pumice clasts as large as 3 cm are common. Well-exposed units in the sequence are 1.5 to 3 m thick. Exposures decrease in height and clast size downstream. The most distal exposure noted by us is at the confluence of the two forks of Rocky Creek. Exposures are inset against metamorphic basement.

The age of the sequence is unknown. It is likely post-Vashon in age, because no discontinuities were found in the section and it is likely that some erosion and compaction would have occurred in the coarse-sand beds if they had been overrun by the Cordilleran ice sheet. Exposures lie just beyond the mapped extent of the glacier of Sumas age in Rocky Creek (fig. 27), so its relation to ice of Sumas age is unknown. The sequence is also not in contact with older till deposits. No tephras have been found in any of the stream exposures, further clouding the possible age of these deposits.

The exposures in the west fork of Rocky Creek resemble those of the Sulphur Creek assemblage and lie about 1.8 km west-southwest of RS–16 (fig. 27*D*). The sequence thus may be a remnant of a once more extensive Sulphur Creek assemblage that extended across the Rocky Creek-Sulphur Creek valley prior to emplacement of the Sulphur Creek lava flow. Alternatively, it could be a separate assemblage filling a paleovalley of Rocky Creek. An eroded, till-draped (likely Vashon Drift) lava flow with an age of 32±14 ka (unit amp of Hildreth and others, 2003) obstructs the west fork of Rocky

Figure 32. Photograph of the sequence of fragmental deposits on the right valley wall of the west fork of Rocky Creek. The sequence includes at least five coarse basal units that consist of angular-to-subrounded Mount Baker andesite dipping about 10 degrees to the south. Rounded pumice clasts as large as 3 centimeters in diameter are common. The age of the sequence is unknown; it is beyond the limit of the glacial deposits of Sumas age and no tephras were found above it. Labels show the unit number and thickness in meters (m). Photograph by D.S. Tucker.

Creek 250 m upstream of the western-most volcaniclastic exposure. The lava lies on metamorphic basement. This flow is unlikely to be the source of the inferred postglacial Rocky Creek sequence. However, a higher, upslope lava flow within the stacked andesites of Mazama Park (unit amp) has a K-Ar age date of 9±11 ka (Hildreth and others, 2003). It or other flows in the stack could also be the source for the Rocky Creek sequence.

Fragmental Deposit in Sandy Creek

Hildreth and others (2003) surmised that a prominent smooth, gently graded topographic surface in Sandy Creek (fig. 27*A*) was possibly a flank assemblage equivalent to or related to the Boulder Creek assemblage. The heavily forested surface between 730 and 1,160 m altitude is bounded on its north and south margins by forks of a stream and is underlain by 15 to 20 m of stratified coarse deposits (fig. 33). The basal 2 m consists of clast-supported angular blocks, 20 cm in diameter. A crudely crossbedded unit of sand and small lithic clasts overlies the angular blocks and is capped by two or, in places, three beds of angular, dense, not-very-fresh-looking andesitic blocks in a sandy matrix. No blocks appear to be prismatically jointed, which is a characteristic of blocks in the other assemblages. The largest measured blocks are 1 m in diameter and rounded alluvial cobbles and metamorphic clasts are rare, even though metamorphic basement rocks compose both valley walls. Soil above the diamict contains the middle Holocene tephra layers O (Mount Mazama) and BA (Mount Baker). Early Holocene tephra set SC was not observed.

The origin of the deposit is equivocal, but the crude stratification, angularity of blocks, lack of fresh-looking andesite material, and scarcity of entrained alluvial and valley-wall clasts lead us to interpret the deposit as the result of one or more landslides from an unknown source area upvalley. Absence of tephra set SC, common in upvalley meadow

Figure 33. Photograph of crudely stratified fragmental deposits at 2,850 feet (975 meters) altitude in the south fork of Sandy Creek of uncertain origin and age. The crude stratigraphy and absence of either fresh andesitic blocks or entrained alluvial and valley wall clasts (such as in a lahar) suggest that this may be the result of one or more landslides. White lines show contacts between coarse, angular blocky units and a crudely crossbedded unit of sand and lithic clasts. The lack of tephra set SC suggests that these deposits postdate the ~9.8-thousand-year Schriebers Meadow cinder cone eruption and therefore are younger than early Holocene in age. Photograph by D.S. Tucker.

exposures and on both east and west ridge crests, and the shallow dissection of the surface suggest that the deposit is younger than early Holocene and therefore considerably younger than the fragmental assemblages discussed above.

Origin of the Boulder Creek, Pratt Creek, Sulphur Creek Assemblages

We interpret the origin of the Boulder Creek, Pratt Creek, and Sulphur Creek assemblages as syneruptive flank deposits produced during largely effusive eruptions. Syneruptive origin is suggested by evidence of heat (prismatic jointing and breadcrusted clasts), by the presence of pumice in the Boulder Creek and Sulphur Creek assemblages, by tracing assemblage lahar and hyperconcentrated-flow deposits upslope to stacks of possible source andesitic lava flows, by the thickness of the deposits indicating a lot of fragmental material being generated, and, in the case of the Boulder Creek assemblage, by interlayering of the fragmental deposits with lava flows. The sequence in Rocky Creek is similar to the other assemblages, but whether it is a separate assemblage or part of the Sulphur Creek assemblage requires further investigation.

Block-and-ash-flow deposits in the Boulder Creek and Pratt Creek assemblages are recognized by their monolithologic nature, relative lack of low-density clasts expectable in column-collapse pyroclastic-flow deposits, and numerous prismatically jointed and breadcrusted clasts. Hyde and Crandell (1978) used a hand-held magnetometer to report a preferred orientation of thermoremanent magnetism in individual clasts, supporting a high-temperature origin for some units in the Boulder Creek assemblage. Flows emplaced at high temperatures are most characteristic of the basal 53 m of the Boulder Creek assemblage section at RS–14b. Some deposits may qualify as hot lahars, in which clasts may show multiple remanent directions (for example, Hoblitt and Kellogg, 1979), although most lahar deposits low on the volcano's flanks probably fall in Hoblitt and Kellogg's category of cold lahars, with no consistent thermoremanent magnetism. There are no known lava domes at Mount Baker and Hildreth and others (2003) inferred that the block-and-ash flows formed by avalanching of summit-derived lava flows over snow and glaciers, an inference compatible with our conclusions (below) about the origins of the associated lahars and hyperconcentrated flows.

We propose that hot avalanches from disintegrating summit-derived lava flows swiftly melted snow and ice to produce the water content to mobilize the lahars. Voluminous lahars generated simply by lava flows are rare to nonexistent as lava flows tend to override and burrow into snow and ice; the heat transfer between them is generally too slow to produce sufficient meltwater (Major and Newhall, 1989). Mechanisms that do generate sufficient meltwater include (1) interaction of hot pyroclasts with snow or ice, (2) ponding and sudden release of water (for example, jökulhlaups or glacial outbursts), or (3) ejection of water from a crater lake (Major and Newhall, 1989). Walder (2000a,b) provided theoretical and experimental arguments for a purely thermal mechanism by which a layer of hot pyroclasts can incorporate underlying snow and transform into a slurry, but he concluded that both thermal and mechanical erosion are probably involved. Lahars in all of the assemblages are clay poor (matrix clay content <3 percent; see Boulder Creek assemblage matrix, table 6), arguing against a flank-failure origin. The lack of time breaks between multiple lahar units argues against a glacial-outburst scenario and there is no evidence that a lake existed at the time in the summit crater area. Most upper edifice deposits are lava flows and there is no evidence of sustained explosive activity or of lava-dome formation to generate the block-and-ash flows other than by lava-flow-front disintegration. Short-duration explosions or low-level lava fountaining, however, may also have occasionally occurred and could account for the pumice seen in units 15 and 17 in the Boulder Creek assemblage (table 5) and in some units of the Sulphur Creek assemblage and Rocky Creek sequence.

Summary of Assemblage Age Data

The Boulder Creek, Pratt Creek, and Sulphur Creek assemblages all overlie Vashon Drift and are, in turn, overlain by tephra set SC from Schriebers Meadow cinder cone; thus, their ages are broadly confined between about 16.3 and 9.8 ka. Evidence suggests, however, that their ages are most likely between 14.2 and 11.6 ka for reasons discussed in the text and summarized below.

At RS–14b, the Boulder Creek assemblage overlies Vashon Drift, but, at RS–14a, it lies within the glacial limit of Sumas age and overlies probable till of Sumas age (figs. 27*B*, 34). This limits the maximum age of the Boulder Creek assemblage to no more than about 13.5 ka. Exposures of the Pratt Creek assemblage, Sulphur Creek assemblage, and Rocky Creek sequence are only found beyond the glacial limit of Sumas age (fig. 27). However, the Sulphur Creek assemblage (and likely the Rocky Creek sequence) would reasonably have contributed to the mixed lacustrine and volcaniclastic facies (Mhc_1) at Horseshoe Cove (figs. 17, 18). Facies Mhc_1 overlies facies Lu (purely lacustrine). We assume that facies Lu correlates with the dated Lsc section (14.2–13.5 ka) at Sandy Creek; thus, these assemblages are likely no older than about 14 ka. The upper age of facies Mhc_1 and Mu is given by the forest bed dated at around 11.6 ka.

The weathered upper horizons of the Boulder Creek, Pratt Creek, and Sulphur Creek assemblages all contain tephra set SC (fig. 34), dated at about 9.8 ka. Tephra set SC corresponds to facies Vhc and Vu in Glacial Lake Baker, which sits above the 11.6 ka forest bed. Thus, the minimum age of the assemblages is likely 11.6 ka. Charcoal in the weathered horizon of the Sulphur Creek assemblage yielded ages of 12.96–12.69 and 13.26–12.66 ka (appendixes 2, 3), consistent with data from the lake record.

The assemblages are not in contact, and, other than a questionable date on the Boulder Creek assemblage, none are directly dated; thus, we are unable to correlate among the

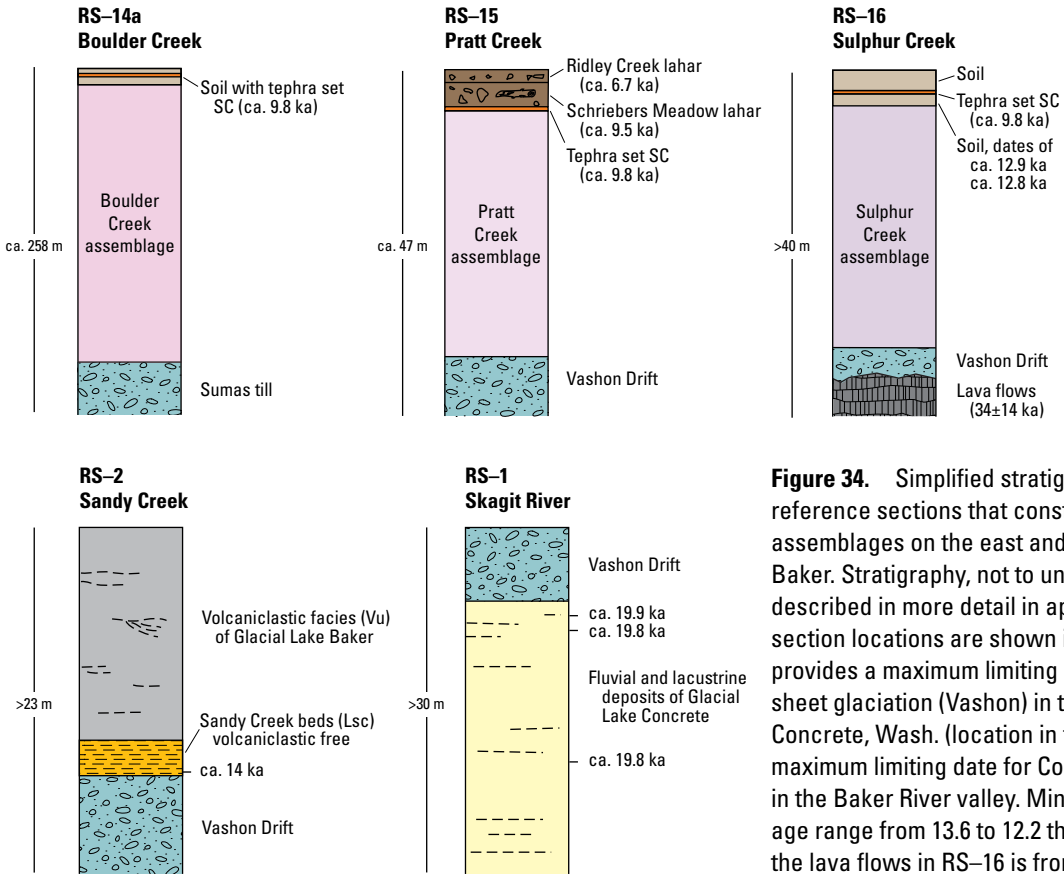

Figure 34. Simplified stratigraphic sections of key reference sections that constrain the age of fragmental assemblages on the east and southeast flanks of Mount Baker. Stratigraphy, not to uniform vertical scale, is described in more detail in appendix 1 and in text. Reference section locations are shown in figures 2 and 3. RS–1 provides a maximum limiting date for the Cordilleran ice sheet glaciation (Vashon) in the Skagit River valley near Concrete, Wash. (location in fig. 2), and RS–2 gives the maximum limiting date for Cordilleran ice sheet deglaciation in the Baker River valley. Minimum ages for the till of Sumas age range from 13.6 to 12.2 thousand years (ka). The age of the lava flows in RS–16 is from Hildreth and others (2003). ca., circa

assemblages on the basis of their ages or stratigraphy. Each appears to have a distinct source as suggested by limited geochemical data and distribution. Nonetheless, the glacial and tephra stratigraphy suggests that all the assemblages could be roughly equivalent in age. The Boulder Creek and Sulphur Creek assemblages can be confined to between about 13.5 and 11.6 ka. Presumably, the Rocky Creek sequence is similar in age to the Sulphur Creek assemblage owing to the similarity of the deposits, but we have neither glacial till nor overlying tephra layers to help constrain its age. Because Pratt Creek does not flow into Baker Lake, we cannot use the Glacial Lake Baker record to help refine the age of the Pratt Creek assemblage beyond between 16.9 and 9.8 ka. These ages are compatible with argon ages of some of the summit lava flows and suggest that the assemblages record the last eruptive activity from the summit vent of Mount Baker.

Summary of Assemblage Deposits

- Thick fills of fragmental deposits, and locally lava flows, are found in the Boulder, Pratt, Sulphur, and Rocky Creek drainages on the east and southeast flanks of the volcano. Each assemblage consists of numerous units ranging from boulder-rich flow deposits containing prismatically jointed and breadcrusted clasts to lahars to sandy hyperconcentrated-flow deposits. In Boulder Creek (Hyde and Crandell, 1978; Hildreth and others, 2003), the assemblage is interbedded with lava flows. At other localities, the assemblages either overlie latest Pleistocene lava flows or potentially correlate to similarly aged lava flows farther upvalley.
- Assemblage lahars are inferred to be syneruptive on the basis of their low clay content and downstream transformation to hyperconcentrated flows. In Boulder and Pratt Creek, the lahars are interbedded with deposits of block-and-ash-flows formed when lava flow fronts collapsed as they advanced over steep terrain. The hot block-and-ash-flow pyroclasts likely intermixed with snow and ice to produce water for the lahars. Minor amounts of pumice in assemblage deposits suggest some explosive activity occurred during emplacement of the assemblages, but that the bulk of the volcanic activity was effusive.
- Several of the assemblages (fig. 34) overlie Vashon Drift (<16.3 ka) and underlie the early Holocene tephra set SC (>9.8 ka). However, the assemblages are more likely between 14.2 and 11.6 ka in age on the basis of facies relations in Glacial Lake Baker and the relation of some of the assemblages to glacial deposits of Sumas age.

- Assemblage deposits do not overlap and only the Boulder Creek assemblage is directly dated (that age, however, is poorly constrained). Thus, we do not know the relative timing of the deposits in the different drainages. Clasts in the Pratt Creek, Sulphur Creek, and Boulder Creek assemblages have slightly different chemical compositions, which suggests that they were emplaced during different summit eruptions. The broader distribution of the Boulder Creek assemblage indicates that it may be the youngest of all the assemblages as it appears to be the best preserved, but that may also reflect a more prolonged or more voluminous eruptive episode.
- Lava flows within the assemblages can be traced to the Carmelo Crater vent. Thus, the assemblages record the last eruptions from the summit vent.

Chapter F

Mount Baker Volcano, Northern Casade Range, Washington

The ~9.8 thousand year old Sulphur Creek lava flow fills the valley floor of Rocky and Sulphur Creeks and originates at the low forested mound of the Schriebers Meadow cinder cone. View looks west; Twin Sisters on skyline. Photograph by John Scurlock, September 9, 2003, used with permission.

Chapter F

Latest Pleistocene to Present Tephras and the Early Holocene Sulphur Creek Lava Flow

The latest Pleistocene to present eruptive history of Mount Baker consists mainly of small- to moderate-volume tephras, summit and off-flank lava flows, and emplacement of the fragmental assemblages discussed in chapter E. Only the latest Pleistocene deposits are from the summit cone, whereas Holocene tephra falls and lava flows are all from peripheral vents. The focus in this chapter is on the age and stratigraphy of post-Vashon tephras and characteristics used for their field identification as time-stratigraphic horizons. Of particular interest is the timing of eruptive activity, and its correlation, or lack thereof, with glacial deposits (chapter C) and lahar-producing events described in chapter G. We also discuss the emplacement of the Sulphur Creek lava flow as the only known Mount Baker lava flow of Holocene age.

As used here, a tephra layer is a discrete depositional unit and a tephra set consists of multiple layers that commonly comprise the thickest and generally most widespread main layer plus other minor layers. The common practice in naming tephras at Cascade Range volcanoes is a letter (or letters) as, for example, tephra layer O from Mount Mazama (Mullineaux, 1974). We have applied this long-standing practice at Mount Baker in this and all previous reports (for example, table 3 of Scott and others, 2001).

Tephra Set SP (Latest Pleistocene)

The oldest known postglacial tephra-fall deposit from Mount Baker (as distinguished from the minor pumice deposits described in the fragmental assemblages; chapter E) is tephra set SP, as designated by Scott and others (2001) but first recognized and dated by Hyde and Crandell (1978). Two deposits, a discrete layer of tephra set SP and a silty soil containing concentrations of angular black, unaltered andesitic vitric ash underlie scoria of tephra set SC from the Schriebers Meadow cinder cone at the Park Butte Trail crossing of Rocky Creek (RS–4, appendix 1). Here the tephra set SP is dark gray (10YR 4/1) to black (10YR 2/1), and consists of fine-sand-size, juvenile pyroclasts. Brown (10YR 4/3) to colorless, unaltered vitric grains compose the bulk of the finest fraction and plagioclase, augite, and hypersthene crystals compose the remainder (≤30 percent). Normalized glass compositions average about 67 percent SiO_2 (appendix 5). Estimated distribution of the layer is shown in figure 35.

Charcoal fragments from the top of the <1.0-cm-thick layer of tephra set SP at RS–4 (unit 3, appendix 1) yield a date of 12.97–12.67 ka. Charcoal fragments in the overlying 4-cm-thick silty soil layer, which contains a significant proportion of tephra particles, yield dates of 12.69–12.42 and 12.73–12.58 ka (appendixes 2, 3). Beneath these two units is a 25-cm-thick soil containing sporadic concentrations of black, vitric silt and fine-sand-size andesite grains. It is unclear if these grains represent early sporadic explosions or have filtered down from above. Geochemical analyses of about 20 shards (table 5) yield a SiO_2 content of 66.9±4.7 percent with relatively high iron compared to other Mount Baker tephras.

Two tephra layers south of the Scott Paul Trail (RS–5, fig. 36) are tentatively assigned to tephra set SP. The locality is 5 km south of the summit and the layers are confined in age between 13.41–13.21 and 9.46–9.14 ka (appendixes 2, 3). The fine-ash fraction is unaltered, light gray, and glassy. Grains

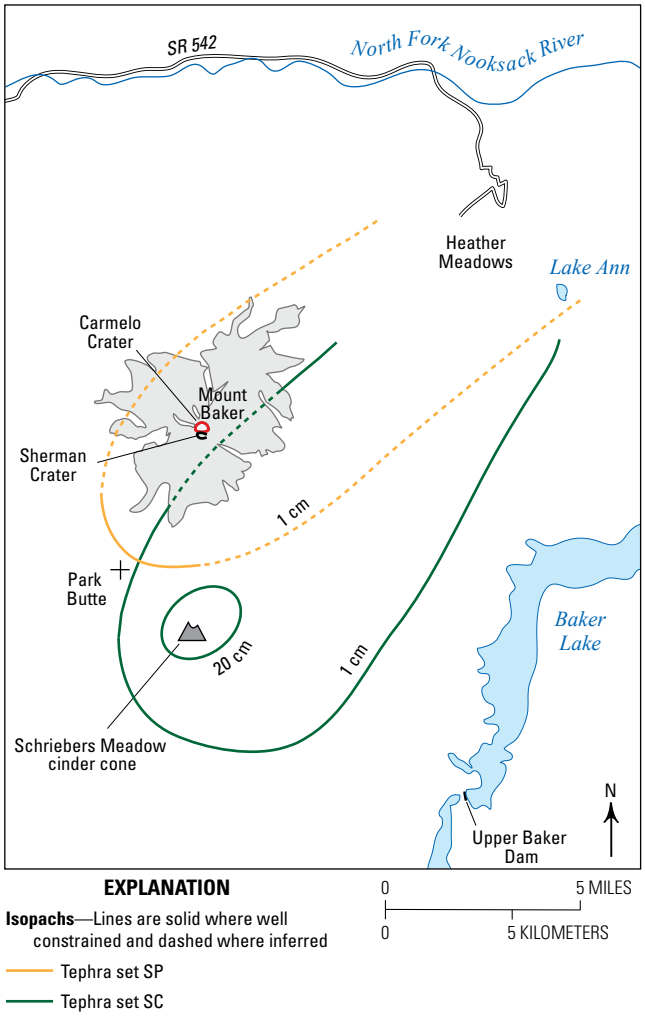

Figure 35. Schematic map showing approximate isopachs for late Pleistocene tephra set SP (1 centimeter, cm) and early Holocene tephra set SC (1 and 20 cm). Note the different source areas. Gray area is the upper edifice of Mount Baker showing present-day glacier distribution. Distal extent of tephras unknown.

in both layers contain about 68 percent SiO_2 and relatively high iron contents (appendix 5); both are within analytical uncertainty of the tephra set SP sample from RS–4.

Hyde and Crandell (1978) dated what is most likely tephra set SP at 12.73–11.20 ka. They described the unit as a 5- to 7-cm-thick tephra in Sulphur Creek valley. We found no exposures with the tephra that thick nor a cutbank in Sulphur Creek that matched their description. From their description of the stratigraphy, we think the location was more likely from RS–5 or some nearby location on Rocky Creek. Their location of Sulphur Creek may be because of confusing nomenclature on the topographic maps at that time—15-minute topographic maps of that era labeled Sulphur Creek, not Rocky Creek, as the outlet drainage of Easton Glacier. Hyde and Crandell (1978) also reported the tephra 15 km northeast of Carmelo Crater at Heather Meadows (fig. 35). Although the isopachs for tephra set SP certainly suggest a northeast elongation of the tephra lobe, subsequent searches by two of the authors and by others (D.J. Easterbrook, oral commun., 2006) have found no tephra set SP at Heather Meadows, nor was it seen in several sediment cores reaching bedrock at Heather Meadows (Burrows and others, 2000; Burrows, 2001).

At RS–5 (fig. 3), tephra set SP overlies a rubbly diamict with a sandy matrix that represents an alpine moraine probably of Sumas age or material reworked from an alpine moraine of that age. Glacial reconstructions (fig. 6) indicate alpine ice would have been at this elevation during Sumas time, which supports the probable age for the moraine. Dates on the tephra set SP place it within the Sumas stade (14–11.6 ka; table 2), as defined by Armstrong and others (1965).

At the Panorama Point boat launch on Baker Lake reservoir (fig. 3) there is an enigmatic section that can only be observed when lake surface drops below full-pool level. There, numerous dark-gray sand layers interbedded with lake sediment may record late Pleistocene explosive activity, but we have not conclusively identified the dark-gray sand layers as tephra set SP or even as tephra per se.

Based on its age, lack of alteration, and distribution, tephra set SP is inferred to have been erupted from Carmelo Crater at the end of the Pleistocene. The tephra shows no hydrothermal alteration, characteristic of most, although not all, tephras from Sherman Crater. Also, there is no evidence that the Sherman Crater vent existed at the end of the Pleistocene. The emplacement of the hydrothermally altered tephra layer MY in the early Holocene may be the first indication of both alteration and eruptive activity at or near Sherman Crater. Only after the emplacement of Mount Mazama tephra layer O in the middle Holocene (ca. 7.6 ka) does highly altered material appear in the alluvial stratigraphy of drainages downslope of the present Sherman Crater.

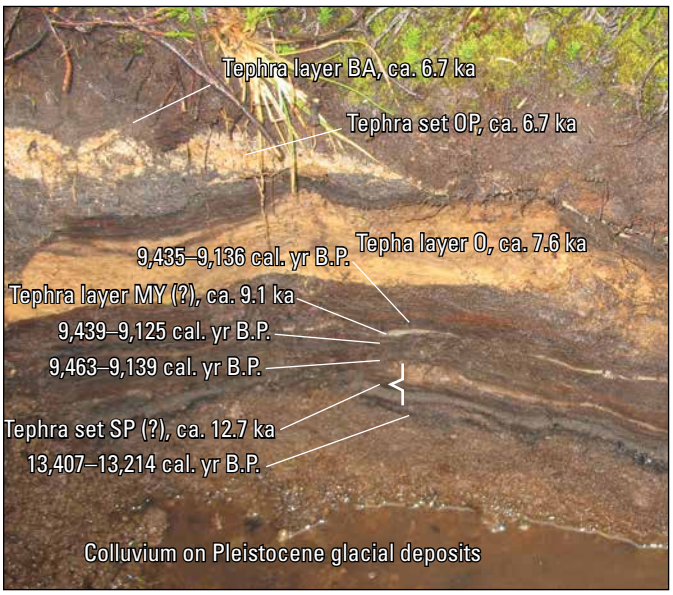

Figure 36. Photograph of tephra stratigraphy at RS–5 (appendix 1), south of Scott Paul Trail and about 5 kilometers south of Carmelo Crater (fig. 3). Exposed section is 0.5 meters thick. Red horizon, 3 centimeters below tephra layer O, may be the result of iron concentration during soil formation. Tephra layer O is from the climactic eruption of Mount Mazama (Crater Lake) 7.6 thousand years ago (Bacon, 1983; Zdanowicz and others, 1999). Limiting ages shown as ranges (in calibrated years before present; cal. yr B.P.), tephras as approximate ages (in thousand years; ka). Photograph by D.S. Tucker; also appears in Osborn and others (2012). ca., circa.

Tephra Set SC and the Sulphur Creek Lava Flow (Early Holocene)

The next younger tephra, tephra set SC, is a distinctive, orangish-to-reddish brown (5YR 4/3) basaltic tephra erupted from the Schriebers Meadow cinder cone. The forested 70-m-high by 500-m-wide Schriebers Meadow cinder cone is located 8 km south of Carmelo Crater in the meadow between Rocky and Sulphur Creeks (figs. 3, 20, 37). The cinder cone hosts twin lakes in craters 100 m apart (fig. 37). Tephra set SC consists of two layers. The main layer, SC_1, (unit 5 in RS–16, appendix 1) consists of fresh black to oxidized orange, lithic-vitric-crystal ash and scoriaceous basaltic lapilli. A second layer, SC_2 (unit 6), is recognized proximal to the cone where it forms a 6-cm layer of ash above SC_1 and resembles the fine-grained distal deposit of SC_1. Hyde and Crandell (1978) recognized SC_2 as the final deposit of the cinder cone eruption.

Layer SC_1 locally consists of multiple normally graded units, reflecting wind shifts or pulses in an intermittent eruption, and possibly some remobilization of the deposits on slopes during the eruption. Grain-size data for layer SC_1 at RS–18 (table 7) reveal moderately poor sorting ($\sigma_G = 3.04$). Scoria bombs are confined to within 1.0 km northeast of the cinder cone whereas lapilli extend to approximately 4.0 km. As much as a meter of 1- to 2-cm-diameter lapilli and dark red (10YR 3/6) to dark reddish-brown (2.5YR 3/4) sandy ash is prominently exposed in dunes and berms in meadows 4 km north of the Schriebers Meadow cinder cone. The dunes and berms are the result of wind and water remobilization. At

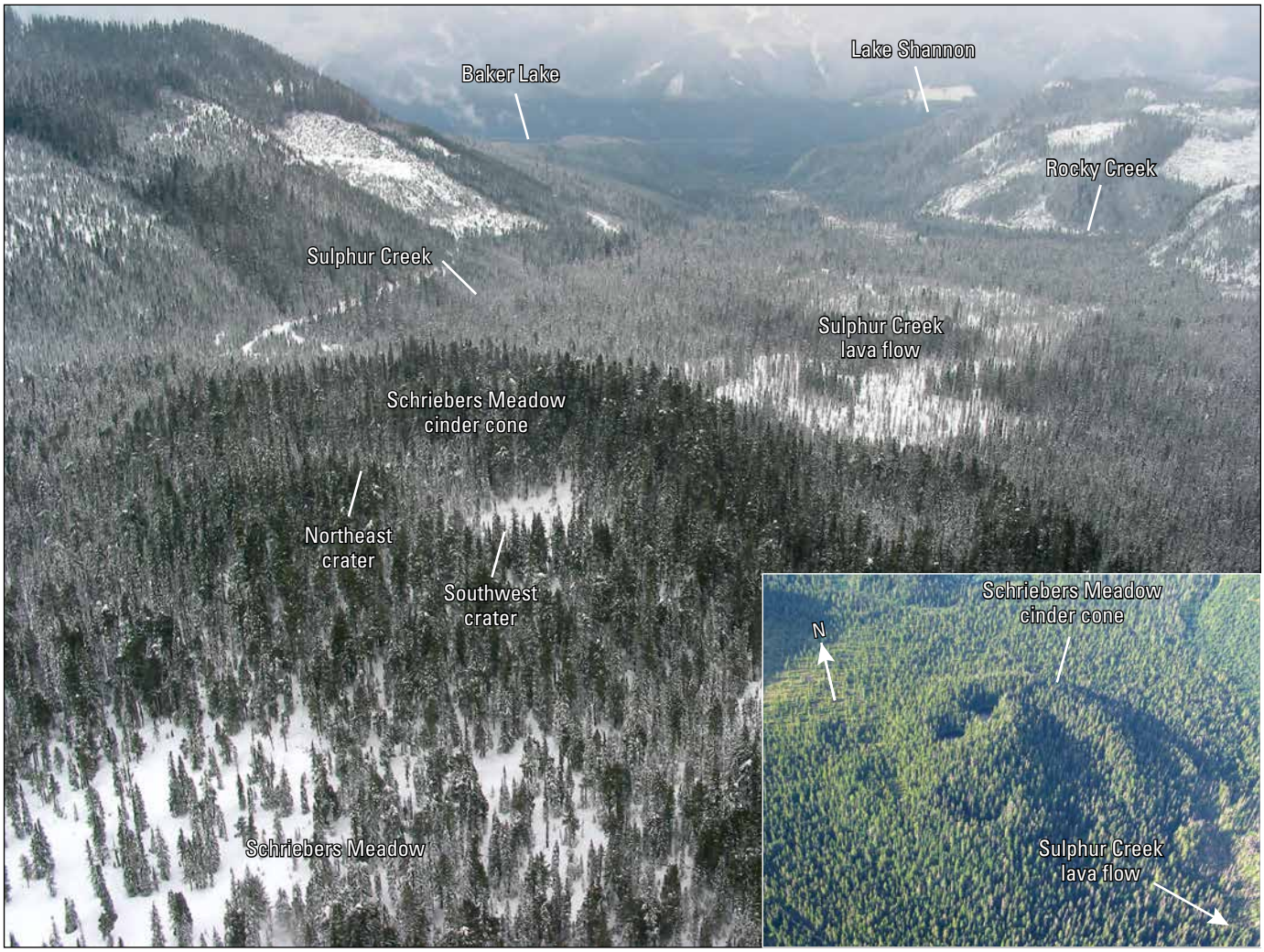

Figure 37. Aerial view of Schriebers Meadow cinder cone looking southeast towards Baker Lake and Lake Shannon reservoirs. The Sulphur Creek lava flow fills the valley between Sulphur Creek and Rocky Creek (fig. 20). Inset photograph, looking north, shows twin lakes in craters approximately 100 meters apart. Photographs by J.H. Scurlock (main photograph, March 8, 2003; inset photograph, July 16, 2006), used with permission.

Table 7. Statistical measurements of grain-size distribution of tephra deposits.

[Graphical measures after Folk (1980); $\phi = -\log_2$ (size in mm). Laboratory analyses by dry or wet sieving. Sedigraph analysis of fine sediment. %, percent; mm, millimeter]

Deposit	Mean diameter (ϕ)	Sorting	Skewness	Kurtosis	Clay[1] (%)	Silt + clay[1] (%)
	Mz	σ_G	Sk_G	K_G	%	%
Tephra on Grant Peak	−1.25	3.27	+0.15	0.78	1.0	6.1
Tephra set YP (upper Park Creek)[2]	1.00	4.14	+0.15	0.64	7.0	22.6
Tephra layer BA (RS–19)	2.16	1.88	+0.11	0.85	1.0	9.7
Tephra set OP (RS–18)	Samples cannot be disaggregated to original fragments with dispersing agents.					
Tephra set SC (RS–17, RS–18)[3]	−2.56	3.04	+0.20	0.97	2.5	12.8

[1]Refers to texture of entire deposit.

[2]Sample collected by J. Fierstein from a bare, glaciated surface in upper Park Creek; thus, it consists of original airfall deposit unmixed with soil.

[3]Channel samples.

Forest Divide (8 km east of the vent; fig. 3), layer SC_1 deposits are 5-cm thick. The axis of maximum thickness, however, extends northeast and layer SC_1 deposits are found at least 18 km from the vent at Lake Ann (fig. 35), where Hildreth and others (2003) report 1–3 cm of fine ash. Kovanen and others (2001) refer to the unit as the "Schriebers Meadow scoria," a unit name that commonly excludes the fine ash that is the main constituent throughout most of its extent.

Recognizable tephra set SC ash in soil beyond 20 km northeast of the cinder cone provides a useful marker to distinguish between surfaces of Pleistocene and Holocene age. As discussed in chapter C, the presence or absence of tephra set SC is often key in interpreting the extent of early Holocene alpine glaciers on the south flank of Mount Baker.

About 40 m south of the first switchback on the Scott Paul Trail, there is an outcrop on the left side of Sulphur Creek (RS–17; appendix 1) that contains charcoal fragments in the top 0.5 m of tephra layer SC_1. We obtained three ages of 10.11–9.55, 10.16–9.70, and 10.17–9.71 ka (appendix 2) from that site. Thomas (1997) reported an age of 9.54–9.28 ka for tephra layer SC_1 that appears at least modestly too young because both the tephra and the overlying Sulphur Creek lava are overlain by the Schriebers Meadow lahar (see chapter G), which we and Thomas (1997) have both dated at about 9.5 ka.

The mantle of tephra set SC that initially choked the headwaters of local drainages was rapidly eroded and redeposited in Glacial Lake Baker to form volcaniclastic facies Vhc and Vu (figs. 17, 18). Charcoal from facies Vhc yielded a date of 9.69–9.54 ka at RS–10 (unit 3, appendix 1), suggesting deposition during and likely soon after the tephra-producing eruptions.

Whole-rock X-ray fluorescence analysis on a single large lapillus yields a composition of 51.4 percent SiO_2 (appendix 5) and microprobe analyses of three glass shards from scoria at the summit of Schriebers Meadow cinder cone averaged 58.6 percent SiO_2. Ryane (2009) conducted an extensive microprobe study of the glass shard population of the scoria and reports a bimodal composition, with two distinct populations of 51–54 percent and 58–62 percent SiO_2. The bimodal composition of tephra set SC could support the contention of Green (1988) that magma mixing was the trigger for the Schriebers Meadow cinder cone eruptions. If glass shard populations in Ryane's 2009 study are microlite free, then the two magmatic components may be basalt and andesite rather than basalt and basaltic andesite, as suggested by Green (1988). It should be noted that the Sulphur Creek lava flow (discussed below) is also bimodal in composition and appears to postdate the tephra-forming portion of the Schriebers Meadow cinder cone eruption.

Sulphur Creek Lava Flow

The Sulphur Creek lava flow erupted from the base of the Schriebers Meadow cinder cone and covers an area of 24 km^2. It extends 8 km downstream in Rocky Creek and more than 11 km downstream in Sulphur Creek and Baker River valleys (fig. 20). Its estimated volume of at least 0.5 km^3 (Tucker and Scott, 2009) makes it the largest Holocene lava flow in the Washington Cascade Range north of Mount Adams. The lava flow overlies the tephra set SC (Kovanen and others, 2001; Hildreth and others, 2003; Tucker and Scott, 2009) and is constrained in age between tephra set SC (ca. 9.8 ka) and the overlying Schriebers Meadow lahar (ca 9.5 ka, chapter G).

Proximal and medial portions of the lava are basaltic andesite (55–56 percent SiO_2; Green, 1988), as is the terminus in Sandy Creek (fig. 26). However, the distal lava exposures near Baker Lake reservoir are basalt (51–52 percent SiO_2; Hildreth and others, 2003; Baggerman and DeBari, 2011; Moore and DeBari, 2011). Except for minor differences in phenocryst sizes and the proportion of pyroxenes (Green, 1988; Tucker and Scott, 2009), the two lava types are difficult to distinguish in the field. Field relations show that the basaltic lava erupted first, followed by the basaltic andesite.

The change in chemical composition indicates that the Sulphur Creek lava flow is either compositionally zoned (Tucker and Scott, 2009), or that multiple flows are present (Hildreth and others, 2003); however, no contacts between two or more flows have been found. At the full-pool shoreline of Baker Lake reservoir, 300 m south of the mouth of Sandy Creek (fig. 26), lava with different compositions is found at two sites 150 m apart: the lower and more distal sample is basaltic andesite, the reverse of the expected relation discussed above. We surmise that the lower elevation and more distal basaltic-andesite lava flowed around the basaltic lava to its shoreline location.

Stream incision exposes the base of the basaltic andesite lava flow in Rocky and Sulphur Creeks below about 440 m altitude. At those locations, a single 4- to 5-m-thick lava flow overlies tephra set SC; contact between units is sharp. Basal breccia is less than 0.5 m thick and is locally absent. Crude, local basal columnar joints, as much as 2.0 m in height and 0.5–0.75 m in width, grade into the vesicular flow interior.

The basalt flow reached the Baker River valley when Glacial Lake Baker filled the valley. Evidence of a high lake level at this time is most dramatically seen where >25 m of deltaic crossbedded lacustrine deposits overlie the lava in Sulphur Creek near the head of Lake Shannon (RS–7, table 3; fig. 15). At Horseshoe Cove, fine-grained lake deposits containing tephra layer O (facies Mhc_2; RS–10, table 3; figs. 17, 18) overlie deltaic volcaniclastic sediment (facies Vhc) from the Schriebers Meadow cinder cone. Additionally, near the mouth of Sandy Creek, lava rests directly on Vashon Drift (fig. 38).

Exposures of basaltic Sulphur Creek lava are found 12 m above the peak reservoir level on the east side of the Baker River valley, at an altitude of 761 ft (232 m; RS–11, appendix 1; fig. 26). The lava flow thickness here is about 15 m and the flow is at least 30 m above the altitude of the fractured dense lava (660 ft, 202 m; Swiger, 1958) on the west side of the reservoir. Prior to construction of the Upper Baker Dam, Stone and Webster Engineering drilled hole S (fig. 25) through the lava on the west side of the Baker River valley at a location that is now in the Horseshoe Cove campground. The base of the lava was found at an elevation of 450 ft (148 m) and the lava's total thickness was measured at about 65 m. As the lava moved down the Sulphur Creek valley, it flowed into Glacial

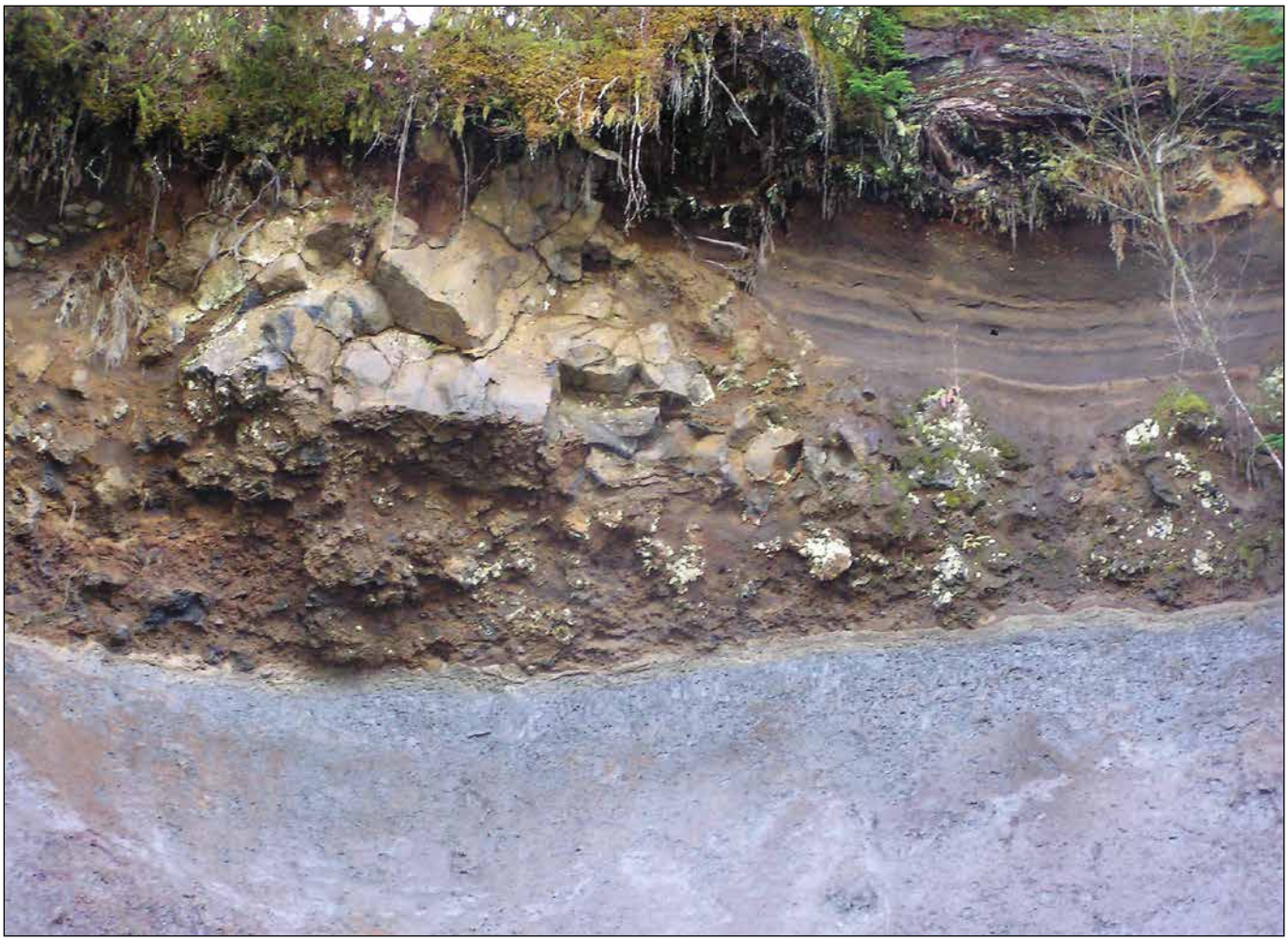

Figure 38. Photograph of Sulphur Creek lava (basaltic andesite) overlying blue Vashon Drift and underlying stratified lake deposits of Glacial Lake Baker (upper right). Location is 150 meters upstream of the mouth of Sandy Creek, right bank. Field of view is approximately 5 meters across. Photograph by D.S. Tucker.

Lake Baker and continued eastward; a thin finger or lobe reached the altitude found at RS–11. We present the following hypotheses to explain this 30 m difference of elevation between the west and east sides that suggests the lava flowed considerably uphill.

1. The Baker River valley was filled with lava. After crossing the valley with hydraulic continuity (more-or-less constant eastward slope) to contact the east valley side, flow was diverted downvalley, partially emptying the initially lava-filled reach (that is, axial drain-away). However, the mapped pre-reservoir lava distribution (fig. 26) records no diversion of flow downstream.

2. As in (1), the Baker River valley was completely filled with lava, but much of it was then removed by erosion to form the existing valley. In this case, a huge volume of lava would have to have been removed during a relatively benign flow regime (meandering river) across the entire valley, after which the erosional regime changed, and vertical incision occurred (as shown by hachure marks in fig. 26) to carve the steep canyon in the meanders. The highest lava on the east valley side is now approximately 50 m above the thalweg of the subsequently incised Baker River and at least 100 m above the lava-buried thalweg at drill hole S. The removal of an erosion-resistant lithology to a depth of 50 m across nearly the entire valley is highly improbable.

3. The lava entered Glacial Lake Baker and invaded the thick lake deposits, continuing to flow internally beneath a chilled upper portion, with confining pressure from a lake that was more than 100 m deep and an overburden of invaded sediment and peperite carapace probably in excess of 10 m thick. The confining hydrostatic and lithostatic pressure allowed the lava, with a prolonged and high rate of flux, to flow uphill on the east valley-side slope.

Although speculative, we favor the last hypothesis as we find no evidence to support hypothesis 1 or 2.

Tephra Layer MY (Early Holocene)

A thin (1–2 mm) lithic tephra composed of altered material at RS–5 (appendix 1; figs. 3, 36) was noted by J.J. Clague during joint investigations of Holocene glacial deposits and tephras (Davis and others, 2005). Subsequent analysis of the tephra did not reveal the presence of juvenile glass (C. Ryane, written commun., 2005), suggesting a phreatic origin. This tephra, designated tephra layer MY, is considered to be the earliest evidence of alteration and eruptive activity at, or near, the vicinity of Sherman Crater—the source for several younger Holocene phreatic tephras. Although we cannot absolutely discount Carmelo Crater as a source, we think it unlikely owing to the lack of alteration in other deposits from this vent area.

Dates obtained by J.J. Clague (written commun., 2006) on a hydrothermally altered tephra (presumably layer MY) at RS–18 (appendix 1) are 9.28–8.78 ka from charcoal in soil directly above the layer and 9.40–8.77 ka from charcoal in soil directly below the layer. At RS–5, tephra layer MY is bracketed between two soil layers with charcoal yielding ages of 9.44–9.13 in the upper soil and 9.46–9.14 and 9.44–9.14 ka in the lower soil. Ages from these two sites overlap and support the correlation. These hydrothermally altered layers are known only on the flank directly south (downslope) of Sherman Crater. We have too little data to constrain volumes for this layer, but suggest it is likely much less than 1×10^6 cubic meters (m^3).

Tephra Layer O (Middle Holocene)

Tephra layer O, erupted during the climactic eruption of Mount Mazama (Bacon, 1983) at the site of Crater Lake in southern Oregon, forms a nearly ubiquitous and useful stratigraphic marker at Mount Baker (figs. 36, 39). It is dated at 7.79–7.60 ka by Bacon (1983), 7.67–7.51 ka by Hallet and others (1997), and at 7.63±150 cal. yr B.P. from ice cores by Zdanowicz and others (1999). We favor the slightly younger age of 7.6 ka from the accelerator mass spectrometer (Hallet and others, 1997) and ice core data (Zdanowicz and others, 1999).

The pale orange-brown (moist 10YR 6/3, dry l0YR 8/3) ash layer ranges from 0.5 cm to as much as 10 cm in thickness where reworked. Scanning electron microscope examination shows that fine-ash glass fragments are well-sorted pumice or bubble-wall shards. Where other tephras are present, tephra layer O is generally separated from underlying tephra set SC or layer MY by a thin soil layer. Particle size of the constituent glass particles is confined to silt- and clay-size ranges (very fine ash). The fine grain size and juvenile glass shards prevent confusion with similarly light-colored deposits, tephra sets OP and YP, from Mount Baker that consist entirely of hydrothermally altered material.

Tephra Set OP (Middle Holocene)

Tephra set OP (Scott and others, 2001; the Rocky Creek ash of Kovanen and others, 2001) forms the basal part of a distinctive black (tephra layer BA) over white tephra couplet on the south flank of Mount Baker that was initially reported to us by W. Hildreth (see discussion in Hildreth and others, 2003). Tephra set OP is a distinctively mottled white (2.5YR 8/0 moist) to pale yellow (2.5Y 8/4 moist) lithic tephra that is typically 1- to >5-cm thick (figs. 36, 39). In places, it mobilized into lahar-like deposits as much as 1-m thick, suggesting wet deposition and downslope movement. The poorly sorted tephra (table 7) consists mainly of angular, 2–4 mm fragments of phreatic lapilli fining distally to ash. The tephra is thickest at altitude 3,980 ft (1,176 m) in the middle-northern tributary of Sulphur Creek, where it may be ponded. There, some intervals are quite coarse (for example, a 15-cm layer contains angular lithic lapilli to 4–6 mm). Where the tephra deposit is >5 cm thick, a 2 cm or less basal ash layer may be present. The presence of the basal ash layer is why we describe the OP tephra as a set rather than a layer. Deposits are thickest on the south flank of Sherman Crater; thus, a source other than Sherman Crater is unlikely.

Tephra set OP (Scott and others, 2001) is widespread on the south side of Mount Baker (fig. 40) but is notably less extensive than succeeding juvenile tephra layer BA. We have not seen tephra set OP without overlying layer BA, although in places layer BA occurs without set OP. We estimate a volume of about 3×10^6 m^3 for tephra set OP, but with high uncertainty.

Macroscopically, tephra set OP may be confused with layer O. The tephras are similar in color, but tephra set OP has a more yellowish hue. Where both are present, they are commonly separated by 2–15 cm of organic-rich soil containing charcoal and decomposed wood (fig. 39) that represents the almost millennium difference in age. Importantly, tephra set OP does not contain juvenile glass shards and is distinctively coarser grained than layer O, with lithic lapilli generally present (except in the local basal ash layer).

Charcoal fragments in the main OP layer at the junction of the Scott Paul and Park Butte Trails yield a date of 6.73–6.49 ka and wood just below the layer yields a date of 6.83–6.50 ka (appendix 2). Wood fragments in the tephra near the junction of the Park Butte and Railroad Grade Trails yield three dates of 7.14–6.79, 6.99–6.73, and 7.17–6.95 ka (appendix 2). Two other dates related to the age of tephra set OP include charcoal at the contact of set OP with the overlying tephra layer BA (6.67–6.44 ka) and charcoal in soil that overlies both tephra set OP and layer BA (6.27–5.95 ka); the latter date provides a minimum limiting age for the OP-BA tephra couplet.

Researchers have described and dated what appears to be tephra set OP at other localities and given it the following names: (1) the undated Morovitz tephra described by Thomas (1997) west of Rocky Creek, (2) the undated Crag View ash

Figure 39. Photograph of the tephra sequence above the early Holocene Schriebers Meadow lahar (ca. 9.5 thousand years [ka]) on Park Butte Trail beyond the junction with the Railroad Grade Trail in Morovits Park (figs. 3, 4). Yellow-colored tephra set OP (6.7 ka) overlies soil above Mount Mazama tephra layer O (ca. 7.6 ka; Zdanowicz and others, 1999) and underlies tephra layer BA (6.7 ka). Photograph by D.S. Tucker. ca., circa.

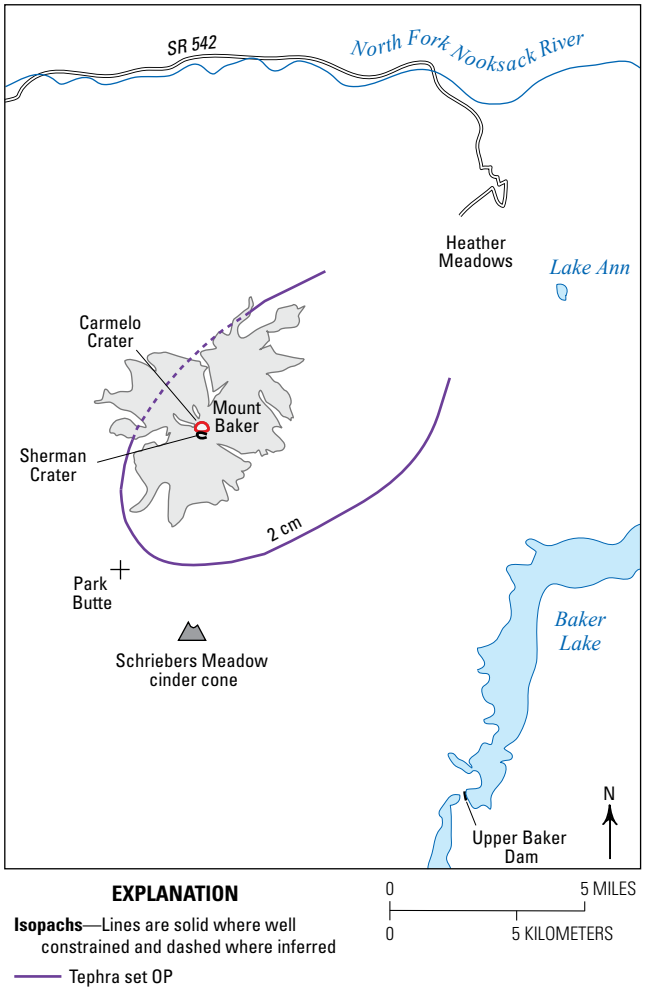

Figure 40. Schematic map of the distribution of tephra set OP showing the 2-centimeter (cm) isopach. Gray area is upper edifice of Mount Baker showing present-day glacier distribution. Distal tephra extent is unknown.

described by Thomas (1997) in terrain east of Sulphur Creek, (3) the unnamed coarse, white tephra with detrital minerals described by Kovanen and Easterbrook (1999), and (4) a tephra initially described as probable layer O (Kovanen and Easterbrook, 1996) and subsequently as the Rocky Creek ash (Kovanen and others, 2001) with an age between 6.72–6.45 and 6.96–6.19 ka (appendix 3).

Tephra Layer BA (Middle Holocene)

Tephra layer BA, a black (2.5YR 2/0 to 2.5 YR 3/0) andesitic tephra, directly overlies and forms the upper part of the distinctive couplet with tephra set OP (figs. 36, 39). Layer BA (Scott and others, 2001; the post-Mazama black ash of Hyde and Crandell, 1978; and the Cathedral Crag ash of Kovanen and others, 2001) is as much as 60 cm thick within 5–6 km northeast of the summit and is extensively exposed on the south, east, and northeast flanks of the volcano (fig. 41). The tephra consists of fully to partially glassy clasts containing the following phenocryst assemblage: plagioclase>clinopy-roxene>orthopyroxene>oxides. Some of the coarsest clasts (4–5 cm lapilli) are prominent on the crest of Lava Divide (figs. 3, 5), 7 km east of Sherman Crater, although the majority of the tephra is much finer grained (table 7). The tephra thins rapidly to the west and was not found in some meadows only 10 km west of Sherman Crater. Because the layer is loose, granular, and easily eroded, extensive remobilization and bioturbation have occurred. Stratification at some localities suggests multiple eruptions or shifting winds. At several localities, the contact between tephra set OP and layer BA consists of interbedded layers of each that may reflect alternating eruptions of lithic and juvenile material in a semicontinuous eruption. A whole-rock X-ray fluorescence analysis of a large lapillus from tephra layer BA

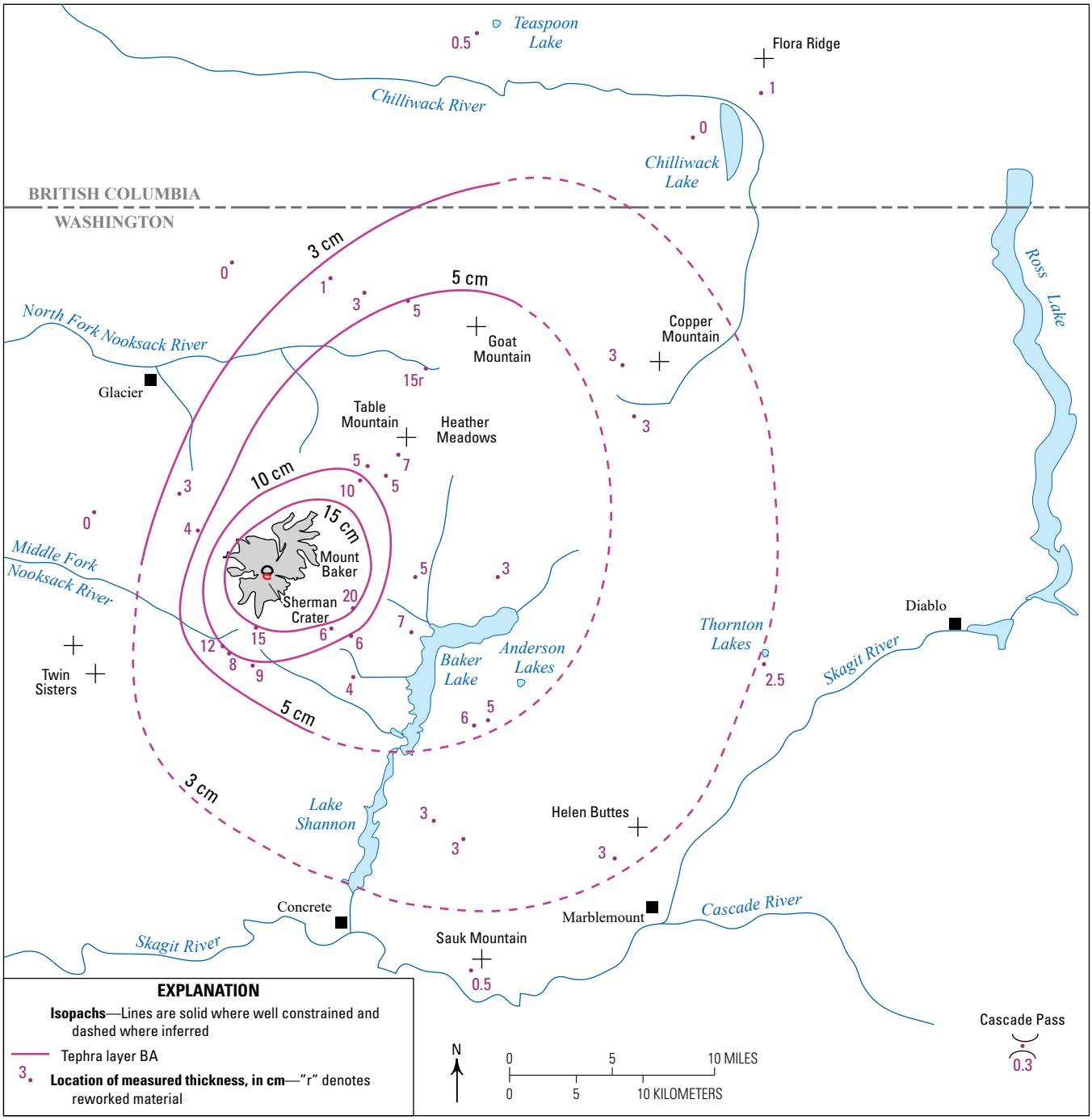

Figure 41. Map of the distribution of tephra layer BA showing isopachs of 15, 10, 5, and 3 centimeters (cm). Gray area is the upper edifice of Mount Baker showing present-day glacier distribution.

(MB-411; Hildreth and others, 2003) yielded a SiO_2 content of 62.1 percent. Microprobe data show a narrow range in glass chemistry from 67.5 to 68.5 percent SiO_2 (appendix 5).

Tephra layer BA is magmatic in origin and is the largest and most extensive post-Vashon tephra from Mount Baker—it is likely the most voluminous of all Mount Baker tephras. It extends at least to Cascade Pass (fig. 41), 66 km southeast of Mount Baker, where a light-gray, 0.3–0.8-cm-thick fine ash has a glass chemistry similar to that of tephra layer BA (Mierendorf and Foit, 2008). At that locality, it lies a few centimeters beneath the Dusty Creek ash of Glacier Peak (Beget, 1984), dated at ca. 5.8 ka (Foit and others, 2004), 6.29–5.81 ka (Beget, 1984), and 5.91–5.73 ka (Hallet and others, 2001). Hyde and Crandell (1978) report a maximum thickness of 60 cm near Table Mountain (fig. 41), 11 km northeast of Mount Baker, but that thickness probably includes

remobilized material because the typical thickness at that distance is closer to 10 cm. The tephra is also reported at the area locally known as Copper Ridge, 33 km northeast of the summit (Mierendorf, 1999). We calculate a volume of 0.2 km^3 bulk (~0.08 km dense-rock equivalent; see table 17) using isopach values (fig. 41) and the method of Fierstein and Nathenson (1992). The volume is at the upper end of previous estimates (Hyde and Crandell, 1978; Gardner and others, 1995) and about twice that estimated by Hildreth and others (2003).

Published ages for tephra layer BA vary over several thousand years. Hildreth and others (2003) report ages of 6.92–6.40 and 6.95–6.28 ka from the Swift Creek watershed, where underlying tephra set OP is not present. Kovanen and others (2001; table 1) report four dates from organic material beneath their Cathedral Crag ash (tephra layer BA) between 7.42–6.81 and 7.57–7.33 ka and two minimum ages of 5.30–4.84 and 4.81–4.15 ka in peat above the Cathedral Crag ash. They reject the minimum ages owing to concerns of contamination by younger rootlets and prefer a maximum limiting age of 7.25–7.00 ka obtained by Burrows and others (2000) from a lake core. Mierendorf (1999) reports an age of 7.16–6.68 ka from charcoal in 5 cm of a "brown sandy tephra" that is likely tephra layer BA.

Tephra layer BA directly overlies (and locally is interbedded with) tephra set OP and therefore their ages should be the same. Charcoal from a trailside exposure (where layer BA overlies set OP) at the junction of the Scott Paul and Park Butte Trails yields a date of 6.66–6.42 ka. At RS–19 (appendix 1), tephra set OP is discontinuous. Charcoal fragments in tephra layer BA where it overlies tephra set OP yield dates of 6.64–6.41 and 6.95–6.28 ka and where set OP is absent, charcoal in a thin organic-rich soil beneath layer BA yields an age of 7.24–6.94 ka (appendixes 2, 3). Charcoal from layer BA on a flat terrace on the right bank of Swift Creek (RS–22, appendix 1) yields ages of 6.62–6.35 and 6.56–6.32 ka. Our tephra set OP and tephra layer BA ages overlap considerably at 2σ uncertainties.

Tephra Set YP (1843 C.E.)

In 1843 C.E., an eruption of Mount Baker "covered the whole country with ashes." The Skagit River reportedly was temporarily dammed by "cinders and ashes brought down by the Hukullum [Baker River]," "all the fish died," and subsequently "smoke [was] frequently seen rising from the mountain" (Gibbs, 1873, p. 358). Several historical accounts (appendix 6) suggest explosive activity that formed the modern configuration of Sherman Crater. The eruption produced tephra set YP (Scott and others, 2001), a poorly sorted (sorting = 4.14; table 7), grayish-yellow (5YR 8/4) to locally light-gray (10R 7/1) tephra composed of highly variable amounts of altered lithic particles (fig. 42). It is typically 1 to 3 cm thick and is widespread as far as 13 km northeast of Sherman Crater (fig. 43). It is best displayed along the Boulder Ridge Trail, where it is 2 to 5 cm thick. In trailside exposures approaching Boulder Glacier, tephra thickness increases to more than 10 cm, grain size coarsens, and the deposit grades to a flowage deposit (similar to tephra set OP), suggesting wet deposition and downslope movement.

Only one significant primary layer of tephra set YP has been seen at a single stratigraphic level, but we designate it as a tephra set rather than a layer to include clearly subsequent minor layers. Thin (several mm) local layers—in cases, simply concentrations of dispersed tephra particles like those in the main layer of tephra set YP—appear as "dusty" zones, probably of airfall origin, within thick forest litter at slightly higher stratigraphic intervals. These layers may correspond with some of the eruptions from Sherman Crater reported between 1843 and 1880 C.E., such those of 1854, 1856, 1858, and 1860 C.E. (appendix 6). The 1860 C.E. report describes eruption clouds "rolling" down the flanks. We include these possibly younger layers in tephra set YP.

The main tephra layer consists of sand-, silt-, and clay-sized particles (table 7), but contains fine lapilli near Sherman Crater. The dominant component is hydrothermally altered clasts where the original mineralogy is obscured by alteration. Much coarser, lithologically comparable debris mantling the crater rim and nearby cleavers is inferred to be, at least in part, the proximal deposits of the tephra and (or) possibly of later 19th-century explosions. Isolated, white altered blocks are found as far as 3–5 km south of Sherman Crater—whether explosively emplaced or transported glacially downslope is unknown. Many such bombs contain opalized silica and are veined with 0.3–1 cm sulphur crystals. These "sulphur bombs" (Thomas, 1997), suggesting violent explosions and ballistic ejection, are also seen in tephra set YP deposits on the Chromatic Moraine north of the volcano, as described below. Distally, the tephra set YP rapidly transitions to a layer of gray dusty ash (silt- and clay-size particles) infiltrated into the root zone.

A tephra sample collected (by J. Fierstein) from bare bedrock in the headwaters of Park Creek, and therefore

Figure 42. Photograph of tephra set YP beneath modern organic-rich duff layer and above colluviated soil layer. Photograph by D.S. Tucker.

uncontaminated by mixing with any pre-19th-century tephra, contains only nonjuvenile components.

The main layer of tephra set YP has a northeastward extent similar to the middle Holocene tephra set OP and layer BA, also inferred to be from Sherman Crater. The 1-cm isopach is estimated to extend as far as 8–10 km to the northeast, transitioning gradually to a dusty concentration in the root zone thereafter (fig. 42). Previously, we proposed that a more widespread gray layer might be a juvenile product of a second tephra set YP eruption (Tucker and Scott, 2006; Tucker and others, 2007). We now discount this hypothesis because field observations with C.A.D. Briggs and T.M. Rodgers, soil scientists with the U.S. Department of Agriculture, indicate that the gray layer is probably the leached, ashen-white E horizon of a spodosol (see Briggs and others, 2006).

We estimate a volume of about $1–2\times10^6$ m^3 for the main tephra set, but with high uncertainty, likely of a factor of two or more.

Sometime between 1843 and 1850 C.E., a major regional storm resulted in flooding throughout the Skagit River floodplain. The event extensively remobilized particles of tephra set YP, depositing them as bright mud coatings on trees that were for decades cause for comment ("marks of the Great Spirit") by Native Americans and pioneers (appendix 8). At RS–20, evidence for flood remobilization includes tephra set YP deposits in the overbank stratigraphy of terraces at locations far outside the area of primary airfall.

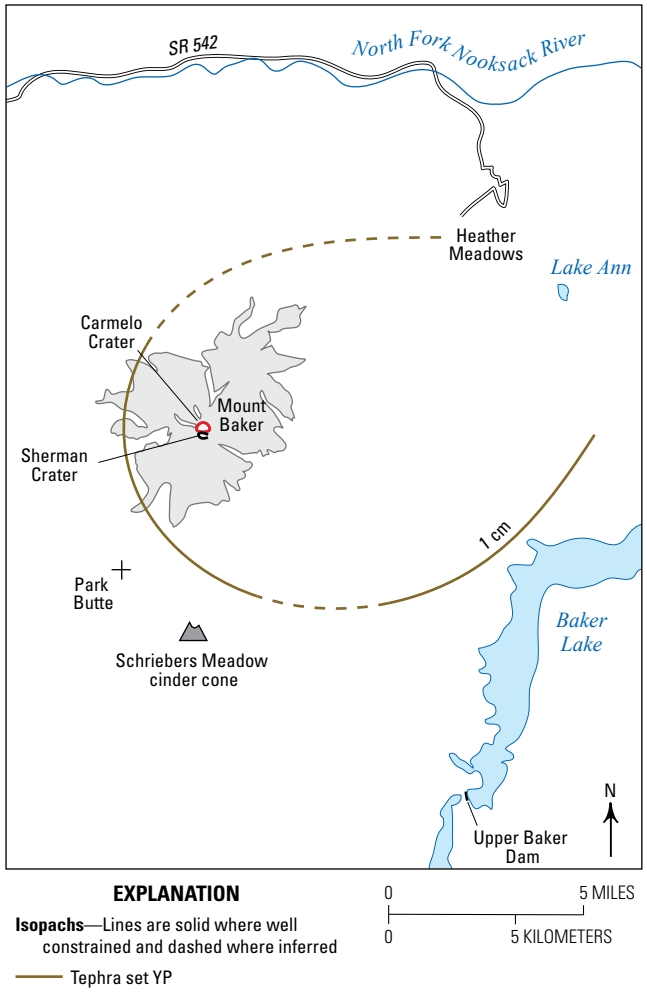

Figure 43. Schematic map of the distribution of tephra set YP showing the 1-centimeter isopach. Gray area is upper edifice of Mount Baker showing present-day glacier distribution. Distal extent of tephra is unknown.

Hydrothermally Altered Deposits Associated with Tephra Set YP Inset on Chromatic Moraine

As described in chapter C, the right-lateral Little Ice Age moraine of Roosevelt Glacier in Glacier Creek is mantled by pale-colored, poorly sorted clastic debris as much as 5 m thick (fig. 12). In addition, approximately 2 m of pale-colored hydrothermally altered material associated with tephra set YP is inset against the lateral moraine. This inset relation suggests that the maximum Little Ice Age extent of Roosevelt Glacier occurred significantly before 1843 C.E. because the highest of the tephra set YP deposits is inset more than 30 m below the morainal crest. Heikkinen (1984) gives a dendrochronologic date on the moraine of 1740 C.E. The inset tephra-set-YP-like deposits include what must have been ballistically ejected blocks, including boulder-size ejecta that may have fallen on upper Roosevelt Glacier or the summit icefield. Either the tephra-set-YP-like deposits traveled as superglacial drift to accrete against the Little Ice Age moraine, or the possibly hot ejecta mixed with meltwater and flowed directly to the moraine.

The inset deposit was analyzed by W. Hildreth (written commun., 2002). Excluding blocks, the deposit consisted of clasts as large as coarse pebbles (32 mm; −5 ϕ) with the following components: fresh andesite with trivial alteration rinds, 45.7 percent; Nooksack Formation, 25.0 percent; highly altered, cream-white andesite, 17.9 percent; slightly altered andesite, 8.6 percent; opalized vein rock, 2.1 percent; and pale-gray altered rhyolite or dike rock, 0.7 percent. A historical account mentions that a huge white boulder, likely native sulfur, was ignited for a campfire by a climbing party that bivouacked in the area in 1891 C.E. (letter from E.H. Thomas preserved by Easton [written commun., 1911–31]).

Tephra on the Carmelo Crater Rim and Grant Peak

In late summer, particularly in low snow years, a dark band of fragmental ejecta appears at the base of the summit ice plateau of Carmelo Crater (report cover; fig. 44). This band also appears in the summit ice in the first vertical aerial photographs of 1940. The band extends 500 m along the top of the Roman Wall (inset in fig. 3), northward from

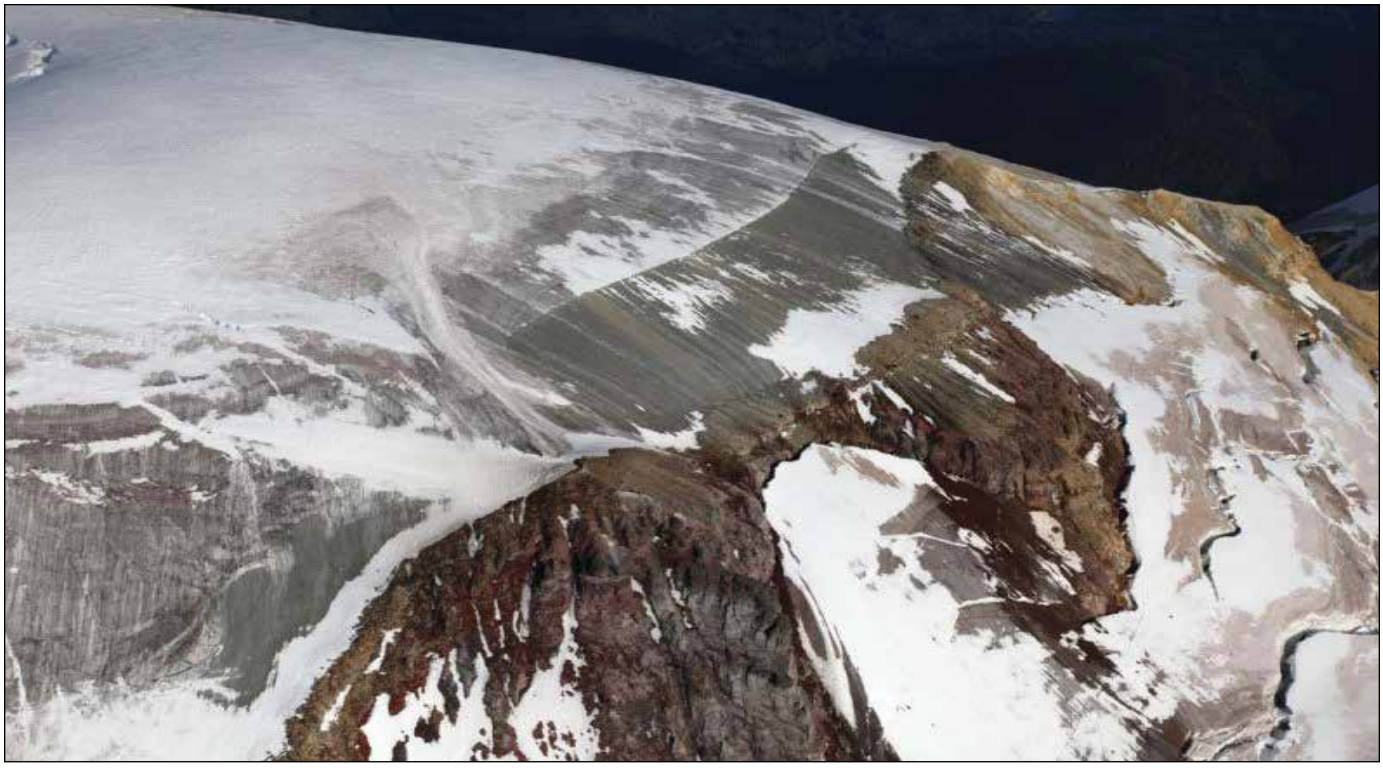

Figure 44. Aerial view to the southeast of fragmental material (dark band) at base of summit ice plateau and Roman Wall. In upper right, the pale-colored, altered bedrock is the northwest rim of Sherman Crater. Photograph by J.H. Scurlock, September 17, 2009, used with permission.

the bedrock crest above the northwest side of Sherman Crater. A geologist crossing the material in 2004 reported that it was fragmental ejecta, "…not ice nor rock contained within ice" (D. McKeever, written commun., 2009). The apparently poorly sorted deposit contains clasts from ash to blocks, coated with pale dust from summit ice meltwater and windblown glacial flour. The few samples we have examined are dense, poorly vesicular andesite, with alteration ranging from sparse pyrite crystals to pervasive argillic alteration; none, however, shows the intense hydrothermal alteration of Sherman Crater deposits.

The summit of Grant Peak, 400 m farther east, is covered with andesitic scoria and bombs (tephra on Grant Peak; size analysis in table 7; samples MB-431 and MB-432 in appendix 5) that is clearly different than the material of the Carmelo Crater rim described above. Glass silica content of the scoria (appendix 5) is similar to tephra set SC from the Schriebers Meadow cinder cone and considerably more mafic in composition than either tephra set SP or tephra layer BA (appendix 5). The tephra on Grant Peak matches the chemistry of a large lapilli lying loose on the surface at altitude 6,500 ft (1,981 m), 500 m northeast of Hadley Peak at the south end of Chowder Ridge (sample MB-651a, appendix 5). Scattered lapilli were lying loose on the surface of deglaciated bedrock. We are unclear of the origin of the tephra on Grant Peak and the lapilli on Chowder Ridge. On the basis of grain size, color, and distribution, they are clearly not from the Schriebers Meadow cinder cone eruption that emplaced tephra set SC. The deposits are clearly magmatic and presumably postglacial. Whether the tephra and lapilli are equivalent to the material forming the fragmental western rim of Carmelo Crater is also unknown. With continued climate amelioration and ice melting, increasing exposure of the fragmental rim and tephra may allow future researchers to decipher the origin and age of these units.

Summary of Latest Pleistocene to Present Tephras at Mount Baker

Tephras at Mount Baker (table 8) are useful local stratigraphic markers for discerning events from latest Pleistocene to historical time periods. Tephra volumes from Mount Baker have been relatively modest ($\leq$0.2 km^3 bulk), especially when compared to the voluminous latest Pleistocene tephras from nearby Glacier Peak (for example, tephra layer B, 6.5 km^3 bulk; Gardner and others, 1998; 1.9–9.4 km^3 bulk, Nathenson, 2017) or to many of the Holocene tephras from Mount St. Helens (0.5–15 km^3 bulk; Gardner and others, 1998; 0.34–9.9 km^3 bulk, Nathenson, 2017). Nonetheless, similar future tephra eruptions from Mount Baker would be both a concern and nuisance for nearby populations and a danger to aviation.

- We infer that tephra set SP was erupted from Carmelo Crater on the basis of distribution and lack of alteration. It is latest Pleistocene in age. All younger tephras from Mount Baker were erupted from satellite vents either at the Schriebers Meadow cinder cone (tephra set SC) or from Sherman Crater (tephra layer MY [inferred], set OP, layer BA, and set YP) during the Holocene.
- Tephra set SC from the Schriebers Meadow cinder cone consists of a basal unit consisting of scoriaceous lapilli and a finer grained ash unit above. It underlies the Sulphur Creek lava flow from the same cinder cone and is the main component of facies Vhc and Vu in Glacial Lake Baker.
- On the basis of distribution and alteration, the phreatic tephra layer MY records the earliest occurrence of hydrothermal alteration likely in the Sherman Crater area.
- At most localities, middle Holocene tephra set OP (phreatic) and layer BA (magmatic) form a couplet with tephra layer BA stratigraphically above set OP and no evidence of a significant time break between them. Locally, however, the tephras are interbedded suggesting periods of alternating phreatic and magmatic activity.
- Tephra layer BA is the most voluminous Mount Baker tephra, with a calculated bulk volume of 0.2 km^3 (about 0.08 km^3 dense-rock equivalent). It is the only magmatic event known from the Mount Baker edifice during the Holocene.
- The youngest dated volcanic deposit from Mount Baker is tephra set YP. Historical accounts (Gibbs, 1873; Easton [written commun., 1911–31]) and dendrochronologic data suggest this eruption took place in the fall of 1843 C.E. It appears to be purely a phreatic deposit as it contains no fresh glass shards. Thin tephra layers in the upper part of the set likely represent smaller sporadic phreatic eruptions that may have persisted until about 1880 C.E.
- The tephras on the rim of Carmelo Crater and Grant Peak remain enigmatic. Glass composition (appendix 5) is similar to the andesite scoria from Schriebers Meadow cinder cone (tephra set SC), but tephra size and distribution make that source unlikely. The tephras appear magmatic and postglacial, but neither source vent nor age is known.

Table 8. Summary of known tephras at Mount Baker showing age, bulk composition and texture, type of eruptive activity, distribution of the main layer, and source vent (glass compositions are in appendix 5).

[ca., circa; ka, thousand years; km, kilometers; NA, not applicable]

Tephra	Age (main layer)	Bulk composition and texture	Volcanic activity	Distribution of main layer	Source vent
Set YP	1843 C.E.	Altered lithic ash and lapilli	Phreatic	13 km northeast	Sherman Crater
Layer BA	ca. 6.7 ka	Andesitic ash and lapilli	Magmatic	33 km northeast[1], 66 km southeast	Sherman Crater
Set OP	ca. 6.7 ka	Altered lithic ash and lapilli	Phreatic	15 km northeast	Sherman Crater
Layer O[2]	ca. 7.6 ka	Rhyodacitic ash	Magmatic	NA	Mount Mazama (Crater Lake)
Layer MY[3]	ca. 9.1 ka	Altered lithic ash	Phreatic	4 km south	Sherman Crater
Set SC	ca. 9.8 ka	Basaltic ash and lapilli	Magmatic	4 km northeast (as scoria lapilli); 20 km northeast (as ash)	Schriebers Meadow cinder cone
Set SP	ca. 12.7 ka	Andesitic ash	Magmatic	5 km south[4]	Carmelo Crater

[1]Reported from Copper Lake by Mierendorf (1999).

[2]Bacon (1983); Zdanowicz and others (1999).

[3]J.J. Clague (written commun., 2005).

[4]Probably was more extensive, but fell during late glacial times.

Chapter G

Mount Baker Volcano, Northern Casade Range, Washington

View looking northeast of altered lava and pyroclastic deposits of the south rim of Sherman Crater. Failure of altered rock gives rise to debris avalanches, lahars, and debris flows at Mount Baker. Photograph by John H. Scurlock, August 8, 2008, used with permission.

Chapter G

Holocene Syneruptive Lahars and Noneruptive Debris Flows

Lahars are the most far-reaching Holocene deposits from Mount Baker, the largest of which are associated with middle Holocene eruptive activity. During Holocene eruptive activity, lahars have resulted primarily from flank failures. During noneruptive periods, lahars are largely associated with meteorological events, glacial outbursts, or landslides of water-saturated glacial material, and are generally much smaller than the lahars from eruption-related flank collapses. To distinguish between eruptive and noneruptive lahars, we designated the latter as debris flows, although they fit the most common definition of a lahar (debris flow on or from a volcano). In addition to Holocene lahars, we describe the two largest debris flows, the ca. 1.7 ka debris flow at Elbow Lake Trailhead (BF–5, appendix 1; figs. 3, 10) and the 1927 C.E. Deming Glacier debris flow, as well as several smaller 19th- and 20th-century debris flows whose deposits crop out primarily in several of the southern and eastern drainages.

Schriebers Meadow Lahar (Early Holocene)

The Schriebers Meadow lahar, the earliest Holocene lahar of consequence, began as a flank collapse on Mount Baker upslope from Schriebers Meadow. The exact location of failure and cause are unknown. It is distributed from Ridley Creek to Sulphur Creek and forms the meadow surface surrounding the Schriebers Meadow cinder cone, where it is between 1.7 and 2.8 m thick (RS–21, appendix 1; fig. 3). Overall, the lahar ranges from 1.5 to 7.0 m thick, is distinctively orange to reddish brown (5YR 3/3 to 5YR 4/3) and is composed of predominantly subangular pebble- to cobble-size clasts of unaltered Mount Baker lithologies in a clay-rich matrix (table 9). Matrix clay and matrix silt and clay are about 9 and 35 percent, respectively. As the lahar

Table 9. Statistical measurements of lahar grain size and sorting at Mount Baker.

[Graphical measures after Folk (1980); $\phi = -\log_2$(size in mm). Laboratory analyses by dry or wet sieving. Sedigraph analysis of fine sediment. Percentages of individual coarse fractions (>−1.0 ϕ; 2 mm) and of total matrix (<−1.0 ϕ; 2 mm) are field measurements. mm, millimeter; NA, not applicable]

Deposit	Mean diameter (ϕ)	Sorting	Skewness	Kurtosis	Clay[1]	Silt + clay[1]	Matrix clay[2]	Matrix silt + clay[2]	Matrix[3]
	Mz	σ_G	Sk_G	K_G	%	%	%	%	%
Schriebers Meadow lahar									
RS–17	−1.84	3.31	+0.46	0.93	2.9	11.5	8.7	34.5	33
Middle Fork lahar									
RS–24	0.45	3.53	+0.16	0.94	6.5	19.7	10.7	32.4	60
RS–26	−1.78	4.89	+0.55	0.76	3.8	14.2	8.8	33.0	43
Ridley Creek lahar									
RS–24	−2.17	3.71	+0.37	0.96	2.5	7.0	8.7	21.8	32
RS-26	1.41	4.67	+0.06	0.89	7.0	25.0	10.1	36.2	69
Park Creek (PC_1) lahar									
RS–22	−0.40	3.69	+0.25	0.82	3.4	13.9	3.6	25.3	55
Morovitz Creek lahar									
RS–27[4]	−0.12	3.54	+0.25	0.83	3.0[4]	12.0[4]	5.8	22.6	53
RS–28[4]	−3.73	4.83	+0.34	0.76	1.0[4]	3.5[4]	5.0	17.5	20
Young lahar at RS–29	−0.55	3.51	+0.31	0.99	5.5	17.5	13.6	30.0	41
Rainbow Creek debris avalanche	1.59	3.92	+0.14	0.82	2.6	16.1	3.8	23.0	70

[1]Refers to texture of entire deposit.

[2]Refers to texture of matrix only.

[3]Proportion of sand, silt, and clay in total deposit.

[4]Dispersing agent treatment not completely effective; clay content underestimated.

descended the southwest flank of the volcano, it incorporated easily erodible tephra set SC (fig. 45)—much of the orange lahar color comes from the tephra. The estimated volume of the lahar is about 30×10^6 m^3 and the estimated runout distance is greater than 20 km (table 10).

The Railroad Grade interfluve (figs. 3, 4) funneled material to the west and to the east. The western branch covered much of the lower Railroad Grade interfluve between the west fork of Rocky Creek and Middle Fork Nooksack River and in this vicinity can be mistaken for the texturally similar, but considerably younger, middle Holocene Middle Fork lahar. In Ridley Creek (RS–15, appendix 1), the 2.2-m-thick Schriebers Meadow lahar lies between two soil layers. The lower soil separates the lahar from the underlying Pratt Creek assemblage and the upper soil separates the lahar from the middle Holocene Ridley Creek lahar. The eastern branch entered Sulphur and Rocky Creek valleys. In Sulphur Creek, it attenuated rapidly on the rough surface of the Sulphur Creek lava flow (see chapters D, F) and did not extend more than 1.5 km beyond Schriebers Meadow. In Rocky Creek, however, the lahar inundated much of the lava-flow surface south of the Schriebers Meadow cinder cone and entered lower Rocky Creek, but it is not documented to have reached the Baker River. On the northwest side of the cinder cone, lahar deposits (unit 2, RS–21, appendix 1) are as much as 5 m above the meadow surface.

The lahar is dated from several localities along Sulphur Creek (appendixes 1, 2, 3). At RS–21, the outermost several rings of two logs with outer bark yield dates of 9.54–9.47 and 9.53–9.42 ka. Other dates from outer rings of logs in the lahar along the reach containing RS–21 are 9.60–9.31, 9.67–9.29, and 9.54–9.15 ka. Thomas (1997) also collected samples of charred wood from the unit that yielded dates of 9.90–9.12 and 9.77–9.03 ka. The similarity of ages constrains the age of the lahar to about 9.5 ka.

Figure 45. Photograph of Schriebers Meadow lahar (~9.5 thousand years old [ka]) near RS–21 (east side of Schriebers Meadow, left bank Sulphur Creek), where it is directly overlain by tephra layer O (7.6 ka) from Mount Mazama (Crater Lake) and reworked material from upstream Ridley Creek lahar. Glove at left is at contact with tephra layer O. Photograph by K.M. Scott.

Table 10. Summary of major debris-avalanche, lahar, and debris-flow activity at Mount Baker during the Holocene.

[C.E., common era; ka, thousand years; m, meters; km, kilometers; NA, not applicable; %, percent]

Lahar	Age	Deposit volume[a] ($10^6\times m^3$)	Estimated bulked sediment[b] (%)	Collapse (failure) volume[c] ($10^6\times m^3$)	Runout distance[d] (km)
Deming Glacier debris flow	June 1927 C.E.	10	100	NA	4.7 as debris flow; 12 as flood
Second Rainbow Creek debris avalanche	Between 1917 and 1932 C.E.	7	10 (?)	6	4.9
Second lahar in Boulder Creek	1858(?) C.E.	2	20	<2	12
First Rainbow Creek debris avalanche	1889–90 C.E.	20	15	15–20	10.2
Morovitz Creek lahar	1845–47 C.E.	20	40	12	>16
Debris flow at Elbow Lake Trailhead	1.715–1.565 ka	10	100	NA	6
Ridley Creek lahar	~6.7 ka[e]	150	15	130	>32
Middle Fork lahar	6.889–6.534 ka	240	25	180	>63
Second Park Creek lahar	After the first lahar	1–2	NA	2–4	>12
First Park Creek lahar	6.889–6.645 ka	35	10	30	>16
Schriebers Meadow lahar	9.665–9.145 ka	27	10	24	>20

[a]Volumes are estimated total volume including material incorporated (bulked sediment) during flow.

[b]Bulked material is identified by composition (percentage of Mount Baker versus non-Mount Baker rocks) and roundness (reflecting previous fluvial transport). Bulking factor of 100 percent reflects flow origin as a flood surge.

[c]Collapse volume of early and middle Holocene events determined by deposit volumes reduced to exclude bulked material.

[d]Runout distances are known runout distances of primary deposits (for example, avalanches, debris flows, or lahars) or of known transitional deposits (for example, floods). In many cases, the total runout distance of either the primary or transitional deposit is unknown; thus, runout distances are known minima.

[e]Wiggle-match age using ^{13}C correction.

Park Creek Lahars (Middle Holocene)

We recognize two middle Holocene clay-rich lahars in Park Creek (fig. 3). The larger one (PC_1) was followed shortly, if not immediately, by a smaller, texturally similar flow (PC_2). The lahars originated as a flank collapse(s) in the headwaters of Park Creek (fig. 46) and have a cumulative thickness of as much as 6.4 m where exposed in lower Swift Creek (RS–22). Both PC_1 and PC_2 have angular to subangular clasts of Mount Baker andesite set in a gray (5Y 6/1) or tan-to-yellowish brown (2.5 YR 6/4) matrix. The PC_1 lahar is more matrix rich and differs significantly in color from the Schriebers Meadow lahar (table 9). Estimated volumes of Park Creek lahars PC_1 and PC_2 are 35×10^6 and $1–2\times10^6$ m^3, respectively, with estimated runout distances of greater than 16 and greater than 12 km, respectively (table 10). The long runout for the PC_2 deposit may be because the PC_1 deposit reduced the hydrologic roughness for the lahar that followed.

The larger Park Creek lahar, PC_1, crossed the interfluves between Park and Rainbow Creeks and between Park and Little Park Creeks; the separate branches then rejoined to inundate the Baker River valley. The flow impounded Baker River to form natural Baker Lake (see fig. 54 in the section on Morovitz Creek lahar below). PC_2 is more limited in distribution. PC_1 and PC_2 are exposed in the right cutbank at the mouth of Swift Creek (RS–22, appendix 1), a distributary drainage on the Park Creek alluvial fan, whereas only PC_1 is exposed in a gravel quarry 1.2 km upstream from Baker Lake Road in Little Park Creek (fig. 47; RS–23, appendix 1). At both localities, PC_1 is log rich, contains large blocks (1.5 to 2.2 m in intermediate diameter) of oxidized and brecciated Mount Baker andesite, and is texturally similar.

Hyde and Crandell (1978) obtained two ages for the Park Creek lahar (presumably PC_1; appendix 3): a date of 8.28–6.78 ka on a wood fragment from an exposure 1 km from the Baker Lake Road along the road to Baker Hot Spring and a date of 7.56–6.50 ka on a wood fragment from an exposure at Baker Lake near the mouth of Swift Creek (likely at or near RS–22; fig. 3). Wood samples from PC_1 deposits at the Little Park Creek quarry (RS–23, appendix 1) yield ages of

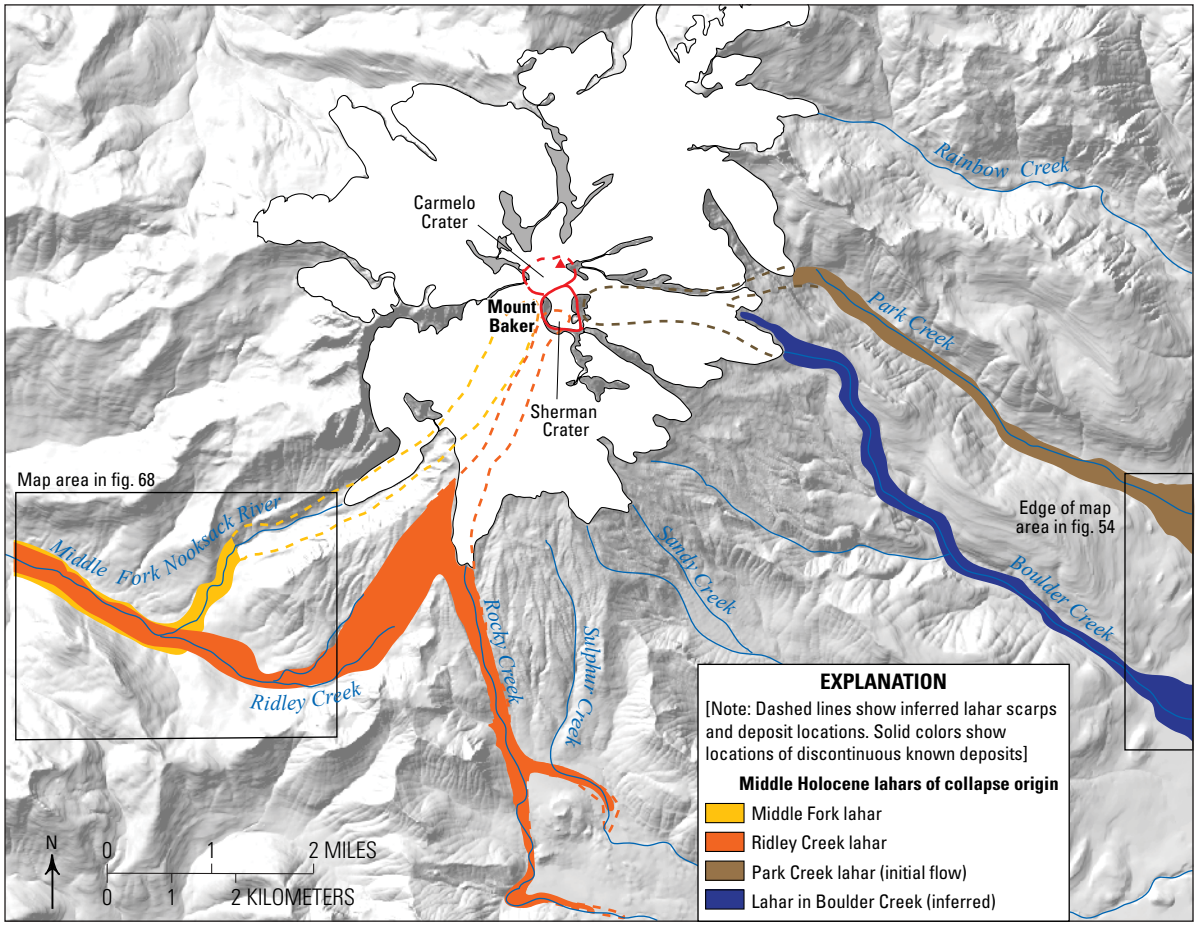

Figure 46. Map of potential initiation scarps and flow paths for the 6.7-thousand-year-old middle Holocene lahars. Source areas are all inferred to be at or near Sherman Crater owing to the high percentage of hydrothermal clay in lahar matrices and abundance of intensely hydrothermally altered clasts. Ridley Creek lahar deposits overlie, or are inset against, the Middle Fork lahar. Sherman and Carmelo Craters outlined in red (dashed where inferred). The lahar in Boulder Creek valley is poorly dated; however, a collapse into Park Creek would likely have spilled over into Boulder Creek as well.

Figure 47. Photograph of the largest Park Creek lahar (PC1) in a quarry in Little Park Creek (RS–23, appendix 1). The lahar consists of angular to subangular boulders and cobbles in a cohesive matrix. At this general locality, the late Holocene Morovitz Creek lahar overlies the Park Creek lahar but is not visible in this photograph. Photograph by K.M. Scott.

7.16–6.79, 7.17–6.80, and 7.75–7.44 ka (appendix 1). The first is from the outer rings of a fir log without bark, the others from wood fragments. Wood samples from PC_1 deposits at the mouth of Swift Creek (RS–22) yielded four ages: 6.88–6.67 ka from the outer rings of a cedar log with bark; two samples with identical ages of 6.89–6.66 ka, and one of 6.80–6.65 ka from outer rings of fir logs. Overall, our ages and those of Hyde and Crandell (1978) overlap, although some just barely. Our preference is towards the younger end of the age range, because we have more confidence in wood samples where bark is still preserved.

Middle Fork Lahar (Middle Holocene)

The largest Holocene lahar from Mount Baker originated as a flank collapse from the area of upper Deming Glacier adjacent to Sherman Crater (Scott and others, 2000, 2001; Tucker and others, 2014; fig. 46). The Middle Fork lahar (RS–24, RS–25, RS–26, appendix 1; figs. 3, 48), as described here, is only the basal part of the long-recognized lahar deposit in the Middle Fork Nooksack River (Hyde and Crandell, 1978; Easterbrook and Kovanen, 1996). We infer that the upper part of the Middle Fork lahar is a separate lahar, which we call the Ridley Creek lahar, described below. The collapse that yielded the Middle Fork lahar immediately transformed to a lahar characterized by a clay-rich (table 9), bluish-gray matrix (5PB 4/1) enclosing dispersed, angular to variably rounded, cobble- to boulder-size clasts and abundant wood. In contrast, the overlying Ridley Creek lahar has a tan-to-pale yellow (2.5Y 8/4) matrix, is finer grained (an abrupt rather than gradual transition) and is wood poor. Hyde and Crandell (1978) interpreted what we call the Ridley Creek lahar as the weathered upper portion of the Middle Fork lahar.

Deposits of the Middle Fork lahar are found in upper Rocky Creek and the length of the Middle Fork Nooksack River. In the Middle Fork Nooksack River, the lahar was as deep as 65 m in the 350-m-wide channel downstream of Ridley Creek, and in excess of 85 m deep in the <200-m-wide gorge downstream from Clearwater Creek (fig. 2). In the Middle Fork Nooksack River valley, bulking—entrainment of valley sediment—caused a gradual change in the matrix from clay-rich, blue mud to light-tan-to-gray, sandy mud, as well as an increase in non-Mount Baker gravel-size clast lithologies to more than 25 percent.

The flow traversed the Middle Fork Nooksack River to its confluence with the North Fork Nooksack River, past the confluence with the South Fork Nooksack River, and downstream in the main Nooksack River to at least as far as Nugents Corner (fig. 2), 48 km downstream of the edifice. Unequivocal deposits of the flow occur in the subsurface at Nugents Corner as observed in well-log samples by P.T. Pringle (written commun., 1997; sample identification confirmed by K.M. Scott). The unit is labeled Qvl in stratigraphic sections (Dragovich and others, 1997), where it is penetrated by six geotechnical borings at Nugents Corner, with a maximum thickness of 14 m. An unknown proportion of that thickness, however, may consist of deposits of the overlying Ridley Creek lahar.

Data from well logs suggest that during the middle Holocene, the Nooksack River most likely flowed north into the Sumas valley (fig. 2; Cameron, 1989; Pittman and others, 2003). Cameron (1989) suggests that the Nooksack River may have flowed northward through the Sumas valley from before the time of tephra layer O (>7.6 ka) to sometime thereafter if, as she notes, she has correctly identified tephra layer O in well logs and drill cores. Her interpretation is based on the presence of volcanic gravels, an interpretation consistent with

Figure 48. Photograph of the log-rich Middle Fork lahar at RS–26 (appendix 1; location in fig. 2), left bank of the North Fork Nooksack River, 35.3 kilometers downstream from the summit. Person at upper right has his hand on the overlying log-poor Ridley Creek lahar. The contact is at his waist. Photograph by D.S. Tucker.

the finding of Mount Baker andesite throughout the valley (P. Pittman, oral commun., 2017). Cameron (1989) notes a log-rich section 4–15 m below the surface, near the town of Sumas and above tephra layer O, which she interprets as the deposits of a lahar (or lahars) from Mount Baker. The stratigraphic position of the log-rich layers is consistent with the Middle Fork lahar, and possibly the Ridley Creek lahar. If correct, the data add at least 20 km to the known extent of the Middle Fork lahar. Regardless of the Nooksack River's course in the middle Holocene, it is also conceivable that if the event happened today, portions of the Middle Fork lahar would top the divide near Everson and flow northward because the divide is relatively low (ca. 2 m). For example, during the past 70 years, the Nooksack River has overflowed its banks near Everson and entered the Sumas valley at least 14 times (Kerr Wood Leidal Associates Ltd., 2005). On the basis of Cameron's (1989) data, well-log data at Nugents Corner, and known thickness through the Middle Fork River valley, we estimate the volume of the Middle Fork lahar to be 240×10^6 m^3, with a runout distance of >63 km.

We dated the outer rings of trunks with retained bark at six Middle Fork lahar sites from successive downstream localities (table 11; appendix 2). The downstream-most date comes from the log-rich locality illustrated in figure 48 at RS–26. The logs are not charred but may appear so where commonly impregnated with black, ferrous iron compounds formed during anaerobic burial. The six dates are tightly constrained between 6.9 and 6.6 ka. Previously reported ages of this flow are 7.42–6.31 ka (Hyde and Crandell, 1978) and 6.72–6.22 and 6.74–6.30 ka (Kovanen and Easterbrook, 2001). The broader age range from previous work is chiefly due to larger uncertainties in the radiocarbon analyses.

The source of the Middle Fork lahar is unclear (figs. 3, 46). On the basis of geometry, it would appear that the source is the upslope portion of the Roman Wall, which today consists of relatively unaltered rock. The Middle Fork lahar, however, has a high clay content (3.8–6.5 percent, table 9) and high proportion of matrix (40–60 percent; table 9), which makes this source questionable. It is conceivable that this portion of the Roman Wall previously had pervasively altered rock that was removed by the flank failure. However, that would require total removal of the altered area. Our preferred source is the largely ice-covered terrain southeast of the Roman Wall and just west of the west rim of Sherman Crater because this area is more likely within the sphere of Sherman Crater alteration.

Table 11. Radiocarbon and calibrated ages of outer rings of trees buried at the base of the Middle Fork lahar at distances between 20.5 and 35.3 kilometers from the source.

[Ages calibrated using OxCal software version 4.3 (Bronk Ramsey and others, 2001; Bronk Ramsey and Lee, 2013; Reimer and others, 2013). ^{14}C yr B.P., radiocarbon years before present; ka, thousand years; m, meters; km, kilometers]

^{14}C yr B.P	Calibrate age (ka)	Distance from summit in Middle Fork Nooksack River (km)	Reference section	Location
5,930±50	6,889–6,656	20.5	RS–24	Olivine mine road bridge
5,920±40	6,835–6,658	21.5		1 km downstream of RS–24, 100 m below confluence with Clearwater Creek
5,890±40	6,831–6,634	21.6		150 m downstream from confluence with Clearwater Creek
5,880±60	6,878–6,535	21.6		150 m downstream from confluence with Clearwater Creek
5,860±50	6,792–6,534	32.4	RS–25	End of Rutsatz Road
5,930±50	6,889–6,656	35.3	RS–26	Log-rich locality, left bank North Fork Nooksack River

Ridley Creek Lahar (Middle Holocene)

The second largest middle Holocene lahar, the Ridley Creek lahar, originated as a collapse of the area of altered rock forming the east portion of the Roman Wall, the west side of Sherman Crater, and Sherman Crater itself (fig. 46) that transformed almost immediately to a lahar. Most of the lahar descended the upper Easton Glacier and entered the Middle Fork Nooksack River by way of Ridley Creek. Smaller portions of the flow spilled down the Easton and Squak Glaciers into Rocky and Sulphur Creeks. The flow did not extend beyond Schriebers Meadow in Sulphur Creek (fig. 46), but it did extend to at least 3 km beyond the meadow along Rocky Creek, where the rugged surface of the Sulphur Creek lava flow had been smoothed by the deposits of the Schriebers Meadow lahar. Flow deposits form the surface of much of Mazama Park and, where exposed in Pratt Creek (RS–15, appendix 1), record a flow more than 30 m deep and at least 200 m wide.

The lahar contains a significant proportion of clay (2.5–7.0 percent, table 9) presumably derived from hydrothermally altered material, and the pale yellow (2.5Y 8/0 to 2.5Y 8/4) matrix contrasts sharply with the bluish-gray color of underlying Middle Fork lahar deposits. A continuous outcrop of more than 100 m along the Park Butte Trail above and below the junction with the Railroad Grade Trail in Morovits Park (fig. 3) shows that either tephra set OP or the Ridley Creek lahar underlies tephra layer BA (fig. 49), suggesting tephra set OP and the Ridley Creek lahar occupy similar stratigraphic horizons. Much of the lahar matrix is similar in color and alteration to that of the tephra. In Sulphur Creek, tephra set OP (RS–21, appendix 1) may underlie the Ridley Creek lahar (fig. 50), suggesting that the collapse may have followed the tephra fall closely in time. Alternatively, what is interpreted to be tephra set OP there may simply be a fines-rich portion at the base of the lahar.

In the Middle Fork Nooksack River downstream from the confluence with Ridley Creek, Ridley Creek lahar deposits form a local terrace 5 to 20 m below peak-flow deposits of the Middle Fork lahar. Ridley Creek deposits are 3 to 7 m thick and commonly overlie the Middle Fork lahar with sharp or, less commonly, transitional contact. As far as the confluence with Clearwater Creek (21.5 km from the summit), the Ridley Creek and Middle Fork lahars are easily distinguished by color, texture, and wood content; however, by RS–25 and RS–26 (table 11) more than 32 km downstream, the distinction in color is much less pronounced (fig. 48). There, the two lahars are mostly differentiated by texture and the presence or absence of wood—the Ridley Creek lahar is finer grained in terms of matrix and clast size, and wood poor. Similar downstream loss of the character and color owing to dilution through bulking of bed and valley-side slope material is observed in other large lahars, such as the Osceola Mudflow at Mount Rainier (Vallance and Scott, 1997). The thickness of the Ridley Creek lahar at RS–26 (2.2 m; appendix 1), 35 km from source, suggests that it likely flowed as far as Nugents Corner (48 km from source) as a lahar. Our estimated Ridley Creek lahar volume is about 150×10^6 m^3, about 60 percent of the volume of the Middle Fork lahar (Tucker and others, 2014).

We obtained one conventional and one wiggle-match age from the Ridley Creek lahar and four conventional ages from tephra set OP (see chapter F; appendix 2). Within 60 m east of the junction of the Park Butte and Railroad Grade Trails in Morovits Park (fig. 3), wood fragments of trees with extremely fine rings in tephra set OP along the lateral edge of the Ridley Creek lahar, yielded four dates from 6.99–6.73 to 7.17–6.95 ka. In the west branch of Sulphur Creek on the north side of Schriebers Meadow, wood in the Ridley Creek lahar yielded a conventional date of 6.94–6.35 ka. The wiggle-match age is from a tree trunk with bark that was buried in 0.5 m of the lahar along the same trailside exposure as the ages obtained from tephra set OP (fig. 51). The log is unusual because of the large number of rings, reflecting their microscopic thickness and slow growth; the trunk contains 285 rings in a radius of only 3.4 cm. Ring density exceeds 30 per mm, approaching the cambium. The wiggle-match age for the log is 6.75–6.71 ka (table 12), which is generally younger than the ages of the wood fragments in the tephra deposit.

Figure 49. Photograph of Ridley Creek lahar overlying tephra layer O from Mount Mazama and underlying tephra layer BA, the magmatic portion of the OP-BA tephra couplet. Just out of the photograph frame to the left, the Ridley Creek lahar is absent, but the stratigraphic position is occupied by tephra set OP (see fig. 39). Age of tephra layer O in thousand years (ka) from Zdanowicz and others (1999). Location is on the Park Butte Trail west of the junction with the Railroad Grade Trail (figs. 3, 4). Penknife handle (10 centimeters) for scale. Photograph by K.M. Scott. ca., circa.

Figure 50. Photograph of a fine-grained layer at the base of the Ridley Creek lahar in Sulphur Creek that may be the hydrothermal tephra set OP. Penknife handle (10 centimeters) for scale. Photograph by K.M. Scott.

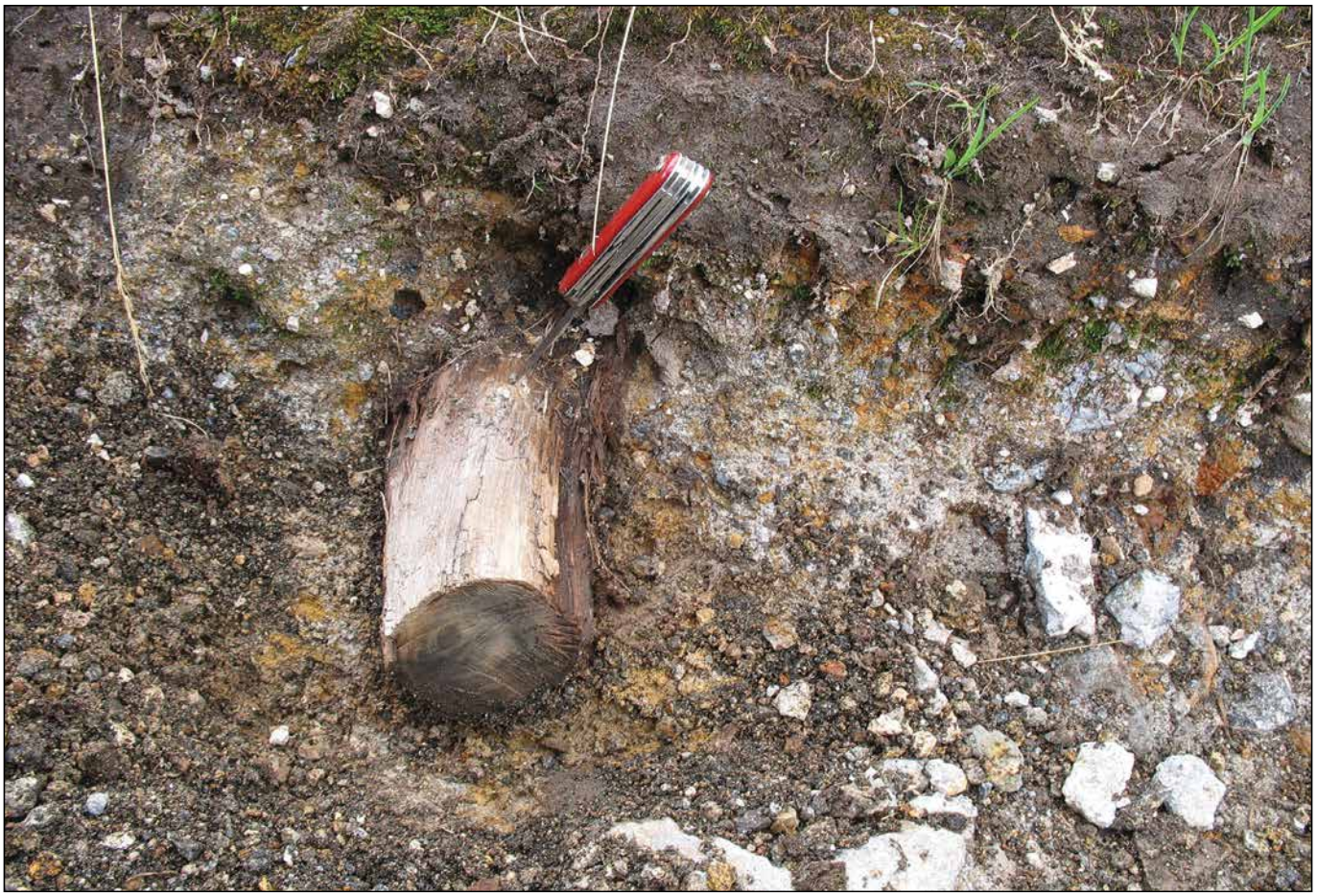

Figure 51. Photograph of the trunk of a tree in the Ridley Creek lahar that was used for wiggle-match age date (table 12). Note preservation of bark. Penknife handle (10 centimeters) for scale. Photograph by K.M. Scott.

Table 12. Wiggle-match age data from ring intervals of a tree buried in Ridley Creek lahar in Morovits Park; trailside exposure about 60 meters east of the junction of Railroad Grade and Park Butte Trails.

[^{14}C yr B.P., radiocarbon years before present; cal. yr B.P., calibrated years before present]

Lab number[a]	δ^{13}C	Age[b] (^{14}C yr B.P.)	Age,[c] uncorrected for δ^{13}C (cal. yr B.P.)[d]	Age, corrected for δ^{13}C (cal. yr B.P.)	Tree ring interval
WW6212	−21.09	5,820±30	6,728–6,536	6,717–6,526	1–16
WW6213	−21.21	6,010±25	6,935–6,785	6,862–6,711	67–77
WW6214	−20.52	5,980±30	6,895–6,736	6,789–6,629	104–110
WW6215	−21.53	6,015±30	6,944–6,782 (95) 6,761–6,759 (0.4)	6,789–6,622	155–160
WW6216	−21.09	6,130±30	7,158–6,941	6,934–6,717	223–227
WW6217	−20.66	6,190±30	7,176–6,990	6,893–6,705	281–285
Wiggle-match age: 6,750–6,710 cal. yr B.P. at 95.4 percent confidence and corrected for δ^{13}C					

[a]Prefix WW refers to U.S. Geological Survey ^{14}C laboratory in Reston, Virginia; values reported use corrected ^{13}C values.

[b]Individual age for each tree ring interval.

[c]Uncorrected age does not account for tree ring interval.

[d]Where multiple ranges occur, the probability of each is shown in parentheses.

Morovitz Creek Lahar (19th Century)

After the middle Holocene, the next significant lahar did not occur until the middle 19th century. Within 2–4 years of the eruption of Sherman Crater that produced tephra set YP in 1843 C.E., the east side of Sherman Crater collapsed to produce the Morovitz Creek lahar (figs. 52, 53). Lahars moved down both Boulder and Park Creeks, ultimately spilling from Park Creek into Morovitz (RS–27, appendix 1), Swift, and Little Park Creeks, and then rejoining to inundate the Baker River valley, probably to several kilometers below the Boulder Creek fan (fig. 54). The Boulder and Park Creek branches of the lahar were likely parts of a single collapse, because a flow into Park Creek from Sherman Crater would also yield a flow into Boulder Creek. We have not found any deposits that suggest the flow reached the confluence with the Skagit River. Extensive deposits in Morovitz Creek (RS–27) give the flow its name. The thickest and coarsest deposits, which are locally log rich, form the terrace of the Boulder Creek Campground on the right bank of Boulder Creek downstream from the highway bridge (fig. 52; RS–28, appendix 1). Left-bank deposits downstream from the highway bridge are described in RS–29 (appendix 1).

Figure 52. Photograph of the boulder-rich Morovitz Creek lahar (base), overlain by a younger lahar (light gray), in terrace of Boulder Creek at campground (RS–28, appendix 1). Units separated by lens of alluvium, thickening to right of pencil (15 centimeters). The lens indicates a time break between the lahars. Light color of younger lahar reflects high proportion of altered matrix. The Morovitz Creek lahar is dominated by rounded boulders of Mount Baker andesite from the Boulder Creek assemblage, which were entrained from bed material of Boulder Creek. Photograph by K.M. Scott.

Morovitz Creek lahar deposits are typically 1.0 to 2.5 m thick (locally as thick as 6 m) and, in Park and Morovitz Creek, consist of acid-stained cobbles and boulders in a light-gray (2.5Y 7/0) to light-yellow (2.5Y 8/4) mottled, clay-rich matrix (RS–27 and RS–30, appendix 1). We hypothesize that the collapsed east wall of Sherman Crater may have consisted of altered rocks rich in hot hydrothermal fluids that stained even the rounded stream clasts incorporated into the flow. At Boulder Creek Campground (fig. 52), rounded alluvial boulders constitute as much as 80 percent of the lahar deposit by volume, indicating that there the lahar had bulked to approximately 5 times its original volume (table 10). Based on the proportion of entrained clasts (determined by fluvial rounding and non-Mount Baker lithologies) in all drainages, the mean bulking factor of all branches of the flow is about 40 percent. In Boulder Creek, however, the mean value is about 55 percent. Estimated volume of the lahar is about 20×10^6 m^3 with an estimated runout of more than 16 km (table 10).

The maximum limiting age of the lahar is 1845 C.E., based on the nearly omnipresent woody layer (1 to >20 cm in thickness) that underlies the lahar in all five drainages in which it is found. The woody layer separates the lahar from the underlying tephra set YP (RS–27, RS–29, RS–30; fig. 53). Historical reports of salmon killed and the "country on fire for miles around" (appendixes 6, 7, 8) suggest that the eruption that deposited tephra set YP occurred in the summer or fall. The woody debris overlying the tephra, however, commonly does not record charring, which questions the veracity of the observation of the "country on fire for miles around."

Although we do not know the exact origin of the woody layer at the base of the lahar, it presumably represents widespread tree kill associated with the 1843 C.E. eruption. Thus, it establishes that the collapse of Sherman Crater that formed the lahar followed the eruption by a significant time interval (months to years rather than hours to days). M.E. Harmon (Department of Forest Sciences at Oregon State University, written commun., 2002) estimated the time interval as a minimum of 2 years on the basis of the layer description. A 2-year time interval is supported by J.S. Hadfield (U.S. Forest Service, written commun., 2002) who, in recording responses of burned, thin-barked trees (such as western

Figure 53. Photograph of the orange-brown woody layer separating underlying tephra set YP (light grey to white ash) and overlying Morovitz Creek lahar (rounded clasts). Location is on the left bank of Swift Creek below Baker Lake Road bridge. Penknife handle (10 centimeters) for scale. Photograph by K.M. Scott.

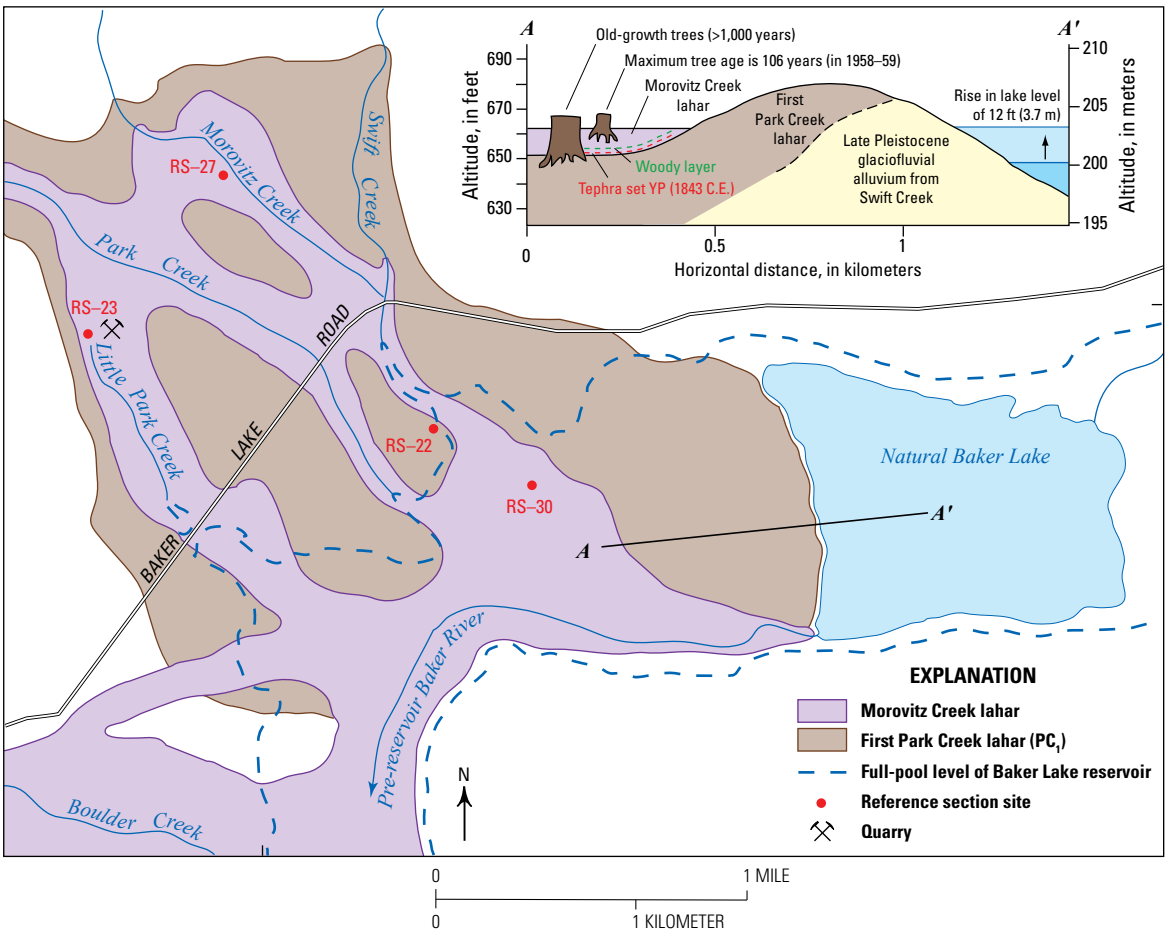

hemlock) in the north Cascade Range, found that after a burn, significant shedding of bark did not occur in the first year, but had begun by the second anniversary of a burn. A study of the disintegration rates of girdled trees found that bark became cracked and began to be shed after 3 years (Helmers, 1948). We thus accept Harmon's estimate of at least 2 years, regardless of origin—whether tephra impacted the forest (for example, by facilitating insect attack), whether the forest was affected by wildfire and for some reason the bark in the woody layer was mostly uncharred, or whether trauma was caused by some process such as elevated volcanic degassing. A minimum limiting date of 1847 C.E. is based on the dendrochronology of trees rooted in the overlying lahar; thus, the time represented by the woody layer is on the order of 2–4 years.

The minimum limiting age of 1847 C.E. (estimated ±1 year) for the lahar is based on the age of Douglas fir growing on the lahar surface and an evaluation of the colonization time gap (Pierson, 2006)—the time between landform creation (lahar deposition) and conifers grown to sampling height. Ring counts of logged stumps were made at four locations (table 13).

The trees show minimum ages between 1852 and 1856 C.E. If the lahar occurred in 1845 C.E., then the colonization time gap is 7–11 years. This value is similar to that of Pierson (2006), who, after surveying lowland (<750 m altitude) Douglas fir sites in southwestern Washington and northeastern Oregon, proposed a colonization time gap of about 10 years, subject to several sources of correction.

An amateur dendrochronologist, A.R. Moore, reported to have dated the Morovitz Creek lahar as 1846 C.E., and was the first worker to report the coeval deposits in Boulder and Park Creeks. He reported "…that the eruption flowed down Boulder and Park Glaciers…I have cut blocks of living trees [presumably with impact scars] that grew along the flow and are still living and find that it happened in 1846 C.E. By counting the annual ring growth of the trees..." (Bellingham Herald, April 26, 1953). The same article also cites Moore for the 1846 C.E. date (appendix 6) of the main eruption, reported by Hudson Bay Company employees. Moore's report is probably accurate for the subsequent collapse and lahar, but unlikely for the main event.

Effects of Morovitz Creek Lahar on Natural Baker Lake

By the middle 19th century, natural Baker Lake was significantly smaller than when formed by the impoundment of the Baker River by the first middle Holocene Park Creek lahar. The lake level was raised about 4 m when the Morovitz Creek lahar inundated the Baker River valley and blocked the lake outlet (figs. 54, 55). The effects were recorded by J. Morovits (appendix 9), who noted, with remarkable accuracy in a letter dated January 26, 1912, that timber 70 years in age had grown on the lahar and that when the flow occurred it "swept down and raised the waters of [natural Baker Lake] some 12 feet [3.7 m]…" (C.F. Easton, written commun., 1911–31). Morovits estimated 100 years as the amount of time since the lahar, but this included his estimate of 30 years for weathering of the deposits, interpreted by him as lava,

Table 13. Summary of tree ring counts in logged stumps on clearcut areas that were inundated by the Morovitz Creek lahar.

[Dates of cuts from U.S. Forest Service records. CTG is the colonization time gap, which is the time between landform (lahar) emplacement and the tree growth to sampling height (Pierson, 2006). yr, year]

Locality	Date of clearcut	No. of stumps	No. of rings	Age (years C.E.)	Minimum CGT range[1] (years)
Park Creek Campground	1993	17	127–138	1866–1855	9–11
Boulder Creek, left bank	1991	13	130–138	1861–1853	7–9
Boulder Creek Campground	2002	4	<146	≤1856	10–12
Natural Baker Lake blockage	1958–59	10	<107	≤1852	6–8

[1]Calculated assuming the Morovitz Creek lahar occurred in 1845±1 year.

Figure 54 (page 78). Map of distal Park Creek and Morovitz Creek lahars where they inundated Baker River valley. Natural Baker Lake was formed in the middle Holocene when the first Park Creek lahar (PC_1; brown color) blocked the Baker River after Glacial Lake Baker had receded from the upper Baker River valley. Lake level dropped between the middle Holocene and prior to inundation of the Morovitz Creek lahar (purple color)—mapped from hydraulic continuity between exposure sites and inferred from vegetation-age boundaries on aerial photographs. The Morovitz Creek lahar blocked the outlet and raised the lake level an estimated 3.7 meters. Diagrammatic cross-section *A*–*A*′ (inset) portrays the rise in lake level caused by the Morovitz Creek lahar, based on the account of J. Morovits (appendix 9).

Figure 55. Photograph of stumps (logged 1958–59) that record two generations of trees on the lahar blockage of natural Baker Lake. The large stump on the right was an old growth tree rooted in the circa (ca.) 6.7-thousand-year-old (ka) Park Creek lahar and subsequently buried by the Morovitz Creek lahar ca. 1846 C.E. The smaller tree on the left is rooted in the Morovitz Creek lahar. Note the lack of flaring on the older tree stump. Ice ax (85 centimeters) for scale. Photograph by K.M. Scott.

before tree growth began. Aerial photographs taken before the filling of Baker Lake reservoir in 1959 allow one to assume a probable flow path for the lahar by comparison of relative tree ages (that is, separating old stands of trees from younger ones). From these photographs, it appears that the Morovitz Creek lahar was the only flow to affect natural Baker Lake in the 19th century. Morovits' observation of tree age on lahar deposits (ca. 70 years in 1912 C.E. equates to ca. 1842 C.E.) supports that flow being the Morovitz Creek lahar.

We were initially puzzled by the fact that the raised level of natural Baker Lake was not reflected in drowned and decayed snags along the lakeshore in the earliest known photographs taken in 1904 C.E. In a 1904 C.E. photograph of the blockage by photographer Darius Kinsey (photograph 0357; Bohn and Petschek, 1978), a few dead trees appear along the shore, but those trees retain small branches, indicating a more recent demise than 1845–47 C.E.. Cline and others (1980) describe a subaerial decay sequence that suggests that only large limbs and the main trunk would have existed in 1904 if killed subaerially in 1845–47 C.E.. However, the report by Morovits when he saw the lake in 1891 C.E. was of "submerged stumps" and "rotting away of all portion[s] of the trees that projected above the water" (appendix 9). This suggests that the trees decayed more rapidly standing in water. The more rapid decay can be ascribed to several factors, including freeze-thaw in the saturated wood at the waterline, and the impacts of ice floes in the spring. The possibly younger dead trees in the Kinsey photograph may reflect changes in outflow level connected with construction of a fish trap at the lake outlet, associated with the 1896 C.E. fish hatchery on the south shore of the lake.

Baker Lake level was reported as 661.7 ft (201.7 m) in 1915 (Herron, 1916), and as 663 ft (202 m) on the 1952 USGS quadrangle map, based on 1947 aerial photography. In 1959, the lake was drowned by the waters of Baker Lake reservoir. In spite of the questionable accuracy of early 20th-century surveying, we can conclude that little if any erosion of the outlet occurred (between 1915 and 1947), although lack of erosion may have been due to outlet stabilization related to the operation of the fish hatchery.

Lahar Younger than the Morovitz Creek Lahar in Boulder Creek (19th Century)

In Boulder Creek Campground, the Morovitz Creek lahar is overlain by a clay-rich lahar, as thick as 1.7 m, with pebble-size clasts set in a white (2.5Y 8/0) to light-gray (2.5Y 7/0) matrix (RS–28, appendix 1; fig. 52). Deposit clay content is 5.5 percent with matrix clay content of 13.6 percent (table 7). This second 19th-century lahar was confined to the proximal part of the Boulder Creek fan and, like its larger predecessor, the Morovitz Creek lahar, originated from a collapse of the east flank of Sherman Crater. Flow was confined to Boulder Creek because of the smaller collapse volume.

Hyde and Crandell (1978) interpreted a hiatus of 100 to 200 years between this lahar and the underlying Morovitz Creek lahar, based on presumed weathering at the top of the older deposit. Based on a historical account (appendix 7), there is a possibility that this second lahar occurred in 1858 C.E. Although the 1858 C.E. account appears to describe a flow that had just occurred, on the basis of the degree of destruction, we interpret that account as juxtaposing the Morovitz Creek lahar and the occurrence of this smaller lahar. In any case, the second smaller lahar (table 10) probably followed the Morovitz Creek lahar by at least several years. Alluvial strata with woody debris locally separate the lahar deposits (RS–28, appendix 1).

Debris Flows Attributed to Glacial or Meteorological Activity

Debris Flow at Elbow Lake Trailhead (4th Century)

A significant debris flow mantles a 7-m-high terrace on the right (north) bank of Middle Fork Nooksack River at the Elbow Lake Trailhead (Tucker and others, 2014; BF–5, appendix 1), 6.4 km downstream from the present Deming Glacier terminus (fig. 10). Exposures at the Elbow Lake Trailhead, exhumed by 2003 flooding, reveal a 1- to 1.4-m-thick debris-flow deposit dominated by angular clasts set in a clay-poor, granular, gray (2.5Y 5/0) matrix. The matrix is mainly composed of angular-to-subangular grains and locally has a well-developed 5-cm sole layer (that is, a texturally distinct basal subunit; Scott, 1988a). The floodplain facies of the terrace deposit has a coarse mode in the pebble-size range. But in an intrachannel exposure just upstream from the post-2003 log bridge, the deposit consists of more than 4 m of blocky channel facies with a coarse mode of angular cobbles. Outer rings of a 25-cm-diameter log buried by the flow yield a date of 1.72–1.57 ka (appendix 2).

Hyde and Crandell (1978) discuss a younger and smaller lahar relative to the Middle Fork lahar, in the Middle Fork Nooksack River drainage near the mouth of Ridley Creek. Their description is of a lahar with a hummocky terrace about 15 m in height. Based on their description and locality, we think that their younger lahar is more likely the 1927 Deming Glacier debris flow described below and is not correlative to the debris flow at the Elbow Creek Trailhead.

The absence of altered clasts and clay-poor matrix indicates that the debris flow at Elbow Lake did not result from the collapse of hydrothermally altered rock. We suggest the following possible origins: (1) volcanic (the result of snow and ice melt by hot volcanic products), (2) meteorological (extreme rain event), (3) glacial outburst (collapse of glacial front or sudden outburst of subglacial water), or (4) collapse of water-saturated morainal material. Lack of any evidence of eruptive activity, such as the presence of a juvenile component, suggests the first hypothesis is not viable. The debris-flow age corresponds to an advance in the first millennium of the Deming Glacier, around 1.81–1.56 ka (Osborn and others, 2012), which suggests the last hypothesis is also unlikely.

The source drainage for this debris flow at the Elbow Creek Trailhead is likely the Middle Fork Nooksack River rather than Ridley Creek. Debris-flow deposits were not seen upstream in either drainage above their confluence; however, if present, they would have been obvious in Ridley Creek because there have been no flow events there since the debris flow exposed at Elbow Lake Trailhead. The apparent absence upstream of debris-flow deposits in the Middle Fork Nooksack River can be explained by subsequent burial by the younger 1927 Deming Glacier debris flow. Although we cannot distinguish between hypotheses (2) and (3) above, the Middle Fork Nooksack River drainage is also much more likely than Ridley Creek for a glacial outburst scenario because the Deming Glacier feeds into the Middle Fork Nooksack River, whereas Ridley Creek does not, and did not, directly drain an alpine glacier.

Easton Glacier Outburst Floods (1911 C.E.)

In 1911, Easton Glacier experienced what was likely an outburst flood. An account in an essay ("Marking and Gauging the Movements of Glaciers" probably by Easton, [C.F. Easton, written commun., 1911–31) gives the following observation "…in 1911, avalanched enormous floods of debris down both outlets." In this case, "both outlets" refers to Rocky and Sulphur Creeks. The "National Forest supervisor" reported that "…he never saw such a gorge of material as there was spit out into the head of Rocky Creek…" (C.F. Easton, written commun., 1911–31). Much of the boulder alluvium spread across the surface of Schriebers Meadow below the trail-crossing bridge was deposited by this flood, including the dynamited boulders reported as lava pillows by Kovanen and others (2001, their fig. 7).

Deming Glacier Debris Flow (June 1927)

In June 1927, the collapse of the distal mile or more (>1.6 km) of the Deming Glacier resulted in what Easton (written commun., 1911–31, p. 158) estimated liberally as an approximately 60-m-deep and 400-m-wide flow of water and ice. This flow transformed rapidly to a debris flow with predominantly subangular clasts of both Mount Baker and non-Mount Baker lithologies in a gray (2.5Y/5.0), muddy sand matrix. The description of this event is analogous to (1) the well-known debris flow (actually a series of flows) resulting from the 1947 collapse of the distal 1.6 km of the Kautz Glacier at Mount Rainier (R.K. Grater[5], National Park Service, written commun., 1948), (2) debris flows spawned from outburst floods or glacier collapses in 1938 and 1963 from the Chocolate Glacier at Glacier Peak (Richardson, 1968; Slaughter, 2005), and (3) numerous outburst floods from the South Tahoma Glacier also at Mount Rainier (Walder and Driedger, 1995). These watery flows transform almost immediately to debris flows. Each occurred after a long period of progressive post-Little-Ice-Age climate amelioration and glacier recession, which likely promoted release of stored water or distal collapse of debris-covered, likely stagnant and saturated ice.

[5]From an unpublished 1948 National Park Service report titled "A report on the Kautz Creek flood studies," 9 p., available at the National Park Service Library in Longmire, Washington.

The 1927 debris-flow deposits form a continuous, well-defined terrace 10–15 m above the present thalweg of the Middle Fork Nooksack River, 1.5 km below the glacier terminus (as of 2013). Approaching the downstream confluence with Ridley Creek, the terrace is 6–10 m above the thalweg and contains megaboulders of volcanic breccia from Black Buttes. The deposits record a single large flow, with several subsequent smaller surges. Fuller (1980) described this flow as a "younger mudflow" (relative to an "older mudflow"—the Middle Fork lahar), which he believed to have been cut by, and therefore older than, a 17th-century moraine.

Easton's estimate of a 9.7 km travel distance (written commun., 1911–31) is high for a continuous, untransformed debris flow. We interpret a series of boulder fronts 1.0 to 1.5 km downstream from the confluence with Ridley Creek, 4.9 km below the toe of the modern glacier, as the end of the debris flow and the beginning of hyperconcentrated flow (fig. 56). The presence of a "house-size" block of ice in the Middle Fork Nooksack River "about a mile" (1.6 km) below the confluence with Ridley Creek that was recalled orally by a member of a U.S. Forest Service crew working on the Ridley Creek Trail at the time (W. Benecke, oral commun., 2000) supports the high concentration of the flow. The first vertical aerial photographs (September 21, 1940) establish the maximum distance of significant runout inundation of the debris and hyperconcentrated flows as slightly more than 12 km, just beyond the confluence with Clearwater Creek (fig. 2).

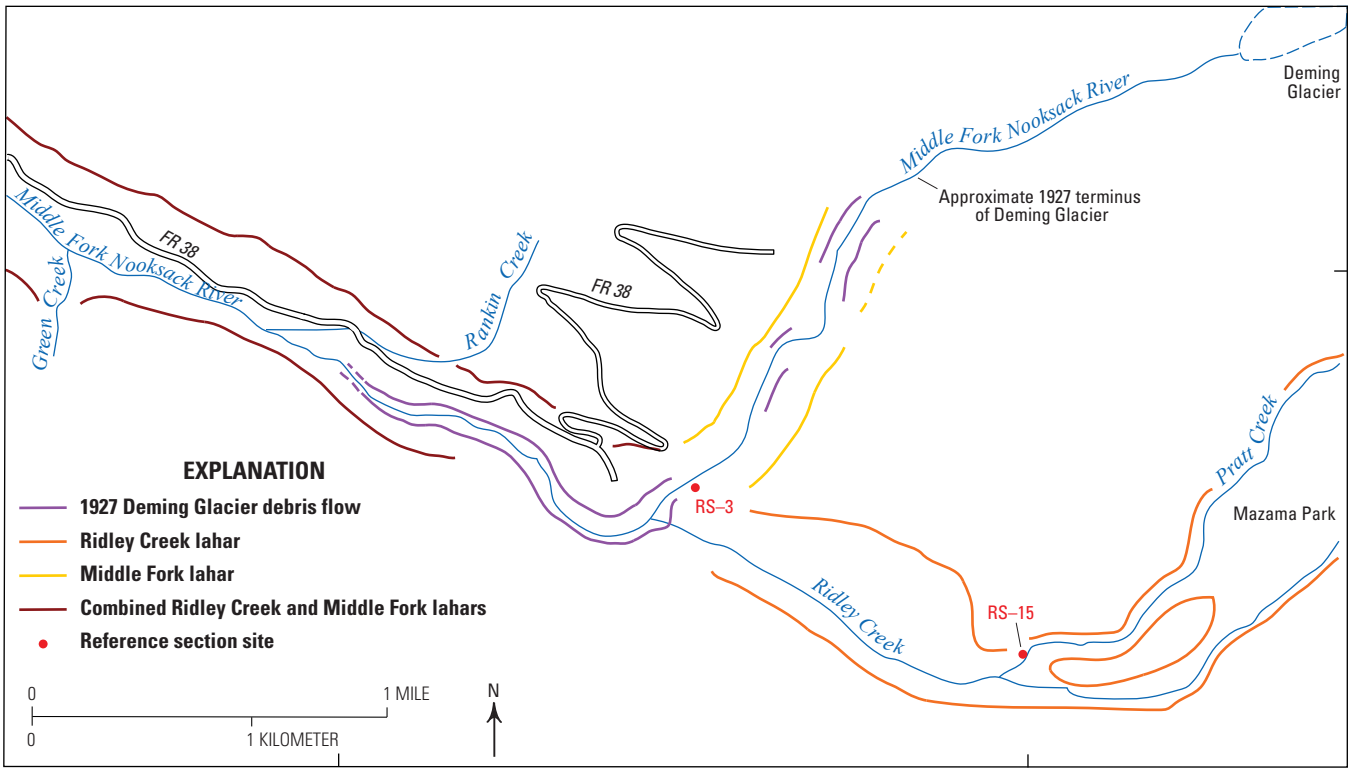

Figure 56. Map of the confluence of Ridley Creek and Middle Fork Nooksack River showing the distribution of Ridley Creek and Middle Fork lahars as well as the 1927 Deming Glacier debris flow. Downstream of the confluence, the yellow wood-poor, finer grained Ridley Creek lahar overlies the blue-gray wood-rich, coarser Middle Fork lahar. The Middle Fork lahar, and likely the Ridley Creek lahar as well, can be traced downstream to Nugents Corner, approximately 33 kilometers downstream from the confluence.

The trigger for this event is unknown. The nearest weather stations in 1927 were at Blaine, Wash., on the coast and at Olga in the San Juan Islands; both recorded normal or below-normal precipitation and temperature for June 1927. Unreported, local and intense precipitation on the flank of Mount Baker could have triggered the flow, although that would be highly unusual in late June. Nonetheless, most of the well-documented glacial collapses and outburst floods at Mount Rainier (all of which transformed to debris flows) occurred after either significant periods of uncommonly hot weather, or prolonged, intense rain (see Scott and others, 1995). For example, the October 1947 Kautz Glacier collapse occurred after several days of heavy rain (Scott and others, 1995).

Easton (written commun., 1911–31) describes one or more earthquakes associated with the flow, felt "50 to 100 miles away." However, he notes that the earthquakes were not reported by seismic stations then located in Victoria and Seattle. Easton's accounts of tremor and noise vastly exceed those of any recorded debris-flow events, even from far larger flows (table 9 of Scott and others, 2001). S.D. Malone (written commun., 2003), a seismologist at the University of Washington, notes that an earthquake as large as that described by Easton in Bellingham, Wash., would have been recorded in Victoria, British Columbia, but that the incomplete records from that station in June 1927 do not record a significant event. Our 1927 witness (W. Benecke, oral commun., 2000) could recall no ground tremor associated with the Deming Glacier debris flow, and he was camped nearby. Owing to the lack of any other seismic reporting and no unusual weather reports for the month, we ascribe the flow to gravitational failure of stagnant glacial ice.

Easton (written commun., 1911–31; 1920) also reported similar flows below the termini of Roosevelt and Mazama Glaciers, based on an apparent trimline defined by removal of older vegetation and "new growth of small trees." We infer that Easton saw only valley-side slopes on which vegetation was slowly returning following late-19th-century glacial recession.

Historical Debris Flows Spawned by Debris Avalanches

Rainbow Creek

A debris avalanche (landslide) recognized by J. Morovits in Rainbow Creek ("the glacier came down") in 1889–90 led to the name "Avalanche Gorge" for the reaches below the Rainbow Glacier (C.F. Easton, written commun., 1911–31). The avalanche transformed into a debris flow, which is the largest historical one in Rainbow Creek, extending to the confluence with Swift Creek (fig. 57). It and a smaller,

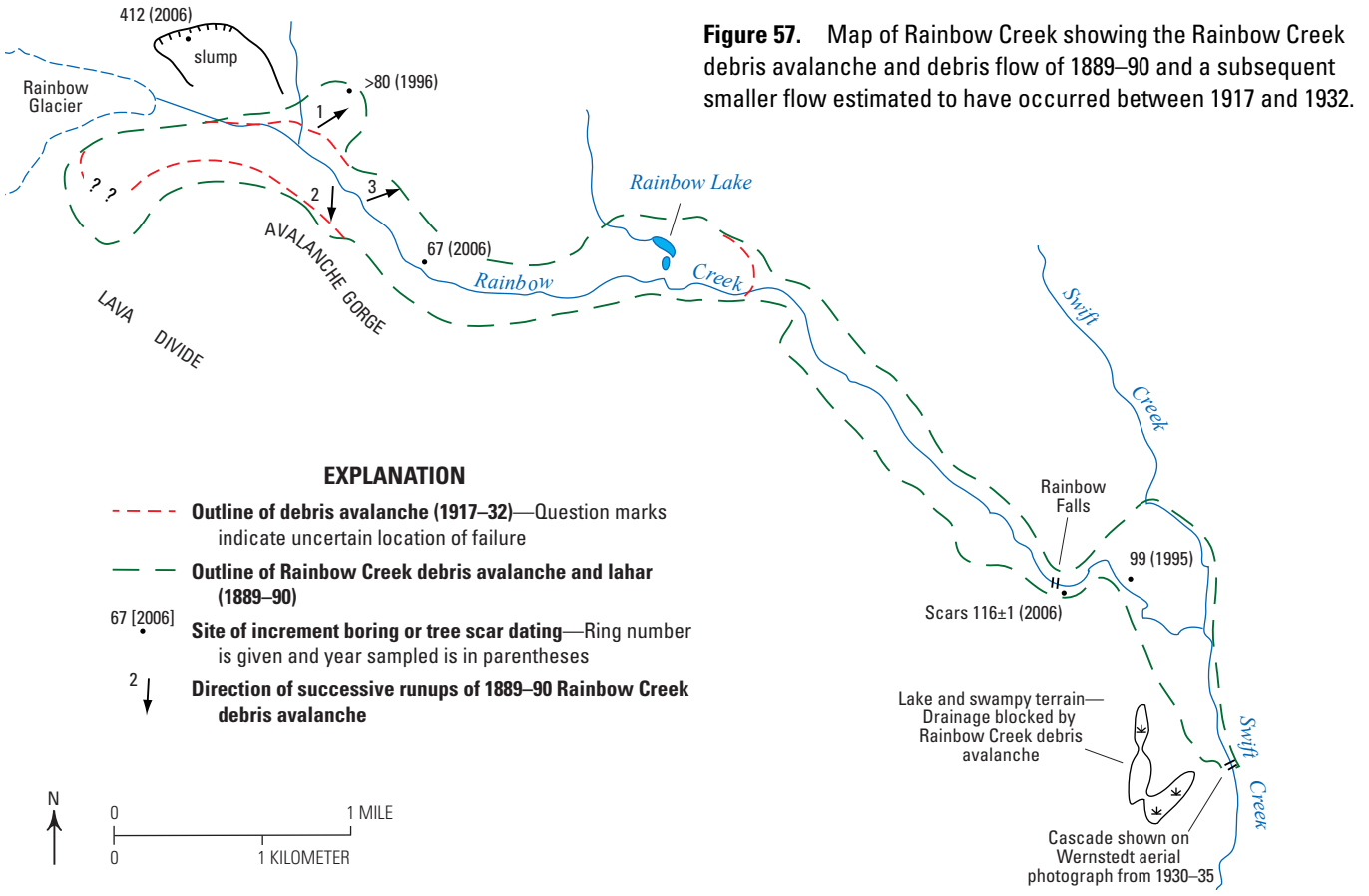

Figure 57. Map of Rainbow Creek showing the Rainbow Creek debris avalanche and debris flow of 1889–90 and a subsequent smaller flow estimated to have occurred between 1917 and 1932.

younger avalanche and debris-flow deposit were described by Hyde and Crandell (1978) and by Fuller (1980).

The source area for the collapse occurred on the northeast side of Lava Divide (Lewis and others, 2006) mainly from rocks older than the late Pleistocene Mount Baker edifice—the andesite of Lava Divide (unit ald) of Hildreth and others (2003)—with a contribution from the underlying metamorphic rocks of the Mesozoic Nooksack Formation. The basal failure plane coincided locally with the contact between the two formations (fig. 58). Crossing the toe of Rainbow Glacier, the flow superelevated on the northeast side of the valley, leaving runup deposits to an altitude of 1,280 m (figs. 57, 59). Using a simplistic equation for flow velocity, $v = \sqrt{2gh}$, where g is gravitational acceleration (9.8 meters per second squared, m/s^2) and h is vertical runup distance (140 m), yields a velocity of ca. 52 meters per second (m/s), assuming complete conversion of kinetic to potential energy, at the base of the runup slope. The initial runup was followed by successive oscillations between opposite valley side slopes (fig. 57) as the flow was progressively oriented to a downstream course and underwent extensive cataclasis and comminution to produce fine sediment that resulted in its eventual distal transformation to a debris flow.

The Rainbow Creek debris avalanche and debris flow had the typical high mobility (height to length ratio H/L = 0.11) of a volcanic debris avalanche (H/L = 0.10; Siebert, 1984; Crandell, 1989; Hayashi and Self, 1992). Such high mobility is generally attributed to intense alteration and rapid disaggregation of failed volcanic rock. The Rainbow Creek debris avalanche consisted of relatively unaltered lava flows, although some alteration apparently exists along interflow breccia layers (W. Hildreth, written commun., 2010). The mobility of the Rainbow Creek debris avalanche was apparently facilitated by fine sediment that was produced by the initial cataclasis and by fine sediment entrained downstream from clay-rich Vashon Drift and glaciolacustrine deposits.

The Rainbow Creek debris avalanche transformed to a clay-rich debris flow below the runup area (from clay-poor,

Figure 58. Photograph of the failure scarp (425 meters thick) of the Rainbow Creek avalanche on the northeast flank of Lava Divide (figs. 3, 5, 57). The floor of the failure lies along a contact between middle Pleistocene andesite of Lava Divide (rough strata dipping to left) that overlies Mesozoic Nooksack Formation (smoother surfaces at lower right). Photograph by D.S. Tucker.

Figure 59. Aerial view of the runup scar documenting superelevation of 140 meters of the Rainbow Creek debris avalanche on the valley-side slope opposite the failure scar in figure 58. Note the lower, younger lateral levee formed by the debris avalanche that occurred between 1917 and 1932. Aerial photograph by J.H. Scurlock, September 27, 2004, used with permission.

block-supported flow to a clay-rich, matrix-supported flow) and extended across the interfluve between Rainbow Creek and Swift Creek (fig. 57). As the avalanche transformed to the debris flow, the clast-supported texture of the upstream rubbly avalanche deposit was gradually replaced distally with cobble- and boulder-sized clasts within a greater and greater proportion of gray (2.5Y 5/0), silt- and clay-rich matrix (fig. 60; table 9) from the Vashon glacial deposits.

At Rainbow Falls (fig. 57), 1.4 km upstream from the Swift Creek confluence, the Rainbow Creek debris avalanche left a well-defined 1- to 2-m levee, 82 m above the channel, defining a cross-sectional area of approximately 10,000 m^2. Based on velocities of similar flows (Pierson, 1998), a mean velocity of approximately 20 m/s at the site yields a discharge on the order of 200,000 m^3/s.

Locally, log-rich debris-flow deposits form gently undulating topography over 1.0 km^2 between Rainbow and Swift Creeks (fig. 57). Several closed depressions about 2 m deep record melt-out of ice blocks transported by the flow, and a few small hummocks reflect disaggregated, possibly originally frozen megaclasts. The toe of Rainbow Glacier was eroded, and then buried, by the failed mass at the foot of the failure scarp; in 2006, ice was still exposed beneath those deposits. A prominent cascade is visible on the earliest aerial photographs by Lage Wernstedt (no. 4034; 1930–35) at what we interpret was the location of the terminal debris-flow front in Swift Creek, 1.0 km downstream from the confluence with Rainbow Creek. Since then, the cascade has been completely removed by erosion.

Fuller (1980) suggested that the older Rainbow Creek avalanche occurred in the 1860s. We suggest it occurred ca. 1889–90, based on statements by Morovits and from the following evidence:

A. J. Morovits observed a barren debris avalanche surface in 1891. In a letter (April 12, 1912; see appendix 9), Morovits stated that, when he homesteaded nearby in October 1891, the deposits of an avalanche

Figure 60. Photograph of a deposit of the Rainbow Creek debris flow in lower Rainbow Creek after the debris avalanche had transformed to a clay-rich debris flow. The debris flow overlies a deformed sandy layer that has a dark humic horizon marking the level of the pre-flow surface. The person points to the base of the debris flow deposit. Photograph by D.S. Tucker.

in Rainbow Creek that formed "when the glacier came down" had "not a bush of any kind" growing on its surface. For comparison, by 1983, we noted that significant regrowth on untreated deposits of the 1980 debris avalanche at Mount St. Helens had begun. We infer that Morovits's comment makes an age for the Rainbow Creek debris avalanche of much more than a couple of years before 1891 unlikely.

B. Coring of the largest Douglas fir (felled by erosion in 2006) on downstream deposits, left bank of Rainbow Creek, about 0.8 km upstream from the confluence with Swift Creek, revealed 99 rings in 1995 (fig. 57). Thus, an age of 1889 is indicated, with a minimum colonization time gap of 7 years (1995−99−7=1889) (table 10). Based on the maximum limiting age from (A), the colonization time gap is unlikely to be more than 8 years. The Morovits account indicates that early 1891 is also possible, but we think it unlikely because it requires a very low colonization time gap of 5 years (given a sampling height of about 1 m).

C. Scars (figs. 57, 61) on old-growth cedars preserved along the right margin of the flow above Rainbow Falls yielded 1890 (±1 year) as the most probable year of the avalanche. Our examination of three sectioned scars did not define a single year.

Fuller (1980) reported two failure deposits. He reported a smaller debris avalanche, dated 1888, extending to the terminal lobe enclosing Rainbow Lake and overlying the larger Rainbow Creek debris avalanche, which he dated as from the 1860s. In spite of his 1980 report of a cored tree with 109 rings near Rainbow Falls, which would give a date ca.

Figure 61. Photograph of a healing scar (left of person) on upstream side of old-growth western redcedar that survived the 1889–90 Rainbow Creek debris avalanche. Site is near peak flow level at Rainbow Falls; note only younger trees are below this level. Photograph by K.M. Scott.

1864 for a 7-year colonization time gap (1980−109−7=1864; see fig. 6 of Fuller, 1980), we are confident of our younger date of 1889–90 for the larger avalanche. Fuller (1980) dated the smaller, younger upvalley debris avalanche as 1888 based, in part, on his sectioning of a tree scar near Rainbow Lake. We suggest that the tree Fuller dated was rooted in the first debris avalanche deposit and scarred by the second debris avalanche; thus, Fuller was dating the older of the two avalanches.

Fuller (1980, p. 33) cited Easton (written commun., 1911–31) for the middle 1860s date of the largest debris avalanche. He is not alone in perpetuating that notion. We suggest that it originated in repeated misinterpretations, attributed and unattributed, to an April 12, 1912, note by Morovits that the flow occurred "about 30 years ago" (C.F. Easton, written commun., 1911–31, p. 54; appendix 9). We suggest that Morovits' comment of "about 30 years ago" is from the date of his note (1912), which would place the event in the early 1880s. His later contemporaries, including Easton, overlooked his comment about the unvegetated surface of the flow when he arrived, and they, as well as possibly Fuller (1980), interpreted his comment to refer to a date about 30 years before 1891. An unattributed report in Easton (written commun., 1911–31) ca. 1915–20 of tree scars dated by counting rings, which "date back to the forties and fifties of 1886," remains a typographical mystery.

Hyde and Crandell (1978) also reported two debris flows in Rainbow Creek. The "most recent" flow was believed to have extended downvalley "at least 1.5 km" from the scarp on the flank of Lava Divide, and "may have occurred within the last 100 years." Like both Fuller (1980) and this study, Hyde and Crandell (1978) recognized the initial large avalanche and a smaller later flow (discussed below).

A younger debris avalanche originated from the same scarp area as the 1889–90 debris avalanche between about 1917 and 1932. The debris avalanche impounds Rainbow Lake and also transformed to a debris flow (figs. 57, 62). We prefer the later part of the age interval based on our confidence that J. Morovits would have reported the flow had it occurred while he still lived several kilometers downstream. He left the area in 1917. The minimum limiting date of 1932 is based on our coring of the largest tree in a large group of Douglas firs in the center of the Rainbow Creek valley at the location shown in figure 57. That tree had 67 rings in 2006, yielding 1932 as a minimum age of the substrate, assuming a 7-year colonization time gap (2006−67−7=1932). In the 1930–35 Wernstedt photograph (fig. 62), the site is entirely barren.

The younger landslide has a broadly hummocky surface reflecting the presence of megablocks on the order of 60–80 m in maximum dimension. They form the elevated darker areas consisting of rubbly debris in the 1930–35 photograph (fig. 62). The steep, lobate front of the flow, 0.4–0.6 km downstream from Rainbow Lake, may also consist of partially disaggregated masses of similar scale. Relative to the larger and earlier 1889–90 Rainbow Creek debris avalanche, the much smaller runup distance of this second flow (ca. 25–30 m; fig. 59) indicates a lower velocity of approximately 17 m/s. Correspondingly, the H/L was approximately 0.20, indicating this avalanche was less mobile than the 1889–90 example and less than those typical of volcanic terrains (Siebert, 1984; Crandell, 1989; Hayashi and Self, 1992). The lower mobility may have been the consequence of less disaggregation of the megaclasts and the production of fine sediment by cataclasis.

Deposits of an older landslide underlying the 1889–90 avalanche were seen at only one site—on the left bank of Rainbow Creek, 0.6 km upstream from the confluence with Swift Creek (fig. 53). Wood in the deposits yielded an age of 677–496 cal. yr B.P. (1273–1454 C.E.). Otherwise, we see no pre-1889–90 deposits other than bedrock in Rainbow Creek, except for Vashon Drift at an altitude of 1,900 ft (580 m) and Vashon glaciolacustrine deposits at an altitude of 2,360 ft (719 m).

Other Debris Flow, Lahar, and Landslide Deposits

Debris Flows and Lahars in North Flank Drainages

All north flank channels have conveyed debris flows that have originated most probably from rainfall-induced or gravity-triggered landslides on valley-side slopes. The landslides typically are channelized as debris flows, or they temporarily block the channel, releasing surges with significant proportions of entrained sediment. Major flood discharges transform locally to clay-poor debris flows, amplified by entrainment of detritus contributed by bank erosion (see Glacier Creek example in table 7). In middle reaches of Glacier and Wells Creek, the Holocene alluvial sections contain tephra layer O (ca. 7.6 ka). We see no significant lahar deposits either underlying or overlying tephra layer O and therefore surmise that no significant lahars of volcanic origin have occurred in those watersheds during the Holocene.

Debris Flows in Middle Fork Nooksack River

Several debris-flow deposits are seen in cutbanks in the lower reaches of the Middle Fork Nooksack River, ending about 30 km downstream from the summit. A debris flow yielding an age of 7.93–7.71 ka occurs below tephra layer O at RS–25 (appendix 1). Kovanen and others (2001) reported an otherwise undescribed debris-flow deposit located downstream from the Mosquito Lake Road bridge across the Middle Fork Nooksack River with an age of 3.45–3.21 ka. A debris flow or lahar, not seen elsewhere, and older than the Middle Fork lahar (and hence covered by those deposits at most locations), is present near the same location, 0.4 km downstream from the Mosquito Lake Road bridge. The origins of these deposits are unknown.

Older Lahar from Sherman Crater in Boulder Creek

A lahar deposit is exposed on the left bank of Boulder Creek, 150 m upstream from the Baker Lake Road bridge (fig. 3). The upper 2 m of the deposit consists of rounded cobble- and boulder-size clasts in a matrix of silt, sand, and fine gravel particles of which 10–15 percent consist of pale-colored, hydrothermally altered lithologies most likely from Sherman Crater. It is overlain by a sequence consisting of 0.4 to 1.5 m of silt-rich overbank flood deposits intercalated with fluvial sand containing particles of tephra layer BA, which in turn is overlain by the Morovitz Creek lahar (1845–47 C.E.). Charcoal 40 cm above the base of the fluvial deposits yields an age of 1.06–0.91 ka (appendix 2), giving a minimum age to the deposit. On the basis of tephra layer BA, the deposit is either time correlative to the middle Holocene lahar deposits in Park Creek or is a younger lahar or debris-flow deposit. It would be reasonable for a collapse into Park Creek to also enter Boulder Creek. Therefore, we favor a middle Holocene age for the deposit, but have no evidence to prove its correlation to the Park Creek lahars.

Figure 62. Lage Wernstedt photograph 3968 of the Rainbow Creek valley circa 1930–35. A, area of landslide failure; B, runup of 1889–90 debris avalanche noted in figures 57 and 59; C, general location of 67-year-old tree cored in 2006; D, terminus of the younger (between 1917 and 1932), less-vegetated Rainbow Creek debris avalanche; and E, well-defined vegetated lateral levees of the 1889–90 Rainbow Creek debris avalanche.

Landslide in Rainbow Creek Valley

Deposits of an older landslide (fig. 57, labeled slump) with limited runout (altitude of 4,320 ft [1,317 wm]) lie below head scarps on the interfluve northeast of the left-lateral moraine of Rainbow Glacier, above the track of the 1889–90 flow. These deposits, also mapped by Fuller (1980) and Hildreth and others (2003), consist mainly of Nooksack Formation. From tree-ring dating, the oldest of several hemlocks growing on the crest of a headscarp levee is at least 412 years in age.

Debris Flows from Sherman Crater in the 20th Century

Periodic small, surficial collapses of the northeast face of Sherman Peak form debris flows of snow, ice, and hydrothermally altered rock that flow down Boulder Glacier (Frank and others, 1975). The flows generally travel 2.5 to 3 km, though one in June 1984 traveled at least 5.8 km before launching off the glacier terminus. The collapse area for these flows is generally about the same for each event. Frank and others (1975) calculated a volume of about 35,000 m^3 for the initial collapse that quickly moved downslope as a debris flow. They argued for a geothermal origin for these events, based on their observation of a weak vapor plume being coincident with a collapse in 1973; however, no such plume has been seen during subsequent collapse events. Gravitational collapse of oversteepened snow and ice on weak hydrothermally altered rock thus may also be a triggering mechanism. During the unrest in 1975, Frank and others (1975) were concerned that erosional undercutting of the slope below the summit of Sherman Peak could destabilize the peak and lead to a much larger debris avalanche.

Frank and others (1975) documented six collapses between 1958 and 1973, thus calculating a 2.5 year average recurrence interval for that time period. Between March 1975 and 1979, two such events occurred (Frank, 1983; table 1). We know of only one debris flow between 1979 and 2006—it occurred in 1984—but it is likely that others occurred as well. The most recent events have occurred in 2006, 2010, 2013,

and 2016. Debris flows have been documented primarily in the late spring to early fall months of June, July, August, and October. The debris flow in October 2013 was detected on seismometers 6 km west and 11 km northeast of the volcano.

Summary of Lahars

- Volumetrically, the Holocene record at Mount Baker is dominated by clay-rich lahars and debris flows, which have largely affected the west, south, and east flanks of the volcano. In most cases the lahars were triggered by flank collapses of altered rock that transformed rapidly to lahars that entrained (bulked) sediments (till, alluvium, lacustrine deposits, and so on) as they moved downstream (table 10).
- North-flank drainages have largely been unaffected by volcanic activity during the latest Pleistocene to present. Absence of clay-rich debris flows in north-flank drainages reflects the mostly unaltered nature of the rocks in those drainages.
- Unusual among the Holocene events is the clay-rich Schriebers Meadow lahar, which overlies eruptive deposits from the Schriebers Meadow cinder cone. Despite the name, the source for this event is on the Mount Baker edifice, not on the cinder cone. No known volcanic unrest or activity is known on the edifice at this time nor is the exact source locality known. The timing of the Schriebers Meadow lahar predates known phreatic activity at Sherman Crater, but is close in age to tephra layer MY, which may signify the beginning of the development of a hydrothermal system near Sherman Crater.
- The most voluminous and far-traveled lahars (table 10)—Park Creek (PC_1), Middle Fork, and Ridley Creek lahars—occurred in the middle Holocene (around 6.7 ka) at about the time of the only Holocene magmatic eruption from Mount Baker.
- The Morovitz Creek lahar resulted from a collapse of the east side of Sherman Crater within 2–4 years of the phreatic eruption that produced tephra set YP in 1843 C.E.
- The late-19th-century Rainbow Creek debris avalanche has the typical high mobility (H/L = 0.11) of a volcanic debris avalanche (H/L = 0.10; Hayashi and Self, 1992), which is attributed generally to intense alteration and rapid disaggregation of failed volcanic rock. The failure occurred in largely unaltered rock, but at the contact between overlying middle Pleistocene lavas and underlying Mesozoic Nooksack Formation. The high mobility is attributed to cataclasis during failure and entrainment of clay-rich Vashon Drift and fine-grained lacustrine deposits.
- Small, meteorologically induced debris flows dominate the most recent record, primarily on the south side of Mount Baker.

Chapter H

Mount Baker Volcano, Northern Casade Range, Washington

Fumaroles inside Sherman Crater. Man on glacier (bottom center) for scale. Photograph by John H. Scurlock, August 12, 2010, used with permission.

Chapter H

Postglacial Eruptive Periods and Implications for Future Hazards

Using data from the previous chapters, we define four postglacial eruptive periods at Mount Baker. From oldest to youngest, they are the latest Pleistocene Carmelo Crater eruptive period, the early Holocene Schriebers Meadow eruptive period, the middle Holocene Mazama Park eruptive period and the historical Sherman Crater eruptive period. The first three eruptive periods produced magmatic deposits, whereas the youngest eruptive period was entirely phreatic. Below we describe each of the eruptive periods and reanalyze age dates to better constrain the timing of the events and durations of the periods. Lastly, we consider the implications for future volcanic hazards based on these past events.

Latest Pleistocene Carmelo Crater Eruptive Period

We call the latest Pleistocene eruptive episode, the Carmelo Crater eruptive period, for the ice-filled summit crater, Carmelo Crater, of Mount Baker (Hildreth and others, 2003). We concur with Hildreth and others (2003) that the origin of the pyroclastic-flow deposits within the Boulder Creek, Pratt Creek, and Sulphur Creek assemblages, and possibly the Rocky Creek sequence, is from collapse of summit lava flows erupted from the summit crater. And we infer that the lahar deposits in these sequences are from the hot pyroclastic flows interacting with snow and ice. Although we have not correlated any of the assemblage deposits to specific summit lava flows, assemblage distribution (fig. 27, chapter E) and lack of lava flows from Sherman Crater (Hildreth and others, 2003) indicate a Carmelo Crater source. The assemblages are confined in age between deposits of Vashon age (~16.3 ka) and before tephra set SC (~9.8 ka). However, the presence of detrital volcanic sediment in Glacial Lake Baker, sediment facies Mhc_1 and Mu, suggests that the assemblages were emplaced between the volcanic-free Sandy Creek lacustrine beds (Lsc; ~14.1 ka) and before the Glacial Lake Baker forest bed (~11.6 ka). This time period correlates to the latest Pleistocene advance of the Cordilleran ice sheet during the Sumas stade (14–11.6 ka) in Puget Sound with correlative alpine glacier advances of Sumas age in the Cascade Range. Thus, these assemblages appear to date the latest construction of the Mount Baker edifice as occurring during the Sumas stade.

We include tephra set SP within the Carmelo Crater eruptive period on the basis of age (~12.8 ka; fig. 63) and stratigraphy. At RS–5, we have limiting dates from charcoal in soil above and beneath tephra set SP. The maximum limiting age of 13.4–13.2 ka (WW6462, fig. 64) is similar to the minimum age of a moraine of presumed early Sumas age at Pocket Lake (13.5–13.1 ka; Osborn and others, 2012). The minimum limiting age of 9.46–9.13 ka is from a soil above tephra set SP and layer MY and is considerably younger than all other tephra set SP ages. Charcoal in soil overlying the Sulphur Creek assemblage (RS–16), which in turn overlies till of presumed Sumas age, is 12.96–12.66 ka. Although the soil and tephra have overlapping ages, it does not appear that any tephra particles are in the soil, although that locality may be outside the preserved distribution of the tephra. At RS–4, where the tephra overlies a diamict of presumed Sumas age, charcoal samples from within the tephra give three similar ages ranging from 12.97 to 12.43 ka. The maximum limiting age on a moraine of Sumas age from the last late glacial advance is 12.6–12.4 ka (RS–3). Thus, tephra set SP appears to have been erupted during the Sumas stade, perhaps before its last phase.

The age of tephra set SP (~12.8 ka) is broadly similar to that of the Boulder Creek assemblage (~13.5–12.1 ka), which overlies till of Sumas age and is the best constrained in age of

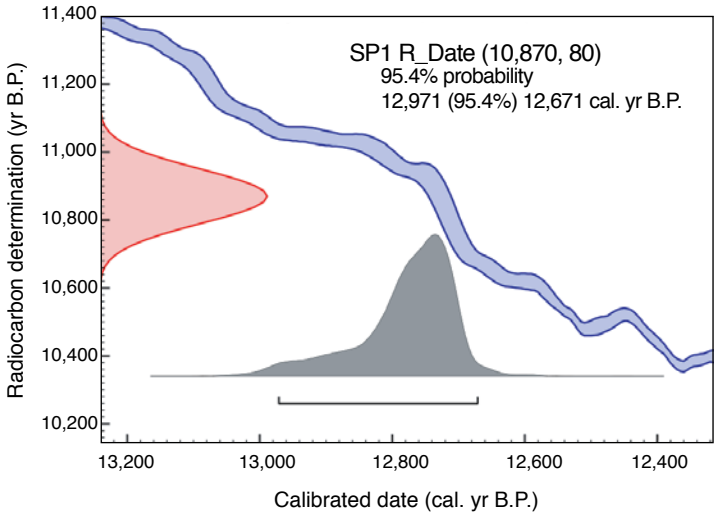

Figure 63. Screenshot of plot showing the calibration curve for charcoal in tephra set SP (radiocarbon sample WW2965) from RS–4. The radiocarbon age (in years before present, yr B.P.) is shown in parentheses at top with the uncertainty. In red is the graphical display of the radiocarbon age; the blue ribbon is the calibration curve for the interval 13,240 to 12,300 calibrated years before present (cal. yr B.P.). The dark gray shows the calibrated probability distribution and the bar shows the 2σ probability range, which is also written in the upper right. On the basis of this and other similar calibrations, we suggest the age of tephra set SP is about 12.8 thousand years old (ka). Radiocarbon analyses from the U.S. Geological Survey Radiocarbon Laboratory in Reston, Va. Calibrated ages and plots developed using 2013 OxCal version 4.2.3 (Bronk Ramsey, 2009; Reimer and others, 2013). %, percent.

the clastic assemblages. Boulder Creek assemblage clasts are plagioclase-rich, two-pyroxene andesite of limited composition (59.7–60.7 percent SiO_2; Hildreth and others, 2003). Tephra set SP has the same mineral constituents as Boulder Creek assemblage lavas and normalized glass compositions average 66.1 percent SiO_2 (appendix 5), higher than the Boulder Creek assemblage bulk-rock composition. (SiO_2 contents in glass are often greater than in bulk rock because of late-stage plagioclase crystallization.) Thus, there is permissive evidence to link tephra set SP to Boulder Creek assemblage lavas, but not absolute evidence because many Mount Baker lavas have similar petrologic and chemical affinities.

Early Holocene Schriebers Meadow Eruptive Period

We define the early Holocene Schriebers Meadow eruptive period (~9.8–9.1 ka) as beginning with eruptions of the cinder cone in Schriebers Meadow that emplaced tephra set SC and the Sulphur Creek lava flow and ending with deposition of tephra layer MY (table 14). Within this time period is also emplacement of sediment facies Vhc and Vu in Glacial Lake Baker that contains tephra set SC and the Schriebers Meadow lahar (~9.5 ka). We name it the Schriebers

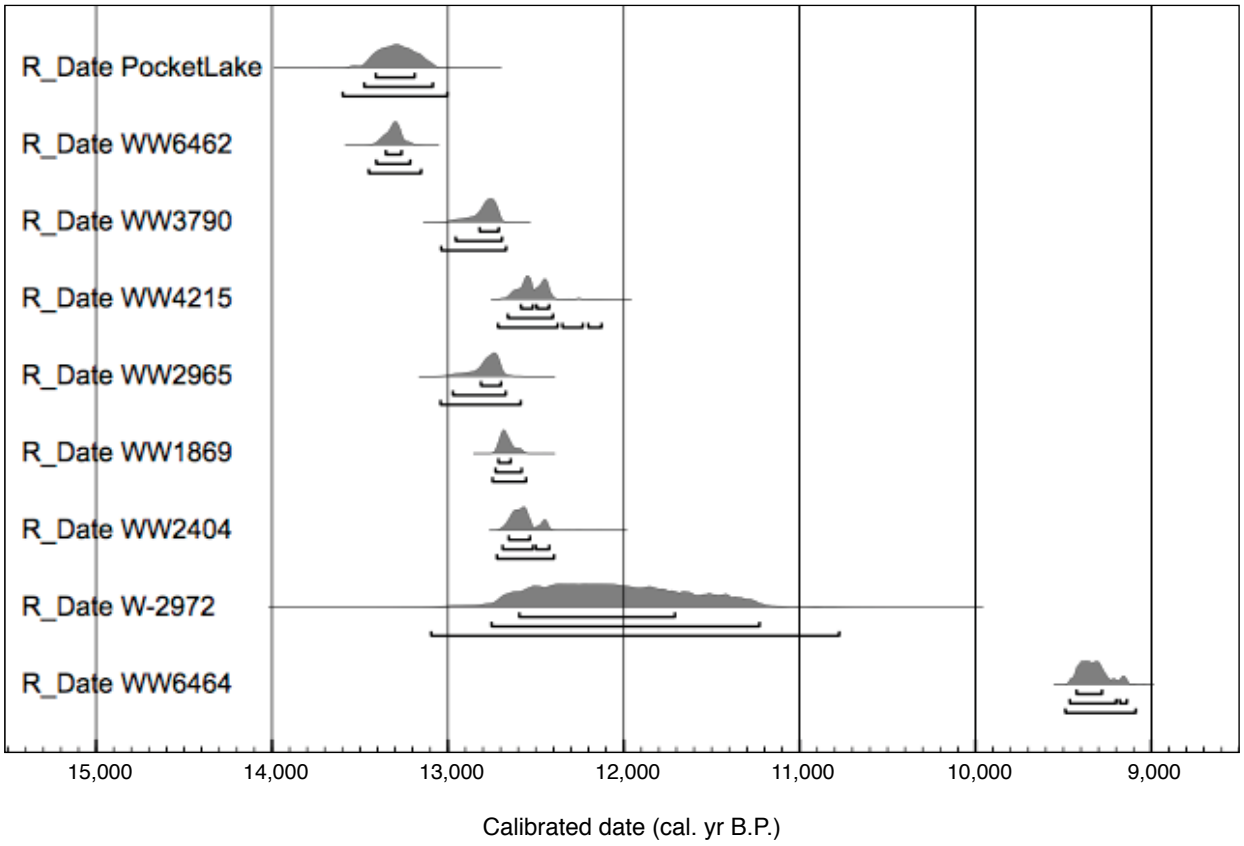

Figure 64. Screenshot of plot showing calibrated age distributions, in calibrated years before present (cal. yr B.P.), of radiocarbon samples related to the age of tephra set SP and latest Pleistocene alpine glacial deposits of Sumas age (appendixes 2, 3). The bars below each gray probability distribution show (from top to bottom) the 1, 2, and 3σ probability ranges. Samples WW6462 and WW6464 are maximum and minimum limiting ages for tephra set SP from RS–5, respectively. Pocket Lake is a minimum age for the oldest moraine of Sumas age at that site (Osborn and others, 2012), which is similar to the maximum limiting age of tephra set SP from RS–5. Sample WW3790 is charcoal from a soil that overlies the Sulphur Creek assemblage—a minimum limiting age for that assemblage—which in turn overlies a diamict of Sumas age (RS–16). WW4215 is an age from wood in the youngest moraine of Sumas age in the upper Middle Fork Nooksack River valley (RS–3). Samples WW2965, WW1869, and WW2404 are from charcoal in tephra at RS–4, where WW2965 represents the main layer of tephra set SP and the others in soil containing concentrations of tephra set SP. Sample W-2972 is wood within tephra set SP from Hyde and Crandell (1978). Radiocarbon analyses from U.S. Geological Survey Radiocarbon Laboratory in Reston, Va. Calibrated ages and plot output from 2013 OxCal version 4.2.4 (Bronk Ramsey, 2009; Reimer and others, 2013).

Table 14. Summary of events during the Schriebers Meadow eruptive period.

[cal. yr B.P., calibrated years before present]

Unit	Calibrated age (cal. yr B.P.)	Process	Source
Tephra layer MY	9,396–9,135[a]	Phreatic eruption	Mount Baker, possibly Sherman Crater area
Schriebers Meadow lahar	9,527–9,472[b]	Flank collapse and lahar runout	Flank of Mount Baker upslope from Schriebers Meadow
Volcaniclastic facies (Vhc, Vu) in Glacial Lake Baker	9,686–9,541	Sedimentation into lake	Reworked tephra set SC
Sulphur Creek lava flow	10,168–9,472[c]	Lava flows in Glacial Lake Baker; deforms and invades lacustrine and volcaniclastic facies	Schriebers Meadow cinder cone
Tephra set SC (layers SC_1 and SC_2)	9,924–9,701[d]	Magmatic flank eruption	Schriebers Meadow cinder cone

[a]This is a combined age of 5 radiocarbon dates (calculated by calibrating each individual age and combining them using OxCal v. 4.2 [Bronk Ramsey, 2009; Reimer and others, 2013]). The total range from individual samples is 9,463–8,846 cal. yr B.P. (appendix 2).

[b]This is a combined age from five radiocarbon dates. The total range from individual samples is 9,665–9,285 cal. yr B.P. (appendix 2).

[c]Minimum-limiting date from age of overlying Schriebers Meadow lahar; maximum-limiting date is age of underlying tephra set SC.

[d]This is a combined age from three radiocarbon dates. The total range from individual samples is 10,168–9,552 cal. yr B.P. (appendix 2).

Meadow eruptive period for the magmatic activity at the cinder cone. Neither the Schriebers Meadow lahar nor tephra layer MY is associated with the cinder cone eruption or with any known magmatic activity at Mount Baker, the source of these deposits. We include the lahar and tephra within the eruptive period because of their broadly similar age. We are not implying that volcanic activity lasted for several hundred years as may be inferred by lumping these events together. We could instead separate the Schriebers Meadow lahar and tephra layer MY from the eruptive period and consider them as orphaned early Holocene events younger than the Schriebers Meadow eruptive period.

The calibration curve for the time period spanning the radiocarbon ages for tephra set SC is flat (fig. 65), which limits the calibrated age precision. Combining the calibrated ages of the individual radiocarbon samples narrows the range to 9.92–9.70 ka (fig. 66), although it also increases the probability that the calibrated age could be around 10.1 ka. Our age of about 9.8 ka is the same as that reported by Hildreth and others (2003).

Five radiocarbon ages of samples taken from outer rings of logs incorporated in the Schriebers Meadow lahar are tightly grouped with a combined calibrated age at 2σ of 9.53–9.47 ka. The calibration curve for this time period is steep, which narrows the age uncertainty (fig. 67).

At 2σ, the combined calibrated ages for tephra set SC (9.92–9.70 ka) and Schriebers Meadow lahar (9.53–9.47 ka) do not overlap, although some individual ages do (appendixes 2, 3). The lack of overlap suggests that these events were likely separated by as much as several centuries. At RS–21 (appendix 1; unit 2), the Schriebers Meadow lahar overlies

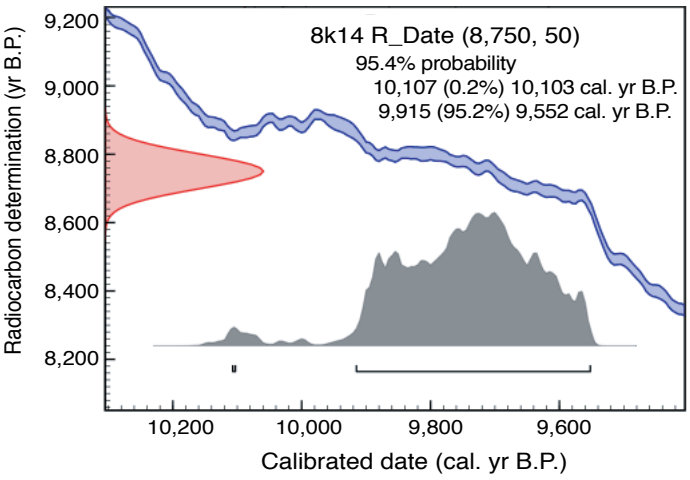

Figure 65. Screenshot of plot showing calibration curve for radiocarbon sample WW954, the youngest age obtained from charcoal in tephra set SC at RS–17. The radiocarbon age (in years before present, yr B.P.) is shown in parentheses at top with the uncertainty. In red is the graphical display of the radiocarbon age; the blue ribbon is the calibration curve for the interval 10,300 to 9,400 calibrated years before present (cal. yr B.P.). The dark gray shows the calibrated probability distribution and the bars below show the 2σ probability range, which is also written in the upper right. Note the relatively flat slope of the blue ribbon above the histogram between 10,200 and 9,600 cal. yr B.P., which limits the calibrated age precision. Radiocarbon analyses from U.S. Geological Survey Radiocarbon Laboratory in Reston, Va. Calibration and plot output from 2013 OxCal version 4.2.3 (Bronk Ramsey, 2009; Reimer and others, 2013). %, percent.

more than 0.9 m of fluvial sand and silt (and presumably the Sulphur Creek lava flow), which represents an unknown time period. Elsewhere, the lahar directly overlies either the lava flow or tephra set SC with little evidence of weathering or soil development between units.

The Sulphur Creek lava flow has not been dated directly but is constrained by the ages of stratigraphically older tephra set SC, stratigraphically younger Schriebers Meadow lahar, and by relations with dated sediment (facies Vhc and Vu) in Glacial Lake Baker. Neither we, nor others (Kovanen and others, 2001; Hildreth and others, 2003) report an instance of primary tephra set SC overlying the Sulphur Creek lava, but consistently find the lava overlying the tephra. We infer a close temporal relation between the cinder cone and lava flow on the basis of historical eruptions, such as Parícutin and Jorullo (for example, Luhr and Simkin, 1993), where only a few years to decades separate tephra emplacement from subsequent lava flows.

Tephra layer MY is a thin (<0.5 cm) lithic tephra found in only two locations, both of which are south of Sherman Crater. It is not in stratigraphic contact with any deposits of the Schriebers Meadow eruptive period. The upper age range of tephra layer MY (~9.4–9.1 ka; appendix 2) is only slightly younger than the lower age range of the combined Schriebers Meadow lahar (9.47 ka), although individual calibrated ages overlap. Like the lahar, the tephra is found only south of present-day Sherman Crater. Both the tephra and lahar contain modest amounts of hydrothermally altered material, the first such evidence of postglacial hydrothermal alteration on the edifice. The similarities in componentry, age, and distribution lead us to speculate that hydrothermal activity in the vicinity of Sherman Crater had commenced by the early Holocene and that the Schriebers Meadow lahar may have been triggered during unrest that produced tephra layer MY. Reid (2004) demonstrated through numerical models of heat and groundwater flow that hydrothermal activity might result in deep-seated collapse of an edifice without accompanying magmatic activity. We reason that similar processes could also result in shallower flank failures.

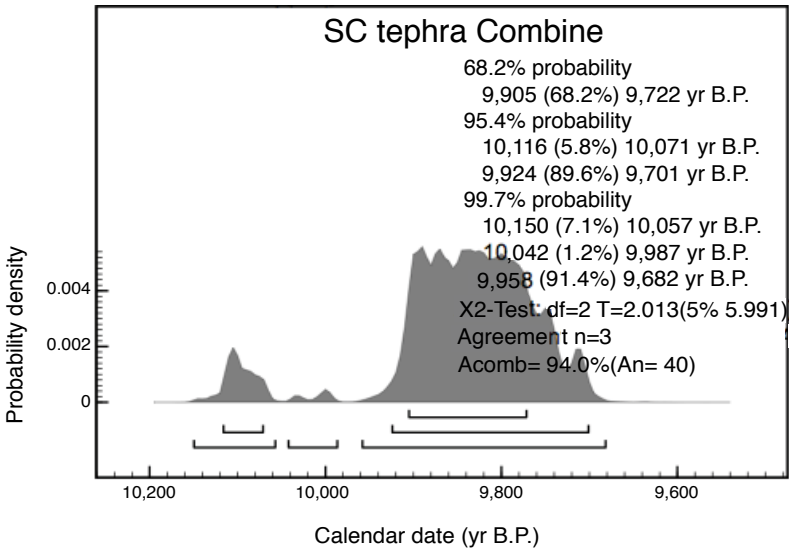

Figure 66. Screenshot of plot showing the calibrated age distribution for tephra set SC determined by combining individual calibrated ages from three charcoal samples in the top 0.5 meters of layer SC_1 in the cutbank of Sulphur Creek (RS–17). The dark gray shows the calibrated probability distribution. The bars below the dark gray histogram show (from top to bottom) the 1, 2, and 3σ probability ranges, which are also written in the upper right. Radiocarbon analyses from U.S. Geological Survey Radiocarbon Laboratory in Reston, Va. Calibration and plot output from 2013 OxCal version 4.2.3 (Bronk Ramsey, 2009; Reimer and others, 2013). %, percent.

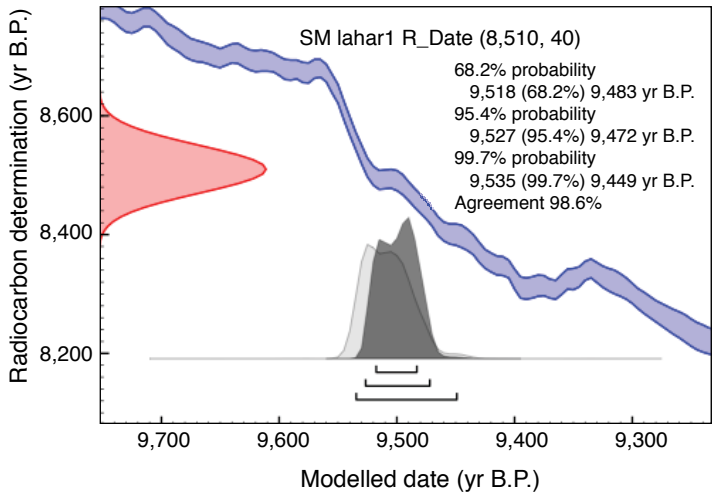

Figure 67. Screenshot of plot showing the calibration curve for radiocarbon sample WW198 from the outer rings of a log in the Schriebers Meadow lahar. The radiocarbon age (in years before present, yr B.P.) is shown in parentheses at top with the uncertainty. In red is the graphical display of the radiocarbon age; the blue ribbon is the calibration curve for the interval 9,800 to 9,200 calibrated years before present (cal. yr B.P.). The dark gray shows the calibrated probability distribution and the bars show (from top to bottom) the 1, 2, and 3σ probability range, which are also written in the upper right. In light gray is the combined age distribution of five ages that has a calibrated 2σ range of 9.53–9.47 thousand years (ka). Radiocarbon analyses from U.S. Geological Survey Radiocarbon Laboratory in Reston, Va. Calibration and plot output from 2013 OxCal version 4.2.3 (Bronk Ramsey, 2009; Reimer and others, 2013). %, percent.

Middle Holocene Mazama Park Eruptive Period

The Mazama Park eruptive period (~6.7 ka) records the most significant Holocene activity at Mount Baker in terms of eruptive volume and far-reaching volcanic events. It consists of a series of events (table 15) that most likely were driven by magmatic intrusion and eruption centered around and at the site of Sherman Crater. The episode began with flank collapses from opposite sides of the crater (see fig. 46, chapter G) and ended with the magmatic eruption of tephra layer BA. This is the only known magmatic eruption from Mount Baker in the Holocene and follows the magmatic late Pleistocene Carmelo Crater eruptive period by more than 5,000 years. The eruptive period is named for Mazama Park (below the Deming Glacier; figs. 3, 4), where the majority of deposits from this episode are found.

Stratigraphic relations suggest the following sequence. The earliest collapse events to the west and east of Sherman Crater (fig. 46) spawned clay-rich (cohesive) lahars down Park Creek, likely Boulder Creek, and the Middle Fork Nooksack River. These cohesive lahars are not in contact, so their relative timing is unknown. The Middle Fork lahar is overlain by the Ridley Creek lahar, whose collapse area is likely near or adjacent to that of the Middle Fork lahar, which forced the flow into different initial drainages (fig. 46). The Ridley Creek lahar contains intensely altered clasts and proximally has a matrix similar to that of phreatic tephra set OP. Tephra set OP forms a couplet with the magmatic tephra layer BA, which caps the eruptive sequence. None of the lahars (Park Creek, Boulder Creek, Middle Fork, or Ridley Creek) contains any juvenile clasts, suggesting that these flank failures and resultant lahars all predate the magmatic activity that emplaced tephra layer BA. Below we couple the stratigraphy with a more detailed look at the ages to suggest that the Mazama Park eruptive episode consisted of a relatively short-lived (weeks to a few years) unrest-to-eruptive event with early lahars occurring during unrest and before magma reached the surface.

The range in radiocarbon ages from individual samples highlights the difficulties in interpreting age data for the timing of events. Individually calibrated ages for the largest Park Creek and Middle Fork lahars span from 7.75 to 6.65 and 6.89 to 6.54 ka, respectively, suggesting the Park Creek event could have occurred anytime within a thousand-year interval. If we restrict Park Creek lahar ages to only those from wood with bark (table 2.15 of appendix 2), we reduce the spread of ages for the Park Creek lahar to 6.89–6.65 ka, which overlaps well with the ages from the Middle Fork lahar, but which still suggests an interval of about 350 years. We can further refine the ages statistically by calibrating individual ages and then combining them to see the time period of best fit to the calibration curve (fig. 68). When done for both the Park Creek and Middle Fork lahars, the spread of ages is further reduced

Table 15. Events of the Mazama Park eruptive period.

[Ages given are full range of calibrated ages from individual layers (appendix 2) as well as combined ages where appropriate. cal. yr B.P., calibrated years before present]

Unit	Calibrated age (cal. yr B.P.)	Process	Source
Older lahar in Boulder Creek (?)	>1,059 and <6,321[a]	Flank collapse and lahar runout	East flank of Sherman Crater
Tephra layer BA	6,617–6,321[b]	Magmatic eruption	Sherman Crater
Tephra layer OP and lahars of remobilized tephra	6,731–6,440[c]	Phreatic eruption (possibly phreatomagmatic)	Sherman Crater
Ridley Creek lahar	6,750–6,710[d]	Flank collapse and lahar runout	West flank of Sherman Crater (altered lava flows dipping downslope)
Middle Fork lahar 2σ combined	6,890–6,533 (individual) 6,754–6,472 (combined)[e]	Flank collapse and lahar runout	Flank below Roman Wall (?), west of Sherman Crater
Park Creek lahars 2σ combined	7,169–6,644 (individual) 6,787–6,676 (combined)[f]	Flank collapse and lahar runout	Flank east of Sherman Crater

[a]Unclear if this deposit is related to the Mazama Park eruptive episode or not, but highly probable on basis of geography.

[b]Tephra is part of a couplet with tephra layer OP and therefore should be of similar age.

[c]Tephra is associated with the Ridley Creek lahar and therefore should have the same age as the lahar.

[d]Wiggle-match age using OxCal v. 4.3 (Bronk Ramsey and others, 2001; Reimer and others, 2013) and ^{13}C analyses by the U.S. Geological Survey radiocarbon laboratory in Reston, Va.

[e]The combined calibrated age at 2σ probability is from five radiocarbon samples with two ranges: 6,777 to 6,764 (6.1 percent) and 6,754 to 6,472 (89.3 percent) cal. yr B.P.

[f]The combined calibrated age at 2σ probability is from four radiocarbon samples.

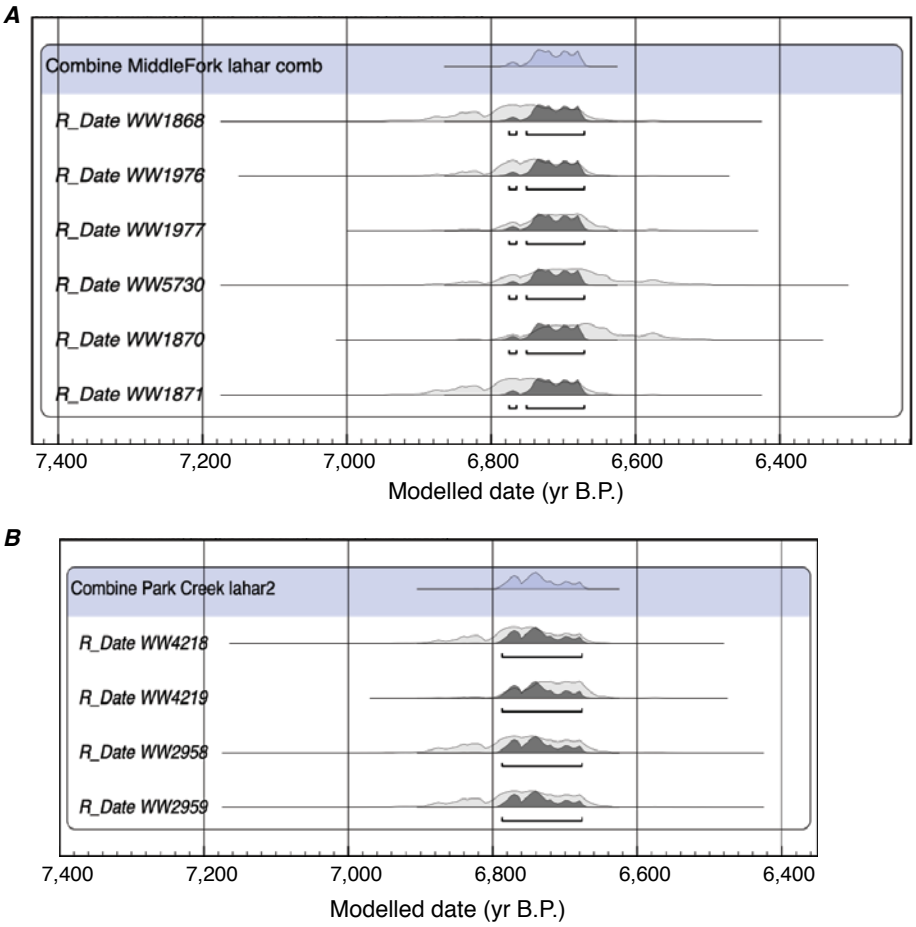

Figure 68. Screenshot of plots showing individual and combined calibrated ages (in calibrated years before present, cal. yr B.P.) for the Middle Fork lahar (*A*) and for the largest of the Park Creek lahars, PC_1 (*B*). In the blue banner at the top of each plot is the combined calibrated probability distribution. Calibrated combined probability distributions (dark gray) are superimposed on the calibrated probability distribution for each sample (light gray corresponding to laboratory numbers; appendixes 2, 3), with bars below showing probability range at 2σ. The combined calibrated age at 2σ for the four Park Creek lahar samples is 6.79–6.68 thousand years (ka) and for the five Middle Fork lahar samples is 6.75–6.67 ka (92 percent) and 6.78–6.77 ka (3.4 percent). The most probable ages are indistinguishable. Radiocarbon analyses from the U.S. Geological Survey Radiocarbon Laboratory in Reston, Va. Calibration and plot output from 2017 OxCal version 4.3.2 (Bronk Ramsey and others, 2001; Reimer and others, 2013).

at 2σ to 6.79–6.68 and 6.76–6.67 ka, respectively, and the interval in which the event likely occurred is reduced to about 120 years.

A complete log in the Ridley Creek lahar (fig. 51) allowed us to obtain a wiggle-match age for the Ridley Creek lahar (fig. 69). This is a technique where the interval between individual radiocarbon samples is precisely known (through tree-ring counting) and thus radiocarbon ages can be better fit to the wiggles of the calibration curve. The wiggle-match age for the Ridley Creek lahar using measured $\delta^{13}C$ values is 6,750–6,710 cal. yr B.P. (table 12). It is instructive to compare the wiggle-match age (fig. 70; appendix 2) with the calibration curves for each of the tree-ring intervals (fig. 70). For ring interval 1–16 (denoted N(8,8), the outermost layer), the wiggle-match age is shifted to the oldest part of the range and beyond—less than 5 percent of the range from this interval overlaps with the wiggle-match age. For intervals 223–225 and 281–285 (denoted N(224,1) and N(283,2)) near the center of the tree, the wiggle-match age is skewed to the younger part of the age distributions. The median calibrated age from wood near the center of the tree (285 rings) is more than 400 years older than the wiggle-match age. Details of the wiggle-match age highlight difficulties in interpreting radiocarbon ages and caution against over interpretation of those ages, especially from wood (including ages from the outer rings of limbs with bark).

Ages for tephra set OP range from 7.17 to 6.44 ka (table 2.11 of appendix 2) and overlap the wiggle-match age for the Ridley Creek lahar (6.75–6.71 ka). However, ages for tephra layer BA, which forms a couplet with tephra set OP, are generally younger than the wiggle-match age. Dates on charcoal from organic soil beneath layer BA, where set OP is absent, give maximum limiting ages that either are older than the lahar (7.25–6.93 ka; appendix 2) or overlap with the lahar, but with broad uncertainties (for example, 6.95–6.28 ka; Hildreth and others [2003]; appendix 3). Dates from charcoal within the tephra at two localities (RS–19, RS–22; appendix 2) are fairly well constrained between 6.65 and 6.31 ka with a combined age of 6.50–6.41 ka. These ages are younger than the lahar age and similar to a charcoal date (6.67–6.44 ka) at the contact between tephra set OP and layer BA (WW2403; appendix 2). We consider the charcoal dates from within tephra set OP and layer BA and at their contact to be minimum ages because there is no known source of charcoal for this eruption. The eruption did not produce pyroclastic flows and it is unlikely that either tephra fall (OP or BA) would have been hot enough to char organic material. Lightning from the BA ash cloud could have produced forest fires, but the areas where charcoal is found within the tephras are areas that were previously swept by the Ridley and Pratt Creek lahars; thus, those areas likely did not support organic material

large enough to form fragments of charcoal. The tephra falls are both relatively thin where the charcoal was sampled, so incorporation of younger charcoal through bioturbation is likely. Alternatively, tephra set OP and layer BA are centuries younger than the Ridley Creek lahar deposits; however, this hypothesis is not supported by the stratigraphic evidence. Thus, our data indicate that the age of the middle Holocene Mazama Park eruptive episode is about 6.7 ka, just slightly older than the 6.5 ka age suggested by Hildreth and others (2003).

Our interpretation of stratigraphic relations and age dates suggests that the duration of hazardous events (lahars and tephra fall) during the middle Holocene Mazama Park eruptive episode was likely short (days, months, years?), but how short is difficult to determine. The contact between the Middle Fork lahar and overlying Ridley Creek lahar is generally sharp (RS–24, RS–25; figs. 2, 48) at the few downstream locations where contact relations are accessible. The sharp contact suggests that enough time occurred between the emplacement of the two flows to allow the Middle Fork lahar to sufficiently dewater and compact before being overridden by the Ridley Creek lahar. Experimental studies show that sequential noncohesive (clay-poor) debris-flow surges of

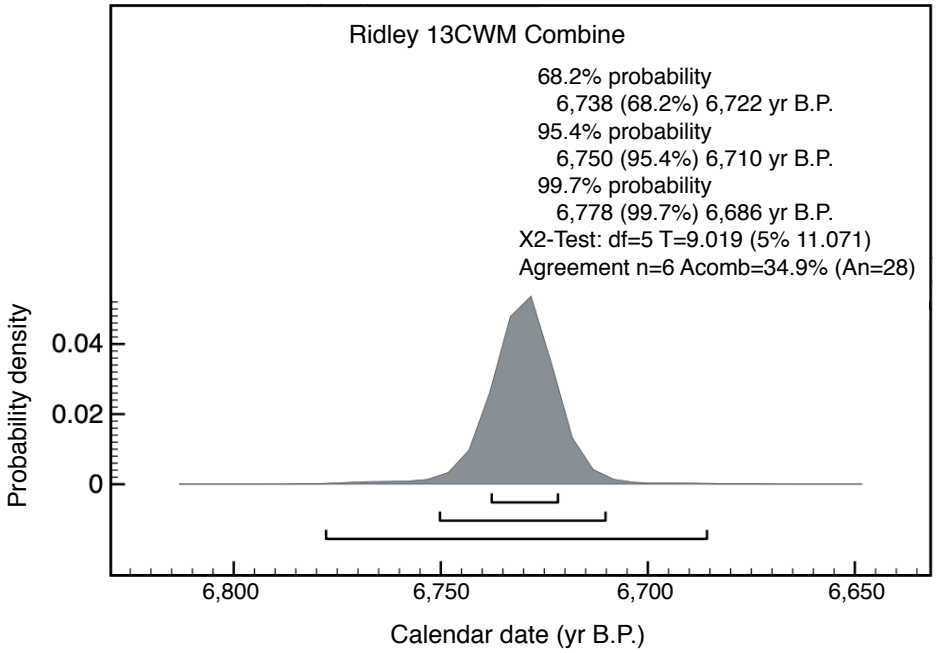

Figure 69. Screenshot of plot showing the Ridley Creek wiggle-match age calibration, in years before present (yr B.P.). The dark gray shows the calibrated probability distribution and the bars show (from top to bottom) the 1, 2, and 3σ probability range, which are also written in the upper right. Radiocarbon analysis from the U.S. Geological Survey Radiocarbon Laboratory in Reston, Va. Plot output from 2013 OxCal version 4.2.3 (Bronk Ramsey, 2009; Reimer and others, 2013). %, percent.

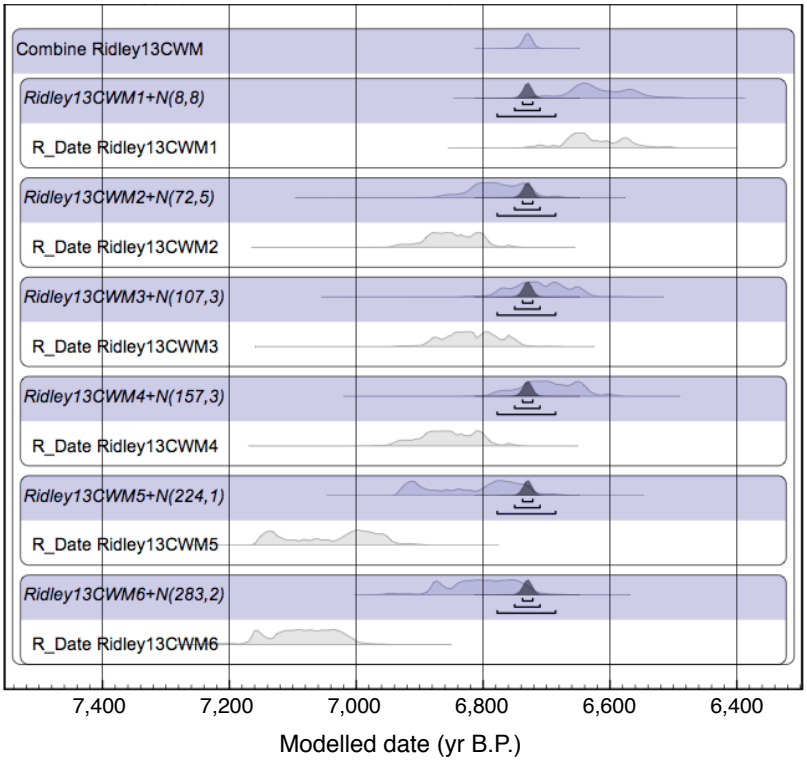

Figure 70. Screenshot of plot showing the wiggle-match ages (in years before present, yr B.P.) for six samples taken from the same log in the Ridley Creek lahar deposit. In the blue banner is the calculated wiggle-match age probability distribution. For each sample, the tree ring interval is given in parentheses as the intermediate ring number followed by the range (for example, (8,8) means tree ring interval 1–16 and (224,1) means tree ring interval 223–225). The outermost tree ring is ring number 1. For each sample, the blue bar shows the individual calibrated age corrected for the tree ring interval (light gray) with the wiggle-match age superimposed (dark gray); the white bar shows the calibrated age without the ring-interval correction. The bars below the wiggle-match distribution show (from top to bottom) the 1, 2, and 3σ probability ranges for the wiggle-match age. Radiocarbon analyses from U.S. Geological Survey Radiocarbon Laboratory in Reston, Va. Calibration and plot output from 2013 OxCal version 4.2.3 (Bronk Ramsey, 2009; Reimer and others, 2013).

similar material may mix sufficiently at their flow boundaries to destroy evidence of separate flows if the underlying unit has not dewatered prior to emplacement of the overlying unit (Major, 1997). Major's 1997 study supports field observations made during the 1989–90 eruption of Redoubt Volcano in Alaska. Scientists on the ground hours after the March 23, 1990, eruption could only distinguish the hot March 23 debris-flow deposits from the underlying cold March 14 debris-flow deposits by clast temperature (Gardner and others, 1994). We assume that cohesive (clay-rich) lahars would take even longer to dewater than noncohesive lahars and therefore more time would be needed to preserve a sharp contact. However, there are two important factors to consider: (1) the above experiments were not designed to study how long it would take to develop a sharp contact, and (2) the Middle Fork and Ridley Creek lahar material may be dissimilar enough to produce very different results than the material used in the experiments or found at Redoubt Volcano. In some of the few exposures in the gorge of the Middle Fork Nooksack River above Clearwater Creek upstream from RS–24 (fig 2), local evidence of erosion and deposition at the contact also suggests some time period between the two flows, but again the time interval is unclear. These observations provide permissible, but not unequivocal, evidence that the Middle Fork lahar may have preceded the overlying Ridley Creek lahar by some time period ranging from hours to perhaps weeks or months. Alternatively, the sharp boundary between the two lahars may reflect grain size or clay content heterogeneities in the Middle Fork lahar, which may have allowed it to dewater quickly, thus preserving contact relations for flows only minutes to hours apart. Although the exact timing is unknown, it is unlikely that the time period separating the flows could be greater than a decade because of the lack of wood at the contact between the lahars. It generally takes only a matter of years to a decade in the Pacific Northwest to reestablish trees on a disturbed or newly emplaced lahar surface (Pierson, 2006).

Regardless of the details, it is significant that the large Middle Fork lahar (and likely the Park Creek lahars) occurred early in the eruptive sequence before the main magmatic activity. The most likely scenario is that these lahars represent flank failures owing to magma intrusion into the edifice. These early flank failures were followed after some time by activity that produced another collapse (Ridley Creek lahar) simultaneously with phreatic explosions that produced tephra set OP. The phreatic eruption quickly culminated in the magmatic eruption that emplaced tephra layer BA.

Our interpretation of the Mazama Park eruptive period stratigraphy differs from that of Kovanen and others (2001, figs. 3, 5) who interpret the Rocky Creek ash (tephra set OP) as underlying the Middle Fork lahar. We suggest that our differences are likely due to conflicting interpretations regarding the stratigraphy at RS–20 (appendix 1, table 16), which is discussed in Kovanen and Easterbrook (1996). At RS–20, a phreatic ash underlies a lahar deposit that we (and they) interpret to be the middle Holocene Middle Fork lahar. However, we interpret the lahar to be reworked at that site, whereas they do not. Age dates from RS–20 (appendixes 1, 2) of <270 years before present support the interpretation that the phreatic tephra at this locality is the late Holocene tephra set YP and that the Middle Fork lahar is reworked. The age dates Kovanen and others (2001) give for the Rocky Creek ash (table 16) are not from this section but from deposits in upper Clearwater Creek (D.J. Kovanen, written commun., 2006), more than 2 km upstream of RS–20. Thus, we conclude

Table 16. Comparison of our interpretation of the stratigraphy at RS-20 (detailed stratigraphy in appendix 1) and the composite middle Holocene stratigraphy deduced by Kovanen and others (as shown in fig. 5 of their 2001 report).

[cal. yr B.P., calibrated years before present; ka, thousand years; m, meters; cm, centimeters]

Unit no.	Thickness	RS–20 stratigraphy, as interpreted in this report	Nearby(?) site(s), as interpreted by Kovanen and others (2001)
6	0.7 m	Redeposited Middle Fork lahar deposits; date from log in deposit is 275 to <0 cal. yr B.P. (flow age is 6.7 ka)	Middle Fork lahar ages are 6,715–6,218 and 6,741–6,296 cal. yr B.P.
5	0.5 m	Overbank deposits, organic rich; charcoal 10 cm above tephra set YP yields age of 420 to <0 cal. yr B.P.	Date above tephra is 6,957–6,192 cal. yr B.P.
4	1–2 cm	Tephra set YP (1843 C.E.); dates from partially carbonized wood in base of tephra are 280 to <0, 460 to <0, and 494 to <0 cal. yr B.P.	Rocky Creek ash (tephra set OP)[1]
3	0–30 cm	Overbank deposits, wood rich; dates from 2–15 cm below tephra are 905–677 and 1,284–1,076 cal. yr B.P.	Date below tephra is 6,719–6,450 cal. yr B.P.
2	2 m	Boulder alluvium	
1	<1 m	Glacial deposits with lacustrine beds, similar to those that are characteristic of late- or post-Vashon age at other localities in the Middle Fork Nooksack River (see unit 2 of RS–3; appendix 1)	Glacial deposits

[1]We believe that misinterpretation of the hydrothermally altered tephra at the RS–20 locality led Kovanen and others (2001) to suggest that tephra set OP underlies the Middle Fork lahar. Their ages above and below the tephra come from a nearby site, not from RS–20. Location of RS–20 is on right bank of Clearwater Creek about 120 m downstream from the bridge; Universal Transverse Mercator 570190 E., 5402480 N.

that they combined the Clearwater Creek and RS–20 sections because their dates on their Rocky Creek ash made sense stratigraphically with their dates of the Middle Fork lahar and led to what we think is an erroneous interpretation of the stratigraphy of middle Holocene events.

Historical Sherman Crater Eruptive Period (1843–80 C.E.)

The Sherman Crater eruptive period began in 1843 C.E. with the eruption of tephra set YP, a violent phreatic eruption that formed the modern configuration, although not size, of Sherman Crater. Several eruptions from Sherman Crater are reported between 1843 and 1880 C.E., such as those of 1854, 1856, 1858, and 1860 C.E. (appendix 6). We recognize from modern (and false) reports of incandescence that the middle-19th-century reports of incandescence may be incorrect, but the sheer number of events reported suggests some validity. Thus, it seems plausible that post-1843 C.E. unrest could have lasted for decades and could have been interspersed with small-volume eruptions that produced deposits that have not been preserved in the geologic record. It is noteworthy that, after ca. 1880 C.E. and specifically after 1891 C.E., when Sherman Crater was ice filled (appendix 6), no reports have been found of lightning or forest fires that were mistaken for eruptions. The late 1800s was a time when an increasing number of miners and homesteaders were aware that Mount Baker was an active volcano and who may have been tempted to report volcanic activity. Therefore, we put the end of the eruptive period around 1880 C.E., after which there were no more reports of incandescence at the volcano.

There is also no evidence that either the tephra, in 1843 C.E., or the lahar deposits, in 1845–47 C.E., effectively dammed the Skagit River (appendixes 6, 7). Nor does the tephra fall seem substantial enough to kill all the fish from miles around, as reported in Gibbs (1873). We speculate that the fish kill in the downstream Skagit River may have resulted from acidic meltwater, perhaps pooled in Sherman Crater, which was ejected or released into the surrounding drainages, either during or close to the time of the eruption. A modern analogy may be the 2005 event at Chiginagak Volcano, a hydrothermally active volcano on the Alaska Peninsula. There, acidic waters drained from a summit lake through tunnels at the base of a glacier that breaches the crater rim (Schaefer and others, 2008). The acidic waters traveled several tens of kilometers and spilled into a large lake, reducing its pH to ~2.9, killing much aquatic life, and preventing the annual salmon run. The Chiginagak event occurred, however, during a time of volcanic quiescence with no concurrent or ensuing eruption.

Age of Formation and Alteration at Sherman Crater

The first appearance of hydrothermally altered material at or near the site of Sherman Crater is during the early Holocene Schriebers Meadow eruptive period, with the emplacement of the Schriebers Meadow lahar (~9.5 ka) and tephra layer MY (~9.1 ka). Sometime before 7.6 ka (before the emplacement of tephra layer O), detrital, hydrothermally altered material began to appear in the stratigraphic record in Sulphur Creek (see RS–18; appendix 1). This suggests that the area of the present Sherman Crater was an area of active hydrothermal alteration prior to the beginning of the Mazama Park eruptive period.

The present volume of Sherman Crater is estimated at 15×10^6 m^3 (table 17) by us and by Hildreth and others (2003). The volume of the 1843 C.E. tephra set YP is a small fraction of that volume (table 17). Thus, modern Sherman Crater

Table 17. Estimated volumes of tephras that originated from Sherman Crater and the estimated volume of Sherman Crater before the 1845–47 collapse of the east side.

[m^3, cubic meters]

Tephra or crater	Volume (m^3)	Notes
YP	$1–2\times10^6$ bulk	Occurs as dispersed dusty ash in root zone beyond area of proximal deposition. Locally concentrated by surface runoff, and locally remobilized as small lahars. Primary extent poorly constrained.
BA	200×10^6 bulk	Granular, noncohesive particles; extensively eroded and much originally deposited on snow and ice. Volume estimated to be $50–100\times10^6$ m^3 by Hildreth and others (2003) and $100–200\times10^6$ m^3 by Hyde and Crandell (1978).
OP	3.5×10^6 bulk[1]	Coarser grained than tephra set YP; synchronous with Ridley Creek lahar. Volume includes local lahars formed of mobilized ejecta on flank downslope from crater.
MY	$<< 0.1\times10^6$ bulk	Probable product of earliest known eruption at or near site of Sherman Crater.
Sherman Crater (after 1843 C.E. and before 1845–47 C.E.)	15×10^6	Assumptions of original topography are subjective. Volume estimated to be 15×10^6 m^3 by Hildreth and others (2003).

[1]Minimum volume because it is difficult to know the proportion that was incorporated into the Ridley Creek lahar.

formed before 1843 C.E. and can be inferred to have resulted mainly from events during the Mazama Park eruptive period. The only deposits with significant volumes of hydrothermally altered material are tephra sets OP and YP and the Ridley Creek lahar. The volume of tephra set OP is also only a fraction of the probable pre-1843 C.E. volume of Sherman Crater.

Obviously, a discrepancy exists between the volume of the crater and the relatively small volumes of the hydrothermally altered tephra layers (table 17). Likely most, or at least some, of the missing volume exists in the 150×10^6 m^3 Ridley Creek lahar, as part of the originating flank collapse (table 10) or perhaps as tephra set OP material ejected and mobilized as part of that lahar or from deposits since eroded. Less likely, but still probable, is that some of the crater volume may have formed from collapse after the eruption of tephra layer BA. The volume of tephra layer BA (table 17), however, far exceeds the missing volume of Sherman Crater, which would suggest that if there was any collapse of the crater owing to tephra withdrawal, the amount of collapse was minor.

Geology and Activity of Modern Sherman Crater

Modern Sherman Crater (frontispiece) drains through the notch referred to as "east breach" at altitude 2,883 m. There appears to be no depression beneath the nearly flat, ice-covered floor, and none was discovered in glacier-cave surveys (Kiver, 1975, 1978), or was indicated by internal drainage of the subglacial lake that was present during the 1975–76 thermal activity (appendix 6). Hundreds of pressurized fumaroles vent within the crater; although the largest are at least 1 m in diameter, most are only a few centimeters across. West and northwest margin fumaroles vent among blocks in the talus apron. A small but vigorous cluster of fumaroles vent from fissured and altered lava on a steep face just inside the west rim. The largest vent, known as the Sulphur Cone fumarole (fig. 71), is at the bottom of a deep pit melted through ice, just inside the east breach below Lahar Lookout (the high point on the north side of the east breach). Fumarole temperatures are the highest in the Cascade Range after those on the 1980–86 and 2004–08 lava domes at Mount St. Helens (Ingebritsen and others, 2014).

Sherman Crater truncates sequences of lava flows, interbedded breccias, and pyroclastic deposits erupted from Carmelo Crater (see frontispiece photograph); apparently, no lava flows have originated from Sherman Crater (Hildreth and others, 2003). Some layers that dip into the crater, principally on the west flank of Lahar Lookout, are breccias banked against the crater wall (see frontispiece photograph). Frank (1983) postulated that these breccias might be correlative with the Boulder Creek assemblage. We note, however, the nearly complete absence of altered material in the Boulder Creek assemblage (RS–14a, RS–14b), and suggest that at the time

Figure 71. Close-up photographic view of Sulphur Cone fumarole in the east breach of Sherman Crater. Main area of crater located to right; Boulder Creek drainage and Boulder Glacier to left. Emission color enhanced for visibility. Aerial photograph by J.H. Scurlock, May 26, 2003, used with permission.

of Boulder Creek assemblage emplacement (ca. 12.7 ka), it is unlikely that Sherman Crater existed. Instead, we hypothesize that the breccia blocks were formed by explosive shattering of Carmelo Crater rocks during formation of Sherman Crater.

The crater rim is mantled with hydrothermally altered ejecta and is surrounded by an aureole of alteration formed in lava flows and breccias erupted from Carmelo Crater. Only the outer 1 cm or so of some lava blocks is altered (Warren and Watters, 2007), whereas the matrix and the smaller blocks in crater breccias are pervasively altered. The dominant alteration products of the crater breccias are silica, alunite, kaolinite, and smectite (Frank, 1983).

Finn and others (2018) conducted high-resolution helicopter magnetic and electromagnetic surveys over several Washington Cascade Range volcanoes, including Mount Baker, to understand the distribution of alteration, water, and ice thickness to aid in evaluating volcanic slope stability. They show that nonmagmatic, water-saturated altered rocks at Mount Baker are restricted to zones about 500 m in diameter to more than 150 m thick beneath Sherman Crater and the Dorr Fumarole Field, the latter located north to northeast of Mount Baker summit. On the basis of their work, they calculate a minimum volume of 0.1 km^3 of alteration around Sherman Crater and suggest its east side is the most likely area to collapse.

The 1975–76 "Aseismic Thermal Event" and Subsequent Activity

On March 10, 1975, local observers reported a dark column rising from Sherman Crater that contrasted sharply with the white vapor emissions frequently seen on clear, cold days (fig. 72). Over the following years, many new fumaroles developed in the crater, yielding plumes darkened with nonjuvenile ash. A ten-fold increase in thermal activity was measured by infrared imaging as the existing thermal areas expanded and new areas developed (Frank and others, 1977). About half the ice and snow in the crater melted in the summer of 1975, and the intracrater glacier became highly crevassed. Melting produced a lake at the bottom of the crater (Easterbrook, 1975). The possibility of a major eruption was considered, and the level of Baker Lake reservoir was

Figure 72. Photograph of a typical vapor plume from Sherman Crater as seen during cold, clear weather. Aerial photograph by J.H. Scurlock, March 23, 2005, used with permission. Inset photograph of backlit plume as seen from near Ferndale, Washington, by D.S. Tucker, February 3, 2008.

drawn down to accommodate potential lahars, a response that subsequent analysis shows to have been both timely and volumetrically appropriate (Scott and others, 2000). No lahars reached Baker Lake reservoir during or subsequent to the middle 1970s activity.

The 1975–76 activity triggered a more intense monitoring effort than had been applied previously at any other Cascade Range volcano, and included seismic, deformation (tiltmeter measurements), gravity, thermal, volcanic gas, and water studies. Descriptions of the 1975–76 activity and monitoring include Crandell (1975), Eichelberger and others (1976), Fretwell (1976), Nolf (1976), Radke and others (1976), Frank and others (1977), Malone (1977; 1979), Rosenfeld (1977), Krimmel and Frank (1980), and Shafer (1980).

During 1975 and 1976, multiple layers of nonjuvenile tephra were deposited on snow and glacier surfaces in Sherman Crater and as much as a few hundred meters away. Heiken and Wohletz (1985) estimated the ejected volume at 500 m^3, with individual layers as thick as 1 cm. The coarse fraction of the ejecta was dominated by fumarolically altered lithic or crystalline clasts. Tridymite and cristobalite composed about 10 percent by volume of the deposits, with accessory sulphur, plagioclase, pyroxene, pyrite, and clay minerals (Babcock and Wilcox, 1977). Finer particles included partially altered clear glass that composed as much as 10 percent of the ejecta in May 1975 (Heiken and Wohletz, 1985). In contrast, altered glass composed 29 percent of the material composing the walls of fumaroles in Sherman Crater.

No seismic activity of volcanic origin was detected during or several years following this period (Frank and others, 1977; Malone, 1977; 1979). The cause of the sharp increase in thermal activity and gas emission was reviewed by Juday (2007), who concluded that possibilities included magma intrusion, or the fracture of a layer of hydrothermally altered clay that had previously prevented volatiles from escaping. The 1975–76 monitoring produced important baseline data against which recent gravimetric, geodetic, and gas chemistry data are compared. For example, Crider and others (2008; 2011) documented gravity increases of as much as 1,800±300 microgals (μGal) between 1977 and 2005. They propose that the increase is consistent with the densification of a stalled magma intrusion. Using GPS, Hodge (2008) resurveyed electronic distance measurement marks installed in 1981–83 and showed that the edifice has deflated slightly in the quarter century between observations. He posits a deformation source approximately 5 km deep beneath the north-flank Dorr Fumarole Field (fig. 3).

Fumarolic gases, sampled annually since 2006, are dominated by H_2O, CO_2, and H_2S (Werner and others, 2009; Ingebritsen and others, 2014). Based on post-1975 changes in degassing, Werner and others (2009) also conclude that magma was intruded in 1975 and then stalled. H_2S emissions, reported as approximately 5.5 metric tons per day (t/d) by McGee and others (2001) and recently as <1 t/d (Werner and others, 2009), are considerably reduced from 1975 when the peak measured rate was 112 t/d (Radke and others, 1976). The peak 1970s CO_2 emission rates from Sherman Crater fumaroles are estimated to have been approximately 950 t/d; since the late 1990s, CO_2 has remained relatively stable at approximately 150 t/d (Werner and others, 2009; Ingebritsen and others, 2014). Declining emission rates are the expected trend from a gradually crystallizing magma, although the continued emission of CO_2, high magmatic $^3He/^4He$ ratios (~7.6; Ingebrietsen and others, 2014), and the long-term hydrothermal system may be the result of some continuing connection between the surface and deep convecting magma (Werner and others, 2009). Fumarolic gas compositions show no SO_2 signature (Werner and others, 2009; Ingebritsen and others, 2014), probably because hydrolysis ("scrubbing") converts SO_2 entirely to H_2S (Doukas and Gerlach, 1995; McGee and others, 2001; Symonds and others, 2001). Visible thermal and fumarolic activity as of 2014 remain significantly above pre-1975 levels, although greatly reduced from peak 1975 levels. Additional evidence for reduced thermal activity includes the absence of particulate material around fumaroles and the relatively smooth, unbroken surface of the intracrater glacier.

Implications for Future Hazards from Mount Baker

Mount Baker produced a variety of eruptive products in postglacial time—lava flows that in turn collapsed to produce pyroclastic flows and spawn clay-poor lahars, phreatic and juvenile tephra falls, and flank failures that transformed to clay-rich lahars. Postglacial time also saw a change in vent location from summit eruptions during the latest Pleistocene (Carmelo Crater eruptive period) to early Holocene eruptions at the distal-flank vent Schriebers Meadow cinder cone, to the middle and late Holocene eruptions at the off-summit vent Sherman Crater. Both eruptive style and vent location have important implications for potential hazards associated with future eruptive activity.

Of the hazardous ground phenomena—lava flows, pyroclastic flows, lahars, and tephra fall—lahars are the most likely to threaten human life at distances greater than 20 km from Mount Baker. Lahars move down river drainages that head on, or are fed by tributaries that head on, the volcano, so the potential pathways are well known. The potential for far-traveled lahars may require evacuation during future unrest and eruption.

Summit eruptions of lava flows during the Carmelo Crater eruptive period resulted in those flows descending the steep upper flanks of the volcano and collapsing to form rapidly moving, hot pyroclastic flows (block-and-ash flows) that quickly melted snow and ice to spawn clay-poor lahars. Accumulated deposits from repeated collapses formed the thick flank assemblages seen on the east and south flanks of the volcano. Under this type of trigger mechanism, the resultant lahar volume depends upon the initial volume of

hot material, the volume of snow and ice that can melt to provide water, and the volume of loose material that the lahar incorporates along its path. In some cases, the lahars transformed into more water-rich hyperconcentrated flows downvalley.

The Schriebers Meadow cinder cone eruption produced local tephra falls and a lava flow. This is the only known distal-flank eruption in postglacial time (Hildreth and others, 2003) and therefore is a low-probability event. Lava flows on the distal flanks traverse low-angle slopes, thus lava-flow collapse is highly unlikely. A similar type of event today would not be very hazardous unless there was a population just downwind of a cinder cone that would be affected by tephra fall or if the lava blocked a river or drainage impounding a lake upstream. Lava flowing through forests could cause wildfires, which could then threaten a larger area.

The shift in vent location during the Holocene from the summit area to Sherman Crater focused hazardous activity on the southwestern to eastern sectors of the volcano. The shift in vent location also coincided with the development of an active near-surface hydrothermal system that has weakened rock in the vicinity of Sherman Crater. Collapses of weakened rock have spawned large clay-rich lahars down most of the drainages from the upper Middle Fork Nooksack River to Park Creek. The largest of these occurred during the ~6.7 ka Mazama Park eruptive period and were likely linked to deformation caused by the intrusion of magma in the upper edifice. Although neither the timing of flank failures nor lava flow-front collapses can be predicted, they differ in terms of when they occur: large flank failures can occur during or before a magmatic eruption begins, whereas lava-flow-front collapses can only occur during active lava-flow extrusion. This distinction is important for evaluating potential hazards during a volcanic crisis.

Flank failures have many of the triggers that are common to all landslides in steep terrain. However, the features of stratovolcanoes—alteration to weak, unstable material; permeable layers acting as aquifers for groundwater of hydrothermal, precipitation, and snow- and ice-melt origin; magma intrusion destabilizing sectors; and slope-parallel deposits—can cause a greater magnitude and frequency of landslides relative to nonvolcanic terrain. Of special concern is whether flank failures or lahars from these failures flow into Baker Lake reservoir. Large enough flows could potentially cause seiches that could affect shorelines or the integrity of the dam itself if the reservoir is at a high pool level (Walder and others, 2006). If the pool level is sufficiently low, however, the reservoir could act as a catchment for flank failures or resultant lahars.

Lahars have a long-term effect on the river drainages they traverse. The sediment from lahar deposition raises the riverbed, resulting in an increased probability of flooding in that part of the channel.With time, the sediment load moves downstream as the river works to reestablish pre-eruption levels. Thus, areas that did not experience a lahar or flooding during the initial activity may be affected months to years later (see Rodolfo and others, 1996). Also, it may take decades for sediment yields to return to pre-eruption levels (for example, Major, 2004; Pierson and others, 2011).

Tephra falls from Mount Baker have been very small (10^2 m^3) to modest (10^8 m^3) in volume. The area within 30 km around Mount Baker is sparse in population, which, coupled with the dominant westerly wind directions, means that most people are likely to experience only minor amounts of tephra fall (<1 cm). Such thicknesses are generally not life threatening, except perhaps to those with an already compromised respiratory system. Easterly winds would reach a greater population, and experience shows that even a millimeter of ash can be a considerable nuisance. It is likely that the explosions that produced tephra layer BA and pumice during the Carmelo Crater eruptive period reached altitudes that would affect aviation, especially aircraft on approach or takeoff from nearby airports. Such activity would require rerouting of aircraft; thus, any explosive activity may be a concern for the aviation sector.

On the basis of past events, the following should be considered when responding to volcanic unrest and eruption at Mount Baker.

- Vent location is important for assessing areas likely to be affected by future activity. A vent at the summit can potentially affect the broadest area as lava flows or lahars could move down any or all sectors of the volcano. Flows from a vent at Sherman Crater will likely affect only the east to southwest portions of the volcano. A vent located off the edifice, such as the Schriebers Meadow cinder cone, is of low probability and likely to affect only a limited area; however, depending on where the vent is located, the impact could be substantial if it were to block a river drainage. Earthquake locations and deformation monitoring will be important to assess the most likely vent area as the volcano reawakens.

- The most likely future vent area is Sherman Crater because it has been the most recently active vent and it has an active hydrothermal system that has weakened the surrounding rocks.

- Most volcanic activity will result in some type of flowage event. Lava flows moving over steep terrain can collapse, resulting in hot, fast moving pyroclastic flows that could reach the base of the volcano in minutes. The pyroclastic flows could quickly melt snow and ice to form lahars that, depending on size, could travel well beyond the flanks of the volcano.

- Flank failures can occur during unrest or eruption and can be difficult to predict. Thus, mitigation measures would need to be considered early in unrest, especially if renewed unrest is centered on the Sherman Crater area with its moderate volume of altered and weakened rock. Based on past behavior, a future collapse will quickly transition to a lahar that may move far downvalley.

- The lahar risk at Mount Baker is amplified by the presence of two reservoirs at the base of the volcano operated for hydroelectric-power generation and flood control. These are of special concern if unrest is centered on the Sherman Crater vent, which is just upslope. Large impulsive lahars into the reservoirs could lead to local tsunami inundation (Walder and others, 2006) or waves overtopping the dams that could lead to dam failure and result in catastrophic flooding of the Skagit River. In 1975, reservoir operators prudently lowered the level of the reservoirs in response to the unrest. The vulnerability of these reservoirs will require reservoir operators to respond to unrest, as in 1975, before the outcome of the unrest is known (Gardner and others, 1995; Scott and others, 2000).
- Lahars can increase in volume as they flow by entraining additional material—a process referred to as bulking (Scott, 1988a). The largest 19th-century flow, the Morovitz Creek lahar, is represented by deposits that contain an average of 40 percent entrained material; locally, the percentage is more than 80 percent. Thus, the flow volume was locally as much as five times (the "bulking factor") the original collapse volume. There is plenty of fragmental material in all valleys surrounding Mount Baker, so the volumes of all potential lahars will increase beyond their initial starting volumes. We calculated the proportion of entrained sediment for Holocene lahars (table 10) as a guide to the significance of the process.
- The effects of lahars on river drainages can last long after an eruption has ceased.
- Although tephra falls are rarely life threatening to those on the ground, even small tephra falls can be disruptive and difficult to clean up. All ash clouds can be life threatening to the aviation sector. The aviation community will need to be alerted quickly to the presence of any ash clouds that might intersect aircraft pathways.

References Cited

Adams, W.C., 1919, Reminiscences of Mt. Baker: Mazama, v. 5, no. 4, p. 338–342.

Armstrong, J.E., Crandell, D.R., Easterbrook, D.J., and Noble, J.B., 1965, Late Pleistocene stratigraphy and chronology in southwestern British Columbia and northwestern Washington: Geological Society of America Bulletin, v. 76, p. 321–330.

Babcock, J.W., and Wilcox, R.E., 1977, Results of petrographic examination of samples, *in* Frank, D., Meier, M.F., and Swanson, D.A., 1977, Assessment of increased thermal activity at Mount Baker, Washington, March 1975–March 1976: U.S. Geological Survey Professional Paper 1022–A, p. 25–26.

Bacon, C.R., 1983, Eruptive history of Mount Mazama and Crater Lake caldera, Cascade Range, U.S.A.: Journal of Volcanology and Geothermal Research, v. 18, p. 57–115.

Baggerman, T.D., and DeBari, S.M., 2011, The generation of a diverse suite of Late Pleistocene and Holocene basalt through dacite lavas from the northern Cascade arc at Mount Baker, Washington: Contributions to Mineralogy and Petrology, v. 161, p. 75–99, https://doi.org/10.1007/s00410-010-0522-2.

Bartlein, P.J., Harrison, S.P., Brewer, S., Connor, S., Davis, B.A.S., Gajewski, K., Guiot, J., Harrison-Prentice, T.I., Henderson, A., Peyron, O., Prentice, I.C., Scholze, M., Seppä, H., Shuman, B., Sugita, S., Thompson, R.S., Viau, A.E., Williams, J., and Wu, H., 2011, Pollen-based continental climate reconstructions at 6 and 21 ka—A global synthesis: Climate Dynamics, https://doi.org/10.1007/s00382-010-0904-1.

Beckey, F., 2003, Range of glaciers: Portland, Oregon Historical Society, 527 p.

Beget, J.E., 1982, Postglacial volcanic deposits at Glacier Peak, Washington, and potential hazards from future eruptions: U.S. Geological Survey Open-File Report 82–830, 77 p.

Beget, J.E., 1984, Tephrochronology of Late Wisconsin deglaciation and Holocene Glacier fluctuations near Glacier Peak, North Cascade Range, Washington: Quaternary Research, v. 21, p. 304–316.

Begg, A., 1894, History of British Columbia from its earliest discovery to the present time: Toronto, William-Briggs, 568 p.

Beverage, J.P., and Culbertson, J.K., 1964, Hyperconcentrations of suspended sediment: Journal of the Hydraulics Division of the American Society of Civil Engineers, v. 90, p. 117–128.

Bohn, D., and Petschek, R., 1978, Kinsey, Photography: San Francisco, Chronicle Books, 319 p.

Booth, D.K., 1987, Timing and processes of deglaciation along the southern margin of the Cordilleran ice sheet, *in* Ruddiman, W.F., and Wright, H.E., Jr., eds., North America and adjacent oceans during the last deglaciation: Geological Society of America, The Geology of North America, v. K-3, p. 71–90.

Bourasaw, N.V., 2003, Four British bachelors clear the wilderness at the site of future Sedro: Skagit River Journal, accessed April 2, 2019, at http://www.skagitriverjournal.com/s-w/pre1900/4bachelors.html.

Brewer, W.H., 1865, Volcanic eruptions in northern California and Oregon: American Journal of Science, v. 90, 264 p.

Briggs, C.A.D., Busacca, A.J., and McDaniel, P.A., 2006, Pedogenic processes and soil-landscape relationships in North Cascades National Park, Washington: Geoderma, v. 137, p. 192–204.

Bronk Ramsey, C., 2001, Development of the Radiocarbon Calibration Program: Radiocarbon, v. 43, no. 2A, p. 355–363.

Bronk Ramsey, C., 2009, Bayesian analysis of radiocarbon dates: Radiocarbon, v. 51, no. 1, p. 337–360.

Bronk Ramsey, C., and Lee, S., 2013, Recent and planned developments in the program OxCal: Radiocarbon, v. 55, no. 3, p. 720–730.

Bronk Ramsey, C., van der Plicht, J., and Weninger, B., 2001, "Wiggle matching" radiocarbon dates: Radiocarbon, v. 43, no. 2A, p. 381–389.

Brown, C.B., 2011, Estimation of annual mass balance and Little Ice Age equilibrium line altitude depression of Mount Baker glaciers: Burnaby, British Columbia, Simon Fraser University, M.S. thesis, 138 p.

Burke, R.M., 1972, Neoglaciation of Boulder valley, Mt. Baker, Washington: Bellingham, Western Washington University, M.S. thesis, 47 p.

Burrows, R.A., 2001, Glacial chronology and paleoclimatic significance of cirque moraines near Mts. Baker and Shuksan, North Cascade Range, Washington: Bellingham, Western Washington University, M.S. thesis, 92 p.

Burrows, R.A., Kovanen, D.J., Easterbrook, D.J., and Clark, D.H., 2000, Timing of extent of cirque glaciations near Mts. Baker and Shuksan, North Cascades Range, WA [abs.]: Geological Society of America Abstracts with Programs, v. 32, no. 6, p. 7.

Cameron, V.J., 1989, The late Quaternary geomorphic history of the Sumas valley: Burnaby, British Colyumbia, Simon Fraser University, M.A. thesis, 154 p.

Clague, J.J., and James, T.S., 2002, History and isostatic effects of the last ice sheet in southwestern British Columbia: Quaternary Science Reviews, v. 21, p. 71–87, https://doi.org/10.1016/S0277-3791(01)00070-1.

Clague, J.J., Mathewes, R.W., Guilbault, J.P., Hutchinson, I., and Rickets, B.D., 1997, Pre-Younger Dryas resurgence of the southwestern margin of the Cordilleran ice sheet, British Columbia, Canada: Boreas, v. 26, p. 261–277.

Cline, S.P., Berg, A.B., and Wight, H.M., 1980, Some characteristics and dynamics in Douglas-fir forests, western Oregon: Journal of Wildlife Management, v. 44, p. 773–786.

Coleman, E.T., 1869, Mountaineering on the Pacific: Harper's New Monthly Magazine, v. 39, p. 793–817.

Coleman, E.T., 1877, Mountains and mountaineering in the Far West: Alpine Journal, v. VIII, no. LVII, p. 232–242.

Connelly, D., 1976, Morovits, the hospitable hermit of Baker Lake: Off Belay, v. 28, August, p. 6–10.

Coombs, H.A., 1939, Mt. Baker, a Cascade volcano: Geological Society of America Bulletin, v. 50, p. 1,493–1,510.

Costa, J.E., 1986, A history of paleoflood hydrology in the United States, 1800–1970: Eos Transactions, American Geophysical Union, v. 67, p. 425, 428–430.

Crandell, D.R., 1971, Postglacial lahars from Mount Rainier volcano, Washington: U.S. Geological Survey Professional Paper 677, 73 p.

Crandell, D.R., 1975, Increased hydrothermal activity at Mount Baker, Washington: U.S. Geological Survey Professional Paper 975, 212 p.

Crandell, R.R., 1989, Gigantic debris avalanche of Pleistocene Age from Mount Shasta Volcano, California, and debris-avalanche hazard zonation: U.S. Geological Survey Bulletin 1861, 29 p.

Crandell, D.R., and Miller, R.D., 1974, Quaternary stratigraphy and extent of glaciations in the Mount Rainier region, Washington: U.S. Geological Survey Professional Paper 847, 59 p.

Crider, J.G., Johnsen, K.H., and Williams-Jones, G., 2008, Thirty-year gravity change at Mount Baker Volcano, Washington, USA—Extracting the signal from under the ice: Geophysical Research Letters, v. 35, L20304, https://doi.org/10.1029/2008GL034921.

Crider, J.G., Frank, D., Malone, S.D., Poland, M.P., Werner, C., Caplan-Auerback, J., 2011, Magma at depth—A retrospective analysis of the 1975 unrest at Mount Baker, Washington, USA, *in* Moran, S.C., Newhall, C.G., and Roman, D.C., eds, Failed eruptions—Late-stage cessation of magma ascent: Bulletin of Volcanology, v. 73, no. 2, p. 175–189, https://doi.org/10.1007/s00445-010-0441-0.

Darwin, L.H., 1921, Biological survey of Washington waters—Baker Lake: Washington State Fisheries Commission, 2 p. [Bathymetric map of Baker Lake by E.L. Smith and M.G. Anderson, July 8–14, 1921.]

Davidson, G., 1885, Recent volcanic activity in the United States—Eruptions of Mount Baker: Science, v. 6, no. 138, p. 262.

Davis, P.T., Menounos, B., and Osborn, G., 2009, Holocene and latest Pleistocene alpine glacier fluctuations—A global perspective: Quaternary Science Reviews, v. 28, p. 2,021–2,033.

Davis, P.T., Osborn, G., Menounos, B., Ryane, C., Clague, J., Riedel, J., Koch, J., and Scott, K., 2005, New evidence for Holocene glacier fluctuations on Mt. Baker, Washington [abs.]: American Geophysical Union Fall Meeting Program and Abstracts, no. U43A–0827.

Davis, P.T., Osborn, G., Ryane, C., Menounos, B., and Clague, J., 2007, Little ice age fluctuations of glaciers on Mount Baker, Washington [abs.]: Geologial Society of America Abstracts with Programs, v. 39, n. 4, p. 82.

Davis, P.T., VanHollen, D., Osborn, G., Ryane, D., Menounos, B., Clague, J., Koch, J., Scott, K.M., and Reasoner, M., 2006, Did Neoglaciation begin as early as 6400 calendar years ago? [abs.]: Geological Society of America Abstract with Programs, v. 38, no. 7, p. 236.

Denton, G.H., and Hughes, T.J., eds., 1981, The last great ice sheets: New York, John Wiley and Sons, 484 p.

De Smet, P.J., 1847, Oregon missions and travels over the Rocky Mountains, in 1845–46: New York, Dunigan, 412 p.

Dethier, D.L., Pessl, F., Keuler, R.F., Balzarini, M.A., and Pewar, D.R., 1995, Late Wisconsinan glaciomarine deposition and isostatic rebound, northern Puget Lowland, Washington: Geological Society of America Bulletin, v. 107, p. 1,288–1,303.

Doukas, M.P., and Gerlach, T.M., 1995, Sulfur dioxide scrubbing during the 1992 eruptions of Crater Peak, Mount Spurr Volcano, *in* Keith, T.E.C., ed., The 1992 eruptions of Crater Peak vent, Mount Spurr Volcano, Alaska: U.S. Geological Survey Bulletin 2194, p. 47–57.

Dragovich, J.D., Dunn, A., Parkingson, K.T., Kahle, S.C., and Pringle, P.T., 1997, Quaternary stratigraphy and cross sections, Nooksack, Columbia, and Saar Creek Valleys, Kendall and Deming 7.5-minute quadrangles, western Whatcom County, Washington: Washington Division of Geology and Earth Resources Open File Report 97–4, 13 p., 8 plates.

Dwelley, C., 1953, History of Skagit country: Skagit River Journal, accessed on March 29, 2019, at http://www.skagitriverjournal.com/scounty/histories/dwelley4-county.html [article has been edited from its original form].

Easterbrook, D.J., 1975, Mount Baker eruptions: Geology, v. 3, p. 679–682.

Easterbrook, D.J., 2000, Correlation of late Pleistocene glaciomarine drift in NW Washington and SW British Columbia and evidence for uplift rates [abs.]: Geological Society of America Abstracts with Programs, v. 32, no. 6, p. 12.

Easterbrook, D.J., and Burke, R.M., 1972, Glaciation of the northern Cascades, Washington [abs.]: Geological Society of America Abstracts with Programs, v. 4, p. 152.

Easterbrook, D.J., and Donnell, C.B., 2007, Glacial and volcanic history of the Nooksack Middle Fork, Washington [abs.]: Geological Society of America Abstracts with Programs, v. 39, no. 4, p. 12.

Easterbrook, D.J., and Kovanen, D.J., 1996, Far-reaching mid-Holocene lahar from Mt. Baker in the Nooksack Valley of the North Cascades, WA [abs.]: Geological Society of America Abstracts with Programs, v. 28, p. 64.

Easterbrook, D.J., Kovanen, D.J., and Slaymaker, O., 2007, New developments in Late Pleistocene and Holocene glaciation and volcanism in the Fraser Lowland and North Cascades, Washington: Geological Society of America Field Guide 9, p. 31–56.

Eichelberger, J.S., Heiken, G., Widdicombe, R., Wright, D., Keady, C.J., and Cobb, D.D., 1976, New fumarolic activity on Mount Baker; observations during April through July 1975: Journal of Volcanology and Geothermal Research, v. 1, no. 1, p. 35–53.

Fagan, B., 2000, The Little Ice Age—How climate made history, 1300–1850: New York, Basic Books, 246 p.

Fierstein, J., and Nathenson, M., 1992, Another look at the calculation of fallout tephra volumes: Bulletin of Volcanology, v. 54, p. 156–167.

Finn, C.A., Deszcz-Pan, M., Ball, J.L., Bloss, B.J., and Minsley, B.J., 2018, Three-dimensional geophysical mapping of shallow water saturated altered rocks at Mount Baker, Washington—Implications for slope stability: Journal of Volcanology and Geothermal Research, v. 357, p. 261–275, https://doi.org/10.1016/j.jvolgeores.2018.04.013.

Foit, F.F., Gavin, D.G., and Feng, S.H., 2004, The tephra stratigraphy of two lakes in south central British Columbia, Canada, and its implications for mid-late Holocene activity at Glacier Peak and Mount St. Helens, Washington: Canadian Journal of Earth Science, v. 41, p. 1,401–1,410.

Folk, R.L., 1980, Petrology of sedimentary rocks: Austin, Texas, Hemphill Publishing Co., 182 p.

Frank, D., 1983, Origin, distribution, and rapid removal of hydrothermally formed clay at Mount Baker, Washington: U.S. Geological Survey Professional Paper 1022–E, 31 p.

Frank, D., Meier, M.F., and Swanson, D.A., 1977, Assessment of increased thermal activity at Mount Baker, Washington, March 1975–March 1976: U.S. Geological Survey Professional Paper 1022–A, 49 p.

Frank D., Post, A., and Friedman, J.D., 1975, Recurrent geothermally induced debris avalanches on Boulder Glacier, Mount Baker, Washington: U.S. Geological Survey Journal of Research, v. 3, no. 1, p. 77–87.

Fretwell, O.M., 1976, Water quality sampling and analysis activities related to Mount Baker's recent volcanic activity [abs.]: Eos Transactions, American Geophysical Union, v. 57, no. 2, p. 89.

Friele, P.A., and Clague, J.J., 2002, Younger Dryas readvance in Squamish River valley, southern Coast Mountains: Quaternary Science Reviews, v. 21, p. 1,925–1,933.

Fuller, S.R., 1980, Neoglaciation of Avalanche Gorge and the Middle Fork Nooksack River valley, Mt. Baker, Washington: Bellingham, Western Washington University, M.S. thesis, 68 p.

Gardner, J.E, Carey, S., and Sigurdsson, H., 1998, Plinian eruptions at Glacier Peak and Newberry volcanoes, United States—Implications for volcanic hazards in the Cascade Range: Geological Society of America Bulletin, v. 110, no. 2, p. 173–187.

Gardner, C.A., Neal, C.A., Waite, R.B., and Janda, R.J., 1994, Proximal pyroclastic deposits from the 1989–1990 eruptions of Redoubt Volcano, Alaska—Stratigraphy, distribution and physical characteristic, *in* Miller, T.P, and Chouet, B.A., eds., The 1989–1990 eruptions of Redoubt Volcano: Journal of Volcanology and Geothermal Resources, v. 62, p. 213–50.

Gardner, C.A., Scott, K.M., Miller, C.D., Myers, B., Hildreth, W., and Pringle, P.T., 1995, Potential volcanic hazards from future activity at Mount Baker, Washington: U.S. Geological Survey Open-File Report 95–498, 16 p.

Geological Society of America, 1995, Rock-color chart with genuine Munsell color chips: Geological Society of America.

Gibbs, G., 1855, Report of George Gibbs on a reconnaissance of the country lying upon Shoalwater Bay and Puget Sound *in* Stevens, I.I., 1855, Reports of Explorations and Surveys to Ascertain the Most Practicable and Economical Route for a Railroad from the Mississippi River to the Pacific Ocean: U.S. War Department, v. 1, p. 465–473.

Gibbs, G., 1873, Physical geography of the north-western boundary of the United States: Journal of the American Geographical Society of New York, v. IV, p. 298–392.

Green, N.L., 1988, Basalt-andesite mixing at Mount Baker volcano, Washington; I. Estimation of mixing conditions: Journal of Volcanology and Geothermal Research, v. 34, p. 251–265.

Grove, J.M., 1988, The Little Ice Age: London, Routledge, 498 p.

Hallett, B., Hills, L.V., and Clague, J., 1997, New accelerator mass spectrometry ages for the Mazama ash layer from Kootenay National Park, British Colombia, Canada: Canadian Journal of Earth Sciences, v. 34, p. 1,202–1,209.

Hallet, B., Mathewes, R.W., and Foit, F.F., 2001, Mid-Holocene Glacier Peak and Mount St. Helens We tephra layers detected in lake sediments from southern British Columbia using high-resolution techniques: Quaternary Research v. 55, p. 284–293.

Hayashi, J.N., and Self, S., 1992, A comparison of pyroclastic flow and debris avalanche mobility: Journal of Geophysical Research, v. 97, no. B6, p. 9,063–9,071.

Heiken, G., and Wohletz, K., 1985, Volcanic ash: University of California Press, 246 p.

Heikkinen, O., 1984, Dendrochronological evidence of variations of Coleman Glacier, Mount Baker, Washington, USA: Arctic and Alpine Research, v. 16, p. 53–64.

Heller, P.L., 1980, Multiple ice flow directions during the Fraser Glaciation in the lower Skagit River drainage, northern Cascade Range, Washington: Arctic and Alpine Research, v. 12, p. 299–308.

Helmers, A.E., 1948, Disintegration of girdled Western Hemlock and Grand Fir: U.S. Forest Service Northern Rocky Mountain Forest and Range Experiment Station Publication 17, 14 p.

Herron, W.H., 1916, Profile surveys in 1915 in Skagit River Basin, Washinton: U.S. Geological Survey Water-Supply Paper 419, 8 p., 12 plates.

Hicock, S.R., and Lian, O.B., 1995, The Sisters Creek Formation—Pleistocene sediments representing a nonglacial interval in southwestern British Columbia at about 18 ka: Canadian Journal of Earth Sciences, v. 32, p. 758–767.

Hildreth, W., 1996, Kulshan Caldera—A Quaternary subglacial caldera in the North Cascades, Washington: Geological Society of America, v. 108, p. 786–793.

Hildreth, W., 2007, Quaternary magmatism in the Cascades—Geologic perspectives: U.S. Geological Survey Professional Paper 1744, 125 p.

Hildreth, W., Fierstein, J., and Lanphere, M., 2003, Eruptive history and geochronology of the Mount Baker volcanic field, Washington: Geological Society of America Bulletin, v. 115, p. 729–764.

Hill, K.S., Crider, J.G., and Williams-Jones, G., 2007, Gravity increase observed at Mount Baker, Washington, 1975–2006 [abs.]: Geological Society of America Abstracts with Programs, v. 39, no. 4, p. 65.

Hoblitt, R.P., and Kellogg, K.S., 1979, Emplacement temperatures of unsorted and unstratified deposits of volcanic rock debris as determined by paleomagnetic techniques: Geological Society of America Bulletin, v. 90, p. 633–642.

Hodge, B.E., 2008, Characterizing surface deformation from 1981 to 1983 on Mount Baker volcano, Washington: Bellingham, Western Washington University, M.S. Thesis, 127 p.

Hodge, B.E., and Crider, J.G., 2007, Edifice contraction from 1981 to 2006 of Mount Baker volcano—Results from campaign GPS resurvey of EDM network [abs.]: Geological Society of America Abstracts with Programs, v. 39, no. 4, p. 65.

Hyde, J.H., and Crandell, D.R., 1978, Postglacial volcanic deposits at Mount Baker, Washington, and potential hazards from future eruptions: U.S. Geological Survey Professional Paper 1022–C, 17 p.

Ingebritsen, S.E., Gelwick, K.D., Randolph-Flagg, N.G., Crankshaw, I.M., Lundstrom, E.A., McCulloch, C.L., Murveit, A.M., Newman, R.H., Bergfield, D., Tucker, D.S., Schmidt, M.E., Spicer, K.R., Mosbrucker, A., and Evans, W.C., 2014, Hydrothermal monitoring data from the Cascade Range, northwestern United States: U.S. Geological Survey data set, https://doi.org/10.5066/F72N5088.

Juday, J.E., 2007, A contemporary view of 1975–1976 elevated activity levels at the Mount Baker complex, Washington, and current community awareness of volcano hazards: Bellingham, Western Washington University, M.S. thesis, 219 p.

Kendrick, J. (trans.), 1991, The voyage of Sutil and Mexicana, 1792—The last Spanish exploration of the Northwest Coast of America: Spokane, Arthur H. Clark Co., 108 p.

Kennard, P.M., and Driedger, C.L., 1987, Estimated ice volumes on Cascade Volcanoes—Mount Baker, Glacier Peak, and Mount Adams in Washington, and Mount Jefferson in Oregon [abs.]: Eos Transactions, American Geophysical Union, v. 68, no. 16, p. 308.

Kerr Wood Leidal Associates Ltd., 2005, Nooksack River sediment management plan—Summary of background information: Whatcom County Flood Control Zone District report, 144 p.

Kiver, E.P., 1975, The first exploration of Mount Baker ice caves: Explorers Journal, v. 53, no. 2, p. 84–87.

Kiver, E.P., 1978, Geothermal ice caves and fumaroles, Mount Baker volcano, 1974–77 [abs.]: Geological Society of America Abstracts with Programs, v. 10, no. 3, p. 112.

Koch, J., Clague, J.J., and Osborn, G.O., 2007a, Glacier fluctuations during the last millennium in Garibaldi Provincial Park, British Columbia: Canadian Journal of Earth Science, v. 44, p. 1,215–1,233.

Koch, J., Osborn, G.O., and Clague, J.J., 2007b, Pre-"Little Ice Age" glacier fluctuations in Garibaldi Provincial Park, Coast Mountains, British Columbia, Canada: The Holocene, v. 17, p. 1,069–1,078.

Kokelaar, P., 1986, Water-magma interactions in subaqueous and emergent basaltic volcanism: Bulletin of Volcanology, v. 48, p. 275–289.

Kovanen, D.J., 1996, Extensive late-Pleistocene alpine glaciation in the Nooksack River Valley, North Cascades, Washington: Bellingham, Western Washington University, M.S. thesis, 186 p.

Kovanen, D.J., 2001, Late glacial ice margin fluctuations (~12.5–10.0 ^{14}C kyr BP) in the Fraser Lowland and adjacent Nooksack Valley, southwestern British Columbia, Canada, and northwestern Washington, U.S.A.: Vancouver, University of British Columbia, Ph.D. dissertation, 306 p.

Kovanen, D.J., and Easterbrook, D.J., 1996, Extensive readvance of Late Pleistocene (YD?) alpine glaciers in the Nooksack River Valley, 10,000 to 12,000 years ago, following retreat of the Cordilleran ice sheet, North Cascades, Washington: Friends of the Pleistocene Field Trip Guidebook, 74 p.

Kovanen, D.J., and Easterbrook, D.J., 1999, Holocene tephras and lahars from Mount Baker, Washington [abs.]: Geological Society of America Abstracts with Programs, v. 31, p. 71.

Kovanen, D.J., and Easterbrook, D.J., 2001, Late Pleistocene, post-Vashon, alpine glaciation of the Nooksack drainage, North Cascades, Washington: Geological Society of America Bulletin, v. 113, p. 274–288.

Kovanen, D.J., and Easterbrook, D.J., 2002, Timing and extent of Allerød and Younger Dryas age (ca. 12,500–10,000 ^{14}C yr B.P.) oscillations of the Cordilleran Ice Sheet in the Fraser Lowland, western North America: Quaternary Research, v. 57, p. 208–224.

Kovanen, D.J., Easterbrook, D.J., and Thomas, P.A., 2001, Holocene eruptive history of Mount Baker, Washington: Canadian Journal of Earth Science, v. 38, p. 1,355–1,366.

Kovanen, D.J., and Slaymaker, O., 2005, Fluctuations of the Deming Glacier and theoretical equilibrium-line altitudes during the Late Pleistocene and early Holocene on Mount Baker, Washington, U.S.A.: Boreas, v. 34. p. 157–175.

Krimmel, R.M., and Frank, D., 1980, Aerial observations of Mount Baker, Washington; 1976–1979 update [abs.]: Eos Transactions, American Geophysical Union, v. 61, no. 6, p. 69.

Landes, H., 1907, Round-about Mount Baker: Mazama, v. 3, no. 1, p. 5–8.

Lewis, D.R., Scott, K.M., and Tucker, D.S., 2006, Long-runout debris avalanche in Rainbow Creek, Mount Baker, Washington: Geological Society of America Abstracts with Programs, v. 39, no. 4, p. 65.

Lisiecki, L.E., and Raymo, M.E., 2005, A Pliocene-Pleistocene stack of 57 globally distributed benthic δ^{18}O records: Paleooceanography, v. 20, https://doi.org/10.1029/2004PA001071.

Luhr, J.F., and Simkin, T., 1993, The volcano born in a cornfield: Geoscience Press, 456 p.

Major, J.J., 1997, Depositional processes in large-scale debris-flow experiments: Journal of Geology, v. 105, p. 345–366.

Major, J.J., 2004, Posteruption suspended sediment transport at Mount St. Helens—Decadal-scale relationships with landscape adjustments and river discharges: Journal of Geophysical Research, v. 109, https://doi.org/10.1029/2002JF000010.

Major, J.J., and Newhall, G.C., 1989, Snow and ice perturbations during historic volcanic eruptions and the formation of lahars and floods: Bulletin of Volcanology, v. 52, p. 1–27.

Majors, H.M., 1978, Mount Baker, a chronicle of its historic eruptions and first ascent: Seattle, Northwest Press, 226 p.

Malone, S.D., 1977, Summary of seismicity and gravity, *in* Frank, D., Meier, M.F., and Swanson, D.A., 1977, Assessment of increased thermal activity at Mount Baker Washington, March 1975–March 1976: U.S. Geological Survey Professional Paper 1022–A, p. 19–22.

Malone, S.D., 1979, Gravity changes accompanying increased heat emission at Mount Baker, Washington: Journal of Volcanology and Geothermal Research, v. 6, no. 3–4, p. 214–256.

Malone, S.D., and Frank, D., 1975, Increased heat emission from Mount Baker, Washington: Eos Transactions, American Geophysical Union, v. 56, no. 10, p. 679–685.

McGee, K.A., Doukas, M.P., and Gerlach, T.M., 2001, Quiescent hydrogen sulfide and carbon dioxide degassing from Mount Baker, Washington: Geophysical Research Letters, v. 28, p. 4,479–4,482.

McNeil, F.H., 1930, Backtracking old trails: Mazama, v. 12, no. 12, p. 7–19.

Menounos, B., Osborn, G., Clague, J.J., and Luckman, B.H., 2009, Latest Pleistocene and Holocene glacier fluctuations in western Canada: Quaternary Science Reviews, v. 28, p. 2,049–2,074.

Mierendorf, R.R., 1999, Precontact use of tundra zones of the northern Cascades Range of Washington and British Columbia: Archaeology in Washington, v. VII, p. 3–23.

Mierendorf, R.R., and Foit, F.F, Jr., 2008, 9,000 years of earth, wind, fire and stone at Cascade Pass—Preliminary Archaeology and Geochronology [abs.]: Society for American Archaeology Abstracts of the 73rd Annual Meeting, p. 385.

Moore, N.E., and DeBari, S.M., 2011, Mafic magmas from Mount Baker in the northern Cascade arc, Washington—Probes into mantle and crustal processes: Contributions to Mineralogy and Petrology, v. 163, p. 521–546, https://doi.org/10.1007/s00410-011-0686-4.

Morrisey, M., Zimanowski, B., Wohletz, K., and Buettner, R., 2000, Phreatomagmatic fragmentation, *in* Sigurdsson, H., Houghton, B., Rymer, H., Stix, J., and McNutt, S., eds., Encyclopedia of Volcanoes (1st ed.): San Diego, Academic Press, p. 431–446.

Mullineaux, D.R., 1974, Pumice and other pyroclastic deposits in Mount Rainier National Park, Washington: U.S. Geological Survey Bulletin 1326, 83 p.

Nolf, B., 1976, Tilt-bar stations on Mount Baker, Washington [abs.]: Eos Transactions, American Geophysical Union, v. 57, no. 2, p. 88.

O'Connor, J.E., and Costa, J.E., 2004, The world's largest floods, past and present—Their causes and magnitudes: U.S. Geological Survey Circular 1254, 13 p.

Osborn, G., Menounous, B., Ryanne, C., Riedel, J., Clague, J., Koch, J., Clark, D., Scott, K., and Davis, P.T., 2012, Latest Pleistocene and Holocene glacier fluctuations on Mount Baker, Washington: Quaternary Science Reviews, v. 49, p. 33–51.

Pelto, M.S., and Riedel, J.R., 2002, Spatial and temporal variations in annual mass balance in North Cascade glaciers, Washington, 1984–2000: Hydrological Processes, v. 15, p. 3,461–3,472.

Pierson, T.C., 1998, An empirical method for estimating travel times for wet volcanic mass flows: Bulletin of Volcanology, v. 60, p. 98–109.

Pierson, T.C., 2006, Dating young geomorphic surfaces using age of colonizing Douglas fir in southwestern Washington and northwestern Oregon, USA: Earth Surface Processes and Landforms, v. 31, p. 811–831.

Pierson, T.P., Pringle, P.T., and Cameron, K.C., 2011, Magnitude and timing of downstream channel aggradation in response to a dome-building eruption at Mount Hood, Oregon: Geological Society of American Bulletin, v. 123, p. 3–20.

Pierson, T.C., and Scott, K.M., 1985, Downstream dilution of a lahar—Transition from debris flow to hyperconcentrated streamflow: Water Resources Research, v. 21, p. 1,511–1,524.

Pittman, P., Maudlin, M., and Collins, B., 2003, Evidence of a major late Holocene river avulsion [abs.]: Geological Society of America Abstracts with Programs, v. 35, no. 6, p. 334.

Plummer, F.G., 1898, Reported volcanic eruptions in Alaska, Puget Sound, etc., 1690 to 1896, *in* Holden, E.S., ed., A catalog of earthquakes on the Pacific Coast, 1769 to 1897: Smithsonian Miscellaneous Collections, no. 1087, p. 24–27.

Porter, S.C., 1976, Pleistocene glaciations in the southern part of the North Cascade Range, Washington: Geological Society of America Bulletin, v. 87, p. 61–75.

Porter, S.C., and Denton, G., 1967, Chronology of Neoglaciation in the North American Cordillera: American Journal of Science, v. 265, p. 177–210.

Porter, S.C., and Swanson, T.W., 1998, Radiocarbon age constraints on rates of advance and retreat of the Puget Lobe of the Cordilleran ice sheet during the last glaciation: Quaternary Research, v. 50, p. 205–213.

Post, A., and LaChapelle, E.R., 1971, Glacier ice: Seattle, University of Washington Press, 110 p.

Radke, L.F., Hobbs, P.V., and Stith, J.L., 1976, Airborne measurements of gases and aerosols from volcanic vents on Mount Baker: Geophysical Research Letters, v. 3, no. 2, p. 93–96.

Ragan, D.M., 1961, Geology of Twin Sisters dunite, northern Cascades, Washington: Seattle, University of Washington, Ph.D. dissertation, 98 p.

Reasoner, M.A., Osborn, G., and Rutter, N.W., 1994, Age of the Crowfoot advance in the Canadian Rocky Mountains—A glacial event coeval with the Younger Dryas oscillation: Geology, v. 22, p. 439–442.

Reid, M.E., 2004, Massive collapse of volcano edifices triggered by hydrothermal pressurization: Geology, v. 32, p. 373–376.

Reimer, P.G., Bard, E., Beck, J.W., Blackwell, P.G., Bronk Ramsey, C., Buck, C.E., Cheng, H., Edwards, R.L., Friedrich, M., Grootes, P.M., Guilderson, T.P., Haflidasen, H., Hajdas, I., Hatte, C., Heaton T.J., Hoffmann, D.L., Hogg, A.G., Hughen, K.A., Kaiser, K.F., Dromer, B., Maning, S.W., Niu, M., Reimer, R.W., Richards, D.A., Scott, E.M., Southon, J.R., Staff, R.A., Turney, C.S.M., and van der Plicht, J., 2013, IntCal13 terrestrial radiocarbon age determination, 0–50,000 years B.P., Radiocarbon, v. 56, p. 1,869–1,887.

Reyes, A., Wiles, G.C., Smith, D.J., Barclay, D.J., Allen, S., Jackson, S., Larocque, S., Laxton, S., Lewis, D., Calkin, P.E., and Clague, J.J., 2007, Expansion of Alpine Glaciers in Pacific North America in the first millennium: Geology, v. 34, p. 57–60.

Richardson, D., 1968, Glacier outburst floods in the Pacific Northwest: U.S. Geological Survey Professional Paper 600–D, p. 79–86.

Riedel, J.L., 1987, Chronology of Late Holocene glacier recessions in the Cascade Range and deposition of a recent esker in a cirque basin, North Cascade Mountains: Madison, University of Wisconsin, M.S. thesis, 94 p.

Riedel, J.L., 2007, Late Pleistocene glacial and environmental history of Skagit Valley, Washington and British Columbia: Burnaby, British Columbia, Simon Fraser University, Ph.D. dissertation, 187 p.

Riedel, J.L., 2011, Quaternary Geology of Skagit Valley unpublished guidebook: Friends of the Pleistocene Fall Meeting, 51 p.

Riedel, J.L., 2017, Deglaciation of the North Cascade Range, Washington and British Columbia, from the Last Glacial Maximum to the Holocene: Cuadernos de Investigacion Geographica [Geographical Research Letters], v. 43, no. 2, p. 467–496.

Riedel, J.L., Clague, J.J., Ward, B.C., 2010, Timing and extent of Evans Creek stade alpine glaciation in Skagit Valley, Washington: Quaternary Research, v. 73, no. 2, p. 313–323.

Riedel, J.L., and Larrabee, M.A., 2016, Impact of recent glacial recession on summer streamflow in the Skagit River: Northwest Science, v. 90, no. 1, p. 5–22.

Rodolfo, K.S., Umbal, J.V., Alonso, R. A., Remotigue, C.T., Paladio-Melosantos, Ma. L., Salvador, J.H.G., Evangelista, D., and Miller, Y., 1996, Two years of lahars on the western flank of Mount Pinatubo—Initiation, flow processes, deposits, and attendant geomorphic and hydraulic changes, *in* Newhall, C.G., and Punongbayan, R.S., eds., 1996, Fire and Mud—Eruption and lahars of Mount Pinatubo, Philippines: Philippine Institute of Volcanology and Seismology, Quezon City and University of Washington Press, Seattle and London, p. 989–1,014.

Rosenfeld, C.L., 1977, Summary of thermal-infrared observations, *in* Frank, D., Meier, M.F., and Swanson, D.A., 1977, Assessment of increased thermal activity at Mount Baker, Washington, March 1975–March 1976, U.S. Geological Survey Professional Paper 1022–A, p. 12–14.

Rusk, C.E., 1978, Tales of a western mountaineer: Seattle, The Mountaineers, 380 p.

Ryane, C., 2009, Holocene glacier fluctuations on Mount Baker, Washington, USA: Calgary, Alberta, University of Calgary, M.S. thesis, 121 p.

Ryder, J.T., and Thomson, B., 1986, Neoglaciation in the southern Coast Mountains of British Columbia—Chronology prior to the late-Neoglacial maximum: Canadian Journal of Earth Sciences, v. 23, p. 237–238.

Scott, K.M., 1988a, Origins, behavior, and sedimentology of lahars and lahar-runout flows in the Toutle-Cowlitz River system: U.S. Geological Survey Professional Paper 1447–A, 74 p.

Scott, K.M., 1988b, Origin, behavior, and sedimentology of prehistoric lahars at Mount St. Helens, Washington: Geological Society of America Special Paper 229, p. 23–36.

Scott, K.M., Hildreth, W., and Gardner, C.A., 2000, Mount Baker—Living with an active volcano: U.S. Geological Survey Fact Sheet 059–00, 4 p.

Scott, K.M., Macias, J.L., Naranjo, J.A., Rodriguez, S., and McGeehin J.P., 2001, Catastrophic debris flows transformed from landslides in volcanic terrains—Mobility, hazard assessment, and mitigation strategies: U.S. Geological Survey Professional Paper 1630, 59 p.

Scott, K.M., and Tucker, D.S., 2006, Eruptive chronology of Mount Baker revealed by lacustrine facies of Glacial Lake Baker [abs.]: Geological Society of America Abstracts with Programs, v. 38, no. 5, p. 75.

Scott, K.M., Tucker, D.S., and McGeehin, J.P., 2003, Island of fire in a sea of ice—The growth of Mount Baker volcano and the Fraser Glaciation in the North Cascades [abs.]: XVI INQUA Congress Programs with Abstracts, p. 162.

Scott, K.M., Vallance, J.W., and Pringle, P.T., 1995, Sedimentology, behavior, and hazards of debris flows at Mount Rainier, Washington: U.S. Geological Survey Professional Paper 1547, 56 p.

Scurlock, J.H., 2007, Austin Post, legendary chronicler of glaciers: Northwest Mountaineering Journal, no. 4, accessed March 29, 2019, at http://www.alpenglow.org/nwmj/07/071_Post1.html.

Sea, D.S., and Whitlock, C., 1995, Postglacial vegetation and climate of the Cascade Range, Central Oregon: Quaternary Research, v. 43, p. 370–381.

Schaefer, J.R., Scott, W.E., Evans, W.C., Jorgenson, J., McGimsey, R.G., and Wang, B., 2008, The 2005 catastrophic acid crater lake drainage, lahar, and acidic aerosol formation at Mount Chiginagak volcano, Alaska, USA—Field observations and preliminary water and vegetation chemistry results: Geochemistry, Geophysics, and Geosystems, v. 9, no. 7, https://doi.org/10.1029/2007GC001900.

Shafer, D.C., 1980, Evaluation and implications of the thermal activity of Mount Baker, Washington from aerial photographs and infrared images [abs.]: Oregon Academy of Science Proceedings, v. 16, p. 15.

Sholes, G.M., 1920, The Mount Baker outing of the Mazamas in 1909: Mazama, v. VI, no. 1, p. 26–32.

Siebert, L., 1984, Large volcanic debris avalanches—Characteristics of source areas, deposits, and associated eruptions: Journal of Volcanology and Geothermal Research, v. 22, p. 163–197.

Skilling, I.P., White, J.D.L., and McPhie, J., 2002, Peperite—A review of magma-sediment mingling, *in* Skilling, I.P., White, J.D.L., and McPhie, J., eds., 2002, Peperite—Processes and products of magma-sediment mingling: Amsterdam, Elsevier, 289 p.

Slaughter, S.L., 2005, The 1938 Chocolate Glacier debris flow, Glacier Peak volcano, North Cascade Washington: Ellensburg, Central Washington University, M.S. thesis, 89 p.

Stearns, H.T., and Coombs, H.A., 1959, Quaternary history of upper Baker Valley, Washington [abs.]: Geological Society of America Bulletin, v. 70, no. 12, p. 1,788.

Stewart, J.E., and Bodhaine, G.L., 1961, Floods in the Skagit River Basin, Washington: U.S. Geological Survey Water-Supply Paper 1527, 66 p.

Stuiver, M., Grootes, P.M., and Braziunas, T.F., 1995, The GISP2 $\delta^{18}O$ climate record of the past 16,500 years and the role of the sun, ocean, and volcanoes: Quaternary Research, v. 44, p. 341–354.

Swanson, T.W., and Porter, S.C., 1997, Cosmogenic isotope ages of moraines in the southeastern North Cascade Range: Pacific Northwest Friends of the Pleistocene Field Excursion Guidebook, 18 p.

Swiger, W.F., 1958, Report on lava bed area, Baker River project, upper Baker River Plant: Stone and Webster Engineering Corporation report prepared for the Puget Sound Power and Light Company, Bellvue, Wash., 27 p.

Symonds, R.B., Gerlach, T.M., and Reed, M.H., 2001, Magmatic gas scrubbing—Implications for volcano monitoring: Journal of Volcanology and Geothermal Research, v. 108, p. 303–341.

Symonds, R.B., Janik, C.J., Evans, W.C., Ritchie, B.E., Counce, D., Poreda, R.J., and Iven, M., 2003a, Scrubbing masks magmatic degassing during repose at Cascade-Range and Aleutian-Arc volcanoes: U.S. Geological Survey Open-File Report 03–435, 22 p.

Symonds, R.B., Poreda, R.J., Evans, W.C., Janik, C.J., and Ritchie, B.E., 2003b, Mantle and crustal sources of carbon, nitrogen, and noble gases in Cascade-Range and Aleutian-Arc volcanic gases: U.S. Geological Survey Open-File Report 03–426, 26 p.

Tabor, R.W., Haugerud, R.A., and Miller, R.B., 1989, Overview of the geology of the North Cascades, *in* Tabor, R.W., Haugerud, R.A., Brown, E.H., Babcock, R.S., and Miller, R.B., eds., Accreted terranes of the North Cascades Range, Washington: American Geophysical Union, Washington, D.C., International Geological Congress Field Trip T307, p. 1–33.

Tabor, R.W., Haugerud, R.A., Hildreth, W., and Brown, E.H., 2003, Geological map of the Mount Baker 30- by 60-minute quadrangle, Washington: U. S. Geological Survey Geologic Investigations Series I-2660, 73 p., 2 sheets.

Thomas, P.A., 1997, Late Quaternary glaciation and volcanism on the south flank of Mt. Baker, Washington: Bellingham, Western Washington University, M.S. thesis, 98 p.

Thomas, P.A., Easterbrook, D.J., and Clark, P.U., 2000, Early Holocene glaciation on Mount Baker, Washington State, USA: Quaternary Science Reviews, v. 19, p. 1,043–1,046.

Troost, K.G., 2016, Chronology, lithology, and paleo-environmental interpretations of the penultimate ice-sheet advance into Puget Lowland: Seattle, University of Washington, Ph.D. dissertation, 239 p.

Tucker, D.S., and Scott, K.M., 2004, Boulder Creek assemblage, Mount Baker, Washington—A record of the latest cone building episode [abs.]: Geological Society of America Abstracts with Programs, v. 36, no. 4, p. 85.

Tucker, D.S., and Scott, K.M., 2006, A magmatic component in 19th century Mount Baker eruptions? [abs.]: Geological Society of America Abstracts with Programs, v. 38, no. 5, p. 75.

Tucker, D.S., and Scott, K.M., 2009, Structures and facies associated with the flow of subaerial basaltic lava into a deep freshwater lake—The Sulphur Creek lava flow, North Cascades, Washington: Journal of Volcanology and Geothermal Resources, v. 185, no. 4, p. 311–322.

Tucker, D.S., Scott, K.M., and Lewis, D.R., 2007, Field guide to Mount Baker volcanic deposits in the Baker River valley—Nineteenth century lahars, tephras, debris avalanches, and early Holocene subaqueous lava, *in* Stelling, P., and Tucker, D.S., eds., 2007, Floods, faults, and fire—Geological field trips in Washington State and Southwest British Columbia: Geological Society of America Field Guide 9, p. 83–98, https://doi.org/10.1130/2007.fld009(04).

Tucker, D.S., Scott, K.M., Grossman, E.E, and Linneman, S., 2014, Mount Baker lahars and debris flows, ancient, modern and future, *in* Dashtgard, S., and Ward, B., eds., Trials and tribulations of life on an active subduction zone—Field trips in and around Vancouver, Canada: Geological Society of America Field Guide 38, p. 33–52, https://doi.org/10.1130/2014.0038(03).

Vallance, J.W., 2000, Lahars, *in* Sigurdsson, H., Houghton, B., Rymer, H., Stix, J., and McNutt, S., eds., Encyclopedia of Volcanoes (1st ed.): San Diego, Academic Press, p. 601–616.

Vallance, J.W., and Scott, K.M., 1997, The Osceola mudflow from Mount Rainier—Sedimentology and hazard implications of a huge clay-rich debris flow: Geological Society of America Bulletin, v. 109, p. 143–163.

Walder, J.S., 2000a, Pyroclast/snow interactions and thermally driven slurry formation. Part 1; Theory for monodisperse grain beds: Bulletin of Volcanology, v. 62, p. 105–118.

Walder, J.S., 2000b, Pyroclast/snow interactions and thermally driven slurry formation. Part 2; Experiments and theoretical extension to polydisperse tephra: Bulletin of Volcanology, v. 62, p. 119–129.

Walder, J.S., and Driedger, C.L., 1995, Frequent outburst floods from South Tahoma Glacier, Mount Rainier, U.S.A.—Relation to debris flows, meteorological origin and implacations for subglacial hydrology: Journal of Glaciology, v. 41, p. 1–10, https://doi.org/10.3189/S0022143000017718.

Walder, J.S., Watts, P., and Waythomas, C.F., 2006, Case study—Mapping tsunami hazards associated with debris flow into a reservoir: American Society of Civil Engineering Journal of Hydraulic Engineering, v. 132, p. 1–11.

Warren, S.N., and Watters, R.J., 2007, Influence of geologic structure and alteration strength on edifice failure at Mount Baker, Washington [abs.]: Geological Society of America Abstracts with Programs, v. 39, no. 4, p. 66.

Werner, C., Evans, W.C., Poland, M., Tucker, D.S., and Doukas, M., 2009, Long-term changes in quiescent degassing at Mount Baker volcano; evidence for a stalled intrusion in 1975 and connection to a deep magma source: Journal of Volcanology and Geothermal Resources, v. 186, p. 379–386.

White, J.D.L., McPhie, J., and Skilling, I., 2000, Peperite—A useful genetic term: Bulletin of Volcanology, v. 62, p. 65–66.

Whitlock, C., 1992, Vegetational and climatic history of the Pacific Northwest during the last 20,000 years—Implications for understanding present-day biodiversity: Northwest Environmental Journal, v. 8, p. 5–28.

Whitney, J.D., 1888, The United States—Facts and figures illustrating the physical geography of the country and its material resources: Boston, Little, Brown, and Company, 472 p. [Reprinted in The Encyclopedia Britannica, 9th ed.: Edinburgh, Adam and Charles Black, v. XXIII, p. 791–817].

Williams, J.H., ed., 1913, The canoe and the saddle, or Klalam and Klickatat, by Theodore Winthrop, to which are now added his western letters and journals: Portland, Franklin-Ward Company, 332 p.

Winthrop, T., 1862, The canoe and the saddle: New York, J. W. Lovell, 375 p.

Zdanowicz, C.M., Zielinski, G.A., and Germani, M.S., 1999, Mount Mazama eruption—Calendrical age verified and atmosphere impact assessed: Geology, v. 27, no. 7, p. 621–624.

Appendixes 1–9

Appendix 1. Reference Sections and Buried Forests

Reference sections (RS) and buried forests (BF) provide key age or stratigraphic control of glacial and volcanic deposits around Mount Baker. Radiocarbon ages (in ^{14}C years before present, yr B.P.) and 2-sigma (2σ) calibrated ages (in cal. yr B.P.) are given here and also collated in appendixes 2 and 3. Table columns show unit number, thickness, and description. Coordinates are given in Universe Transverse Mercator (UTM) zone 10 projection using the North American Datum of 1927 (NAD 27).

Reference Sections

RS–1

Key.—Maximum date for Vashon Drift and envelopment of Mount Baker by the Cordilleran ice sheet; age of Glacial Lake Concrete. Upper part of section (Vashon in age) in south (left) cutbank of bluff opposite confluence of the Skagit River and Jackman Creek, 1.7 river kilometers (km) upstream from confluence with the Baker River at Concrete, Wash. This is the "Big Boy" section (named Big Boy after a bull pastured on the terrace above the section) of Riedel and others (2010). Coordinates: UTM 582710 E., 5396670 N.

[m, meters; cm, centimeters; ^{14}C yr B.P., ^{14}C years before present; cal. yr B.P., calibrated years before present]

Unit no.	Thickness (m)	Description
7	10–12	Vashon Drift; silty gravel with rounded clasts but containing angular clasts of exotic lithologies as large as 1 m across.
6	0.6–1.0	Coarse sand and gravel grading to stratified silt at top. Age of outer rings of 5-cm-thick log, 20 cm below top of unit is 16,545±45 ^{14}C yr B.P. (20,147–19,760 cal. yr B.P.). Age of flattened reed stems from topmost silt layer is 16,425±50 ^{14}C yr B.P. (20,019–19,615 cal. yr B.P.). Age of Sitka spruce cone from near top of unit is 16,400±80 ^{14}C yr B.P. (20,027–19,565 cal. yr B.P.; Riedel and others, 2010).
5	4	Interbedded lacustrine and fluvial gravel; coarse pebble mode is well stratified, with large-scale crossbedding.
4	0–1	Clay-rich lacustrine silt; lenticular and locally eroded from section.
3	2–3	Fluvial gravel; pebble mode, with scour channels.
2	2	Clay-rich lacustrine silt with abundant plant macrofossils. Interpreted by Riedel and others (2010) as from Glacial Lake Concrete, formed by damming of Skagit River valley by Evans Creek stade valley glaciers flowing out of Baker River valley. Basal date: 19,880±80 ^{14}C yr B.P. (24,175–23,663 cal. yr B.P.; Riedel and others, 2010).
1	>8	Interbedded fluvial and lacustrine strata.

RS–2

Key.—Age of earliest known deposits of Glacial Lake Baker (Sandy Creek beds). Exposure along right bank of Sandy Creek where it enters Baker Lake and observable only at times of maximum reservoir drawdown. Site buried by alluvium in 2003. Labeled facies described in chapter D. Coordinates: UTM 596960 E., 5393570 N.

[m, meters; ^{14}C yr B.P., ^{14}C years before present; cal. yr B.P., calibrated years before present]

Unit no.	Thickness (m)	Description
5	0.8–1	Soil, brown, silty.
4	2 to >3	Alluvium; cobble mode, sandy matrix, scour channels at base.
3	>10	Volcaniclastic facies (Vu) of Glacial Lake Baker, which grades upward into sandy alluvium. Volcanic sedimentation in response to eruption of Schriebers Meadow cinder cone. 2 m of Sulphur Creek lava is exposed about 70 m upstream.
2	1.7	Sandy Creek beds; lacustrine facies (Lsc) of Glacial Lake Baker. The unit transitions from till (below) to 0.9 m of blue-gray, laminated silt and clay with plant fossils, overlain by 0.8 m of tan to blue-gray, thinly laminated rhythmite-like beds with abundant plant macrofossils. Ages of 12,200±45 ^{14}C yr B.P. (14,241–13,951 cal. yr B.P.) from a lodgepole pinecone and 11,820±45 ^{14}C yr B.P. (13,762–13,546 cal. yr B.P.) from a 2-cm piece of charcoal.
1	>8	Vashon Drift; massive grayish-blue (5PB 5/2) till with less than 3 percent gravel (>2 mm). Clasts mainly exotic but include Mount Baker and Black Buttes lithologies. Dominates valley walls upstream.

RS–3

Key.—Dated moraines of Sumas age in the Middle Fork Nooksack River; Vashon Drift documented by upstream transport of Twin Sisters Dunite. Left bank of Middle Fork Nooksack River 100–500 meters (m) upstream of confluence with Ridley Creek at altitude of 2,640 feet (805 m), 3.0 km downstream of present terminus of Deming Glacier. Tephras and lahars described in chapters F and G, respectively. Coordinates: UTM 581250 E., 5397460 N.

[m, meters; cm, centimeters; ca., circa; ka, thousand years; ^{14}C yr B.P., ^{14}C years before present; cal. yr B.P., calibrated years before present; *n*, number]

Unit no.	Thickness (m)	Description
6	7–9	Deming Glacier debris flow (June 1927); boulders and cobbles in a granular matrix. Deposit is inset against older units; contains boulders of Black Buttes volcanic breccia >5 m along trail to site of log bridge (destroyed 2003). (Unit may correlate with part of unit 3 of Kovanen and Slaymaker, 2005.)
5	0–2.5	Middle Fork lahar (middle Holocene); debris-flow deposit with blue-gray cohesive matrix. Deposit caps section. (Unit may correlate with part of unit 3 of Kovanen and Slaymaker, 2005.)
4	0–8	Colluvium; locally intercalated with 2–3 cm of early Holocene tephra set SC (ca. 8,800 yr B.P.; 9.7 ka). Not shown on fig. 3 cross-section diagram. (Unit may correlate with part of unit 3 of Kovanen and Slaymaker, 2005.)
3b	9	Alpine till (Sumas in age); rubbly sandy diamict above distinct contact with unit 3a. Unit includes platy andesite typical of Mount Baker lava flows and a lens of lacustrine strata near top. (Unit correlates with part of unit 3 of Kovanen and Slaymaker, 2005.)
3a	7	Alpine till (Sumas in age); rubbly sandy diamict. Age of outer rings of log at base of unit, resting on unit 2, is 10,600±40 ^{14}C yr B.P. (12,691–12,433 cal. yr B.P.). Ages of outer rings of two logs, probably both from the same tree, 2 m above base of unit is 10,520±50 and 10,510±50 ^{14}C yr B.P. (12,655–12,237 and 12,644–12,173 cal. yr B.P.). Age of outer rings of log 3.5 m below top of unit is 10,550±40 ^{14}C yr B.P. (12,640–12,415 cal. yr B.P.). (Unit correlates with unit 2 of Kovanen and Slaymaker, 2005.)
2	0.5–3.5	Glaciofluvial and glaciolacustrine clay; finely laminated with silt-rich interbeds and dropstones. (Unit correlates with unit 1b of Kovanen and Slaymaker, 2005.)
1	>20	Vashon Drift; interbedded with lacustrine deposits and flow till. Contains Mount Baker lithologies, mainly metavolcanics and metasediments of the Nooksack Formation exposed in gorge upstream. Twin Sisters Dunite indicates ice movement up the Middle Fork Nooksack River. Clast composition (*n* = 50): volcanic, 52 percent (20 percent Black Buttes lithologies distinguished by olivine content, greater alteration, and filled vesicles relative to Mount Baker lithologies, 2 percent andesite, and 30 percent uncategorized); metasedimentary and metavolcanic, 38 percent; dunite, 8 percent; limestone, 2 percent; and granitoid, 2 percent. (Unit correlates with unit 1a of Kovanen and Slaymaker, 2005.)

RS–4

Keys.—Age of tephra set SP and relation to moraines of Sumas age. Right bank of easternmost (2013) dry channel of Rocky Creek, 40 m downstream from abutments of washed-out footbridge. This is the section described by Hyde and Crandell (1978, p. 4) as from "the bank of Sulphur Creek [Rocky Creek] 1.8 km northwest of the Schriebers Meadow cinder cone." Coordinates: UTM 586250 E., 5395850 N.; 3,690 feet (1,125 m) altitude.

[m, meters; cm, centimeters; mm, millimeters; ^{14}C yr B.P., ^{14}C years before present; cal. yr B.P., calibrated years before present]

Unit no.	Thickness	Description
7	1.8 m	Diamict of pebble-size clasts in sand matrix. Inferred neoglacial alpine moraine.
6	15 cm	Stratified and reworked middle Holocene tephra layer BA.
5	85 cm	Orange early Holocene tephra from Schriebers Meadow cinder cone (tephra set SC); angular, openwork scoria lapilli, 2–12 mm.
4	4 cm	Brown silty soil containing thin concentrations of angular sand-size fragments of gray-black andesite tephra. Charcoal fragments yield ages of 10,720±50 ^{14}C yr B.P. (12,729–12,580 cal. yr B.P.) and 10,590±50 ^{14}C yr B.P. (12,689–12,423 cal. yr B.P.).
3	0.1–1.0 cm	Black sand-size ash representing the main layer of tephra set SP. Date of charcoal fragments in upper part of layer is 10,870±80 ^{14}C yr B.P. (12,971–12,671 cal. yr B.P.).

RS–4—Continued

Unit no.	Thickness	Description
2	25 cm	Soil; brown sandy silt containing dispersed particles of angular gray-black andesite.
1	>6 m	Diamict, probable alpine moraine of Sumas age. Rubbly gravel with andesite-sand matrix. Facets on prisms of disaggregated prismatically jointed blocks are round.

RS–5

Keys.—Section constraining ages of tephra set SP (?) and layer MY (?) overlying likely moraine of Sumas age. Excavated pit near base of swale, 225 m south of Scott Paul Trail, on interfluve below Scott Paul Trail. Coordinates: UTM 587350 E., 5397550 N.; 4,870 feet (1,484 m) altitude.

[cm, centimeters; mm, millimeters; ka, thousand years; ^{14}C yr B.P., ^{14}C years before present; cal. yr B.P., calibrated years before present]

Unit no.	Thickness (cm)	Description
14	20	Soil with grains of middle Holocene tephra layer BA near base.
13	0–3	Middle Holocene tephra set OP.
12	2–7	Organic-rich soil.
11	2–5	Middle Holocene tephra layer O (7.6 ka) from Mount Mazama.
10	3	Organic-rich soil.
9	0.5	Red-stained peaty soil layer without visible particles of tephra set SC.
8	1	Organic-rich soil with charcoal yielding date of 8,298±46 ^{14}C yr B.P. (9,435–9,136 cal. yr B.P.)
7	0.2	Tephra layer MY (?), angular lithic particles.
6	4	Organic-rich soil; date 8,285±35 ^{14}C yr B.P. (9,439–9,125 cal. yr B.P.), from charcoal fragments 3 mm below unit 7; date of 8,315±50 ^{14}C yr B.P. (9,463– 9,139 cal. yr B.P.) from charcoal fragments in center of unit 6.
5	0.3–2.5	Layer of tephra set SP (?) containing poorly sorted angular, mainly lithic tephra with minor juvenile andesite.
4	1.5–2.0	Organic-rich soil.
3	0.4–1.2	Layer of tephra set SP (?); granular juvenile andesite.
2	1	Charcoal-rich stratum just below tephra yielding date of 11,460±35 ^{14}C yr B.P. (13,407–13,214 cal. yr B.P.)
1	>10	Colluvium developed on probable alpine moraine of Sumas age.

RS–6

Key.—Site of dated middle Holocene and Little Ice Age advances of Easton Glacier (Osborn and others, 2012). Left-lateral moraine of Easton Glacier where exposed over approximately 50 m between bedrock outcrops at 5,260 feet (1,603 m) altitude. Coordinates: UTM 586330 E., 5397790 N.

[m, meters; cm, centimeters; ^{14}C yr B.P., ^{14}C years before present; cal. yr B.P., calibrated years before present]

Unit no.	Thickness (m)	Description
6	4	Late neoglacial till dated at 410±40 ^{14}C yr B.P. (524–319 cal. yr B.P.) by Osborn and others (2012).
5	~20	Neoglacial till.
4	0.3–1	Deformed peat and soil containing abundant wood, including logs dated at 5,260±70 and 5,240±70 ^{14}C yr B.P. (6,263–5,907 and 6,263–5,893 cal. yr B.P., respectively; Osborn and others, 2012).
3	0–2	Distinctive light-colored, glacially deformed strata including early Holocene tephra set SC (lapilli as large as 1.5 cm), and middle Holocene tephra layer O, tephra set OP, and grains of tephra layer BA.
2	1–2.3	Debris-flow deposit of morainal sediment.
1	2–4	Alpine till of probable Sumas age overlying lava flows.

RS–7

Keys.—Section of deltaic units above Sulphur Creek lava, documenting post-lava sedimentation into Glacial Lake Baker at a minimum altitude of about 760–770 feet (232–235 m). Exposures are 100 m upvalley from end of road in lower Sulphur Creek. Coordinates: UTM 595980 E., 5389520 N.

[m, meters; cm, centimeters; ft, feet; ^{14}C yr B.P., ^{14}C years before present; cal. yr B.P., calibrated years before present]

Unit no.	Thickness	Description
5	2 m	Horizontally bedded terrace gravels with silt interbeds unconformably overlying deltaic section.
4	>18 m	Deltaic volcaniclastic deposits in Glacial Lake Baker. Dramatic deltaic crossbedding records migration of Sulphur Creek delta into lake. Altitude of unit records high level of Glacial Lake Baker after emplacement of the Sulphur Creek lava flow.
3	5–8 m	Horizontally stratified volcaniclastic facies of Glacial Lake Baker.
2	0–25 cm	A thin layer of volcaniclastic-free, yet post-lava sediment may represent sedimentation during a very brief interval when Sulphur Creek may have been temporarily blocked. Sharp contact with overlying volcaniclastic facies, representing reestablished drainage courses from terrain mantled with early Holocene tephra set SC. A 1.3-m megaclast of pre-lava lacustrine facies (volcaniclastic free) on top of the lava flow was eroded by flowing lava.
1	>5 m	Distal sub-lacustrine Sulphur Creek lava (altitude of top, 600 ft; 183 m). A large spring of remarkably pure water (according to Puget Sound Power and Light[1]) issues from beneath the lava upstream from this reference section and is interpreted as discharge from an aquifer formed by the buried channel of Sulphur Creek pre-lava flow.

[1]Predecessor to Puget Sound Energy.

RS–8

Key.—Deposits of Glacial Lake Baker documenting lake level at 770 feet (235 m) altitude postdating tephra set SC (early Holocene). Roadcut is in terrace above primitive campground north of Sandy Creek mouth. Coordinates: UTM 597000 E., 5393800 N.

[m, meters; ft, feet]

Unit no.	Thickness (m)	Description
3	0.6	Silty soil forming top of terrace, 770 ft (235 m) altitude interpreted as deposit of Glacial Lake Baker.
2	0.2	Sandy pebble gravel consisting of eruptive products from early Holocene eruptions of Schriebers Meadow cinder cone.
1	>1.8	Laminated, horizontally bedded lacustrine silt.

RS–9

Key.—Age of lacustrine deposits documents the existence of Glacial Lake Baker in the late Holocene. Cutbank on west side of Lake Shannon, 300 m upvalley from Bear Creek exposed at times of maximum reservoir drawdown. Coordinates: UTM 594600 E., 5384800 N.

[m, meters; ^{14}C yr B.P., ^{14}C years before present; cal. yr B.P., calibrated years before present]

Unit no.	Thickness (m)	Description
3	6	Lacustrine strata of Glacial Lake Baker. Charcoal 1.5 m from top of sequence yields date of 3,205±35 ^{14}C yr B.P. (3,550–3,360 cal. yr B.P.).
2	0.5–1.2	Pebble-cobble gravel; well rounded, alluvial, partly cemented, resting directly on Vashon Drift and surrounding a large granitoid erratic.
1	>3	Vashon Drift; clay rich, blue gray, with 2.1-m angular granitoid erratic resting on upper surface.

RS–10

Keys.—Horseshoe Cove section of Glacial Lake Baker; Sulphur Creek lava with peperite carapace invaded Glacial Lake Baker sequence beneath decollement (glide plane); evidence of high levels of Glacial Lake Baker after emplacement of early Holocene Sulphur Creek lava flow. Horseshoe Cove is on west side of Baker Lake reservoir, with complete sequence visible when lake level is <680 feet (207 m). Site is 70–300 m south and east of the boat ramp. Coordinates: UTM 597550 E., 5391340 N.

[m, meters; cm, centimeters; ft, feet; ^{14}C yr B.P., ^{14}C years before present; cal. yr B.P., calibrated years before present]

Unit no.	Thickness (m)	Description
5	0–2.3	Mixed (Mhc_2) deltaic facies of Holocene Glacial Lake Baker; ripple cross-laminated and horizontally stratified sand, unconsolidated sand and pebble gravel, lacustrine silt and clay. Includes log with outer rings yielding date of 6,135±35 ^{14}C yr B.P. (7,158–6,952 cal. yr B.P.) and ponded deposits of middle Holocene tephra layer O (Mount Mazama) weathered blue (5B 5/6) and not its characteristic orange color. Layer indicates that the deltaic flux of detrital tephra from the Schriebers Meadow cinder cone (unit 4) was largely complete by the middle Holocene, and that Glacial Lake Baker still existed at a high level, greater than about 700 ft (213 m).
4	2–4	Volcaniclastic facies (Vhc) of Glacial Lake Baker; coarse deltaic sand and pebble gravel, rich with tephra set SC, and has deltaic crossbeds with amplitudes >2 m. Unit tapers in thickness toward center of reservoir.
3	1	Volcaniclastic facies (Vhc) of Glacial Lake Baker; fine sand with silty interbeds, well stratified, consolidated. Charcoal 10 cm below top of unit yields date of 8,655±35 ^{14}C yr B.P. (9,686–9,541 cal. yr B.P.).
2	>4	Mixed facies (Mhc_1) of Pleistocene Glacial Lake Baker; silt and clay, lacking volcaniclastic material, well laminated; interbedded with sand-mode strata with volcaniclastic material. Uppermost clay-rich unit contains two 1-cm conifer-needle-rich layers of the forest bed, 15 cm apart. Outer rings of log in lower stratum of forest bed yield date of 9,975±35 ^{14}C yr B.P. (11,610–11,267 cal. yr B.P.). Near base, sequence contains peperite sills invaded from carapace of Sulphur Creek lava flow, and a 1.2-m-thick layer of rip-up clast conglomerate in which clasts are Pleistocene facies Lsc.
1	>5	Early Holocene Sulphur Creek lava flow with 0.3–1.0 m carapace of peperite consisting of lava fragments in a matrix of clay-rich Glacial Lake Baker facies Lsc (correlation based on plant fragments). Carapace contains fewer lava fragments toward upper margin, which is a decollement along which the early Holocene lava flow invaded the overlying Pleistocene sequence. Drill logs show lava is as much as 65 m thick.

RS–11

Keys.—Lacustrine deposits of Glacial Lake Baker where intruded by the peperite carapace of the lava, locally along a decollement, on the east side of Baker River valley; lava forms invasive "pillow"-like masses; age of forest bed and facies Mu. Exposures in reservoir bank on north side of prominent point on the east side of Baker Lake reservoir, near Anderson Creek, opposite Horseshoe Cove boat ramp. Unit 1 is younger than and intrudes overlying units 2–7. Coordinates: UTM 598100 E., 5390830 N.

[m, meters; cm, centimeters; ^{14}C yr B.P., ^{14}C years before present; cal. yr B.P., calibrated years before present]

Unit no.	Thickness	Description
8	>1.5 m	Basalt-rich gravel, sand, and silt; horizontally bedded, containing concentrations of tephra set SC. Forms wide terrace around Glacial Lake Baker (with archaeological sites).
7	1–2 m	Volcaniclastic facies (Vu).
6	0.5 m	Lacustrine facies (Lu) separated from underlying unit by decollement.
5	<4 m	Lacustrine and volcaniclastic facies (Mu) of Glacial Lake Baker, as in RS–6. Displaced, deformed, and elevated like unit 2. Unit contains invasive "pillow"-like masses.
4	15 cm	Variable thickness of mixed volcaniclastic and lacustrine facies (Mu) like unit 2.
3	1 cm	Forest bed: wood- and conifer-needle-rich mat yielding dates from the outer rings of 5-cm-thick log of 10,355±50 ^{14}C yr B.P. (12,406–12,010 cal. yr B.P.) and from needles 9,985±35 ^{14}C yr B.P. (11,614–11,271 cal. yr B.P.). The needle date is probably more accurate.

RS–11—Continued

Unit no.	Thickness	Description
2	2–5 m	Mixed volcaniclastic and lacustrine facies (Mu) of Glacial Lake Baker; section displaced, deformed, and elevated by the intruding Sulphur Creek lava flow. Twig 12 cm below forest bed yields date of 10,205±50 ^{14}C yr B.P. (12,110–11,715 cal. yr B.P.).
1	>5 m	Sulphur Creek lava invading older, overlying sediment of units 2, 4, and 5, with invasive "pillows."

RS–12

Key.—Documents intrusion and complex deformation of Glacial Lake Baker sediment and Vashon Drift by peperite breccia sill. Composite from exposures in steep banks 10–250 m downvalley from mouth of Dry Creek when drawdown of Baker Lake reservoir is below 685 feet (209 m) altitude. Coordinates: UTM 597980 E., 5391640 N.

[m, meters; cm, centimeters; ka, thousand years]

Unit no.	Thickness	Description
6	0–30 cm	Pebble alluvium mainly derived from Sandy Creek fan.
5	0–20 cm	Ponded deposits of tephra layer O (7.6 ka) from climactic eruption of Mount Mazama in Glacial Lake Baker.
4	0–1.5 m	Facies Mu; alluvial and lacustrine sand and silt locally deposited on lava and peperite.
3	0–4 m	Facies Vu; sediment of Glacial Lake Baker, interbedded turbidite-like strata and well-laminated silt and clay with deformation by microfaulting. Inferred to contain tephra set SC. Locally intruded by peperite dikes and sills.
2	>5 m	Sulphur Creek lava flow; vertical contact with till and Pleistocene (facies Mu) and early Holocene (facies Mu and Vu) lacustrine strata of Glacial Lake Baker. A 2×8-m mass of peperite with sediment matrix abuts upvalley side of main till exposure. Peperite sill, 0–20 cm thick, appears invaded from that mass into the lacustrine section below the forest bed dated ~11.6 (see RS–10 and RS–11).
1	4 m	Vashon Drift; blue gray with granitoid clasts as large as 0.6 m. Vertical contact with Sulphur Creek lava flow on downvalley side.

RS–13

Keys.—Sulphur Creek lava directly overlies deformed deposits of Glacial Lake Baker and is overlain by probable deposits of Glacial Lake Baker. Lava on left bank of Sulphur Creek at base of waterfall, 300 m downstream from Baker Lake Road bridge over Sulphur Creek. Coordinates: UTM 595060 E., 5390150 N., 800 feet (245 m) altitude.

[m, meters; cm, centimeters]

Unit no.	Thickness	Description
7	30 cm	Soil and forest duff.
6	2 m	Rubbly debris flow consisting of angular and subrounded basalt blocks in sandy matrix; thin sole layer (see Scott, 1988a) with rounded pebbles.
5	1 cm	Buff silt containing organic fragments.
4	4 m	Alternating 10- to 30-cm-thick horizontal beds of tephra-set-SC-bearing medium sand and 2- to 5-cm-thick beds of pale gray silt. Probable lacustrine deposit.
3	10 m	Sulphur Creek lava with angular basal breccia. Lava is fine grained, glassy, poorly jointed, and only slightly vesicular at the base, increasingly so upwards.
2	>1 m	Laminated, buff lacustrine clay, baked and deformed in contact with overlying lava. Base covered.
1	0–1 m	Thin-bedded to crossbedded gray slack-water sand, with void cavities, banked against and under the eroded base of units 2 and 3.

RS–14a

Key.—South (right bank) section of Boulder Creek assemblage overlying probable alpine glaciation deposits of Sumas age; assemblage underlies early Holocene tephra set SC. Deposits on south (right) valley-side slope of Boulder Creek, from thalweg at 1,800 feet (549 m) altitude to top of slope at 2,600 feet (792 m) altitude, 3.1 km upstream from bridge. Coordinates: UTM 593180 E., 5398210 N.

[m, meters; cm, centimeters]

Unit no.	Thickness	Description
7	1–2 m	Soil on sandy colluvium with coarse pebble clasts.
6	3–4 cm	Tephra set SC (early Holocene).
5	3–4 cm	Gray, organic-rich silt.
4	0–3 m	Diamict; rubbly colluvium probably derived from alpine glacial till of Sumas age.
3	~230 m	Boulder Creek assemblage; sequence of fragmental deposits consisting of block-and-ash flows, lahar deposits, hyperconcentrated-flow deposits and alluvial interbeds.
2	~25 m	Diamict; alpine drift, undated but inferred to be of Sumas age. Clasts of local metamorphic rocks (~40 percent) and Mount Baker andesite (~25 percent) in compacted sandy mud matrix. Basal contact dips 20 degrees and conforms with present valley-side slope and channel axis.
1	1 m	Fluvial sand overlying compacted, glacially deformed clay and silt.

RS–14b

Key.—North (left bank) type section of Boulder Creek assemblage containing block-and-ash flows. More detailed description of assemblage in table 7. Deposit on north (left) valley-side slope of Boulder Creek 2.0 km above highway bridge. Top of slope and section at 2,040 feet (622 m) altitude. Coordinates: UTM 594330 E., 5398800 N.

[m, meters]

Unit no.	Thickness (m)	Description
2	81	Boulder Creek assemblage; sequence of fragmental deposits consisting of block-and-ash flows, lahar deposits, hyperconcentrated-flow deposits and alluvial interbeds.
1	0 to >3	Diamict, angular-to-subrounded clasts of Mount Baker andesite and pre-Mount Baker volcanics and rare, locally derived metamorphic clasts in a matrix of clay and sand. Site is beyond reach of glaciers of Sumas age, therefore likely Evans Creek alpine glacial deposit.

RS–15

Key.—Block-and-ash-flow deposits overlie Vashon Drift; Pratt Creek assemblage and the Ridley Creek lahar (see chapter G). Exposure along Pratt Creek, right bank, 50–250 m upstream of confluence with Ridley Creek. Coordinates: UTM 583540 E., 5396720 N.

[m, meters; cm, centimeters; ka, thousand years]

Unit no.	Thickness	Description
10	1.7 m	Ridley Creek lahar (middle Holocene); debris-flow deposit consisting of pebble- to cobble-size clasts mainly of Mount Baker andesite in a distinctively light gray (7.5YR 6/0) to pale yellow (2.5Y 8/4) cohesive matrix.
9	740 cm	Soil; rust colored, containing 5–20 cm of middle Holocene tephra layer O (7.6 ka) 0–15 cm above base.

RS–15—Continued

Unit no.	Thickness	Description
8	2.2 m	Schriebers Meadow lahar (early Holocene); rubbly debris-flow deposit consisting of subangular pebble- to cobble-size clasts in an orangish-brown cohesive matrix.
7	0–1.5 m	Soil; upper 0.2 to 0.3 m containing and stained by tephra set SC (early Holocene).
6	20 m	Pratt Creek assemblage; noncohesive, stratified, monolithologic block-and-ash flow, debris flow, and fluvial deposits dominated by sand-size sediment, including 0.5- to 1.5-m-thick layers of pebble-to cobble-size subangular clasts of Mount Baker andesite. Coarse intervals contain prismatically jointed clasts and fragments.
5	1–2 m	Pratt Creek assemblage; block-and-ash flow deposit with breadcrusted and strongly prismatically jointed blocks with rusty colored ash matrix. Syneruptive origin indicated by abundance of prismatically jointed and breadcrusted clasts showing evidence of high emplacement temperatures.
4	2 m	Pratt Creek assemblage; well-stratified yellow-brown sand containing both andesite and hydrothermally altered and stained lithologies.
3	6 m	Pratt Creek assemblage; well-stratified black andesite sand, with 10 percent pebble-size clasts. Several clay interbeds as thick as 1 cm near middle of unit.
2	>7 m	Vashon Drift containing exotic lithologies, including granodiorite, and Twin Sisters Dunite. Gray-blue to black matrix with significant amounts of Mount Baker andesite lapilli; more granular than matrix of other Vashon deposits around Mount Baker.
1	>4 m	Evans Creek (?) alpine drift with no exotic lithologies. Granular matrix similar to that of overlying Vashon Drift.

RS–16

Key.—Minimum age of the Sulphur Creek assemblage from charcoal in overlying soil and colluvium. Valley-side slopes of left bank (east side) of the middle fork of Sulphur Creek, at 3,725–3,900 feet (1,135–1,189 m) altitude. Tephra set SC and older units exposed at top of left valley-side slope; younger units exposed on left bank near stream level, about 75 m downstream. Coordinates: UTM 587290 E., 5396380 N.

[m, meters; cm, centimeters; mm, millimeters; ka, thousand years; ^{14}C yr B.P., ^{14}C years before present; cal. yr B.P., calibrated years before present]

Unit no.	Thickness	Description
11	0.5 m	Soil with middle Holocene tephras BA and YP (not seen in situ).
10	0.7 m	Debris-flow deposits that may correlate with a distributary of the Ridley Creek lahar exposed on the right bank, upstream from confluence with west fork of Sulphur Creek.
9	3–8 cm	Organic-rich silty sediment with masses of middle Holocene tephra layer O.
8	1 cm	Middle Holocene tephra layer O (7.6 ka).
7	0–1 m	Soil stained orangish brown by tephra set SC, locally organic rich.
6	6 cm	Tephra layer SC_2 (at top of upstream part of section); discrete layer of ash-size tephra.
5	1.8–3 m	Tephra layer SC_1 (orangish-brown scoria lapilli in size range of medium pebbles, 8–16 mm).
4	0.3 m	Soil and silty colluvium; dates of 10,901±68 and 11,020±180 ^{14}C yr B.P. (12,956–12,692 and 13,256–12,656 cal. yr B.P., respectively) from charcoal several centimeters above the base of the unit.
3	>25 m	Sulphur Creek assemblage; sand-mode clay-poor flow deposits representing hyperconcentrated and alluvial runouts of block-and-ash flows and lahars; significant content of prismatically jointed blocks. Contacts sharp; units separated by multiple silt laminae deposited from meltwater. Some units contain 5–15 percent pumice.
2	3 m	Vashon Drift containing exotic lithologies, including granitoids and exotic metamorphic clasts in a blue-gray matrix.
1	>10 m	Lava flows and flow breccias, with minor intercalations of fragmental detritus like unit 2.

RS–17

Key.—Age of tephra set SC; tephra dated and shown to be overlain by Sulphur Creek lava and the Schriebers Meadow lahar. Exposure along left cutbank of Sulphur Creek, 40 m south of first switchback in the Scott Paul Trail, 200 m from trailhead at parking lot (note drainages are incorrectly plotted on the 7.5-minute quadrangle map in this area). Part of section covered by slumping in 2003. Coordinates: UTM 587350 E., 5395350 N.

[m, meters; cm, centimeters; ka, thousand years; ^{14}C yr B.P., ^{14}C years before present; cal. yr B.P., calibrated years before present]

Unit no.	Thickness	Description
7	1 cm	Diffuse tephra set YP (historical) in soil.
6	0.8–1.6 m	Interval including middle Holocene Ridley Creek lahar in upstream exposures, replaced here by detrital sediment that contains >20 percent hydrothermally altered grains.
5	2–4 cm	Middle Holocene tephra layer O (7.6 ka) from Mount Mazama.
4	0–0.7 m	Detrital sediment containing hydrothermally altered clasts.
3	2.4 m	Early Holocene Schriebers Meadow lahar, mainly angular pebble-size clasts as dispersed phase in reddish-brown matrix, with this distinctive color from entrained tephra set SC. Here, the lahar overlies tephra set SC.
2	>2 m	Early Holocene Sulphur Creek lava exposed in stream channel downstream but not in direct contact with (underlying) tephra at this site. The lava is overlain by the Schriebers Meadow lahar.
1	>1.2 m	Tephra set SC, lapilli-size scoria at base grading to silty ash with charcoal yielding ages 8,750±50 ^{14}C yr B.P. (10,107–9,552 cal. yr B.P.), 8,830±50 ^{14}C yr B.P. (10,156–9,698 cal. yr B.P.), and 8,850±50 ^{14}C yr B.P. (10,168–9,710 cal. yr B.P.). Base not exposed.

RS–18

Keys.—Postglacial tephras at Mount Baker; section yielding dates of tephra layer MY. Excavated pit 150 m south of the Scott Paul Trail, on interfluve between second and third minor tributaries of Sulphur Creek east of the Metcalfe Moraine, the left-lateral Little Ice Age moraine of Easton Glacier; 4,800 feet (1,460 m) altitude. Coordinates: UTM 586330 E., 5397790 N.

[m, meters; cm, centimeters; ka, thousand years; ^{14}C yr B.P., ^{14}C years before present; cal. yr B.P., calibrated years before present]

Unit no.	Thickness	Description
12	>1 cm	Root zone.
11	1 cm	Lithic and vitric ash, lapilli of glass, and particles of hydrothermally altered material dispersed in soil; historical tephra set YP.
10	8 cm	Soil.
9	12 cm	Granular ash (fine sand mode) dispersed in soil; middle Holocene tephra layer BA.
8	2 cm	Aggregated small hydrothermally altered lapilli, middle Holocene tephra set OP.
7	4 cm	Organic-rich soil.
6	2–3 cm	Middle Holocene tephra layer O (7.6 ka) from Mount Mazama.
5	5 cm	Soil, with charcoal yielding date of 8,110±70 ^{14}C yr B.P. (9,278–8,775 cal. yr B.P.) (J.J. Clague, written commun., 2006).
4	0.2 cm	Tephra layer MY, <2 mm lithic ash (silt and sand size) in organic-rich soil; grains of hydrothermally altered material.
3	7 cm	Soil, with charcoal yielding date of 8,130±80 ^{14}C yr B.P. (9,395–8,774 cal. yr B.P.) (J.J. Clague, written commun., 2006).
2	5–65 cm	Tephra set SC, dominated by scoriaceous lapilli but containing much fine ash.
1	>0.4 m	Colluvium and soil on late Pleistocene or early Holocene alpine moraine. Includes dispersed andesitic ash (fine sand size), possibly tephra set SP (see RS–15).

RS–19

Key.—Age dates for tephra layer BA. Channel-side exposures 10 m above the Ridley Creek Trail crossing of the western fork of Pratt Creek, the main tributary of Ridley Creek. Trail is grossly misplaced on the Mount Baker 7.5-minute topographic quadrangle. Coordinates: UTM 583440 E., 5397490 N.

[cm, centimeters; ka, thousand years; ^{14}C yr B.P., ^{14}C years before present; cal. yr B.P., calibrated years before present]

Unit no.	Thickness (cm)	Description
6	10	Colluvium and soil.
5	20–30	Tephra layer BA. Charcoal fragments yield dates of 5,730±50 and 5,670±60 ^{14}C yr B.P. (6,642–6,410 and 6,628–6,315 cal. yr B.P., respectively).
4	0–2	Charcoal-rich organic layer. Yields date of 6,170±50 ^{14}C yr B.P (7,240–6,940 cal. yr B.P). Underlies tephra layer BA where tephra set OP is not present.
3	16–23	Tephra set OP. Poorly sorted diamict of silt, sand, and blocks of hydrothermally altered andesite as large as 13 cm.
2	1–2	Soil.
1	~3	Middle Holocene tephra layer O (7.6 ka).

RS–20

Key.—Water-deposited tephra set YP overlain by displaced Middle Fork lahar, at site where previously interpreted by others as a much older tephra. Location is on right bank of Clearwater Creek, about 120 m downstream from bridge. Negative calibrated ages are indicated by 0. Coordinates: UTM 570190 E., 5402480 N.

[m, meters; cm, centimeters; ^{14}C yr B.P., ^{14}C years before present; cal. yr B.P., calibrated years before present]

Unit no.	Thickness	Description
6	0.7 m	Redeposited Middle Fork lahar deposits; 100±50 ^{14}C yr B.P. (275 to <0 cal. yr B.P.) date from log in deposit.
5	0.5 m	Overbank deposits, organic rich; charcoal 10 cm above tephra that yields a date of 200±50 ^{14}C yr B.P. (420 to <0 cal. yr B.P.).
4	1–2 cm	Tephra set YP; partially carbonized wood in base of tephra yields dates of 140±50 ^{14}C yr B.P. (280 to <0 cal. yr B.P.), 260±50 ^{14}C yr B.P. (469 to <0 cal. yr B.P.), and 310±50 ^{14}C yr B.P. (494–287 cal. yr B.P.).
3	0–30 cm	Overbank deposits, wood rich; 840±50 ^{14}C yr B.P. (905–677 cal. yr B.P.), 1,260±40 ^{14}C yr B.P. (1,284–1,076 cal. yr B.P.) dates from 2–15 cm below tephra.
2	2 m	Bouldery alluvium.
1	<1 m	Glacial deposits with lacustrine beds similar to those that are characteristic of late- or post-Vashon age at other localities in the Middle Fork Nooksack River (see RS–3, unit 2).

RS–21

Keys.—Description of and age of Schriebers Meadow lahar. Location on right bank of Sulphur Creek, 150 m downstream of bridge constructed for snowmobiles in Schriebers Meadow. Overlain by numerous middle Holocene tephra layers. Coordinates: UTM 587690 E., 5395230 N.

[m, meters; cm, centimeters; ka, thousand years; ^{14}C yr B.P., ^{14}C years before present; cal. yr B.P., calibrated years before present]

Unit no.	Thickness	Description
11	10–25 cm	Soil, organic debris.
10	3–15 cm	Middle Holocene tephra layer BA, also seen as multiple redistributed units throughout Schriebers Meadow.
9	2.1 m	Middle Holocene Ridley Creek lahar, mainly as a debris flow, but represented in this same stratigraphic interval by detrital sediment from the recession phase of the flow or fluvial reworking. Weathering of components, dominated by altered lithics, may create a clay-rich matrix like that of a debris flow.
8	0.0–0.8 cm	Middle Holocene tephra set OP or basal, fine-grained layer of Ridley Creek lahar.

RS–21—Continued

Unit no.	Thickness	Description
7	0.5–3 cm	Organic-rich, fine-grained sediment.
6	1–4 cm	Middle Holocene tephra layer O (7.6 ka).
5	2 cm	Organic-rich, fine-grained sediment.
4	0.3–0.8 m	Sequence of stratified fluvial sand including silt-rich overbank deposits, locally cut by a channel deposit of alluvium. Contains concentrations of black angular sand-size andesite particles.
3	1.0–1.5 m	Alluvium with sandy matrix and rounded-to-subrounded pebbles and cobbles.
2	1.7–2.8 m	Schriebers Meadow lahar; orangish-brown sandy silt and clay matrix containing angular to subrounded cobbles and boulders. Isolated boulders >1 m. Locally log and wood rich. Bulking of coarse phase <15 percent. Logs yield dates of 8,510±40 and 8,450±40 ^{14}C yr B.P. (9,543–9,470 and 9,533–9,423 cal. yr B.P., respectively).
1	>0.9 m	Fluvial sand and silt, including overbank deposits with scattered fine pebbles and at least two layers of black angular sand-size andesite particles. Basal contact, probably with the Sulphur Creek lava flow, is below streambed level; upstream, the Schriebers Meadow lahar rests directly on tephra layer SC_1 or the lava flow (overlying the tephra).

RS–22

Key.—Dated logs from Park Creek lahar PC_1 overlain by lahar PC_2. Exposure on right bank of Swift Creek where it enters Baker Lake and forms a near-vertical cliff 5 to 7 m in height. Baker Lake Resort is located on the terrace surface; the section is near campsite numbers 68 to 70. Section described during low reservoir levels. Coordinates: UTM 599010 E., 5398130 N.

[m, meters; cm, centimeters; ^{14}C yr B.P., ^{14}C years before present; cal. yr B.P., calibrated years before present]

Unit no.	Thickness	Description
6	2.1 m	Historical Morovitz Creek lahar; intensely altered, tan-to-yellow matrix with both altered and unaltered pebble- and cobble-size clasts. Inset as a berm against base of PC_1. Base covered.
5	0.3–2.5 m	Sandy soil and colluvium forming main terrace surface. Local clay-rich unit representing deposition in pond on lahar surface after tephra layer BA.
4	5–20 cm	Tephra layer BA; massive, graded (maximum grain size 1 to 3 cm above base) unit with modal class in fine-sand fraction (primary thickness about 5 cm); two dates from charcoal in tephra, 5,670±40 and 5,680±40 ^{14}C yr B.P. (6,560–6,322 and 6,618–6,349 cal. yr B.P., respectively).
3	1.3–2.0 m	Park Creek lahar PC_2; finer grained, texturally identical unit to PC_1, but with coarsest clasts of dispersed phase in pebble class.
2	2.3–4.4 m	Park Creek lahar PC_1; cohesive lahar with blue-gray, locally tan or yellowish, clay-rich matrix that forms 55 percent of deposit. Clasts of dispersed phase are typically angular to subangular pebbles or fine cobbles, with a few boulders consisting of altered, fractured andesite. Wood rich. Outer rings of cedar log with bark yield date of 5,935±40 ^{14}C yr B.P. (6,880–6,668 cal. yr B.P.); outer rings of fir logs with bark yield two dates of 5,930±50 and one of 5,900±35 ^{14}C yr B.P. (6,889–6,656 and 6,795–6,645 cal. yr B.P., respectively).
1	>1.5 m	Alluvium; pebble-cobble mode.

RS–23

Keys.—Exposure of largest Park Creek lahar and historical Morovitz Creek lahar. Deposit in quarry in Little Park Creek, 1.15 km upstream from the Baker Lake Road. Coordinates: UTM 597300 E., 5398610 N.

[m, meters; cm, centimeters; ^{14}C yr B.P., ^{14}C years before present; cal. yr B.P., calibrated years before present]

Unit no.	Thickness	Description
7	0.5–1.6 m	Morovitz Creek lahar; intensely altered matrix that encloses altered and unaltered pebble- and cobble-size clasts.
6	2–10 cm	Woody layer.
5	0–2 cm	Tephra set YP.
4	0–20 cm	Pebble-mode alluvial gravel.

RS–23—Continued

Unit no.	Thickness	Description
3	5 m	Park Creek lahar PC_1; pebbles and cobbles dispersed in clayey gray matrix. Deposit yields three age dates: 6,070±50; 6,120±50; and 6,740±90 ^{14}C yr B.P. (7,156–6,788; 7,169–6,800; and 7,751–7,437 cal. yr B.P., respectively). The first age date is from a log without bark, the other two are from wood fragments.
2	0 to >2 m	Alluvium.
1	>12 m	Glaciofluvial sand and gravel, well stratified with deltaic crossbedding. Deposited in Glacial Lake Baker or its Holocene remnant.

RS–24

Key.—Age of Middle Fork lahar with overlying Ridley Creek lahar. Exposure on left bank of Middle Fork Nooksack River, 100 m downstream from bridge on the road leading to the olivine mine in the Twin Sisters range, 20.5 km downstream from summit. Coordinates: UTM 570570 E., 5401730 N.

[m, meters; ^{14}C yr B.P., ^{14}C years before present; cal. yr B.P., calibrated years before present]

Unit no.	Thickness (m)	Description
5	0.1–0.3	Organic debris; forest litter.
4	2–3	Ridley Creek lahar as described at RS–15 (chapter G). Tan-yellow matrix with sharp basal contact here but gradational in exposures 40 m downstream. One of many exposures downstream from confluence of Middle Fork Nooksack River and Ridley Creek where the Ridley Creek lahar may appear to be the upper weathered part of a single flow, the original "Middle Fork lahar."
3	5–8	Middle Fork lahar; blue-gray clay-rich matrix with dispersed phase dominated by rounded cobbles and pebbles. Basal half suggests high bulking factor as coarse material entrained from underlying alluvium. The clay-rich matrix of this alluvium-dominated basal portion, however, identifies it as a lahar. Date from outer rings of fir trunk with bark is 5,930±50 ^{14}C yr B.P. (6,889–6,656 cal. yr B.P.).
2	1.7	Cobble-mode alluvium with sandy matrix, similar in gross appearance to overlying lahar but origin is revealed by the sandy matrix.
1	>~12	Vashon glacial deposits, dominated by non-Mount Baker lithologies with 1–3 percent of Mount Baker andesite. Interbedded lacustrine strata, clayey till, unconsolidated pebble-mode gravel, all locally deformed likely by upvalley-flowing ice overriding deposit.

RS–25

Key.—Middle Fork lahar overlain by Ridley Creek lahar and underlain by older non-Mount Baker debris-flow deposits. Exposure on left bank of Middle Fork Nooksack River, 2.9 km upstream from confluence of Middle Fork and North Fork Nooksack Rivers, 75 m upstream from end of Rutsatz Road, 32.4 km downstream from summit. Coordinates: UTM 563620 E., 5407690 N.

[m, meters; cm, centimeters; ka, thousand years; ^{14}C yr B.P., ^{14}C years before present; cal. yr B.P., calibrated years before present; *n*, number]

Unit no.	Thickness	Description
7	0.6 m	Ridley Creek lahar; sharp basal contact. Coarse pebble mode. Matrix same color as Middle Fork lahar.
6	0.5–1.5 m	Middle Fork lahar; more of a floodplain facies relative to thicker, log-rich exposure at RS–26. Date 5,860±50 ^{14}C yr B.P. (6,792–6,534 cal. yr B.P.).
5	5 cm	Silt-rich overbank flood deposits and soil.
4	2–5 cm	Tephra layer O (7.6 ka); forms flame structure that points downstream in response to shearing by Middle Fork lahar.

RS–25—Continued

Unit no.	Thickness	Description
3	15–25 cm	Silt-rich overbank flood deposits and soil.
2	1.7 m	Debris-flow deposit with tan mud-rich matrix containing altered or weathered material that contains subordinate Mount Baker lithologies. Probably not a lahar from the Mount Baker edifice, but a large debris flow with source in the Middle Fork Nooksack River headwaters (inferred from subangular dunite clasts). Charcoal fragments from uppermost 20 cm yield age of 6,990±50 ^{14}C yr B.P. (7,934–7,705 cal. yr B.P.). 56 percent of clasts rounded to subrounded. Clast composition (n = 100): sedimentary (Chuckanut Formation), 40 percent; andesite and basalt, 36 percent; dunite, 6 percent; and other (argillite, quartzite, and metasedimentary), 18 percent.
1	>2.8 m	Debris-flow deposit with angular clasts of fossiliferous (palm fronds), consolidated sandstone (Chuckanut Formation), and black shale in black clay-rich matrix. A landslide-runout flow originating from opposite side of the Middle Fork Nooksack River valley.

RS–26

Key.—Log-rich Middle Fork lahar overlain by Ridley Creek lahar. Exposure on left bank of North Fork Nooksack River 125 m downstream from confluence with Middle Fork Nooksack River, 35.3 km downstream from summit. Coordinates: UTM 562100 E., 5408920 N.

[m, meters; cm, centimeters; km, kilometers; ^{14}C yr B.P., ^{14}C years before present; cal. yr B.P., calibrated years before present]

Unit no.	Thickness	Description
5	1.5 m	Granular debris-flow or grain-flow deposit consisting of predominantly pebbles with little interstitial matrix, which was probably removed by post-depositional processes. Probable origin is as a flood surge resulting from failure of blockage in tributary dammed by the Ridley Creek lahar.
4	2.2 m	Ridley Creek lahar. Debris-flow deposit where, after more than 20 km of flow, it has eroded deposits of the Middle Fork lahar and lost its distinctive pale-yellow upstream color. Matrix similar to Middle Fork lahar, but deposit is wood poor, with few coarse clasts larger than the medium-pebble fraction.
3	>5.4 m	Middle Fork lahar. Mottled tan to blue-gray matrix enclosing hydrothermally stained cobbles, few boulders, and abundant logs. Limb molds common in upper half. Overall normal grading. Date from outermost rings of large log with bark is 5,930±50 ^{14}C yr B.P. (6,889–6,656 cal. yr B.P.).
2	1 cm	Layer of charcoal, deformed by emplacement of overlying lahar.
1	0.4 m	Fluvial sand.

RS–27

Key.—Morovitz Creek lahar on the floodplain of lower Morovitz Creek. Exposure on right bank of Morovitz Creek, 1.15 km upstream of confluence with Swift Creek, near ruins of the Morovitz cabin, where drainage crosses swampy area that reflects drainage disruption by the lahar (creek grossly mislocated on 7.5-minute quadrangle). Coordinates: UTM 597920 E., 5399350 N.

[m, meters; cm, centimeters]

Unit no.	Thickness	Description
5	0.8 m	Morovitz Creek lahar; pebble mode; altered, cohesive, clay-rich matrix.
4	8–10 cm	Wood layer.
3	1–2 cm	Tephra set YP.
2	0.5–0.7 m	Soil.
1	>0.5 m	Park Creek lahar; base not exposed.

RS–28

Key.—Section records two historical lahars separated by alluvium in Boulder Creek. Exposure on right bank of Boulder Creek at campground downstream from highway bridge, adjacent to campsite 9. Coordinates: UTM 596350 E., 5396380 N.

[m, meters]

Unit no.	Thickness (m)	Description
4	0.5	Lahar younger than the Morovitz Creek lahar. Pebbly, intensely altered matrix; similar to unit 1 but contains less rounded alluvium, suggesting a bulking factor of about 10 percent.
3	0.6	Alluvium with woody debris.
2	0.4	Fluvial sand in channel on surface of unit 1.
1	>1.7	Branch of Morovitz Creek lahar in Boulder Creek; contains boulders with rounded to subrounded clasts consisting of Mount Baker andesite derived from erosion of Boulder Creek assemblage. Local bulking factor of ~80 percent estimated from rounded alluvium.

RS–29

Key.—19th-century lahar stratigraphy on Boulder Creek fan. Composite section based on exposures on the left bank of Boulder Creek for 0.8 km, beginning 0.4 km below bridge and including a distributary cut into the east side of Boulder Creek fan and formed after clearcut of 1991. Coordinates: UTM 596950 E., 5396150 N.

[m, meters; cm, centimeters]

Unit no.	Thickness	Description
6	0–0.5 m	Stratified sandy alluvium that represents overbank flood deposits after emplacement of 19th-century lahars.
5	0–2.0 m	Lahar possibly correlating with the observations of 1858 (appendixes 5, 6). Cohesive, tan to light-gray, clay-rich matrix composed of hydrothermally altered particles. Mainly pebble-size dispersed clasts are both angular material from source and rounded, unaltered andesite bulked into flow; both types are stained yellow to orange by reaction with acid-rich matrix.
4	1 to >2.6 m	Morovitz Creek lahar; cohesive, clay-rich matrix like that of overlying unit but with more sand; dispersed clasts as large as boulders are unaltered andesite bulked during flow. Clasts are stained yellow to orange by reaction with matrix. Sheared old-growth stumps at base of deposit.
3	0–15 cm	Woody debris, generally not burned.
2	0–1 cm	Tephra layer YP.
1	>2.0 m	Sandy, brown soil and alluvium; well stratified.

RS–30

Key.—Deposits form the 19th-century blockage of natural Baker Lake. Deposits exposed where cut by Swift Creek when it flows across the exposed bottom of modern Baker Lake reservoir at times of low water levels. Coordinates: UTM 599410 E., 5397800 N.

[m, meters; cm, centimeters]

Unit no.	Thickness	Description
6	15–60 cm	Lacustrine silt; reservoir deposits with abundant modern charcoal.
5	1.9 m	Morovitz Creek lahar; yellow-orange stained pebbles and cobbles in pale-colored, clay-rich matrix of hydrothermally altered particles, wood and log rich. Ring counts of flared stumps of 10 trees growing on the surface of this unit near this site have a range of 91 to 106 years. The trees were probably cut in 1958 or 1959, the year Upper Baker Dam was completed. Note that unflared stumps of old-growth trees protrude through this layer, rooted on unit 2, including those of huge cedars with rotted heartwood and possibly in excess of 1,000 years in age.
4	2 cm	Woody debris layer.
3	1 cm	Tephra set YP, uniform in thickness across 5 m of exposure.

RS–30—Continued

Unit no.	Thickness	Description
2	>0.2 m	Soil; brown, silty. The old-growth trees protruding through overlying deposits are rooted in this layer.
1	>3 m	Sandy, well-rounded pebble and cobble alluvium.

Buried Forests

BF–1, BF–2, and BF–3

Buried forest(s) at base of neoglacial moraines. Southeast (left) valley-side slope 1.9–2.0 km downstream from present terminus of Deming Glacier. BF–1 and BF–3 are high on valley-side slope, near 3,180 feet (957 m) altitude; BF–2 is downslope, near 3,090 feet (942 m) altitude, and 0.1 km upstream. No deposits of Middle Fork lahar on surface. Coordinates: BF–1 and BF–3, UTM 581880 E., 5398140 N.; BF–2, UTM 581840 E., 5398200 N.

[m, meters; km, kilometers; ^{14}C yr B.P., ^{14}C years before present; cal. yr B.P., calibrated years before present]

Unit no.	Thickness (m)	Description
3	>3	Till with logs at base (BF–3). Age of outer rings of log is 430±30 ^{14}C yr B.P. (530–335 cal. yr B.P.).
2	>12	Till with logs at base (BF–1). Age of outer rings of log is 1,595±30 ^{14}C yr B.P. (1,549–1,410 cal. yr B.P.). The same buried forest, with numerous in situ old-growth tree trunks, is exposed 0.1 km upstream at BF–2; date from outer rings of in situ buried stump is 1,595±45 ^{14}C yr B.P. (1,595–1,381 cal. yr B.P.).
1	>15	Till.

BF–4

Date from base of moraine. Located 1.4 km downstream from terminus of Deming Glacier on right valley-side slope at 3,640 feet (1,109 m) altitude. Coordinates: UTM 582240 E., 5399040 N.

[m, meters; ^{14}C yr B.P., ^{14}C years before present; cal. yr B.P., calibrated years before present]

Unit no.	Thickness (m)	Description
2	>10	Moraine without deposits of Middle Fork lahar on surface. Age of outer rings of 1-m-diameter log probably at base of till is 1,070±40 ^{14}C yr B.P. (1,061–926 cal. yr B.P.).
1	>8	Till.

BF–5

Buried forest at base of debris-flow deposit that caps a 7-m terrace on right bank of Middle Fork Nooksack River exposed at the Elbow Lake Trailhead. Exposure is 5.2 km downstream from present terminus of Deming Glacier at altitude 670 m. Coordinates: UTM 578990 E., 5398300 N.

[m, meters; cm, centimeters; ^{14}C yr B.P., ^{14}C years before present; cal. yr B.P., calibrated years before present]

Unit no.	Thickness (m)	Description
3	0.2	Soil supporting mature forest.
2	1–4	Noncohesive diamict seen in both channel and flood-plain facies; channel facies with coarse mode of angular cobbles in noncohesive matrix, with 5-cm sole layer. Outer rings of 25-cm log with bark at base of flood-plain facies yield date of 1,740±30 ^{14}C yr B.P. (1,715–1,565 cal. yr B.P.). Deposit interpreted as a glacial-outburst flow.
1	>3	Alluvium.

Appendix 2. Radiocarbon and Calibrated Ages of Samples Collected by Authors

Here we document radiocarbon ages of samples collected or submitted by authors or, in the case of tephra layer MY, previously unpublished information provided by a colleague. Calibrated ages were determined using 2013 OxCal software versions 4.2.3 and 4.2.4, based on work by Bronk Ramsey (2009). For the wiggle-match ages, we used 2017 version 4.3.2, based work by Bronk Ramsey and others (2001). In both cases we used the IntCal13 atmospheric calibration curve of Reimer and others (2013). Calibrated ages (cal. yr B.P.), shown in bold, are the total range of possible ages at a 2σ confidence level (95.4 percent probability); where multiple intervals occur, the ranges are shown and followed by percent probability in parentheses. The ranges may contain intervals that are excluded as possible ages. Some recently analyzed samples are corrected for isotopic fractionation ($^{13}C/^{12}C$), otherwise the standard value of −25 is given. Significant ages are noted with their stratigraphy in reference sections (RS) and buried forest (BF) locations (appendix 1). Initial letters of laboratory numbers identify the analytical laboratory: WW, U.S. Geological Survey, Reston, Va.; TO, IsoTrace Laboratory Radiocarbon Analytical Services, Toronto, Canada; and B, Beta Analytic, Inc., Miami, Fla. Coordinates are given in Universe Transverse Mercator (UTM) zone 10 projection (easting, northing) using North American Datum of 1927 (NAD 27).

Table 2.1. Lacustrine and fluvial deposits preceding arrival of Vashon ice in Skagit River valley.

[cm, centimeters; km, kilometers; ^{14}C yr B.P., ^{14}C years before present; cal. yr B.P., calibrated years before present]

Lab no.	Field no.	^{13}C	^{14}C yr B.P.	Cal. yr B.P.	Material	Location	UTM
WW5458	B-05-01	−25	16,425±50	**20,019–19,615**	Flattened reed (?) stems	RS–1	582710, 5396670
WW5459	B-05-02	−25	16,545±45	**20,147–19,760**	Outer rings 5-cm log	RS–1	582710, 5396670
B220961	NOCA 125a	−26.6	16,333±60	**19,941–19,528**	Wood	2 km upstream from RS–1	

Table 2.2. Left-lateral Sumas moraine, Middle Fork Nooksack River above confluence with Ridley Creek.

[^{14}C yr B.P., ^{14}C years before present; cal. yr B.P., calibrated years before present]

Lab no.	Field no.	^{13}C	^{14}C yr B.P.	Cal. yr B.P.	Material	Location	UTM
WW1872	B-98-09	−25	10,600±40	**12,691–12,433** 12,691–12,525 (90.0) 12,469–12,433 (5.4)	Outer rings of log	RS–3	581250, 5397460
WW1873	B-98-10	−25	10,510±50	**12,644–12,173** 12,644–12,376 (88.7) 12,346–12,298 (2.2) 12,290–12,235 (3.9) 12,199–12,187 (0.4) 12,176–12,173 (0.1)	Outer rings of log	RS–3	581250, 5397460
WW1874	B-98-11	−25	10,520±50	**12,655–12,237** 12,655–12,378 (92.0) 12,330–12,304 (0.9) 12,279–12,237 (2.5)	Outer rings of log	RS–3	581250, 5397460
WW4215	B-02-07	−25	10,550±40	**12,640–12,415**	Outer rings of log	RS–3	581250, 5397460

Table 2.3. Left-lateral moraines, Middle Fork Nooksack River, 1.9–2.0 kilometers below terminus of Deming Glacier.

[cm, centimeters; ^{14}C yr B.P., ^{14}C years before present; cal. yr B.P., calibrated years before present]

Lab no.	Field no.	^{13}C	^{14}C yr B.P.	Cal. yr B.P.	Material	Location	UTM
WW6081	B-06-16	−23.47	1,595±30	**1,549–1,410**	Outer rings of log	BF–1	581880, 5398140
WW6463	B-07-31	−25	1,595±45	**1,595–1,381** 1,595–1,585 (0.9) 1,570–1,381 (94.5)	Outer rings of buried 35-cm stump	BF–2	581840, 5398200
WW6082	B-06-17	−23.23	430±30	**530–335** 530–452 (90.7) 443–439 (0.6) 350–335 (4.1)	Outer rings of log	BF–3	581880, 5398140

Table 2.4. Right-lateral moraine, Middle Fork Nooksack River, 1.4 kilometers below terminus of Deming Glacier.

[km, kilometers; ^{14}C yr B.P., ^{14}C years before present; cal. yr B.P., calibrated years before present]

Lab no.	Field no.	^{13}C	^{14}C yr B.P.	Cal. yr B.P.	Material	Location	UTM
WW2660	B-99-01	−25	1,070±40	**1,061–926**	Outer rings of log?	BF–4	582240, 5399040

Table 2.5 Left-lateral moraine, Coleman Glacier (site of Davis and others, 2007); samples collected by G. Osborn.

[^{14}C yr B.P., ^{14}C years before present; cal. yr B.P., calibrated years before present]

Lab no.	Field no.	^{13}C	^{14}C yr B.P.	Cal. yr B.P.	Material	Location	UTM
WW6076	BW-2	−22.0	595±30	**652–540** 652–579 (69.7) 572–540 (25.7)	Wood	Buried forest in left-lateral moraine (same site as 940 ^{14}C yr B.P. age of Davis and others, 2007)	
WW6084	BBBB#5	−20.05	515±30	**625–506** 625–606 (7.7) 564–499 (89.5)	Wood	Buried forest in left-lateral moraine (same site as 940 ^{14}C yr B.P. age of Davis and others, 2007)	

Table 2.6. Lacustrine strata of Glacial Lake Baker.

[cm, centimeters; ^{14}C yr B.P., ^{14}C years before present; cal. yr B.P., calibrated years before present]

Lab no.	Field no.	^{13}C	^{14}C yr B.P.	Cal. yr B.P.	Material	Location	UTM
WW4074	B-02-04	−25	12,200±45	**14,241–13,951**	Lodgepole pinecone	RS–2	596960, 5393570
WW4088	B-02-03	−25	11,820±45	**13,762–13,546**	Charcoal, 2-cm piece	RS–2	596960, 5393570
WW4851	B-04-02	−25	3,205±35	**3,550–3,360** 3,550–3,534 (2.3) 3,492–3,360 (93.1)	Charcoal	RS–9	594600, 5384800

Table 2.6. Lacustrine strata of Glacial Lake Baker.—Continued

Lab no.	Field no.	^{13}C	^{14}C yr B.P.	Cal. yr B.P.	Material	Location	UTM
WW6991	B-08-21	−23.97	6,135±30	**7,158–6,952**	Outer rings of 25-cm log	RS–10	597550, 5391340
WW4852	B-04-03	−25	9,975±35	**11,610–11,267** 11,610–11,520 (21.0) 11,506–11,267 (74.4)	Outer rings of log in forest bed	RS–10	597550, 5391340
WW4853	B-04-05	−25	8,655±35	**9,686–9,541**	Charcoal	RS–10	597550, 5391340
WW5731	B-06-05	−25	10,205±50	**12,110–11,715**	Twig 12 cm below forest bed	RS–11	598100, 5390830
WW5732	B-06-06	−25	10,355±50	**12,406–12,010**	Outer rings of 5-cm log in forest bed	RS–11	598100, 5390830
WW6077	B-06-08	−25.47	9,985±35	**11,614–11,271**	Pine needles in forest bed	RS–11	598100, 5390830

Table 2.7. Silty soil and colluvium overlying the Sulphur Creek assemblage.

[^{14}C yr B.P., ^{14}C years before present; cal. yr B.P., calibrated years before present]

Lab no.	Field no.	^{13}C	^{14}C yr B.P.	Cal. yr B.P.	Material	Location	UTM
WW3790	B-01-04	−25	10,901±68	**12,956–12,692**	Charcoal fragments in soil	RS–16	587290, 5396380
WW3791[a]	B-01-05	−25	11,020±180	**13,256–12,656**	Charcoal fragments in soil	RS–16	587290, 5396380

[a]Sample consisted of 0.2 milligrams of carbon.

Table 2.8. Tephra set SP.

[^{14}C yr B.P., ^{14}C years before present; cal. yr B.P., calibrated years before present]

Lab no.	Field no.	^{13}C	^{14}C yr B.P.	Cal. yr B.P.	Material	Location	UTM
WW1869	B-98-05	−25	10,720±50	**12,729–12,580**	Charcoal fragments in soil containing tephra	RS–4	586250, 5395850
WW2404	B-98-27	−25	10,590±50	**12,689–12,423** 12,689–12,516 (79.5) 12,500–12,423 (15.9)	Charcoal fragments in soil containing tephra	RS–4	586250, 5395850
WW2965	B-00-10	−25	10,870±80	**12,971–12,671**	Charcoal fragments in tephra	RS–4	586250, 5395850
WW6464	B-07-33	−25	8,315±50	**9,463–9,139** 9,463–9,199 (89.2) 9,180–9,139 (6.2)	Charcoal in soil between tephra set SP (lower) and layer MY (upper)	RS–5	587350, 5397550
WW6465	B-07-34	−25	8,285±50	**9,439–9,125**	Charcoal in soil between tephra set SP (lower) and layer MY (upper)	RS–5	587350, 5397550
WW6462	B-07-30	−25	11,460±35	**13,407–13,214**	Charcoal fragments below tephra set SP	RS–5	587350, 5397550

Table 2.9. Tephra set SC.

[^{14}C yr B.P., ^{14}C years before present; cal. yr B.P., calibrated years before present]

Lab no.	Field no.	^{13}C	^{14}C yr B.P.	Cal. yr B.P.	Material	Location	UTM
WW954	B-95-5	−25	8,750±50	**10,107–9,552** 10,107–10,103 (0.2) 9,915–9,552 (95.2)	Charcoal in tephra	RS–17	587350, 5395350
WW1456	B-97-7	−25	8,850±50	**10,168–9,710** 10,168–9,736 (95.0) 9,715–9,710 (0.4)	Charcoal in tephra	RS–17	587350, 5395350
WW1468	B-97-18	−25	8,830±50	**10,156–9,698** 10,156–9,981 (33.3) 9,970–9,698 (62.1)	Charcoal in tephra	RS–17	587350, 5395350

Table 2.10. Tephra layer MY.

[mm, millimeter; ^{14}C yr B.P., ^{14}C years before present; cal. yr B.P., calibrated years before present]

Lab no.	Field no.	^{13}C	^{14}C yr B.P.	Cal. yr B.P.	Material	Location	UTM
TO12444[a]	MB-14A	−25	8,110±70	**9,278–8,775** 9,278–8,850 (89.1) 8,839–8,775 (6.3)	Charcoal in soil above tephra	RS–18	586330, 5397790
TO12445[a]	MB-14C	−25	8,130±80	**9,395–8,774** 9,395–9,385 (0.4) 9,372–9,363 (0.3) 9,307–8,846 (89.9) 9,941–8,774 (4.8)	Charcoal in soil below tephra	RS–18	586330, 5397790
WW6111	B-06-10	−25	8,298±46	**9,435–9,136**	Charcoal in organic-rich soil above tephra layer MY	RS–5	587350, 5397550
WW6464	B-07-33	−25	8,315±50	**9,463–9,139**	Charcoal below tephra layer MY in organic-rich soil	RS–5	587350, 5397550
WW6465	B-07-34	−25	8,285±35	**9,439–9,125**	Charcoal 3 mm below tephra layer MY in organic-rich soil	RS–5	587350, 5397550

[a]Age from J.J. Clague, written commun., 2007.

Table 2.11. Tephra set OP and Ridley Creek lahar (synchronous with tephra set OP).

[m, meter; cm, centimeter; ft, feet; ^{14}C yr B.P., ^{14}C years before present; cal. yr B.P., calibrated years before present]

Lab no.	Field no.	^{13}C	^{14}C yr B.P.	Cal. yr B.P.	Material	Location	UTM
WW1459	B-97-10	−25	5,800±50	**6,731–6,488**	Charcoal in tephra	Scott Paul Trail at junction with Park Butte Trail	
WW1460	B-97-11	−25	6,010±50	**6,986–6,733**	Wood in tephra transitional to Ridley Creek lahar	Park Butte Trail 60 m before Railroad Grade Trail	

Table 2.11. Tephra set OP and Ridley Creek lahar (synchronous with tephra set OP).—Continued

Lab no.	Field no.	^{13}C	^{14}C yr B.P.	Cal. yr B.P.	Material	Location	UTM
WW1464	B-97-09	−25	5,860±60	**6,826–6,499** 6,826–6,820 (0.4) 6,797–6,499 (95.0)	Wood in 3-cm organic layer between tephra layer O and set OP	Scott Paul Trail at 3,860 ft altitude	
WW1973	B-98-12	−25	6,060±40	**7,144–6,791** 7,144–7,130 (1.3) 7,010–6,791 (94.1)	Wood fragments in tephra set OP	Junction of Park Butte and Railroad Grade Trails	
WW1974	B-98-13	−25	6,060±40	**7,144–6,791** 7,144–7,130 (1.3) 7,010–6,791 (94.1)	Wood fragments in tephra set OP	Junction of Park Butte and Railroad Grade Trails	
WW1975	B-98-14	−25	6,160±40	**7,166–6,949**	Wood fragments in tephra set OP	Junction of Park Butte and Railroad Grade Trails	
WW2403	B-98-26	−25	5,760±50	**6,670–6,440**	Charcoal at contact of tephra set OP and layer BA	Scott Paul Trail at junction with Park Butte Trail	
WW1112	B-96-24	−25	5,320±50	**6,271–5,948** 6,271–6,241 (4.3) 6,215–5,988 (88.8) 5,967–5,948 (2.3)	Charcoal overlying tephra set OP and layer BA	Scott Paul Trail in upper Sulphur Creek	
B56322	B-92-20	−25	5,800±120	**6,936–6,349** 6,936–6,349 (94.6) 6,368–6,349 (0.8)	Wood in Ridley Creek lahar	West branch of Sulphur Creek, north side of Schriebers Meadow	

Table 2.12. Tephra layer BA.

[^{14}C yr B.P., ^{14}C years before present; cal. yr B.P., calibrated years before present]

Lab no.	Field no.	^{13}C	^{14}C yr B.P.	Cal. yr B.P.	Material	Location	UTM
WW1458	B-97-06	−25	6,170±50	**7,240–6,940** 7,240–7,196 (3.8) 7,180–6,940 (91.6)	Charcoal in organic layer below tephra	RS–19	583440, 5397490
WW3604	B-01-01	−25	5,730±50	**6,642–6,410**	Charcoal fragments in tephra	RS–19	583440, 5397490
WW3605	B-01-02	−25	5,670±60	**6,628–6,315** 6,628–6,585 (5.8) 6,569–6,315 (95.0)	Charcoal fragments in tephra	RS–19	583440, 5397490
WW4216	B-02-08	−25	5,670±40	**6,560-6,322** 6,560–6,392 (89.6) 6,372–6,322 (5.8)	Charcoal in tephra	RS–22	599010, 5398130
WW4217	B-02-09	−25	5,680±40	**6,618-6,349** 6,618–6,609 (0.6) 6,603–6,588 (1.2) 6,567–6,395 (91.7) 6,369–6,349 (1.8)	Charcoal in tephra	RS–22	599010, 5398130

Table 2.13. Tephra set YP.

[cm, centimeter; ^{14}C yr B.P., ^{14}C years before present; cal. yr B.P., calibrated years before present]

Lab no.	Field no.	^{13}C	^{14}C yr B.P.	Cal. yr B.P.	Material	Location	UTM
WW1463	B-97-14	−25	200±50	**420 to <0** 420–412 (0.6) 315–59 (77.7) 42 to <0 (17.0)	Charcoal 10 cm above tephra	RS–20	570190, 5402480
WW1413	B-97-02	−25	140±50	**280 to <0** 284–166 (41.8) 155 to <0 (53.6)	Partially carbonized wood at base of tephra	RS–20	570190, 5402480
WW5724	B-06-02	−25	260±50	**469 to <0** 469–267 (73.1) 215–145 (17.2) 20 to <0 (5.1)	Partially carbonized wood at base of tephra	RS–20	570190, 5402480
WW1414	B-97-03	−25	310±50	**494–287**	Partially carbonized wood at base of tephra	RS–20	570190, 5402480
WW1461	B-97-12	−25	1,260±40	**1,284-1,076** 1,284–1,171 (74.1) 1,163–1,076 (21.3)	Overbank deposits, wood rich, 2–15 cm below tephra	RS–20	570190, 5402480
WW1462	B-97-13	−25	840±50	**905–677** 905–854 (12.6) 831–677 (82.8)	Overbank deposits, wood rich, 2–15 cm below tephra	RS–20	570190, 5402480

Table 2.14. Schriebers Meadow lahar.

[m, meter; ^{14}C yr B.P., ^{14}C years before present; cal. yr B.P., calibrated years before present]

Lab no.	Field no.	^{13}C	^{14}C yr B.P.	Cal. yr B.P.	Material	Location	UTM
WW1980	B-98-19	−25	8,450±40	**9,533–9,423**	Outer rings of log	RS–21	587690, 5395230
WW1981	B-98-20	−25	8,510±40	**9,543–9,470**	Outer rings of log	RS–21	587690, 5395230
WW2962	B-00-07	−25	8,410±80	**9,542–9,14**6 9,542–9,245 (93.9) 9,171–9,146 (1.5)	Outer rings of log	Confluence of middle and west forks of Sulphur Creek	
WW2963	B-00-08	−25	8,500±70	**9,600–9,314** 9,600–9,398 (92.6) 9,358–9,314 (2.8)	Outer rings of log	Right bank of Sulphur Creek	
WW2964	B-00-09	−25	8,490±90	**9,665–9,285**	Outer rings of log	Left bank of Sulphur Creek, 50 m downstream of RS–21	

Table 2.15. Largest Park Creek lahar (PC_1)

[^{14}C yr B.P., ^{14}C years before present; cal. yr B.P., calibrated years before present]

Lab no.	Field no.	^{13}C	^{14}C yr B.P.	Cal. yr B.P.	Material	Location	UTM
WW4218	B-02-10	−25	5,935±40	**6,880–6,668** 6,880–6,870 (1.5) 6,860–6,668 (93.9)	Outer rings of cedar log with bark	RS–22	599010, 5398130
WW4219	B-02-11	−25	5,900±35	**6,795–6,645**	Outer rings of fir log with bark	RS–22	599010, 5398130

Table 2.15. Largest Park Creek lahar (PC_1)—Continued

Lab no.	Field no.	^{13}C	^{14}C yr B.P.	Cal. yr B.P.	Material	Location	UTM
WW2958	B-00-01	−25	5,930±50	**6,889–6,656**	Outer rings of fir log with bark	RS–22	599010, 5398130
WW2959	B-00-02	−25	5,930±50	**6,889–6,656**	Outer rings of fir log with bark	RS–22	599010, 5398130
WW2960	B-00-03	−25	6,070±50	**7,156–6,788** 7,156–7,099 (7.1) 7,086–7,078 (0.6) 7,069–7,044 (1.8) 7,030–6,788 (85.9)	Outer rings of log without bark	RS–23	597300, 5398610
B57709	B-8		6,120±60	**7,169–6,800** 7,169–6,846 (94.2) 6,815–6,800 (1.2)	Wood fragments (knot)	RS–23	597300, 5398610
B56314	B-9		6,740±90	**7,751–7,437**	Wood fragment	RS–23	597300, 5398610

Table 2.16. Middle Fork lahar from outermost rings of trees knocked down by the flow.

[m, meters; ^{14}C yr B.P., ^{14}C years before present; cal. yr B.P., calibrated years before present]

Lab no.	Field no.	^{13}C	^{14}C yr B.P.	Cal. yr B.P.	Material	Location	UTM
WW1415	B-97-04	−25	100±50	**275 to <0** 275–173 (33.9) 151 to <0 (64.5)	Log in reworked lahar deposit	RS–20	570190, 5402480
WW1868	B-98-04	−25	5,930±50	**6,889–6,65**6	Outer rings of fir trunk with bark	RS–24	570570, 5401730
WW1976	B-98-15	−25	5,920±40	**6,853–6,658** 6,853–6,812 (8.1) 6,806–6,658 (87.3)		100 m below confluence of Middle Fork Nooksack River and Clearwater Creek	
WW1977	B-98-16	−25	5,890±40	**6,831–6,819** 6,831–6,819 (0.8) 6,798–6,634 (94.6)		150 m downstream from confluence of Middle Fork Nooksack River and Clearwater Creek	
WW5730	B-06-3	−25	5,880±60	**6,878–6,535** 6,878–6,873 (0.3) 6,858–6,535 (95.1)		150 m downstream from confluence of Middle Fork Nooksack River and Clearwater Creek	
WW1870	B-98-07	−25	5,860±50	**6,792–6,534**	Outer rings of fir trunk with bark	RS–25	563620, 5407690
WW1871	B-98-08	−25	5,930±50	**6,889–6,656**	Outer rings of fir trunk with bark	RS–26	562100, 5408920

Table 2.17. Ridley Creek lahar, where all data are from the same 285-year-old log as determined from careful counting of ring intervals; resultant wiggle-match age is 6,750–6,710 calibrated years before present at 95.4 percent probability.

[^{14}C yr B.P., ^{14}C years before present; cal. yr B.P., calibrated years before present]

Lab no.	Field no.	^{13}C	^{14}C yr B.P.	Cal. yr B.P.	Material	Location	UTM
WW6212	RC1-16	−21.09	5,820±30	**6,717–6,526**	Rings 1–16 (outermost)	Park Butte Trail before Railroad Grade Trail	
WW6213	RC67–77	−21.21	6,010±25	6,862–6,711	Rings 67–77		
WW6214	RC104–110	−20.52	5,980±30	6,789–6,629	Rings 104–110		
WW6215	RC155–160	−21.53	6,015±30	6,789–6,622	Rings 155–160		
WW6216	RC223–227	−21.09	6,130±30	6,934–6,717	Rings 223–227		
WW6217	RC281–285	−20.66	6,190±30	6,893–6,705	Rings 281–285		

Table 2.18. Ridley Creek lahar, where all data are from the same 285-year-old log as determined from careful counting of ring intervals and conventional ^{13}C assignment; not corrected for ring interval.

[^{14}C yr B.P., ^{14}C years before present; cal. yr B.P., calibrated years before present]

Lab no.	Field no.	^{13}C	^{14}C yr B.P.	Cal. yr B.P.	Material	Location	UTM
WW6212	RC1–16	−25	5,790±35	**6,653–6,496**	Rings 1–16 (outermost)	Park Butte Trail before Railroad Grade Trail	
WW6213	RC67–77	−25	5,980±30	**6,895–6,736**	Rings 67–77		
WW6214	RC104–110	−25	5,945±35	**6,880–6,674** 6,880–6,870 (1.8) 6,860–6,674 (93.6)	Rings 104–110		
WW6215	RC155–160	−25	5,990±35	**6,930–6,740**	Rings 155–160		
WW6216	RC223–227	−25	6,100±35	**7,157–6,882** 7,157–7,095 (13.3) 7,087–7,042 (4.7) 7,032–6,882 (77.4)	Rings 223–227		
WW6217	RC281–285	−25	6,155±35	**7,162–6,957**	Rings 281–285		

Table 2.19. Debris Flow at Elbow Lake Trailhead.

[^{14}C yr B.P., ^{14}C years before present; cal. yr B.P., calibrated years before present]

Lab no.	Field no.	^{13}C	^{14}C yr B.P.	Cal. yr B.P.	Material	Location	UTM
WW6083	B-06–18	−22.9	1,740±30	**1,715–1,565**	Outer rings of log	BF–5	578990, 5398300

Table 2.20. Other deposits.

[m, meters; ft, feet; ^{14}C yr B.P., ^{14}C years before present; cal. yr B.P., calibrated years before present]

Lab no.	Field no.	^{13}C	^{14}C yr B.P.	Cal. yr B.P.	Material	Location	UTM
WW2995	B-00-04	−25	1,050±40	**1,059–914**	Charcoal	Fluvial sediment between older lahar in Boulder Creek and Morovitz Creek lahar; left bank Boulder Creek 200 m upstream of bridge	
WW1978	B-98-17	−25	6,990±50	**7,934–7,705**	Charcoal	In lahar (?) underlying tephra layer O at RS–25	
WW1467	B-97-17	−25	3,710±40	**4,219–3,926** 4,219–4,209 (0.8) 4,155–3,958 (91.1) 3,951–3,926 (3.5)	Charcoal	Pale-colored lithic tephra over tephra layer BA at Baker Pass	
B56319	B-15		770±50	**790–653**	Outer rings of log	On Little Ice Age moraine of Easton Glacier under opal- and sulphur-bearing deposits at 4,360 ft altitude	
B56327	B-29		570±80	**677–496**	Wood	Deposit stratigraphically beneath Rainbow Creek debris avalanche, 200 m upstream from 2009 Rainbow Creek bridge crossing	

Table 2.21. Lahar from Glacier Peak in Sauk River.

[km, kilometers; ^{14}C yr B.P., ^{14}C years before present; cal. yr B.P., calibrated years before present]

Lab no.	Field no.	^{13}C	^{14}C yr B.P.	Cal. yr B.P.	Material	Location	UTM
WW6430	B-02-04	−22.74	40,000±600	44,785–42,752	Wood	Left bank Sauk River, >50 km below volcano (7 km below Darrington, Wash.)	
WW6992	B-02-03	−25	38,790±740	44,145–41,820	Outer rings log	Left bank Sauk River, >50 km below volcano (7 km below Darrington, Wash.)	

Appendix 3. List of All Radiocarbon Ages Cited in this Report

Shown are the laboratory ^{14}C ages with uncertainties (where known), the calibrated age range at a 2σ confidence level (95.4 percent probability), the laboratory number where known, the reference for the radiocarbon or calibrated age, the unit being dated, and in which chapter the age is first cited. Initial letters of laboratory numbers identify the analytical laboratory: AA, University of Arizona, Tucson, Ariz.; B, Beta Analytic Inc., Miami, Fla.; CAMS, Lawrence Livermore National Laboratory, Livermore, Calif.; GSC, Geological Survey of Canada, Ottawa; I (?) and TO, IsoTrace Laboratory, University of Toronto, Canada; U and UCI, University of California, Irvine, Calif.; WW*, Western Washington University, Bellingham, Wash.; and W and WW, U.S. Geological Survey Radiocarbon Laboratory in Reston, Va.

[yr B.P., years before present; cal. yr B.P., calibrated years before present]

^{14}C age (yr B.P.)	Error (years)	Calibrated 2σ age range (cal. yr B.P.)	Lab no.	Source	Event or unit dated	Chapter
100	50	275 to <0	WW1415	This report	Reworked Middle Fork lahar	F
140	50	280 to <0	WW1413	This report	Tephra layer YP	F
200	50	420 to <0	WW1463	This report	Overlying tephra layer YP	F
260	50	469 to <0	WW5724	This report	Tephra layer YP	F
310	50	494–287	WW1414	This report	Tephra layer YP	F
375	15	500–331	U68591a	Osborn and others (2012)	Little Ice Age	C
410	40	524–319	B221569	Osborn and others (2012)	Little Ice Age advance	C
430	30	530–335	WW6082	This report	Little Ice Age advance	C
515	30	625–506	WW6084	This report	Little Ice Age	C
570	80	677–496	B56327	This report	Older Rainbow Creek debris avalanche	G
595	30	652–540	WW6076	This report	Little Ice Age	C
770	50	790–653	B56319	This report	Little Ice Age advance of Easton Glacier	C
840	50	905–677	WW1462	This report	Overbank deposit below tephra layer YP	F
970	50	967–766	B207929	Osborn and others (2012)	Late neoglacial	C
1,050	40	1,059–914	WW2995	This report	Lahar in Boulder Creek	G
1,070	40	1,061–926	WW2660	This report	Late neoglacial advance of Deming Glacier	C
1,260	40	1,284–1,076	WW1461	This report	Overbank deposit below tephra layer YP	F
1,595	30	1,549–1,410	WW6081	This report	Neoglacial advance of Deming Glacier	C
1,595	45	1,595–1,381	WW6463	This report	Neoglacial advance of Deming Glacier	C
1,740	30	1,715–1,565	WW6083	This report	Debris flow at Elbow Lake in Middle Fork Nooksack River	G
1,750	50	1,812–1,556	B234087	Osborn and others (2012)	Late neoglacial	C
2,115	15	2,146–2,010	U68591d	Osborn and others (2012)	Middle neoglacial advance of Deming Glacier	C
2,285	15	2,349–2,211	U68591c	Osborn and others (2012)	Middle neoglacial	C
2,940	35	3,207–2,976		Easterbrook andDonnell (2007)	Middle neoglacial advance of Deming Glacier	C
2,960	30	3,212–3,005		Easterbrook and Donnell (2007)	Middle neoglacial advance of Deming Glacier	C
3,120	50	3,447–3,214	AA22223	Kovanen and others (2001)	Younger Middle Fork lahar (?)	G
3,205	35	3,550–3,360	WW4851	This report	Glacial Lake Baker remnant in Lake Shannon	D
3,710	40	4,219–3,926	WW1467	This report	Younger lithic tephra (?)	F

^{14}C age (yr B.P.)	Error (years)	Calibrated 2σ age range (cal. yr B.P.)	Lab no.	Source	Event or unit dated	Chapter
3,970	100	4,814–4,149		Kovanen and others (2001)	Minimum age of Cathedral Crag ash (tephra layer BA)	F
4,390	90	5,295–4,837		Kovanen and others (2001)	Minimum age of Cathedral Crag ash (tephra layer BA)	F
4,600		5,432–5,304		Porter and Denton (1967)	Early reference on beginning of neoglaciation	C
4,600	70	5,576–5,045		Porter and Denton (1967)	Early reference on beginning of neoglaciation	C
		5,830–5,780		Foit and others (2004)	Dusty Creek tephra of Glacier Peak	F
5,080–5,000		5,901–5,725		Hallet and others (2001)	Dusty Creek tephra of Glacier Peak	F
5,240	70	6,263–5,893	B207279	Osborn and others (2012)	Early neoglacial	C
5,260	70	6,263–5,907	B207260	Osborn and others (2012)	Early neoglacial	C
5,320	50	6,271–5,948	WW1112	This report	Charcoal above tephra set OP and layer BA	F
5,500–5,100		6,290–5,809		Beget (1984)	Dusty Creek tephra of Glacier Peak	F
5,650	110	6,715–6,218		Kovanen and others (2001)	Middle Fork lahar	G
5,670	60	6,628–6,315	WW3605	This report	Tephra layer BA	F
5,670	40	6,560–6,322	WW4216	This report	Tephra layer BA	F
5,680	40	6,618–6,349	WW4217	This report	Tephra layer BA	F
5,710	110	6,741–6,296	I18414	Kovanen and others (2001)	Middle Fork lahar	G
5,730	50	6,642–6,410	WW3604	This report	Tephra layer BA	F
5,730	170	6,957–6,192	AA22215	Kovanen and others (2001)	Minimum age of Rocky Creek ash (tephra set OP)	F
5,760	50	6,670–6,440	WW2403	This report	Contact between tephra set OP and layer BA	F
5,760	155	6,950–6,278		Hildreth and others (2003)	Tephra layer BA	F
5,785	55	6,719–6,450	AA22214	Kovanen and others (2001)	Maximum age of Rocky Creek ash (tephra set OP)	F
5,800	120	6,936–6,349	B56322	This report	Ridley Creek lahar	G
5,800	50	6,731–6,488	WW1459	This report	Tephra set OP	F
5,830	110	6,923–6,401		Hildreth and others (2003)	Tephra layer BA	F
5,850		6,719–6,642		Easterbrook and Burke (1972)	Advance of Boulder Glacier, earliest neoglaciation	C
5,860	60	6,826–6,499	WW1464	This report	Wood in tephra set OP	F
5,860	50	6,792–6,534	WW1870	This report	Middle Fork lahar	G
5,880	60	6,878–6,535	WW5730	This report	Middle Fork lahar	G
5,890	40	6,831–6,634	WW1977	This report	Middle Fork lahar	G
5,900	35	6,795–6,645	WW4219	This report	Park Creek lahar	G
5,920	40	6,853–6,658	WW1976	This report	Middle Fork lahar	G
5,930	50	6,889–6,656	WW1868	This report	Middle Fork lahar	G
5,930	50	6,889–6,656	WW1871	This report	Middle Fork lahar	G
5,930	50	6,889–6,656	WW2958	This report	Park Creek lahar	G
5,930	50	6,889–6,656	WW2959	This report	Park Creek lahar	G

^{14}C age (yr B.P.)	Error (years)	Calibrated 2σ age range (cal. yr B.P.)	Lab no.	Source	Event or unit dated	Chapter
5,935	40	6,880–6,668	WW4218	This report	Park Creek lahar	G
5,980	250	7,415–6,311	W2944	Hyde and Crandell (1978)	Middle Fork lahar	G
6,000		6,882–6,795		Ryder and Thompson (1986)	Later reference on beginning of neoglaciation	C
6,010	50	6,986–6,733	WW1460	This report	Tephra set OP	F
6,040	90	7,159–6,678		Mierendorf (1999)	Tephra layer BA	F
6,060	40	7,144–6,791	WW1973	This report	Tephra set OP	F
6,060	40	7,144–6,791	WW1974	This report	Tephra set OP	F
6,070	50	7,156–6,788	WW2960	This report	Park Creek lahar	G
6,120	60	7,169–6,800	B57709	This report	Park Creek lahar	G
6,135	30	7,158–6,952	WW6991	This report	Mhc_2 facies, Glacial Lake Baker	D
6,160	40	7,166–6,949	WW1975	This report	Tephra set OP	F
6,170	50	7,240–6,940	WW1458	This report	Tephra layer BA	F
6,170	250	7,562–6,495	W3224	Hyde and Crandell (1978)	Park Creek lahar	G
6,210	40	7,245–7,004		Burrows and others (2000)	Tephra layer BA	F
6,230	120	7,419–6,809	AA32092	Kovanen and others (2001)	Maximum age of Cathedral Crag ash (tephra layer BA)	F
6,545	50	7,566–7,332	AA32901	Kovanen and others (2001)	Maximum age of Cathedral Crag ash (tephra layer BA)	F
6,650	350	8,277–6,780	W2971	Hyde and Crandell (1978)	Park Creek lahar	G
6,730	40	7,667–7,513		Hallet and others (1997)	Mount Mazama tephra layer O	F
6,740	90	7,751–7,437	B56314	This report	Park Creek lahar	G
6,845	50	7,787–7,592		Bacon (1983)	Mount Mazama tephra layer O	F
		7,627±150		Zdanowicz and others (1999)	Mount Mazama tephra layer O	F
6,990	50	7,934–7,705	WW1978	This report	Older lahar, non-Mount Baker edifice	G
8,110	70	9,278–8,775	TO12444	J.J. Clague (written commun., 2009)	Tephra layer MY	F
8,130	80	9,395–8,774	TO12445	J.J. Clague (written commun., 2009)	Tephra layer MY	F
8,285	35	9,439–9,125	WW6465	This report	Soil between tephra set SP and layer MY	F
8,298	46	9,435–9,136	WW6111	This report	Soil above tephra layer MY	F
8,315	50	9,463–9,139	WW6464	This report	Soil between tephra set SP and layer MY	F
8,410	80	9,542–9,146	WW2962	This report	Schriebers Meadow lahar	G
8,420	70	9,537–9,283	AA22225	Thomas (1997)	Tephra set SC	F
8,450	40	9,533–9,423	WW1980	This report	Schriebers Meadow lahar	G
8,460	140	9,768–9,032	I18545	Thomas (1997)	Schriebers Meadow lahar	G
8,490	90	9,665–9,285	WW2964	This report	Schriebers Meadow lahar	G
8,500	70	9,600–9,314	WW2963	This report	Schriebers Meadow lahar	G
8,500	140	9,904–9,124	I18544	Thomas (1997)	Schriebers Meadow lahar	G
8,510	40	9,543–9,470	WW1981	This report	Schriebers Meadow lahar	G
8,655	35	9,686–9,541	WW4853	This report	Vhc facies, Glacial Lake Baker	D
8,700	1,000	12,749–7,792	WW*31	Burke (1972)	Boulder Creek assemblage	E
8,750	50	10,107–9,552	WW954	This report	Tephra set SC	F
8,830	50	10,156–9,698	WW1468	This report	Tephra set SC	F

^{14}C age (yr B.P.)	Error (years)	Calibrated 2σ age range (cal. yr B.P.)	Lab no.	Source	Event or unit dated	Chapter
8,850	50	10,168–9,710	WW1456	This report	Tephra set SC; minimum age of clastic assemblages	E
9,975	35	11,610–11,267	WW4852	This report	Forest bed, Glacial Lake Baker	D
9,985	35	11,614-11,271	WW6077	This report	Forest bed, Glacial Lake Baker	D
10,000		11,604–11,340		Stuiver and others (1995)	Minimum age for Cordilleran ice sheet re-advance; general age of forest bed in Glacial Lake Baker	D
10,205	50	12,110–11,715	WW5731	This report	Mu facies below forest bed in Glacial Lake Baker	D
10,350	300	12,730–11,210	W2972	Hyde and Crandell (1978)	Tephra set SP	F
10,355	50	12,406–12,010	WW5732	This report	Mu facies below forest bed in Glacial Lake Baker	D
10,510	50	12,644–12,173	WW1873	This report	Till of Sumas age	C
10,520	50	12,655–12,237	WW1874	This report	Till of Sumas age	C
10,550	40	12,640–12,415	WW4215	This report	Till of Sumas age	C
10,590	50	12,689–12,423	WW2404	This report	Tephra set SP (minimum age of Sumas till)	C
10,600	40	12,691–12,433	WW1872	This report	Till of Sumas age	C
10,720	50	12,729–12,580	WW1869	This report	Tephra set SP	F
10,870	80	12,971–12,671	WW2965	This report	Tephra set SP	F
10,901	68	12,956–12,692	WW3790	This report	Sulphur Creek assemblage (minimum age)	E
11,020	80	13,053–12,732	AA22226	Thomas (1997)	Sulphur Creek assemblage (minimum age)	E
11,020	180	13,256–12,656	WW3791	This report	Sulphur Creek assemblage (minimum age)	E
11,300	80	13,311–13,033		Clague and others (1997)	Later Sumas stade Cordilleran ice sheet re-advance	C
11,450	110	13,570–13,111		Osborne and others (2012)	Age of Pocket Lake	E
11,460	35	13,407–13,214	WW6462	This report	Tephra set SP	C
11,820	45	13,762–13,546	WW4088	This report	Sandy Creek beds and early Glacial Lake Baker	C
11,900	110	14,011–13,480		Clague and others (1997)	Early Sumas stade Cordilleran ice sheet re-advance	C
12,000		13,976–13,749		Dethier and others (1995)	Sumas stade, Cordilleran ice sheet re-advance in Fraser Lowland	C
12,200	45	14,241–13,951	WW4074	This report	Sandy Creek lacustrine beds, earliest age of Glacial Lake Baker	C
12,700		15,254–15,012		Dethier and others (1995)	Deglaciation in lower Skagit Valley	E
13,500		16,554–16,277		Dethier and others (1995)	Everson interstade type locality age	C
14,000		17,164–16,817		This report	Maximum age of clastic assemblages	E
14,450	90	17,895–17,358	CAMS21360	Porter and Swanson (1998)	Maximum Cordilleran ice sheet extent around Mount Baker	C
15,000		18,357–18,079		This report	Extrapolated date, volcano surrounded by Cordilleran ice sheet	C
16,000		19,470–19,182		Porter and Swanson (1998)	Cordilleran ice sheet crosses 49th parallel	C
16,333	60	19,941–19,528	B220961	This report	Maximum age for Vashon Drift, Mount Baker area	C
16,400	80	20,027–19,565		Riedel and others (2010)	Pre-Vashon Drift, Skagit River valley, Mount Baker area	D

^{14}C age (yr B.P.)	Error (years)	Calibrated 2σ age range (cal. yr B.P.)	Lab no.	Source	Event or unit dated	Chapter
16,425	50	20,019–19,615	WW5458	This report	Pre-Vashon Drift, Skagit River valley, Mount Baker area	C
16,545	45	20,147–19,760	WW5459	This report	Pre-Vashon Drift, Skagit River valley, Mount Baker area	C
17,570	90	21,540–20,930	B195976	Riedel and others (2010)	End of Evans Creek stade, Mount Baker area	C
17,600	130	21,686–20,892	B38907	Riedel (2007)	Port Moody interstade	C
18,000		21,953–21,632		Denton and Hughes (1981); Porter and Swanson (1998)	Global last glacial maximum	C
19,880	80	24,175–23,663		Riedel and others (2010)	Glacial Lake Concrete	C
21,800	240	26,612–25,628	GSC6009	Riedel (2007)	Glacial recession during Evans Creek stade	C
25,000		29,265–28,800		This report	Early Glacial Lake Concrete	C
25,160	140	29,565–28,837	UCI44540	Riedel and others (2010)	Ice advance, Evans Creek stade, Mount Baker area	C
30,000		34,237–33,855		Armstrong and others (1965)	Start of Fraser glaciation and Evans Creek stade	C

Appendix 4. Origin of the Name Chromatic Moraine

Austin Post, renowned aerial photographer of glaciers, revealed the origin of the present name of the Chromatic Moraine (on modern topographic maps) in email correspondence with J.H. Scurlock on June 2, 2009. See the history of Post's career by Scurlock (2007) and examples of his glacier photographs in Post and LaChapelle (1971). Post writes,

> My first knowledge of the name was from some early map—Mount Baker National Forest, most likely, although there was a small scale topo map that might have been the source.[1] At any rate the name was applied to varicolored ablation moraine on the stagnant ice in the bottom of the Glacier Creek valley portion of the glacier. I presume some turn-of-the century mountain climbers that had knowledge of glaciology and recognized moraine deposits, came up with this imaginative name to describe the feature.
>
> By the time I became active in the Forest Service and later USGS, this ice had melted and the moraine long gone. So, when the Survey drafted new topo maps of the area, I took advantage of this opportunity to up-date the place names obtained from various sources that were not shown on published maps. By this time, I had submitted upwards of ~30 place names in the North Cascades, generally obtained from miners' or mountain climbers' publications, such as nearby "Chowder Ridge" after the amusing fossil clam story.[2] At any rate, Chromatic Moraine was too good a name to let die along with the deposit it originally described, as the melting ice exposed a suitable colorful lateral moraine on the north side of the valley.[3] So, the name was transferred to this feature and was duly approved by the State and National place-name boards.

---

[1]Post probably refers to the 1:250,000-scale map published in 1915 by the U.S. Geological Survey; moraine name is not on that map.

[2]C.F. Easton, written commun., 1911–31.

[3]See figure 10, chapter C.

[Microprobe analyses by F.F. Foit, Jr., GeoAnalytical Laboratory, Washington State University. Standard deviations in parentheses. XRF, X-ray fluorescence; km, kilometer]

Tephra	Stratigraphy; sample no.	UTM[1]	SiO_2	Al_2O_3	Fe_2O_3	TiO_2	Na_2O	K_2O	MgO	CaO	Cl	MnO	P_2O_5	Total	No. of shards analyzed
YP[2]	Surface deposit dt-081105c	58480, 539622	68.56 (0.86)	15.10 (0.46)	2.07 (0.25)	0.89 (0.06)	4.25 (0.27)	4.34 (0.17)	0.80 (0.10)	2.07 (0.25)	0.08 (0.01)			100	13
YP	Surface deposit dt-090306a	580180, 540615	68.67 (1.30)	15.09 (0.80)	3.78 (0.28)	0.84 (0.06)	4.54 (0.26)	4.58 (0.44)	0.67 (0.18)	1.74 (0.58)	0.09 (0.02)			100	8
YP	Surface deposit dt-090306c	58280, 540542	69.32 (0.75)	14.81 (0.43)	3.66 (0.20)	0.83 (0.05)	4.44 (0.34)	4.85 (0.35)	0.58 (0.13)	1.43 (0.34)	0.08 (0.02)			100	15
YP	Surface deposit dt-031506	595890, 538976	68.61 (0.64)	14.89 (0.13)	3.92 (0.26)	0.89 (0.08)	4.53 (0.25)	4.75 (0.45)	0.74 (0.09)	1.60 (0.14)	0.07 (0.03)			100	7
BA	Unknown MB-511[3]	596690, 541275	68.42 (0.80)	15.10 (0.62)	3.70 (0.41)	0.83 (0.07)	4.90 (0.34)	4.66 (0.60)	0.55 (0.12)	1.76 (0.52)	0.07 (0.01)			100	20
BA	Unknown Sc4c[4] ejecta	Unknown	67.45 (1.38)	14.48 (1.06)	4.02 (0.05)	0.88 (0.10)	4.96 (0.62)	4.11 (0.60)	0.73 (0.18)	2.26 (0.66)				98.9	17
BA?	5.5 km north of Sherman Crater MB-651a[5]	587060, 540771	57.90	17.04	6.51	1.03	3.96	1.62	4.31	6.78				98.21	XRF lapillus
Grant Peak scoria	Mount Baker summit MB-430[5]	587120, 540329	59.74	17.36	5.86	0.90	3.56	1.55	4.32	5.93		0.12	0.26	1.79	XRF lapillus
Grant Peak scoria	Mount Baker summit MB-431[5]	587120, 540329	59.37	17.17	5.88	0.89	4.04	1.84	3.66	6.38		0.11	0.27	0.49	XRF lapillus
Grant Peak scoria	Mount Baker summit MB-432	587120, 540329	58.60	17.78	6.19	0.89	3.99	1.54	3.61	6.59		0.11	0.29	1.04	XRF lapillus
OP	Glacier Creek GC-1[5]	Unknown	68.28 (1.06)	15.39 (0.65)	3.91 (0.47)	0.78 (0.09)	4.44 (0.34)	3.90 (0.16)	0.85 (0.21)	2.33 (0.38)				99.9	16
SC(?)[6]	Pocket-Lake pl-0703-116	585150, 539593	58.20 (1.31)	14.52 (0.65)	9.85 (0.64)	2.16 (0.14)	4.29 (0.20)	2.25 (0.25)	2.92 (0.41)	5.75 (0.53)	0.06 (0.02)			100	18

Chemical Composition of Mount Baker Tephras.—Continued

Tephra	Stratigraphy; sample no.	UTM[1]	SiO_2	Al_2O_3	Fe_2O_3	TiO_2	Na_2O	K_2O	MgO	CaO	Cl	MnO	P_2O_5	Total	No. of shards analyzed
SC	Surface sample, road to Schriebers Meadow MB-442	588090, 539476	51.40	18.07	9.16	1.67	4.16	0.78	5.58	8.17		0.17	0.50	98.4	XRF lapillus
SC	Schriebers Meadow scoria cone CR-67	587180, 5394700	58.57	17.49	5.90	0.91	3.89	1.67	3.87	6.92		0.10	0.29	0.01	XRF spatter
SP(?)	Unit 3, RS–17 dt-091305t	587350, 539755	68.04 (1.91)	14.89 (0.69)	4.25 (0.8)	1.04 (0.16)	4.29 (0.62)	3.77 (1.01)	1.08 (0.28)	2.54 (1.01)	0.1 (0.03)			100	15
SP	Unit 3, RS–16 dt-092606a	58710, 5395300	66.85 (4.69)	14.49 (0.92)	5.51 (2.07)	1.24 (0.53)	4.37 (0.34)	3.46 (0.68)	1.07 (0.58)	2.92 (1.39)	0.09 (0.03)			100	20
SP	Unknown dt-091305t3	587350, 539755	67.68 (0.38)	14.91 (0.18)	5.00 (0.12)	1.13 (0.03)	4.42 (0.29)	3.89 (0.08)	0.84 (0.08)	2.05 (0.13)	0.08 (0.02)			100	18

[1]Universe Transverse Mercator (UTM) zone 10 grid coordinates give easting, northing.

[2]Tephra layer YP may contain a mix of glass compositions. Only glass with Mount Baker affinity is reported here.

[3]F.F. Foit, Jr., written commun., 2007.

[4]Kovanen and others (2001) data repository (correlations herein use our conventional terminology).

[5]XRF analyses (Hildreth and others, 2003, data repository).

[6]Pocket Lake sediment core, 2 kilometers northwest of Schriebers Meadow cinder cone. Composition is anomalously mafic and stratigraphically assigned to tephra set SC.

Appendix 6. Reports of Volcanic Activity at Sherman Crater and, where noted, Dorr Fumarole Field and Glacier Peak

Sources include Majors (1978), the many accounts in Easton (written commun., 1911–31), the U.S. Geological Survey's Cascades Volcano Observatory Mount Baker website (https://volcanoes.usgs.gov/volcanoes/baker/baker_geo_hist_115.html), Coombs (1939), Easterbrook (1975), Malone and Frank (1975), and Beckey (2003). See Whitney (1888), the United States part reprinted in the 9th edition of Encyclopedia Britannica, for events of 1854, 1858, and 1870. See appendix 7 for the original field notes of George Gibbs, a source for the description of the 1843 eruption(s) and the effects of subsequent lahar(s) in Boulder Creek.

1792

An account from Spanish exploration of the Strait of Juan de Fuca, June 12, 1792 (Kendrick, 1991):

> During the night we constantly saw light to the south and east of the mountain of Carmelo and even at times some bursts of flame, signs which left no doubt that there are volcanoes with strong eruptions in those mountains.

Interpretation.—The lack of any corresponding geologic evidence at Mount Baker indicates this account is the result of volcanic activity at Glacier Peak (note the location is described as "south and east of the mountain of Carmelo [Mount Baker]"). Beget (1982) reports eruptive activity at Glacier Peak, including magmatic ejecta, approximately 200–300 calendar years before present in age. Majors (1978) incorrectly attributed the activity to Mount Baker.

1810(?) and 1820(?)

Approximate dates for a possible eruption from memories of elderly Native Americans recorded later in the century (for example, Coleman, 1877; Majors, 1978; and F.G. Plummer, Tacoma Daily Ledger, February 28, 1893, cited by Majors, 1978). Eruption dates are based on gross over-estimations of the ages of the Native Americans; see parallel example in appendix 9.

Interpretation.—These and all similar reports refer to events of 1843 or later, based on the findings of this study where dates of events are verified by dendrochronology. See comments with interpretation of 1843 reports below. There exists no good evidence, either historical or geological, of any activity at Mount Baker before 1843 in the 19th century.

1842

There is a listing of an eruption by Plummer (1898, p. 27). However, there is no description and the eruption is not mentioned in Plummer's 1893 address to the Academy of Sciences.

Interpretation.—Possibly a report of the 1843 eruption.

1843

Gibbs (1873, p. 357–359) writes "…both on the authority of officers of the Hudson's Bay Company, and also of Indians, the eruption of 1843 was the first known…covered the whole country with ashes." and "The natives told a Mr. Yale, [Richard Yale, Chief Factor at Fort Langley] that the Skagit River was obstructed in its course [at its confluence with the Hukullum or Baker River], and all the fish died...the country was on fire for miles round." Two earthquakes at Fort Langley occurred "after" the eruption of Mount Baker. Gibbs reports, "The first was tremulous…but its greatest peculiarity was perhaps the loud report that preceded or attended it, and the roaring noise, which continued for some time" (p. 359).

Interpretation.—Certainly the same event that is recorded by George Gibbs in his handwritten field notebook of 1853–58, "Expedition up Skagit River" for July 28, 1858, on the overleaf of p. 57, where he recorded his observations from the confluence of the Baker and Skagit Rivers. Appendix 7 includes the complete field notes for July 28, 1858.

C.E. Finkboner describes, "Indians have a tradition that about thirty years ago [ca. 1837]…Mount Baker was an active, burning volcano. They could see the fire plainly, on dark nights; but about that time a tremendous convulsion took place, changing the whole aspect of the mountain, and killing most all the Salmon in the Skagit River…" (Pacific Tribune, March 26, 1867, cited by Majors, 1978).

In a letter dated February 15, 1844, and published by De Smet (1847), as reported by Majors (1978), 1843 is also reported as the year Mount St. Helens and Mount Baker "became volcanoes."

Interpretation.—The modern configuration of Sherman Crater was formed by the eruption that possibly caused the "loud report" and first earthquake at Fort Langley (72 kilometers north, 51 kilometers west of Mount Baker). That earthquake, however, because of its duration and reported timing "after the eruption" of Mount Baker, may

have recorded the later collapse of Sherman Crater that we date to have occurred in 1845–47, during which the main layer of tephra set YP was produced. E.T. Coleman (1877) reported a remarkably similar eruption as occurring in about 1810(?) that actually refers to this eruption, when he writes "…an old Indian told us that when he was a boy he recollected the mountain bursting out with a terrible fire and great smoke; that all the fish in the river [Skagit River] were poisoned, and that it was two years before they could catch any more…" The March 1867 account also refers to the 1843 eruption and the 1845–47 collapse. Likewise, we infer that an 1893 newspaper account by F.G. Plummer (Tacoma Daily Ledger, February 28, 1893, cited in Majors, 1978) of a Native American "tradition" that Mount Baker "…was formerly much higher and that a tremendous explosion threw down the entire south side…" also refers to the events at Sherman Crater in the 1840s.

1843 (dated herein as 1845–47)

The failure of "the entire south side" associated with reports of the above eruption.

Interpretation.—The east rim of Sherman Crater collapsed to form the Morovitz Creek lahar in Boulder, Park, Little Park, Morovitz, and Swift Creeks. It did not accompany the 1843 eruption, but occurred in 1845–47, based on geological evidence. This is probably an account of an actual event, later embellished as the collapse of the entire summit area that changed the profile of the stratocone as described below.

1846

From a newspaper clipping (Bellingham Herald, April 26, 1953), "An old history of British Columbia states that employees of the Hudson Bay Company saw an eruption of great force from Mount Baker in 1846." Furthermore, material "…flowed down the Boulder and Park Glaciers and left over a thousand acres of ashes and lava."

Interpretation.—Accurate report of the most probable year for the Morovitz Creek lahar (but not for the main explosive eruption of Sherman Crater), supposedly based on dendrochronology of tree scarring by the lahar. See text discussion of the Morovitz Creek lahar for our skepticism of this account occurring in 1846 and our determination of the age of the collapse and its lahar runout. An eruption in this year is also listed by Plummer (1898).

1850

From a newspaper account cited by Majors (1978), "Smoke issuing in dense masses from center of the summit." Additionally, the Oregon Spectator of March 21, 1850, reports "…both mounts, St. Helen and Baker, were sending forth volumes of smoke…"

Interpretation.—Possible emplacement of a minor layer of tephra set YP. The vent was probably Sherman Crater, but appeared to be from the main summit when Mount Baker is viewed from the south.

1852

Winthrop (1862, p. 47) writes that there were "…flame and smoke for several days." Williams (1913, p. 38, 280) writes, "There was an earthquake in October [felt in Victoria, B.C.]" and "They [from Vancouver Island] saw it blaze the winter before this journey of mine [1852–53]."

Interpretation.—Possible emplacement of a minor layer of tephra set YP.

1853

F.G. Plummer recounts a "long black streak. 1,000–2,000 ft in width" on Mount Baker's southwest slope (Tacoma Daily Ledger, February 28, 1893).

Interpretation.—Lahar from west side of Sherman Crater, onto Easton Glacier, perhaps produced by explosive ejection of debris over the west rim of the crater but also possibly the result of collapse of the crater rim.

January 1853

Plummer (1898) lists a "slight lava flow" and eruption.

Interpretation.—Possibly a lahar.

1853–54

"Mount Baker...has, during this winter, been in action, throwing out light clouds of smoke..." (Gibbs, 1855, p. 469).

Interpretation.—Probable cold-weather increase in visibility of gas emission.

1853

G. Davidson (1885), an engineer making triangulation measurements of Mount Baker, reports of the summit being suddenly obscured by "vast rolling masses of dense smoke, which in a few minutes reached an estimated height of two thousand feet"…followed by snow apparently "melted away for two or three thousand feet…" Eruption is also listed for August by Plummer (1898).

Interpretation.—Emplacement of a minor layer of tephra set YP; the "melting" probably represents the covering of snow with dark ash.

1854

In a handwritten note in the margin of his field notebook for January 21, 1954, G. Gibbs wrote "it [Mount Baker] has been smoking this winter" (p. 59).

Interpretation.—Probably the source and actual date of the 1853–54 observation above. We employ the same interpretation, that cold weather caused an increase in the visibility of gas emissions.

1856

"Tree-staining flood of about 1856," described by Stewart and Bodhaine (1961).

Interpretation.—Re-dated herein as 1843–50. Bright-colored "stain" inferred to have derived from 1843 tephra set YP.

A local newspaper reported, "…recently…a dense smoke had, for several weeks, completely shrouded the summit…" (Olympia Pioneer and Democrat, May 2, 1856).

Interpretation.—Probably clouds or a forest fire.

1858

In a newspaper cited by Majors (1978), the crater belched "fire and smoke" and "whole forests [were] swept away by descent of its rivers of burning lava" (The Northern Light, July 24, 1958). A Science article cites "night clouds…brilliantly illuminated" (Davidson, 1885). G. Gibbs writes, "at the foot of the mountain was a level plain two or three miles wide, of black volcanic rock and sand, upon which were vast piles of half burned timber" (Gibbs, 1873, p. 334). On his entry for July 28, 1858, in his handwritten field notebook no. II for "Expedition up Skagit River," Gibbs adds, "The country around [Boulder Creek fan] was a plain for 2 or 3 miles, level, perfectly bare of vegetation and composed of black rock and sand. They saw lava here and sulphur scattered around…[and] great piles of burnt timber seemingly swept by a current of lava (?) into this place." Gibbs' descriptions are based on the accounts of prospectors referred to as "Buffington's party." See appendix 7.

Interpretation.—Gibbs' report of the prospectors' trip up the Baker River to Boulder Creek and to the head of the Boulder Creek fan appears to mainly record widespread evidence of the large Morovitz Creek lahar that occurred 11–13 years before and would have still been relatively fresh. However, the fan surface locally "perfectly bare of vegetation" suggests recent occurrence of the second smaller lahar in Boulder Creek that followed the Morovitz Creek lahar. Gibbs (1873, p. 334) correctly deduced that the timber was more likely swept down by a water-mobilized flow than, as reported by the prospectors, lava. See Gibbs' field notes in appendix 7.

1859

November 25.—"Two large and bright jets of flame… as if issuing from separate fissures…seen but a few days" (Olympia Pioneer and Democrat, November 25, 1859).

December 3.—"Bright flashes as of lightening with report [sic] like heavy cannon," from the diary of J.G. Swan (cited by Majors, 1978) in University of Washington manuscript collection.

December 4.—J.G. Swan also writes of a "great cloud of smoke and steam" and that "others saw the flash last night and thought it was the steamer." The second quote refers to the sound of a steamboat exploding.

Eruption is listed in Plummer (1898).

Interpretation.—Possible continuing phreatomagmatic activity.

1860

"Mount Baker…smokes considerably, and occasionally shows a red light at night." (Commonwealth [newspaper from Des Moines, Iowa], reprinted in Scientific American, July 21, 1860).

"The passengers by steamer [to Victoria, B.C.]…on the 26th of November, reported [Mount Baker]…in a state of active eruption, puffing out large volumes of smoke, which upon breaking, rolled down the snow-covered sides of the mountain…" (Begg, 1894, p. 333).

Interpretation.—Continuing phreatic (?) activity.

December 26.—Reports of a "column of smoke" gave the "appearance of steamboat blowing off…steam" (Port Townsend Register, December 26, 1860; reprinted in the Olympia Pioneer and Democrat, December 28, 1860). Eruption listed in Plummer (1898).

Interpretation.—Continuation of November 1860 activity.

1863

July.—"…volcano is beyond all doubt in a state of eruption, the flames were plainly seen from Beacon Hill." (British Colonist, July 27, 1863, Victoria, B.C.).

Interpretation.—Continuing episodic phreatic and probably phreatomagmatic activity.

1864

October.—Reports of an "...earthquake shook the coast..." and "collapse of top 1,000–1,500 feet of summit, fell in, so that the appearance of the peak was decidedly altered as seen from Victoria, Vancouver Island, it being no longer conical and sharp…" (E.T. Coleman, Whatcom Reveille,

August 3, 1883, cited by Majors, 1978). Another adds, "…a large portion of the mountain having descended into the crater…top of Mount Baker, probably upwards of a mile in width, has entirely collapsed within the past week." (Victoria British Colonist, from the North Pacific Times; reprinted by Deseret News, December 21, 1864).

Interpretation.—False reports of summit collapse, refuted by contemporary observers, including G. Gibbs, in a letter to the editor of Science, and G. Davidson (1885, p. 262), who reported the 1854 eruption. An idealized woodcut by E.P. Bedwell from the Illustrated London News of 1862 (see Majors, 1978, p. 31) shows a sharply pointed summit; another Bedwell engraving, also pre-1864, shows the true, flattened profile more accurately, as well as Sherman Peak (see Majors, 1978, p. 29). Other pre-1864 renderings do not document any change in the summit profile.

1865

"It is asserted that the mountain has fallen one thousand or fifteen hundred feet, and that its summit, which was formerly a sharp point, is now much flattened. This peak has been for some time in a state of active eruption. Dense clouds of smoke have of late issued from it." (Portland Oregonian, April 18, 1865, and other newspaper reports cited by Brewer, 1865, p. 264).

Interpretation.—False report. See discussion above for 1864.

1867

March 30.—"Mount Baker is in active eruption... During the last twelve or fifteen days...dense volume of smoke...from southern peak near the summit..." (C.E. Finkboner, Pacific Tribune, March 30, 1867, as quoted by Coleman, 1877).

October 1.—"There is great excitement at Victoria over the supposed volcanic eruption, sixty-five miles distant, in the Cascade Range" (New York Times, October 1, 1867).

Interpretation.—"Clear, cold northerly winds" during this time period suggest atmospheric effects rather than an eruption.

1867–72

"...Mount Baker...has, since 1867, suffered loss of height and change of form..." (newspaper report cited by Majors, 1978).

Interpretation.—False report, originally from 1864 and 1865.

1868

First Mount Baker summit climbers report that Sherman Crater is clear of snow (Coleman, 1869, p. 793).

1870

Eruption reported as similar to that of 1854 by the same observer, G. Davidson (1885).

Interpretation.—Unlikely an eruption; this report was doubted by contemporaries, unlike his 1854 report.

September 1880–January 1881

September 7.—One account reports a "…violent eruption, flames streaming up from the summit and large volumes of smoke…" (Washington Standard [Olympia], September 17, 1880, cited by Majors, 1978).

November 27.—More than two months later, a newspaper correspondent in northern Whatcom County (including Mount Baker) reported "…fire shot up far above the mountain top" and "…bright flashes and huge red sparks" were seen at 3 a.m. (Morning Oregonian, November 27, 1880, cited by Majors, 1978).

December 13.—"…Mount Baker has been in eruption, and…a sharp shock of earthquake was felt last evening" (New York Times, December 13, 1880).

January 24.—"…Mount Baker is in a state of active eruption, and is throwing out clouds of smoke and ashes" (New York Times, January 31, 1881).

Report from March 20, 1881, which originated from the San Francisco dispatch, reports "streams of fire" seen at night, probably from Mount Baker.

Interpretation.—Last accounts of eruptive activity with possible incandescent ejecta.

Post-1881

Many reports only of steam emissions.

1884

On the northeast flank of Mount Baker, "a steaming crater" was reported by W.H. Dorr (C.F. Easton, written commun., 1911–31).

Interpretation.—First report of Dorr Fumarole Field indicates a level of activity similar to later reports and probably to that of the present.

1884

No reports of eruptive activity other than steam emissions after this year (Beckey, 2003).

1891

Sherman Crater was "...filled with snow except in the center, where there is a circular opening about fifty

feet in diameter, from which steam and sulphurous vapors are constantly escaping" (E.S. Ingraham, Seattle Post-Intelligencer, September 5, 1891, p. 5).

Interpretation.—Establishes a limiting date for the end of significant activity at Sherman Crater in the 19th century. Note the contrast with the 1868 report from Mount Baker summit climbers.

1892

J. Morovits reported in a 1908 newspaper that the central ice pit had shifted 900 feet west of its position in this year. Morovits first climbed Mount Baker in 1892.

Interpretation.—Morovits was possibly misoriented (uncharacteristically) and was viewing a second ice pit.

Post-1892

Many reports of steam emissions. A 1900 photograph described by Frank and others (1977) shows mainly an ice-filled crater with an "ice pit."

Interpretation.—Continuing thermal emissions.

March 1897

"Smoke curling upward in great quantity…in regular puffs…" (New York Times, March 16, 1897).

Interpretation.—Continuing thermal emissions.

March 1900

"Tremendous upheaval of earth and rocks ten miles west of the snow-capped peak…Genuine eruption…likely to burst out anew as a volcano…Great fissures were opened…in valley of the Nooksack…a huge mound of earth, seventy feet high and a quarter of a mile long, was raised across the valley. The stream was dammed and rose to a considerable height, forming a lake before breaking through. The earth trembled and there was a rumbling noise lasting several minutes [heard in Hamilton, Wash.]" (New York Times, April 7, 1900, in reference to March 27, 1900).

Interpretation.—Landslide and landslide dam of the Nooksack River occurred on March 27, 1900, probably in the South Fork Nooksack River valley (based on a report from Hamilton, Wash., located 10 kilometers south of that drainage, on the floodplain of the Skagit River). Report describes the location as 10 miles from Hamilton, without relation to Mount Baker.

September 1900

Climbing party guided by J. Morovits reports the crater was filled with snow and ice except for an "orifice in the snow, about thirty feet in diameter…" with sulphur "crustations" and thick vapor rising 1,000 feet (San Francisco Call; September 2, 1900).

Interpretation.—Continuing thermal emissions.

September 1903

Report of a large volume of black smoke rising from a fumarole in ice that filled Sherman Crater (Rusk, 1978).

Interpretation.—Continuing fumarolic activity.

1906

During the Mazamas trip of 1906 (reported in Recreation Magazine in May 1907), steam jets issued from myriad vents from Sherman Crater with great violence. There were "2 acres with hundreds of vents from which steam is constantly escaping" (Landes, 1907).

Interpretation.—Continuing fumarolic activity.

Debris avalanche into Sherman Crater noted by Adams (1919) from the report by Easton (written commun., 1911–31). May be the last example known before the sequence of activity that began in 1958, reported by Frank and others (1975), on the surface of Boulder Glacier (see 1958–73). Frank and others (1975) note that an undated photograph published in 1930 (p. 16 of McNeil, 1930) may show debris avalanche detritus on Boulder Glacier.

Easton often lectured on the occurrence of an avalanche on April 18, 1906, that he witnessed while viewing Mount Baker with a telescope at the time of the San Francisco earthquake. He described it as from the west side of Mount Baker, of ice (and presumably rock) from a wedge-shaped area 150 to 250 feet deep and 3,000 feet wide, "stripping the mountain bare" (Sholes, 1920). He attributed the avalanche to the earthquake and reported a Sherman Crater that was filled with ice and rocks on his next visit after 1906. He also reported in many venues that Sherman Peak had "sunk" 500 feet in height after 1867, because he mistakenly believed that it and the main summit, Grant Peak, were reported by Coleman (1869) as being the same height, from observations made during the first ascent. Later investigators note that Coleman was actually comparing two elevations on the main peak. While Easton was lecturing on "his scientific investigations" on this subject to the Mazamas at their 1909 camp on the mountain, they conceived the idea of naming their newly discovered glacier after him (Sholes, 1920).

Interpretation.—C.F. Easton's observations were often fanciful.

1907

Extent of Dorr Fumarole Field described (Landes, 1907).

Interpretation.—Frank and others (1977) compared the 1907 report to conditions in 1975–76 and noted similarity in emissions at the Dorr Fumarole Field, at the time when activity at Sherman Crater had greatly increased.

1908

Photograph of Sherman Crater by A. Curtis (fig. 4 in Frank and others, 1977) showing "ice pit" approximately in the same position as in an 1891 photograph by W.A. Amsden, the Bellingham photographer who, with H. Clark, took the first summit photographs (Majors, 1978). Frank and others (1977, fig. 4 caption) note that the "pit" is the same that was reported as emitting sulphurous vapors in the 1890s (see description for 1891 above). It is probably the modern Sulphur Cone fumarole.

Interpretation.—Approximately static conditions persisted between 1891 to at least 1908. No reports of significant activity in this period.

1909–14

Photographs from 1909 and 1914 show west-rim fumaroles and hot ground (figs. 5 and 6 of Frank and others, 1977). A photograph in Easton (written commun., 1911–31) from ca. 1910 shows an ice-filled crater with "ice pit" near the lowest point of the crater rim, known as "East Breach."

Interpretation.—Continuing fumarolic activity.

Circa 1940–75

Oblique aerial photographs from the 1930s, vertical photographs from beginning in 1940 taken during late summer, as well as an infrared survey (1972) and field surveys document a progressive increase in snow-free and geothermally heated ground at Sherman Crater (Frank and others, 1977).

Interpretation.—Frank and others (1977) note that this occurred during the post-1940 period, when climate change (characterized by cooler temperatures and more precipitation in the Pacific Northwest) would have caused a decrease in snow-free conditions and less visible geothermally heated ground.

1958–1973

Six debris avalanches were reported on the surface of Boulder Glacier, the largest in 1973, by Frank and others (1975). They also note the previous occurrence of a debris avalanche into Sherman Crater in 1906 (see description for that year) and photographs of flows predating and apparently identical to the recent examples (McNeil, 1930).

Interpretation.—Interpreted as geothermally induced by Frank and others (1975), and thus as evidence for an increase in heat flux prior to 1975.

1971

Newspapers report Mount Baker as "steaming away" or "steamed up" beginning on March 1, 1971 (Majors, 1978).

1975–76

Comprehensive descriptions and interpretations of increased thermal activity in Sherman Crater first reported on March 10, 1975 (Frank and others, 1977; Malone, 1977, Rosenfeld, 1977). Speculation of an imminent eruption ("Is Mount Baker about to blow its top?," Bellingham Herald, March 16, 1975).

2000

"General migration of activity to the west and northwest side of the [Sherman] crater over the past 10 years." (S.D. Malone, written commun., 2003).

Interpretation.—Possible increased future risk of lahars into Sulphur and Rocky Creeks.

Appendix 7. Notes by George Gibbs on July 28, 1858, in his Field Notebook "Expedition up Skagit River" (starting on p. 57), with Annotations

July 28, Wednesday.—River extremely rapid and during the morning made but about 5 miles as estimated. The few Indians we have met seem very poor. The salmon have not come in abundance and their potatoes are not ripe. In the afternoon passed through a very narrow gorge [The Dalles] above which is the first strong rapid. We reached and passed the…, or as our Indians pronounced it, Hŭ-Kúll-um [Baker River], at the mouth of which is the Ima-léh-hu village. This point is about south of Mt Baker.

The Imalehu [referring to the Baker River] is the branch ascended by Buffington's party [prospectors]. No Whiteman as we were assured by the Indians having ever ascended the main river to a point above this. The branch [Baker River] heads in Mt Baker itself, as ascertained by the prospecting party. They state that about a mile above the mouth of the stream [it] is cañoned and not over 50 feet wide. There is a fall of about 15 feet where it is still narrower. They ascended as they think 25 or 30 miles, traveling 2 days. The foot of the mountain is about 15 miles. Some 8 miles below the base they left the main stream and took a smaller lefthand fork [Boulder Creek], wh. they followed to within 2 or 3 miles of the snow as they saw the water coming out of it [probably to the head of Boulder Creek fan]. The country around was a plain for 2 or 3 miles, level, perfectly bare of vegetation and composed of black rock [andesite] and sand [the surface of Boulder Creek fan]. They saw lava here and sulphur scattered round. There was no ashes and no appearance of a glacier. There were in the plain great piles of burnt timber, seemingly swept by a current of lava [the Morovitz Creek lahar and possibly the younger lahar in Boulder Creek] into their place. They saw smoke or steam ascending from the mountain on eastern [south] side about 2/3 the way up the snow [Sherman Crater].

The Indians remember an eruption undoubtedly that referred to by Mr. Yale [Chief Factor at Fort Langley]. The story they told that they were then living at the foot of the mountain and that a great number of them were killed. The country was on fire for miles around. The survivors crossed the river and went up the mountain. I think however this is incorrect, for others told me that the fish in the Skagit river were destroyed. They said also that they had seen fire and smoke from the mountain but no ashes or stones. I gathered on the bar at the mouth of the Imalehu specimens of trachyte [Mount Baker andesite] and noticed the same below that point on the main River, but saw none above [in the Skagit River above the confluence with the Baker River].

The Imalehu seems to be about 100 yds wide above the gravelly delta over which it spreads at the mouth. The water is whitish and very different in appearance from that of the Skagit. Camped on island, left bank.

Appendix 8. The 19th-Century Flood History of the Skagit River, Interpreted with Events of the Sherman Crater Eruptive Period

History of "Great Floods"—Were Any Related to Volcanic Activity?

This section interprets the 19th-century history of so-called "great floods" by re-evaluating the Native American and pioneer accounts on which they were based and adding evidence from volcanic activity of the Sherman Crater eruptive period (1843 to present). Was the largest historical flood on the Skagit River the indirect result of volcanic activity, and, thus, does the presence of two active volcanoes (including Glacier Peak) in the watershed increase the potential for future catastrophic flooding? Could a pre-settlement "great flood" have been caused by or associated with the failure of a natural dam that originated as either a lahar from Mount Baker or a landslide in the Baker River valley? These and other questions about early, apparently huge floods in the 8,030-square-kilometer (km^2) (3,100-square-mile, mi^2) watershed have been raised by citizens that are concerned with whether the expenditures and strategies for flood control are adequate and if the conditions leading to those early floods can recur. We seek to provide some useful answers in this appendix.

Historical flood peaks in the Skagit River basin were first determined by J.E. Stewart, who compiled the flood history as a hydraulic engineer with the U.S. Geological Survey from about 1915 to 1923. The information compiled by this pioneer paleohydrologist (Costa, 1986) is summarized by G.L. Bodhaine (Stewart and Bodhaine, 1961). The 1961 summary followed a series of unpublished evaluations during the 1950s that focused on hydraulic analysis and recommended changes in the discharges determined by Stewart. Stewart's investigations are recorded in greater detail in field notes from 1922–23 and in unpublished reports from 1918, 1923, 1929, and after 1932. Most of the information on the "great floods" is in three unpublished reports from 1918 and 1923: (1) "Skagit River flood report," 11 p. (J.E. Stewart, U.S. Geological Survey, 1918); (2) "Floods in Skagit River basin, Washington," 120 p. (J.E. Stewart, U.S. Geological Survey, 1923); and (3) "Stage and volume of past floods in Skagit Valley and advisable protective measures prior to the construction of permanent flood controlling works," 29 p. (J.E. Stewart, U.S. Geological Survey, November 1923). The information in all his reports, notes, and letters is also unpublished other than as edited in the 1961 summary; those accounts are cited here as direct quotations from Stewart and his correspondents (where we can deduce them from archival information).

Stewart and Bodhaine (1961) summarized the 19th-century flood history from The Dalles, a bedrock-walled reach 3 kilometers (km) downstream from the confluence of the Baker and Skagit Rivers (the modern gaging station, "Skagit River near Concrete"), as follows:

1. 1815—Highest flood discharge of 500,000 cubic feet per second (ft^3/s), termed the "Indian-legend flood" of about 1815.
2. 1856—Second highest flood discharge of 350,000 ft^3/s, termed the "tree-staining flood of 1856."
3. 1897—Highest flood of the post-settlement period; discharge estimated at 275,000 ft^3/s.

Discharges for the 1815 and 1856 floods are downgraded to estimates in the present compilation of peak-flow data by the U.S. Geological Survey. Stewart based their heights on the height of a flood sand just upstream from The Dalles and on a high-water mark on the bedrock canyon wall at The Dalles, respectively.

Stewart assigned the "1815" flood various dates at various times as described here.

1814.—This year was reported in a letter from Stewart to T.H. Judd, August 22, 1923. In each of the eight typed references to the date, the date of 1814 can be seen to have been added once another date was erased after the letter was initially prepared. The year of "about 1814 (within 10 years either way)" was stated in a letter from Stewart to Frank Davis, July 6, 1923.

1815.—Stewart and Bodhaine (1961) described the "flood of legend" as having occurred "about 1815" simply from "stories which were told by the Indians" (table 8.1). Originally, Stewart (written commun., 1923) described the year 1815 as the mean of the probable range of dates (1805–25) estimated from the ages of Native Americans. He believed it was confirmed by "the size of the unmarked spruce trees" described by early settlers as less than 1.5 feet (ft) (J.E. Stewart, written commun., 1923, p. 7) or 2.5 ft (J.E. Stewart, written commun., 1918, p. 8) in diameter. The smaller of these diameters was the size intended.

1820.—Stewart's 1918 report recorded observations from Joseph Hart (1852–1933), an Englishman who settled, living with and learning from Native Americans, on the north side of the Skagit River, 1.6 km south of the present center of Sedro Woolley (Bourasaw, 2003, and oral commun., 2009). Hart arrived in August 1878 (table 8.1).

1856.—The "tree-staining flood of about 1856" was thought by Stewart and Bodhaine (1961) to be younger than the "great flood" of ca. 1815–20. That both may represent a single flood was first indicated by a handwritten note on the cover of Stewart's 1918 report. The note from an unknown reviewer—"H.E.B.," whose identity remains unknown in U.S. Geological Survey records and recollections of personnel from the era)—addressed to "G.L.B." (G.L. Bodhaine) probably in the 1950s reads, "I believe all references to 1820 flood in this draft for Sedro Woolley and Concrete are for 1856 flood in later reports."

This assertion is identical to the conclusion reached here, probably after review of the same archival material that we examined. The note is credible because of the practice of the U.S. Geological Survey of internal peer review before publication. The specific year of 1856 is based on dendrochronology in 1923, discussed and reassessed below, but the year is otherwise undefined (other than by boyhood recollections of Native Americans described in table 8.1). There was no permanent settlement at that time on the mainland, although settlers had arrived on Fidalgo Island near the Skagit River delta ca. 1855–56 (Dwelley, 1953).

December 4, 1861.—This specific day is from Stewart's field notes ("flood notes") of September 16, 1922, at Reflector Bar, 37 km upstream from the confluence of the Baker and Skagit Rivers. Stewart notes that the rapid "dimming" of recent flood marks[1] (although not reported from upstream locations), and observations at this location lead to his "assumption that the great flood was that of December 4, 1861." He adds, "The old Indian who told Hart in 1879 and others in Sedro Woolley that the flood was when he was a boy either referred to another flood or they did not understand him."

Stewart's source for that specific day is almost certainly the date of the regional flood recorded in Oregon by annual peak flows from the Willamette River at Salem (sta. no. 14191000) and the Willamette River near Albany (sta. no. 14174000), which extend back to December 4, 1861 (M.C. Mastin, written commun., 2009). The flood of that date (December 4, 1861) is the first flood recorded in Washington and Oregon; it is also the peak of record for both sites.

Was There More Than One 19th-Century "Great Flood"?

To both J. Hart's and J.E. Stewart's assumptions can be added the possibility that the Native Americans were simply not as old as originally assumed. Between 29 and 35 years elapsed between the time of the first Hart account (table 8.1) and the most probable date of what here is determined as the only substantiated "great flood" (occurring between 1843 and 1850, as defined below). This is plenty of time for young Native Americans to become "old" in an era of famine and introduced disease. This time interval is also sufficient to explain why young spruce trees were not marked or stained by a flood when Hart recalled memories from 1879, as reported by Stewart (written commun., 1918).

To indicate that the Native American of the first Hart account of 1879–80 probably describes the flood dated herein as 1843–50 and not any earlier flood, we propose an analogy to the report by E.T. Coleman describing his first attempt to climb Mount Baker in 1866, from another "old Indian" (Coleman, 1877). Coleman's report was of an eruption of Mount Baker that occurred when the Native American was a boy, estimated to be about 1810 on the basis of his assumed age by Majors (1978). That eruption is documented herein as occurring in 1843, 23 years before the assumed 1866. Thus, "… the one big flood the Indians tell about" (Hart's 1923 account; table 8.1) logically identifies the 1843–50 "tree-staining" flood.

Stewart later identified the (one) great flood as having occurred in 1856 or even on a single day, December 4, 1861, even after recording the Hart accounts on which the 1815 and 1820 dates were based. The dates of two "great floods" (1815–20 and 1856) are based on the extrapolated memories of different Native Americans—that is, no single recollection is of two large floods. A person remembering a flood of ca. 1815–20 in 1880–81 could be expected to remember a comparable flood from 1856 (or 1843–50, as dated below).

No credible evidence or any recorded oral history survives of flooding that occurred in the early 19th century, referring to the record before ca. 1840. Nevertheless, Stewart (written commun., 1923) did recognize earlier floods "approximately as large" as the assumed 1815 flood on the basis of stratigraphy consisting of interbedded flood sand and "ground surface material" at Reflector Bar. The highest sand layer there was interpreted as the deposit of a flood not exceeded "for thousands of years." At The Dalles, the assumed 1815 flood was interpreted as not exceeded "in thousands of years" based on the lack of any higher flood sand than the one attributed to that flood.

19th-Century "Great Flood(s)" Possibly Related to a Natural-Dam Failure

The initial evidence for the origin of the "great flood" as the breakout from a natural dam comes from Hart's and Stewart's retellings that it came "very quick." Nevertheless, both Hart, in his 1896 pre-Stewart account, and Stewart (written commun., 1918, p. 10–11) attribute this rapid rise to snowmelt with a "Chinook" wind. Other evidence of "sudden arrival" not mentioned by Stewart is the Devin account from the Skagit County Times (November 19, 1896) that suggests a landslide-dam failure near the mouth of the Baker River close to the present site of Lower Baker Dam (table 8.1). A series of "mudslides" destroyed part of the dam powerhouse near the assumed site of the natural dam in 1965. However, our field work has not revealed any evidence of a large landslide-dam failure or of a paleoflood at and downstream from the possible blockage location. The dam and reservoir could obscure the evidence of a blockage but not the paleohydrologic evidence of a huge recent discharge below the blockage. The downstream Baker River gorge was first traversed in July 1858 by a party of prospectors, as reported by George Gibbs (appendix 7). The prospectors' trip is

[1]We use, as did Stewart, the term "flood marks" to refer to mud coatings deposited by large floods. He also used the term for high-water lines on a rock wall, flood sand, and silt deposits on leaves and grass. Hydrologists use these marks to determine the cross sections of peak flow that, if combined with estimates of velocity, yield indirect measurements of flood discharge.

Table 8.1. Selected Native American and pioneer accounts of 19th-century floods in the Skagit River.

Source	Account	Original interpretation
Joseph Hart and other settlers, 1879	One "old [Sedro Woolley] Indian" said that when he was a boy (about 10 years old), stains on trees were made by "a very quick and terrible flood…one winter night" and that there were "traditions handed down of drownings." Source: J.E. Stewart (written commun., 1923); similar account provided by J.E. Stewart (written commun., 1918).	Flood of about 1815 (median age based on range of assumed age of 1805–25); staining also ascribed to 1856 flood (J.E. Stewart, written commun., 1923, p. 7–8).
Joseph Hart, ca. 1896	Shortly after the flood of 1880, two Native Americans [later perished of smallpox] took Hart "to a tree nearby [on "Skiyou Island"] and directed my attention to a water mark at least six feet higher than the present freshest [reference to a spring flood]." No mention of a rapid rise. Source: Skagit County Times (November 19, 1896).	Hart noted, from the account of the Native Americans, that the flood resulted from an early winter snowpack followed by a "Chinook" wind.
Joseph Hart, ca. 1918	"Some of the oldest Indians, judged to be about seventy years of age [said in 1879] when they were small boys a big water came very quick…Mr. Hart estimated at the time, from the age of the Indians, that this flood must have occurred about sixty years previous to 1879." Source: J.E. Stewart (written commun., 1918).	Flood of about 1820, "confirmed by my [Stewart's] study at Reflector Bar and by young spruce trees which did not have a high-water mark in 1879" (J.E. Stewart, written commun., 1918)
Joseph Hart, 1923 (in letter to J.E. Stewart)	"…the one great flood the Indians tell about." Source: personal letter to J.E. Stewart, June 21, 1923.	Did not alter Stewart's interpretation of two "great floods."
Anonymous ("one white man"), 1909	Johny Towne ("old Sauk Indian") told of a flood "much higher than that of 1909 when he was a boy." He was considered to be about 70 years old. Source: J.E. Stewart (written commun., 1923) and J.E. Stewart's field journal of 1922–23 for January 28, 1923.	Flood in 1856 (J.E. Stewart, written commun., 1923, p. 12). The year 1856 is based on dendrochronology.
James Cochraham, 1923	"Old Indian thought to be 90 years old" in 1923 did not remember a flood that drowned Native Americans, but that when he was young, he had known Native Americans who remembered such a flood. Source: J.E. Stewart (written commun., 1923).	Rapid rise as evidence for possible failure of a natural dam.
H.L. Devin, 1896	Devin recalls, "…was some years ago…surveying in the…vicinity of [natural] Baker Lake [probably for hatchery built in 1896]. … in an Indian camp, he was told…of a great flood. They said that about 60 years ago a great slide had choked up the narrow outlet of the Baker valley…until the whole valley was an immense lake, full 80 feet deep. By this time the imprisoned waters had burst through the dam and…precipitated into the Skagit flooding the whole valley. The water marks still plainly visible up the sides of Baker valley and…upon the trees as you come down the Skagit would indicate that this was the real cause of that terrible disaster [as opposed to snowmelt origin]." Source: Skagit County Times (November 19, 1896).	Legend leading to origin of "great flood" interpreted as from failure of a landslide dam. Legend possible but unlikely because of evidence of flood origins in the upper Skagit River drainage. Possible origin of account was a relatively small breaching of the lahar blockage of natural Baker Lake after the lahar of 1845–47 (see section on lahars, chapter G).
Native American tradition, 1820	"…that a number of their tribe were drowned, in a great flood at night…" near the confluence of the Skagit and Sauk Rivers, "probably the great flood previously noted at Reflector Bar [based on flood sand]." Source: J.E. Stewart (written commun., 1918, p. 5–6).	Stewart apparently believed the account was of the "great flood" until dating it as December 4, 1861 (see text). Possible source of reports of rapid rise caused by that flood at Sedro Woolley downstream (both accounts "at night").
Mox Tatlem (Native American)	When he was age 10 (estimated to be in 1811), "there came a winter of great snow, December, January and into February…then came rains and floods…and a great slide filled Diablo Canyon, damming the river. When this broke a great flood raced down the river—ice, logs, and debris—a solid wall of death forty feet high." Source: account via a "medicine man" (D. Buller, Concrete Herald, March 5, 12, and 19, 1936).	"True tale" postdating era of Hart and Stewart; probable version of previous accounts from Stewart (written commun., 1918) and Cochrawham (J.E. Stewart, written commun., 1923 and November 1923).

reported elsewhere (Concrete Herald, June 21, 1951) and the two groups apparently met in the area before Gibbs continued up the Skagit River. The prospectors described a 50-ft-wide gorge and a 15-ft "fall" about a mile above the confluence of the Baker and Skagit Rivers, close to the modern dam site and possible natural-dam location.

A "great flood" origin in the Skagit River caused by natural-dam failure in the Baker River is unsupported by evidence; it is contradicted by Stewart's correlations of paleo-hydrologic evidence ascribed to the 1815 and 1856 floods at locations in the Skagit River upstream of its confluence with the Baker River. In the following section, a possible 19th-century breaching of the 1845–47 lahar-blockage that impounded natural Baker Lake is described. This is the logical source of the Devin account (table 8.1), especially in light of the fact that the Native Americans reporting to Devin lived on the shore of that lake.

A final possibility of "great-flood" origin from a breached natural dam is from a Native American believed to have been born around 1811, 125 years before the account in table 8.1, described as from his son and as interpreted by a "medicine man" (D. Buller, Concrete Herald, March 5, 12, and 19, 1936). The location, Diablo Canyon, is the present site of Diablo Dam in the Skagit River headwaters. This account could correlate with the "tradition among the Indians," reported by Stewart (written commun., 1918, p. 5–6), that "a great number of their tribe were drowned, in a great flood at night…" on a terrace near the Skagit and Sauk River confluence (upstream from the Baker-Skagit River confluence). In apparently attempting to reconcile the legends with the lack of evidence of a former natural dam, Stewart noted in a letter to Frank Davis on May 23, 1923, "It may be that at some time an enormous snow slide dammed the canyon [upstream of] Reflector Bar, and then broke loose. Such an occurrence would check with the old Indian tradition of a flood about 1820 that came unexpectedly in the night and so quick they hardly escaped…"

Lahar Blockage of Natural Baker Lake in the Sherman Crater Eruptive Period

A possible origin of the lake-blockage failure in the Devin account (table 8.1) is a relatively small-scale failure of the blockage of natural Baker Lake. The sources of the account were Native Americans living on the shore of that lake. The original blockage of natural Lake Baker was formed by the largest Park Creek lahar in the middle Holocene. The blockage and the level of the lake were raised in 1845–47 when the east side of Sherman Crater collapsed and yielded branches of the Morovitz Creek lahar down Boulder, Park, Morovitz, and Swift Creeks into the Baker River valley (fig. 50). Although that mobile, multibranched flow raised the level of the lake, impoundment of an 80-ft (24-meter, m) depth of water in the Devin account is not possible. Figure 50 includes a cross section of the blockage showing the 12 ft (3.7 m) rise in lake level reported by pioneer Joseph Morovits (see appendix 9). An early 20th-century bathymetric survey of the lake (Darwin, 1921) reported a surprisingly large maximum depth of 116.5 ft (35.5 m). Based on reconstruction of the lake-bottom profile from that survey, the 2.9-km^2 lake can be estimated to have had a total volume of approximately 50,000,000 cubic meters (m^3). Morovits estimated that a subsequent fall in lake level of 4 feet (1.2 m) occurred by the time he first saw the lake in 1891. That decline could reflect the reported natural-dam breaching. If so, the total maximum volume released was less than 2,700,000 m^3. This volume, the evidence of the flood(s) in the Skagit River valley upstream of the Baker River confluence, and the material forming the blockage—cohesive lahar deposits of relatively low erodibility (indicating gradual breach incision)—indicate that a surge from Baker Lake did not alone account for a "great flood" in the Skagit River.[2]

Native American accounts of the Skagit River being dammed by ash from the 1843 eruption of Sherman Crater (tables 8.1, 8.2) may have been related to the necessarily small dam that could have been formed if the Morovitz Creek lahar extended to the confluence of the Baker and Skagit Rivers in 1845–47. Entrained tephra set YP washed to the confluence also could not have formed a significant blockage, and neither of these deposits could have formed a blockage that with failure conceivably could have yielded a "great flood." Detailed examination by boat of the deposits in the bank of the Skagit River opposite the mouth of the Baker River reveals no stratigraphic evidence of a significant blockage. Tephra set YP does, however, explain the "tree-staining" character of a middle-19th-century "great flood."

[2]M.C. Mastin (written commun., 2009) estimates the discharge based on a breach over one hour (a logical duration of a rapid or sudden breach) as "…[an] average of 26,500 ft^3/s, or about a 2.5 ft change in stage at Skagit River near Concrete [The Dalles] during extreme flood conditions (273,500 to 300,000 ft^3/s) assuming steadily-rising conditions—not a flood wave." An increase of 2.5 feet at The Dalles, a bedrock-walled reach, would occur over a relatively small channel width, whereas downstream the increase would be spread across a flood plain several kilometers in width and would not increase stage sufficiently to create, by itself, a significantly more noteworthy flood. Mastin's analysis deals with association of the dam breaching with a large regional flood.

Table 8.2. Revisions of dates and origins for proposed 19th-century "great floods" in the Skagit River and the tributary Baker River.

[See text and table 8.1 for explanation of sources]

Flood and assumed date	Original evidence for date	Reason(s) for revision
"Indian legend flood of about 1815"	The 1879 Hart report (table 8.1) of Native American(s) who remembered that, when they were children, a "big water" came "very quick."	Age of the Native American is greatly overestimated, leading to a date of the flood ca. 60–65 years too early (another remarkably similar account ascribes excessive age to "old" Native Americans).
		No individual recalled two floods, but if they recalled a flood in 1815, they would have also recalled the "1856 tree-staining flood." The logical inference is that the "1856" flood was the source of this account and, thus, that there are no accounts of an early-19th-century flood, either because no "great flood" occurred or that no oral history survived.
		No credible report of a "great flood" can be linked to the period before ca. 1840. In 1923, Hart refers to "the one big flood the Indians tell about," believed here to be the "tree-staining flood of 1856."
"Tree-staining flood of 1856"	Stewart (written commun., 1923), and in his field journal, records that a Native American said during the 1909 flood that when he [the Native American] was a boy, he saw the river even higher.	This flood is interpreted as the single "great flood" of the middle 19th century, confined to the period between 1843 and 1850.
	The flood deposited coatings of distinctive fine-grained sediment on cedar trees in downstream reaches (below the confluence with the Baker River).	The distinctive "tree-staining" is inferred to include particles of tephra set YP, erupted in 1843 and deposited throughout much of the Baker River watershed. This inference suggests a date for the flood of 1843 or later.
	The year 1856 was based on 62 rings in a tree cut in 1923 from a flood bar on the Skagit River below the Baker River confluence, with 4 years added as the estimated colonization time gap.	Four years is too brief a colonization time gap (Pierson, 2006) for a conifer on a fluvial bar in the northern Cascade Range. A colonization time gap of at least 10 years is probable, indicating a date of 1850 or earlier.
"Great flood" from failure of a natural dam in the Baker River valley ca. 1836	The Devin account (table 8.1). A surveyor near Baker Lake was told by Native Americans of a "great flood" ca. 60 years earlier that resulted from failure of a landslide dam of the Baker River and flooded the "whole" Skagit River valley.	The natural Baker Lake (pre-reservoir) was raised 3.7 meters in 1845–47 (see text) by the Morovitz Creek lahar. Partial failure of this addition to the existing blockage is the most probable source of this legend (see text). The scale of any flood surge from natural Baker Lake could not have produced a "great flood" in the Skagit River.

"Mark by the Great Spirit"—The "Tree-Staining Flood of About 1856"

Origin of the "Staining" from Tephra Set YP of the 1843 Eruption(s) from Sherman Crater and Evidence for a "Great Flood" between 1843–50

Evidence for the maximum limiting age of a "great flood."—Stewart (written commun., 1918) found that the flood he first estimated as occurring about 1815 had been more readily traced than younger floods on the basis of an unusual tree-staining. "At that time they [the first settlers ca. 1878] noticed that the bark on all the larger fir and cedar trees and on all spruce trees more than 1.5 ft [0.46 m] was stained up to a certain height" (Stewart and Bodhaine, 1961). The Hart account from 1879 (elsewhere 1880–81) and later reports indicated that the unusual stain that was "…quite clear in 1879…dimmed rapidly so that by 1900 it was no longer noticeable." This suggested that the staining was from a "flood prior to the coming of the white man but subsequent to the flood of about 1815" (anonymous report titled "History of Floods," from after 1932 but probably by Stewart, who continued to work on Skagit River flood history) and that the staining as seen by settlers "must have been caused by a flood more recent than about 1815" (Stewart and Bodhaine, 1961).

The "bright" color of the "staining" is interpreted here as reflecting a probably small content, in terms of percentage, of suspended hydrothermal particles—silt- and clay-size particles of tephra set YP, distinctively yellow and creamy white in color, that originated from the explosive eruption(s) of Sherman Crater in 1843 (fig. 11). The freshly deposited hydrothermal particles were eroded by storm runoff and concentrated in the highest level of the suspended load of the following flood because of their high clay content and lower specific gravity, estimated as about 2.0–2.2, relative to that of detrital silica, 2.7. Thus, the highest coatings on tree trunks were "stained" with the unusually light-colored mud coating that entered the oral history of both Native Americans and settlers. Tephra set YP was originally described as like a blanket of snow. The staining ascribed to the flood was clearly different from the normal mud coatings, of a nondescript gray color and never "bright" in color, deposited on trees by overbank floods in the Skagit River. Some of the coating material may also have been derived from erosion of the Morovitz Creek lahar consisting of the same hydrothermal particles—but more cohesive and less erodible—that was emplaced in 1845–47 in much of the Baker River valley. The staining was apparently reported only from areas downstream of the confluence with the Baker River (Stewart and Bodhaine, 1961, p. 26–27). References to the "staining" that supports this conclusion include the following.

1. Stewart (written commun., 1923, p. 7): "When… settlers first came into Skagit Valley, the bark on all the fair-sized fir and cedar trees, and all of the spruce over one and one-half feet in diameter, was stained up to a certain height. There were many speculations and arguments among the settlers as to the cause of this staining." On the basis of the Hart accounts (table 8.1), the staining was first attributed by Stewart to the 1815 flood.

2. Later, however, Stewart (written commun., 1923, p. 8) believed "the old Indian was in error in ascribing to the flood of 1815 the flood stains seen by the…settlers. …the stains seen in 1879 were from a flood of about 1856." It was "well marked."

3. Stewart writes, "It is known that the stains on the trees in the late 1870's were remarkably plain, and could be seen for long distances through the forest" (written commun., 1923, p. 11).

4. Stewart reports, "In the floods since the coming of the white man, however, only a few trees have been stained. The cause of the staining [by the pre-settlement flooding] is not known…" (written commun., 1923, p. 7–8). Thus, the staining was thought to be characteristic only of a pre-settlement flood that was somehow different from post-settlement floods.

5. In discussing the 1856 flood, Stewart notes that staining he thought must have accompanied that flood "has apparently all faded…" (written commun., 1923, p. 9). In 1918, he found "mud" (but not the staining) he attributed to the 1856 flood on one cedar. He noted, "The stain from the 1856 flood had disappeared, but the 1909 and 1917 mud marks were clear." Stewart consistently makes a distinction between the "staining," which he apparently never observed directly, and "mud marks."

6. Stewart writes, "…the bright staining of all the cedar trees…" was possibly seen by the Native Americans as "a mark left by the great spirit" (written commun., 1923, p. 15). Clearly, the "staining" was seen as unusual and distinct from other flood-deposited mud coatings by those who saw it directly.

Mobilization and transport of tephra set YP particles is evidenced, firstly, by overbank deposits of the tephra where they must have been water-deposited. Reference section RS–20 includes a discrete 1–2 centimeter (cm) layer of water-deposited particles confined to a flood terrace 2–3 m above the bedrock channel of Clearwater Creek. The layer is distinctly white and if seen as a coating on a tree trunk would appear "bright." Away from the bank surface at RS–20, the tephra is only rarely present as a barely detectable "dusting" of particles

in the root zone. The site is more than 12 km west of any location with a comparable primary airfall thickness (fig. 41). Nearby, it is similarly found where it apparently records material redeposited by water on flood-inundated terraces in terrain now otherwise devoid of the tephra, apparently because it was washed away by a major rainstorm or was initially deposited on snow and flushed from the surface by a rain-on-snow event. Lastly, tephra set YP mobilization is also indicated by the Native American account of "all salmon" killed in the Skagit River with the eruption. Effects of the eruption on salmon in the Skagit River could logically be related to high suspended-sediment concentrations of tephra particles. Normal levels of suspended sediment, even those associated with floods, would not adversely impact salmon to that degree, if at all.

Evidence for the minimum limiting age of a "great flood."—Stewart (written commun., 1923) reveals that the origin of the specific 1856 date is related to cutting of a tree in February 1923 (last growth year was 1922) that was growing on a deposit believed to have been formed by the second ("tree-staining") of the two floods he based on legends. The tree was one of "a number of young [Douglas] fir trees, apparently all of the same age and much younger than the surrounding trees," located on a "sand-bar bench" (inset alluvial terrace) on the north side of the head of the canyon at The Dalles. The tree had 62 rings at the height cut (2.5 ft; 0.8 m). Stewart asked a "Forest Service official" for the period required to grow to that height (colonization time gap; Pierson, 2006), and that official estimated 4 years. This calculation (1922−62−4 = 1856) was the basis for the year of the flood. However, 4 years is too brief a colonization time gap. The minimum colonization time gap for even Douglas fir sprouting in the fines-rich lahar deposits in the area is 7 years (see previous discussions on the Morovitz Creek lahar and Rainbow Creek debris avalanche in chapter G). The colonization time gap for fines-poor sandy alluvium is more likely in the range of 10–20 years and, applying a colonization time gap of 10 years, proposed by Pierson (2006) for Douglas fir on alluvial surfaces farther south in the Cascade Range, the flood can be dated as pre-1850 (1922−62−10 = 1850). Stewart added that, on the basis of other unspecified information, the "tree-staining" flood could be as early as 1850, noting that date was "the year the Willamette River in Oregon had a great flood" (J.E. Stewart, written commun., 1923). As noted above in explanation of Stewart's identification of December 4, 1961, as the date of the "tree-staining" flood, records of annual peak flows from the Willamette River at Salem and near Albany extend back to December 4, 1861, the date of the flood peak of record for both sites. A date that young for the Skagit River flood, however, is precluded by the dendrochronology reported by Stewart.

Summary of 19th-Century Flood History Risk as Related to Mount Baker and Glacier Peak

After comparison of the 19th-century flood record with the events of the Sherman Crater eruptive period (1843–80), we found no evidence of any significant direct or indirect effect of volcanism on floods. This review indicates, in agreement with an anonymous reviewer of hydrologic data ca. the 1950s, that the largest reported pre-settlement flood—the 1815 "flood of legend"—did not exist. The only evidence is a second-hand account, dating from ca. 1879, of memories of Native American(s) from their youth—"stories which are told by the Indians" (Stewart and Bodhaine, 1961). Just as an 1866 account of the 1843 Mount Baker eruption was interpreted on the basis of an "old" Native American's memories as occurring in 1810 (Majors, 1978), the 1879 account of a "great flood" could well be from the 1840s.

The second largest pre-settlement flood—the equally notable "tree-staining flood of 1856"—is re-dated to between 1843 and 1850 based on the correlation of the unusual "staining" of tree trunks with flood-entrained particles of tephra set YP, which erupted in 1843. The minimum limiting date of 1850 is based on our re-evaluation of the historically memorable early attempt at dendrochronology described above. The evidence supports only a single "great flood," of rainfall runoff and snowmelt origin, between 1843 and 1850. Pre-1843 "great floods" certainly occurred, but all the historical accounts can be explained by this middle-19th-century flood—a conclusion shared with the anonymous reviewer cited above.

Several reports link the large 19th-century flood(s) to failures of natural dams. None of the following possible 19th-century blockages by ash or lahars from Mount Baker, either of Baker Lake or of the Skagit River at the confluence with the Baker River, could have accounted for a significant flood surge in the Skagit River.

1. The reported and geologically verified blockage of natural Baker Lake by the Morovitz Creek lahar.
2. The reported blockage of the Skagit River by the 1843 tephra set YP transported by the Baker River.
3. Possible blockage of the Skagit River by the Morovitz Creek lahar in 1845–47.

One of these blockages, probably the first, is the most likely source of the 1897 Devin account from Native Americans living on the shore of natural Baker Lake (table 8.1). The account is geologically possible, but the size

of the blockage and the magnitude of the partial breaching that could have followed are too large. Origin of a significant flood as a breakout of a lake impounded by a natural dam is possible, based on the sudden ("very quick") arrival of the flow according to one account, but this blockage did not occur in the Baker River valley. The Buller account (table 8.1) records a more logical site for a natural dam, upstream from Diablo Canyon in the Skagit River headwaters (fig. 2). More probably, however, the origin of the largest verified 19th-century flood was the same as that of most subsequent floods—a rapid snowmelt or "rain-on-snow" event. The entrainment of tephra set YP could only have occurred with such an origin.

Although there is no evidence of volcanic activity at Mount Baker having contributed to any 19th-century flood in the Skagit River, the future potential for volcanism to increase flood risk rises as the planning horizon lengthens. Significant present risk is mainly confined to the potential for collapse-runout lahars entering the reservoirs. Other potential future effects of volcanic activity in the Skagit and Nooksack Rivers include the formation of natural dams emplaced by volcanic landslides and large lahars analogous to floods and extending to the coastal lowlands. For example, the 1980 eruption of Mount St. Helens was accompanied by emplacement of a landslide blockage of a lake that—like a parallel ancient example ca. 2,500 years before present (ca. 2.6 thousand years ago) previously at the volcano—would have failed and produced a huge flood had not the post-1980 engineering response lowered the level of the lake that was impounded by the landslide. The ancient flood had a discharge greater than the Amazon River at flood stage (Scott, 1988b), and is one of the five volcanism-related examples of the 27 largest global floods described by O'Connor and Costa (2004). The primary point regarding volcanism and floods is that, although present flood risk is not significantly increased by Mount Baker and Glacier Peak, rapid escalation of volcanic activity (phreatic or magmatic) in the future may create significantly increased risk.

Appendix 9. Accounts and Letters Written by Joseph Morovits

The following is an excerpt from a letter written by Joseph Morovits dated April 12, 1912, to C.F. Easton, with original grammar (C.F. Easton, written commun., 1911–31).

> On rainbow creek the glacier came down about 30 years ago end swiped all the timber for 7 miles. went clear into swift creek be fore it stopped. it took every thing for a half mile wide. when I came here 21 years ego [1891] their was ent a bush of any kind on it. but now it is pretty well covered with willows end cottonwood. and ever green timber starting. a person...could tell to egsact date when this happened by cutting down a tree that was on the edge of the slide. and was partly ground off on one side. and green on the other. then count the years the layers of growth since this happened. many trees standing along the edge of this strip have rocks sticking in the sides of them as high. As 30 feet from the roots as big as a mans 2 fists and much biger.

Author's note.—We include the preceding in the original to illustrate the genius of Morovits in spite of his lack of schooling. By his account, he did not attend school and did not read and write until taught by a fellow miner. Some of the spelling and punctuation errors may lie in the first transcription of the original. This letter is quoted, with grammar corrected, in the essay, "Joe Morovits: The Hermit of Baker Lake," by A.J. Craven (C.F. Easton, written commun., 1911–31). There the third sentence is: "A person could tell the date when this happened by cutting down a tree on the edge of the slide which was partly ground off on one side and green on the other, and then count the years that have grown since it stopped growing on the dead side."

The Craven essay mentions a letter (by Morovits to Easton) dated January 26, 1915, but indicates that another letter (probably that of April 12, 1912, to Easton) is the original source of the following edited statement, "I located here two miles west of Baker Lake, at the very foot of Mt. Baker, on the 13th day of October 1891..."

Accompanying the Craven essay in Easton (written commun., 1911–31) is a picture of the Morovits "cabin," with Morovits's writing on the back of the photograph that reads, "Morovits Ranch Cabin was build in October 1891. Where Joe Morovits lived for 25 years alone. Foot of Mt. Baker Whatcom County. Washington near park creek."

Author's note.—J.S. Scurlock and K.M. Scott located the now collapsed remains of the cabin near RS–27.

The following two excerpts are from the Craven essay, without note of a specific letter.

> …he [Morovits] says there are only two places on the Baker River watershed which show evidence of volcanic eruption, one at the head of Swift Creek, about a mile south of Austin Pass, and the other Mount Baker. The former was gigantic in area and violence, the extinct crater being nearly three miles across and the outflow and fissures indicating unusual volcanic disturbance. He thinks the lava from this disturbance is throughout the wash [glacial outwash] of the district. Baker River he says has cut a channel one hundred feet into this lava from the first eruption without cutting through.

Author's note.—The eruptive center mentioned above remained unknown by geologists until recognized by W. Hildreth in 1992 and described by him as the Kulshan caldera and dated to 1.15 million years (Hildreth, 1996; Hildreth and others, 2003). The account of the channel records the incised meanders of the Baker River channel in the Sulphur Creek lava flow (see fig. 25).

> Baker's second lava flow occurred after the glacial age and is in evidence at the head of Park Creek and Rainbow Creek, a comparatively light flow which piled up in high ridge and is different in quality and structure from the other flows.

Author's note.—This refers to the pre-Mount Baker unit, the andesite of Lava Divide, as defined by Hildreth and others (2003).

The Craven essay also refers to the collapse of the east flank of Sherman Crater that produced the Morovitz Creek lahar, dated herein as 1845–47. The estimate of the age of trees growing on the lahar (interpreted by Morovits as disintegrated lava) and dating of the raised blockage of Baker Lake are remarkably accurate.

> The third [last] eruption of Mount Baker came down from between the two peaks [from Sherman Crater, between Sherman Peak and Mount Baker] by Park and Boulder Creeks, and occurred only about a hundred years ago…timber that has grown on this flow is only seventy years old and it probably took thirty years for the lava to disintegrate and become adapted for arboreal vegetation…this is the flow that swept down and raised the lake [natural Baker Lake] some twelve feet for many years, the surface of Baker Lake being now some eight feet higher than before the flow. This is shown by submerged stumps of trees extending out for considerable distance from the present lake shore, and, Joe figures that about one hundred years will account for the rotting away of all portion of the trees that projected above the water. His study of geology, at first hand, is characteristic of the man; confronted with the facts he has [resolved them] into reasonable solutions and the deduction and conclusions are not much different than those reached by men of more learning.

What follows is a description of Joe Morovits from Connelly (1976).

> He was a squat man of such bull strength that he could wrap his skookum big arms around a fallen tree and lift it off the trail. Yet he was the picture of gallantry as he carried bloomered lady mountain climbers across glacial torrents. He was a man of enormous good spirits and gregariousness who would advertise in Seattle newspapers his arrival in town…he had no schooling whatever yet his studied geologic observations on the Cascades of the Mount Baker group still are respected.

Author's note.—The life of Joseph Morovits after he left his "ranch" in the Baker River valley has been a mystery to historians. Nevertheless, a letter has emerged from Morovits to a "Vic," very likely Victor Galbraith, the winner of the 1913 Mount Baker marathon. It reports that Morovits was seriously injured in a car accident in the early 1920s and returned to mining in the Black Diamond coal field, the work that originally brought him and his brother to the Pacific Northwest from Wisconsin in the 1880s.

Menlo Park Publishing Service Center, California
Manuscript approved for publication April 9, 2020
Edited by Monica Erdman
Layout and design by Kimber Petersen
Illustrative support by JoJo Mangano

ISSN 2330-7102 (online)
https://doi.org/10.3133/pp1865